VIEWSHED UNCERTAINTY IN A FORESTED, MOUNTAINOUS LANDSCAPE

by

DOUGLAS LOCKHART

(Under the Direction of Marguerite Madden)

ABSTRACT

Visibility analysis is critical in a variety of applications, and many geographic information systems (GIS) are equipped with analysis functions, such as the viewshed, that provide visibility results based on digital elevation data. These GIS analyses are affected by uncertainty associated with input data and software systems, which limit the reliability of results. This thesis investigates numerous factors (different software and algorithms, elevation data models and spatial resolutions, observer positional errors, visualization approaches, and earth curvature) that can impact GIS-based visibility analysis in mountainous terrain. The results indicate that a raster digital elevation model (DEM) is a better data structure for visibility analyses than a triangulated irregular network (TIN), and higher resolution data tend to generate less variability and better agreement. The algorithms tested normally have high levels of agreement, but discrepancies can exist. There is a need for incorporating surface features into analyses and for field validation of results.

INDEX WORDS: Viewshed, Line of sight, Visibility, Geographic information systems, Uncertainty, Terrain model, Digital elevation model, Triangulated irregular network

VIEWSHED UNCERTAINTY IN A FORESTED, MOUNTAINOUS LANDSCAPE

by

DOUGLAS LOCKHART

B.B.A., The University of Georgia, 1998

A Thesis Submitted to the Graduate Faculty of The University of Georgia in Partial Fulfillment of the Requirements for the Degree

MASTER OF SCIENCE

ATHENS, GEORGIA

2009

VIEWSHED UNCERTAINTY IN A FORESTED, MOUNTAINOUS LANDSCAPE

by

DOUGLAS LOCKHART

Major Professor:	Marguerite Madden
Committee:	Thomas R. Jordan Xiaobai Yao

Electronic Version Approved:

Maureen Grasso
Dean of the Graduate School
The University of Georgia
August 2009

ACKNOWLEDGEMENTS

I would like to thank my wife, Dora, for being willing to move to Athens while I attended graduate school. She worked hard and took care of me daily so that I could pursue my studies and research. Thank you so much for your love and support. This was a team effort.

I would like to thank my family, Wayne, Judy, and Sondra, for always believing in me and supporting me in my decisions. I know that you have always been behind me.

Thanks to Dr. Madden, who has been such a fantastic advisor. She is so full of ideas and supportive of her students. Your guidance to me has been very helpful. Thanks, also, to Tommy and Dr. Yao for serving on my committee and helping to make this department what it is.

Thanks to Rick Smith, who created a function in ArcScene that helped me with my visualizations in Chapter 8. Good luck on your Ph.D.

Most importantly, thanks be to God for giving me the opportunity to come back to school and immerse myself in this field of study. Whatever gifts and abilities I have come from Him, Father, Son, and Holy Spirit.

TABLE OF CONTENTS

LIST OF TABLES

Page

LIST OF FIGURES

Page

CHAPTER 1: INTRODUCTION

Sight is one of the five primary senses for human beings (Coren et al., 2004). It may be the sense that humans are most dependent upon and aware of, as the stimuli of reflected light is usually constant in our field of view, and light is an agent that can transmit detailed information over long distances. Some consider the purpose of vision "is to inform us about our world by using the medium of reflected light" (Enns, 2004). The importance of vision is explained by others as being the function that enables one to move and perform successfully in one's surroundings (Paternoster, 2007). People rely on vision, and the visibility of objects is important in many fields of research, including physical and social sciences. Visibility may be defined as the "condition of being visible," the likelihood of being visible under certain situations, a "range of vision," or "the ability to provide an unblocked view" (Agnes and Guralnik, 2006).

Knowledge of topography, like vision, may be taken for granted, but it plays an important role in scientific research and in people's everyday lives. Nearly all our activities are linked, if only indirectly, to the shape of the ground beneath our feet.

Visibility is dependent on the terrain. Many geographic information systems (GIS) are equipped with analysis functions that provide visibility results in a straightforward manner (Wang et al., 2000). In GIS, visibility is normally expressed as intervisibility between points, also termed line of sight (LoS), or as a viewshed, the total area that is visible from a location (Goodchild and Lee, 1989; Fisher and Farrelly, 1997). Visibility analysis is critical in applications of military maneuvers, communications tower siting, landscape planning, land development, and recreational hiking.

Description of Problem

Visibility analysis in GIS is affected by uncertainty associated with elevation data and software systems. That geographic data and systems used in visibility analysis are not perfect, but are infused with uncertainties, has been well researched (Fisher, 2009). The concept of uncertainty includes not only errors, but also the issues of imprecision, ambiguity, vagueness, and other sources of incomplete information (Shi, 2009). Uncertainty refers to what is unknown and can result from a lack of knowledge about the reliability of data or geographic analyses (Wechsler and Kroll, 2006). If the data or systems cannot unambiguously predict accurate results, decisions can lead to detrimental outcomes (Agumya and Hunter, 2002).

Unfortunately, not all GIS users and decision makers are aware of the questionable nature of results from visibility analyses. Sources of uncertainty that can affect computed visibility include: (1) the software and algorithms used; (2) interpolation techniques employed to create digital elevation data of various data models or structures; (3) the choice of data resolution; (4) observer positional errors; (5) visualization versus algorithm solutions; (6) the curvature of the earth; (7) errors in elevation data; (8) the consideration that most analyses are based on bare earth terrain and ignore surface features (e.g., vegetation and buildings); and (9) other conditions that lead to uncertain results (atmospheric conditions, target distance, color, shape, or size). The fundamental question, then, concerns the confidence that users can have in GIS-generated visibility analyses, given inherent uncertainty and variability in geographic data, algorithms, and software.

Purpose and Objectives

Measures of visibility computed with digital data in a GIS environment have proven to be very useful, but research has demonstrated that results should be viewed with a certain level of

skepticism (Fisher, 1993; Maloy and Dean, 2001). The purpose of this thesis is to investigate various factors that can impact GIS visibility analyses and to quantify the uncertainty and variability of results due to those factors.

This research involves both field and lab work. Vistas from certain field locations were re-created in the lab with various combinations of software systems, elevation data of various data structures and spatial resolutions, positional variabilities, and other software options. Specific objectives of this study include the following:

1) Perform field work in Great Smoky Mountains National Park (GRSM) to observe and photographically record visibility from the perspective of an observer on the ground, using field site locations as measured by the Global Positioning System (GPS).

2) Evaluate the performance and products of different visibility algorithms and software programs. Two visibility algorithms within ESRI ArcGIS, the Viewshed and Line of Sight functions, are compared to determine whether the visibility of certain locations or features in ArcGIS is dependent on the analysis method used. Viewshed results are also compared between ArcGIS and ERDAS Imagine to quantify the agreement between these programs.

3) Create triangulated irregular networks (TINs) and raster digital elevation models (DEMs) with various interpolation techniques from bare-earth, lidar point data. Examine the implications of data structure and interpolation choices through the generation of viewsheds.

4) Demonstrate the uncertainty of viewsheds that can result from GPS variability by assessing the precision and accuracy, where possible, of field-collected GPS coordinates. Find the relationship between GPS-stated accuracy, precision, and tree cover.

5) Determine whether 3D visualizations are a viable alternative to visibility algorithms by comparing the visibility of randomly distributed features between the ArcGIS viewshed function

and the perspective view of ArcScene. Quantify the level of agreement and assess ArcScene for its suitability as a quantitative, visibility analysis tool.

6) Discover whether commonly used map projections and coordinate systems can seriously affect viewshed results. Investigate the distance at which earth curvature becomes an important factor for viewshed analyses.

Throughout the various tests of visibility analysis, the effects of DEM resolution and data structure utilized will be addressed to evaluate the trade off between elevation source data, data volume, computation time, and visibility results. It is anticipated that this research will provide guidance so that users can make informed decisions on input data, software, and processing algorithms. Ultimately, results of this research should enable GIS users to develop an estimate of the confidence they should have in their viewshed results.

Significance

Many issues that impact GIS-based visibility analyses have been researched over the past couple of decades. This thesis seeks to expand the literature by providing examples of numerous disparate sources of visibility uncertainty and assessing their effects in a region of rugged topography. Some new examinations of visibility uncertainty are presented, such as how GPS variability can impact viewsheds, a comparison of different visibility algorithms within the same software package, whether map projections can significantly effect viewsheds, and the feasibility of employing perspective views for determining visibility.

There are a variety of parties who have an interest in visibility, and applications abound (Table 1.1). My hiking background led me to this research. Many hikers, like me, get very excited about views, and we revel in the distant vistas across the landscape from a summit, bald, exposed ridge, or opening through the trees (Figure 1.1). Hikers travel across the country and

plan trips and routes with possible views in mind, yet existing maps do not provide hikers with the information necessary to judge whether distant views will exist from trails. Most hikers can only estimate the geometry from contour lines on a topographic map, and some maps include, in the most general way, areas that are forested versus those that are not. This information is inadequate for hikers to ascertain whether a trail will provide views of certain desirable features. A recreational map or software that could incorporate the probability of views from certain locations would be welcomed by the hiking community.

Table 1.1: Partial list of visibility applications.

Agencies and Parties Interested in Visibility	Visibility Applications
▪ U.S. Army Topographic Engineering Center ▪ National Geospatial-Intelligence Agency, Central Intelligence Agency, Defense Intelligence Agency, Department of Homeland Security, other U.S. intelligence agencies ▪ U.S. Military ▪ Communications companies ▪ Academic geography researchers and historians ▪ Archaeologists ▪ Land developers ▪ Real estate agents ▪ Public land resource managers (National Park Service, U.S. Forest Service, Bureau of Land Management, state Departments of Natural Resources, etc.) ▪ Urban planners ▪ Private businesses ▪ Recreational land users (hikers) ▪ Law enforcement agencies ▪ Federal Aviation Administration ▪ Civil engineering firms ▪ Timber companies ▪ Energy companies ▪ Wildlife biologists and conservancy groups ▪ NASA	▪ Concealment of sensitive materiel ▪ Planning of defense installations, such as surface-to-air missile batteries ▪ Least visible routes for flight paths and military personnel and equipment maneuvering ▪ Visual impact analysis ▪ Fire tower positioning ▪ Communications tower siting optimization (radio, cell, microwave) ▪ Archaeological research into past locations of cultural objects ▪ Environmental impact assessment ▪ Urban view corridors ▪ Recreational trip planning ▪ Visibility of new construction ▪ Radar systems siting optimization ▪ Business location and facilities expansion ▪ Visibility of timber harvesting ▪ Landscape planning and architecture ▪ Environmental management ▪ Windmill location optimization ▪ Wildlife population estimation ▪ Identifying scenic viewpoints ▪ Spacecraft landing site selection ▪ Reconstruction of historical events (e.g., military battles, migration and settlement patterns, etc.)

Figure 1.1: Vista in the North Cascades of Washington, 2007. (Photo by Dora Lockhart.)

This thesis is organized in manuscript style. Chapter 1 is a brief introduction of the topic, a description of the problem, purpose and objectives of the study, and significance. Chapter 2 reviews the literature on visibility studies, organized by the major issues. Chapter 3 describes the study location. Chapter 4 is an overview of the data and methods used. Chapters 5 through 9 are written as manuscripts with each chapter being a self-contained study with a different study area, data, methods, and objectives. Chapter 10 ties together the results of the various studies with a summary, conclusions, and a discussion of future work. Manuscript references are organized by chapter, and introductory (1-4) and concluding (10) chapters are combined into one reference section.

CHAPTER 2: LITERATURE REVIEW

Visibility, in both the natural world and in GIS, is based on the terrain surface and the geometry between an observer and a target. Intervisibility, or LoS, refers to whether two locations are visible to each other (Huss and Pumar, 1997). These two terms can be used interchangeably (Fisher and Farrelly, 1997). Two locations are intervisible if a straight line of sight between them does not intersect the terrain at any point (Maloy and Dean, 2001). In a GIS environment, a ray between an observer and target is evaluated as it passes over the digital elevation surface. If the ray encounters interference from the surface, then the two points are not visible to each other, i.e., one point is masked from the other (Lee and Stucky, 1998; Rana, 2003). In some contemporary GIS packages, visibility along the entire length of an LoS can be determined, in addition to whether the target itself is visible (Figure 2.1). Traditional LoS and viewshed analyses yield a binary result (0 for not visible, 1 for visible) for the locations in question (Fisher, 1993; Nackaerts et al., 1999).

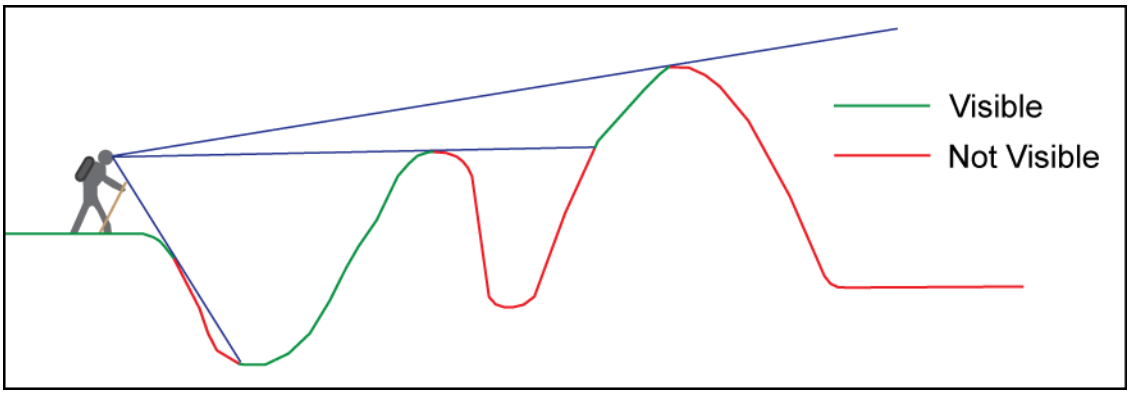

Figure 2.1: Lines of sight in rough terrain. Adapted from Sorensen and Lanter (1993).

A viewshed is an extension of the LoS concept. The term "viewshed" originated with the U.S. Forest Service in the 1970s (Ervin and Steinitz, 2003). The Forest Service's Pacific Southwest Forest and Range Experiment Station developed the first computerized viewshed application, named VIEWIT, in 1968 (Amidon and Elsner, 1968). Instead of considering only two locations, the observer and target, a viewshed considers the total area that is visible from one point (Goodchild and Lee, 1989). The viewshed is normally used to describe what can be seen from a location, but some use it to refer to the area from which a target is visible (Maloy and Dean, 2001; Ervin and Steinitz, 2003). Since a viewshed considers visibility between an observer and every location within the elevation surface, it is more computationally intensive than determining a single LoS, although the same general concept is employed by both the viewshed and LoS functions. To determine a viewshed, all that is needed is a digital representation of the terrain, the point designated as the observer's location, and an algorithm for computation (Dean, 1997). Research into GIS-computed visibility has been ongoing for several decades (Yoeli, 1985; Goodchild and Lee, 1989; Fisher, 1991; Dean, 1997; Izraelevitz, 2003; Llobera, 2007).

Data describing the surface of the earth can be represented and stored in a variety of digital models and formats. Confusion may result unless clear definitions are stated regarding the data, since common terms and acronyms are sometimes used with different substantive meanings. Digital elevation data may refer to bare earth topography, heights of features above ground level, such as buildings and trees, or bathymetric surfaces. Elevation data can be stored digitally as contour lines of equal elevation, a uniformly spaced horizontal grid of elevation values stored as a raster, irregularly spaced mass points, or contiguous, non-overlapping triangles stored as a TIN (Maune et al., 2001).

The term digital elevation model, or DEM, is often used interchangeably with digital terrain model (DTM) (Lillesand et al., 2008). A DEM normally refers to a regularly spaced grid of bare earth elevations, and the US Geological Survey (USGS) has been the major producer of American DEMs (Maune et al., 2001). A DTM may also refer to bare ground elevation at regularly spaced intervals, but, in addition, a DTM may include breaklines, which are important topographic features at irregular intervals, such as rivers or ridges. Bare ground elevation data produced by the US National Geospatial-Intelligence Agency (NGA) are called digital terrain elevation data (DTED) (Maune, 2001).

A digital surface model (DSM) would be identical to a bare earth DEM in areas of terrain devoid of vegetation or man-made or natural objects that extrude above ground level. What differentiates a DSM is that it represents the highest surface at a specific location, whether that surface be the bare ground, the top of a building, or a tree top (Kidner et al., 2000; Maune et al., 2001).

The digital elevation data upon which visibility analyses are based is often a raster of bare earth elevations (DEM), but results can be generated in some software from a vector data model or structure, such as a TIN. Some of the confusion in terminology among DEM, DTM, and DSM stems from different usage in various countries. In this paper, the term DEM will be used to refer to a grid of bare earth elevation in raster format.

Research has uncovered numerous sources of uncertainty that can affect the results of visibility analyses, of which many GIS users are often unaware. As previously stated in Chapter 1, these include: (1) the software and algorithms used; (2) interpolation techniques employed to create digital elevation data of various data models or structures; (3) the choice of data resolution; (4) observer positional errors; (5) visualization versus algorithm solutions; (6) the

curvature of the earth; (7) errors in elevation data; (8) the consideration that most analyses are based on bare earth terrain and ignore surface features (e.g., vegetation and buildings); and (9) other conditions that lead to uncertain results (atmospheric conditions, target distance, color, shape, or size).

GIS Software and Algorithms

As with any computer program, the results of visibility analyses are based on the coded procedures, or algorithms. The basic concept involved in calculating visible areas is fairly simple, but its implementation is a complex function and differs across GIS packages. The practical reality is that algorithms developed by different individuals or companies may generate different results even if they are designed to compute the same phenomenon (Fisher, 1993). Many people are undoubtedly using visibility functions within numerous GISs, but anecdotal evidence suggests that few people who use these functions are questioning their results. Even some researchers make the assumption that the choice of GIS software, with its associated viewshed algorithm, will not affect the results of their project (Yu et al., 2007). However, the field testing of commonly used commercial GIS programs by Riggs and Dean (2007) demonstrated that this is a faulty assumption, because the choice of software program does indeed affect visibility results.

Riggs and Dean (2007) compared field-surveyed viewsheds with viewsheds generated in three popular software programs: ESRI ArcGIS, ERDAS Imagine, and IDRISI by Clark Labs. The level of spatial agreement among the viewsheds ranged from 89-93%. Their elevation data was very accurate and various resolutions of DEMs were used, but in no case were viewsheds better than 85% accurate (ArcGIS), and in some cases accuracy was as low as 66%. In addition, the study area in which viewshed accuracy was evaluated was small, only 0.07 km^2 (7.28 ha, or

17.98 ac). A similar level of viewshed accuracy, validated by field work, was obtained with ArcGIS from coarser resolution DEMs (30-m DTED2, military data). In two study areas, accuracy was 80.3% and 84.0%, but the study area sizes are not known (Swanson, 2004).

Researchers have been, and continue to be, frustrated by the fact that algorithm details are not widely published by software vendors (Fisher, 1993; Riggs and Dean, 2007). A consequence is that users are unable to thoroughly understand the viewshed calculation process or know what to do to improve the final results. Some GIS programs offer multiple visibility functions (e.g., viewshed and LoS functions), and while it is assumed that they will generate the same results, no published studies have been found that verify this assumption, either by independent researchers or by the software vendors.

Elevation Data Structure and Interpolation Techniques

The most important input, and the basis of visibility analyses, is the digital terrain representation. However, the two basic data models used for visibility analysis, DEMs and TINs, have fundamentally different data structures. A DEM is a raster model of uniformly sized square cells (Longley et al., 2005) (Figure 2.2). The DEM structure has appeal because it is simple and is a very common format for publicly available digital elevation data. A TIN is a vector model of contiguous, non-overlapping triangles developed by Peucker et al. (1978) that relies on Delaunay triangulation. The TIN structure is made up of nodes (triangle vertices), edges (triangle sides), and facets (the triangle planes). A TIN's facet is cast at an angle in 3D space (Maloy and Dean, 2001). Thus, different points on a TIN facet may have different elevations while the TIN surface is assumed to be homogeneous in terms of slope and aspect. One of the major differences in the creation of these models from point data is that irregularly spaced input points are retained in the

TIN structure and become TIN nodes, but a DEM "loses" these explicit points in the interpolation process.

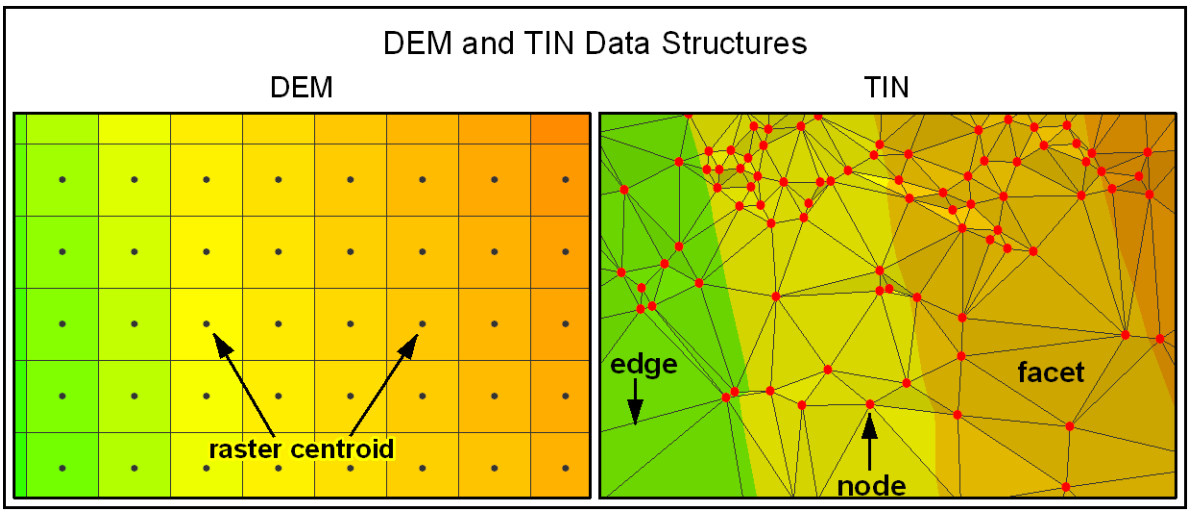

Figure 2.2: DEM and TIN data structures.

When a DEM is generated from point data, the surface must be interpolated (Franke, 1982). Watson (1992) refers to interpolation as "an informed estimate of the unknown." In the interpolation of an elevation surface, sample points with measured z-values are used to estimate the elevation at locations that do not have measured z-values. Various interpolation methods will produce different elevation surfaces, and many GIS packages offer multiple interpolation routines for creating DEMs (Yilmaz, 2007). There is no single interpolation method that is the "best" for all situations (Lam, 1983; Doucette and Beard, 2000; Fisher and Tate, 2006). Published studies are varied in their results. For example, Lloyd and Atkinson (2002) found that kriging produced a more accurate DEM from lidar point data than the inverse distance weighted (IDW) method, but Su and Bork (2006) reached the opposite conclusion. There are also numerous algorithms for creating a TIN via Delaunay triangulation (Goodchild and Lee, 1989; El-Sheimy et al., 2005). Gong et al. (2000) found that in rough terrain, TINs are preferred to

interpolated DEMs, while Yilmaz (2007) reported that a DEM created by kriging was more accurate than a TIN.

Many have theorized that the TIN structure is superior to a raster model for various representations and analyses, including viewsheds (Goodchild and Lee, 1989; De Floriani et al., 1994). However, field-based accuracy assessments have not entirely supported this view. Dean (1997) found that TIN-based viewsheds were more accurate than DEM-based viewsheds, but more recent studies by Maloy and Dean (2001) and Riggs and Dean (2007) found that DEM-derived viewsheds were more accurate.

Data Resolution

Scale and resolution issues are inherent in the nature of digital elevation data since there are a finite number of sample points modeling a continuous surface (Goodchild and Lee, 1989). Different resolutions of data are often available for the same study area. In a DEM, resolution refers to the grid size, or post spacing, while a TIN normally has variable resolution. A DEM composed of very large cells (e.g., 90-m post spacing) oversimplifies the terrain, while a DEM with small post spacing (e.g., 2 m) may not be necessary in all applications. Ziadat (2007) reported that for DEMs interpolated from contours, their accuracy decreased as the post spacing increased. The availability, or lack thereof, of elevation datasets may constrain a user, but the user should choose the resolution that is appropriate for the study, if at all possible.

The choice of elevation data resolution will affect terrain products derived from those data. Kienzle (2004) reported that terrain derivatives, such as slope and aspect, varied significantly with different DEM resolutions. Viewsheds are also derived from the terrain, and results will vary based on the resolution of the elevation surface. Two studies cited by Huss and Pumar (1997), namely Marlin (1992) and O'Rourke (1992), found that intervisibility results were

sensitive to DEM resolution, and both researchers postulated that higher resolution data would yield more accurate results. Maloy and Dean (2001) reported that viewshed accuracy varied by resolution, with results derived from 30-m DEMs found to be more accurate than coarser resolution data. Oversampling to a higher resolution (10 m) did not improve accuracy. Riggs and Dean (2007) found that the most accurate viewsheds were generated from a DEM with a resolution (4 m) that most closely matched the average spacing of the input point data used to construct the DEM. Accuracy declined as resolution became coarser. Swanson (2003) reported that field validation of viewsheds, generated from several software programs, indicated that viewshed accuracy declined with lower resolution DEMs. For example, in the same study area, average viewshed accuracy was 95.8% with 5-m data and was slightly less than 90% with 30-m DEMs. Other factors could have influenced these results, however, because these DEMs were derived from different sources.

Observer Positional Errors

The Global Positioning System is a relatively new geospatial tool, becoming fully operational in 1995 (Rizos, 2002). It has revolutionized field-based data collection and mapping, but for GPS coordinates to be valuable, users must have some idea about their accuracy. There are numerous factors that can impact the accuracy of GPS coordinates, including the user's environment and the spatial distribution of GPS satellites relative to the user. Measurement errors can stem from signal biases and random errors (Arnaud and Flori, 1998). Examples of biases are atmospheric effects, satellite orbital positions, and satellite clock error. These biases can be accounted for and corrected. Errors that cannot be accounted for include receiver clock error and multipathing (Rizos, 2002; Deckert and Bolstad, 1996). Multipath errors occur when

GPS signals reflect off surrounding objects before reaching the receiver, which is a problem in areas covered by dense vegetation and urban settings with buildings (Abidin, 2002).

GPS-estimated positional error, or simply error, is the horizontal distance between a GPS receiver's computed location and its true location. The direction of the error is not considered (Oderwald and Boucher, 2003). It can be thought of as the radius of a circle of error. Without differential corrections, typical GPS accuracy is about 10-20 m (Shi, 2009). Differential corrections can reduce GPS errors in the field by utilizing a reference receiver to account for and correct errors that are common to both receivers (Lillesand et al., 2008). In the U.S., the Federal Aviation Administration provides real-time differential corrections for free via the Wide Area Augmentation Service (WAAS). Officially, WAAS provides 7.6-m horizontal accuracy at a 95% confidence level, but actual results are usually better than this (Lachapelle et al., 2002).

An empirical study of the Garmin GPS V, a popular GPS receiver, demonstrated that its average horizontal accuracy over a range of canopy closure conditions is 3.5 m, and its computed location is within 6.5 m of the true location 95% of the time. Accuracy was dependent on tree cover, as its average accuracy was 2.6 m (4.8 m, 95% confidence level) under open skies, 3.8 m (6.8 m, 95% confidence level) under 40-50% canopy closure, and 4.7 m (9.5 m, 95% confidence level) under a closed canopy (Wing et al., 2005). In a similar study of horizontal accuracy under dense tree cover, the GPS V fared worse, having an average accuracy of 8.9 m (Wing and Eklund, 2007).

The variability of GPS coordinates, especially those obtained in areas of dense tree cover and high ridges, could affect GIS analyses that are heavily dependent on these point coordinates, such as the viewshed function. Huss and Pumar (1997) found that viewsheds are sensitive to horizontal position in rugged terrain because a change of position alters the geometry between an

observer and nearby ground features or obstacles. Although the DEM used in their tests was of coarse resolution (100-m post-spacing), relocating an observer to the nearest grid cell (100 m away), which had the same elevation, caused the visible area to be reduced by 75%.

Visualization versus Algorithm Solutions

Some GIS programs provide more than one way to determine the visibility of surface or near-surface features. ArcGIS provides three methods, including two algorithms, the viewshed and the LoS, and 3D visualizations within ArcScene. Although it was not specifically designed for the purpose of determining visibility like the viewshed or LoS functions, perspective views within ArcScene can be used to simulate a landscape vista, and therefore, visibility. Visualization tools, such as ArcScene, are not designed to provide quantitative or statistical analyses of data (Gahegan, 1999). Whether perspective views in programs like ArcScene can be used for quantitative viewshed analyses is a worthwhile question.

Germino et al. (2001) used a unique approach to assess the accuracy of landscape visualizations with the traditional viewshed function. They compared panoramic photographs taken in the field (ground truth) with visibility determined from a viewshed algorithm and 3D perspective views in ArcInfo. Their goal was to quantify viewshed areas and visible landcover classes. This was accomplished by determining the visibility of landcover data, based on the viewshed function, and test points that were digitized both inside and outside of the algorithm-delineated viewsheds. These two datasets were draped over the same DEMs used in the viewshed function, and the visibility of landcover and test points in perspective view was compared with their visibility as determined from the viewshed algorithm.

Good agreement in the visible areas was found between the viewshed algorithm and the perspective views by Germino et al. (2001). Test points that were far (50 m) from the boundary

of the delineated viewsheds had 100% agreement. As the distance between test points and viewshed boundaries decreased, agreement decreased. For example, at a 2-m distance, agreement was between 75% and 80%. The 3D perspective views of landcover in ArcInfo proved to be very accurate, as assessed by field data. There was only about 2% of error in the estimates of the visible area of each landcover class. Despite these positive findings, no other literature has been discovered that quantifies visibility using both viewshed functions and visualizations.

Earth Curvature

It can be advantageous to simplify and represent the curved earth as a flat plane. A map projection is the representation of a portion, or all, of the curved earth surface as a flat plane. All map projections result in some type of distortion (Habib, 2002). The impact of various coordinate systems and map projections is that errors are introduced into data when transformations between coordinate systems/map projections take place. For example, if a DEM is in geographic latitude/longitude coordinates and the data are projected, an interpolation process takes place. The interpolation shifts DEM grid points in east-to-west and north-to-south directions by variable distances (Franklin and Guth, 2005). Latitude and longitude at a particular location, when transformed into a planar coordinate system, may result in X,Y coordinates that are slightly “off the mark,” or inaccurate.

It is not unusual for GIS viewshed functions to require DEMs to be in a square grid, and this necessitates that data be in a coordinate system such as Universal Transverse Mercator (UTM) or State Plane. According to Franklin and Guth (2005), the errors introduced by shifting grid points during interpolation between a latitude/longitude and a rectangular coordinate system can affect visibility computations significantly. They state that the greatest impacts will occur when dealing with rugged, mountainous terrain.

The curvature of the earth should be taken into consideration in visibility analyses over great distances (Ervin and Steinitz, 2003). Yoeli (1985) developed formulas that could be implemented into visibility algorithms to model this phenomenon. In 1993, Fisher pointed out that earth curvature is normally ignored by viewshed algorithms, but is important because it "causes direct lines of sight to be different from the actual lines viewed along." Fourteen years later, Riggs and Dean (2007) stated that many GIS functions have incorporated earth curvature effects, but not adequately, since GIS documentation does not cite studies that have validated the implemented adjustments. The distance at which earth curvature becomes an important factor for visibility analyses is not widely discussed in the literature or software documentation.

Elevation Data Errors

While many DEMs are of high quality, a DEM is a model, by definition, and should be treated as a simplified representation of reality and not reality itself. All digital elevation data contain errors which cause uncertainty when used in analyses (Fisher, 1991; Wechsler and Kroll, 2006). An elevation error is the difference at a specific point between the digital elevation value and the true elevation (Riggs and Dean, 2007). Errors may exist in the original dataset, or they may get generated in DEM production. Types of errors include photogrammetric errors, digitizing errors, GPS errors, survey errors, interpolation errors, coordinate system and projection transformation errors, scanning distortions, etc. (Huss and Pumar, 1997; Nackaerts et al., 1999). Many users do not examine the potential negative effects of these errors, which is understandable, since dealing with uncertainty is not a single, simple step in GIS (Wechsler and Kroll, 2006). There are limited methods available to users for dealing with DEM errors (Wood and Fisher, 1993). The downside is that elevation errors, even if small, are propagated into

visibility results and can have a serious impact on generated viewsheds (Huss and Pumar, 1997; Kidner et al., 2001; Riggs and Dean, 2007).

While the USGS removes systematic errors and blunders from its National Elevation Dataset (NED) products, random errors remain (Wechsler and Kroll, 2006). Accuracy of elevation data is normally expressed as root mean square error (RMSE). Although this is a good indicator of the quality of the DEM compared with its source, RMSE does not have a spatial component and provides no information regarding the spatial distribution or autocorrelation of error across an area (Holmes et al., 2000; Fisher, 2009).

Visibility will usually be overestimated if elevation errors are not considered (Fisher, 1991). Simulating the error that may be present in a DEM can be accomplished through the Monte Carlo method. This type of stochastic simulation uses random variables to create multiple realizations (Sobol', 1994).

The process of generating probable viewsheds is described by Fisher (1995) and Nackaerts et al. (1999). Error images are created through Monte Carlo simulation, in which pseudorandom values are generated that correspond to the magnitude and statistical distribution of DEM error, which can sometimes be obtained from metadata, through empirical tests, or other published materials. These pseudorandom values are assigned to cells of a raster that have the same extent as the original DEM, thus producing an error image. Each error image is added to the original DEM, and this new DEM can be considered one of many valid samples from a population. A traditional binary viewshed is calculated for each sample DEM, and the probable viewshed is found by averaging all cell values of binary viewsheds. Each cell in the probable viewshed will have a value between 0 and 1, which can be converted to a percentage and considered a probability. By taking DEM errors into consideration, probabilistic visibility is

considered a more robust portrayal of visibility than traditional binary viewsheds. Nackaerts et al. (1999) found that the probabilistic visibility stabilizes for 30 to 60 simulations.

Other, more advanced methods of measuring and simulating error have been used. Fisher (1998) found spatial autocorrelation of DEM errors and used geostatistics to model the distribution of error. Kyriakidis et al. (1999) advocated the use of geostatistics to incorporate high accuracy spot heights with DEMs. Holmes et al. (2000) tested the accuracy of a USGS Level 2 30-m DEM using field-collected GPS points. Kriging was used to generate multiple realizations of the error surface, and these were added back to the original DEM. Maloy and Dean (2001) utilized standard USGS 30-m DEMs and evaluated viewsheds derived from them over intermediate distances (less than 3 km). They were surprised at the low levels of viewshed accuracy, which averaged just 57%, and they theorized that DEM errors were partly responsible. Riggs and Dean (2007) found that DEM errors had a greater negative impact on the accuracy of viewsheds than DEM resolution or software program.

Surface Features

Surface features are one of the most often overlooked, or simply unaccounted for, causes of visibility misrepresentation (Llobera, 2007). The inclusion of features that extrude above the ground surface is necessary for large scale, local visibility analyses from the point of view of a person on the ground or slightly above ground level (Riggs and Dean, 2007). Surface features in urban environments are often man-made structures, such as elevated roads and bridges, buildings, and elevated signage (Kidner et al., 2000). In more natural settings, views are frequently blocked or hampered by coniferous and deciduous trees and other types of vegetation (Winterbottom and Long, 2006). Dean, in 1997, stated, “There is room for considerable improvements in the prediction of forest viewsheds.” The need for improvements was still

evident ten years later, according to Llobera (2007), who asserted, “The inability to incorporate vegetation remains one of the most important, if not the main, Achilles' heel surrounding GISc [geographic information science] approaches to visibility analysis.”

The presence of surface features, such as vegetation or buildings, has been dealt with in various ways. It is sometimes never mentioned (Fisher, 1991; Wang et al., 2000). Other times it is acknowledged but essentially ignored (Huss and Pumar, 1997). Some studies have side-stepped the issue by locating observers at the level of tree tops during viewshed computation when vegetation was thought to impact visibility (Germino et al., 2001). Studies that have assessed viewshed accuracy with field-based techniques have purposely been located in areas without significant vegetation (Maloy and Dean, 2001; Riggs and Dean, 2007). Only recently have various researchers used novel techniques to begin accounting for surface features (Dean, 1997; Llobera, 2007; Sander and Manson, 2007).

One of the many difficulties in modeling vegetative obstructions is the fact that, unlike buildings, vegetation does not create a solid, opaque wall, and defining vegetation boundaries is problematic (Kidner et al., 2000). It is a "fuzzy phenomenon" that does not always totally block visibility (Riggs and Dean, 2007). The screening effects of vegetation may be cumulative over distance, and visual permeability may be a function of understory and overstory species and density. Most algorithms assume all obstacles to be totally opaque, but this does not accurately represent reality (Dean, 1997).

Atmospheric and Other Fuzzy Conditions

Visibility may vary for other reasons. Atmospheric conditions can limit visibility due to clouds, fog, or haze (Ogburn, 2006). This is an example of perceptual uncertainty, which is a type of fuzziness (Fisher, 1994; Fisher, 1995). Pollution can severely decrease visible distances,

even in remote wilderness settings. Visibility in the Southern Appalachian Mountains has decreased by 80% in summer and 40% in winter from 1948 to 2006. Scenic views have been reduced in GRSM, where average annual visibility is 53 km (33 mi), whereas visibility would be 182 km (113 mi) in unpolluted conditions (NPS, 2006).

Traditional viewshed and LoS analyses yield a binary result for each spatial unit of the area in question (Nackaerts et al., 1999). But due to the numerous issues that bring uncertainty into the equation, a fuzzy or probabilistic visibility result is more appropriate than a binary one (Fisher, 1994; Fisher, 1995; Huss and Pumar, 1997; Ogburn, 2006; Llobera, 2007). Probable visibility is the likelihood of a location being visible. This probability can be due to the imprecision of measurements, such as the positional errors of the observer or target, or errors in the digital elevation data. Fuzzy visibility deals with the clarity of a location or object (i.e., whether it is distinguishable or not). This may be affected by atmospheric conditions or the distance, color, shape, or size of a target (Fisher, 1994).

CHAPTER 3: STUDY LOCATION

Overview of Great Smoky Mountains National Park

The GRSM, established in 1934, is the largest national park in the Eastern United States (Figure 3.1). Attracting 8-10 million visitors each year, GRSM is the nation's most visited national park. The park is known for many attributes, including over 1,280 km (800 mi) of trails, spectacular autumn colors, and rich plant and animal life (NPS, 2008).

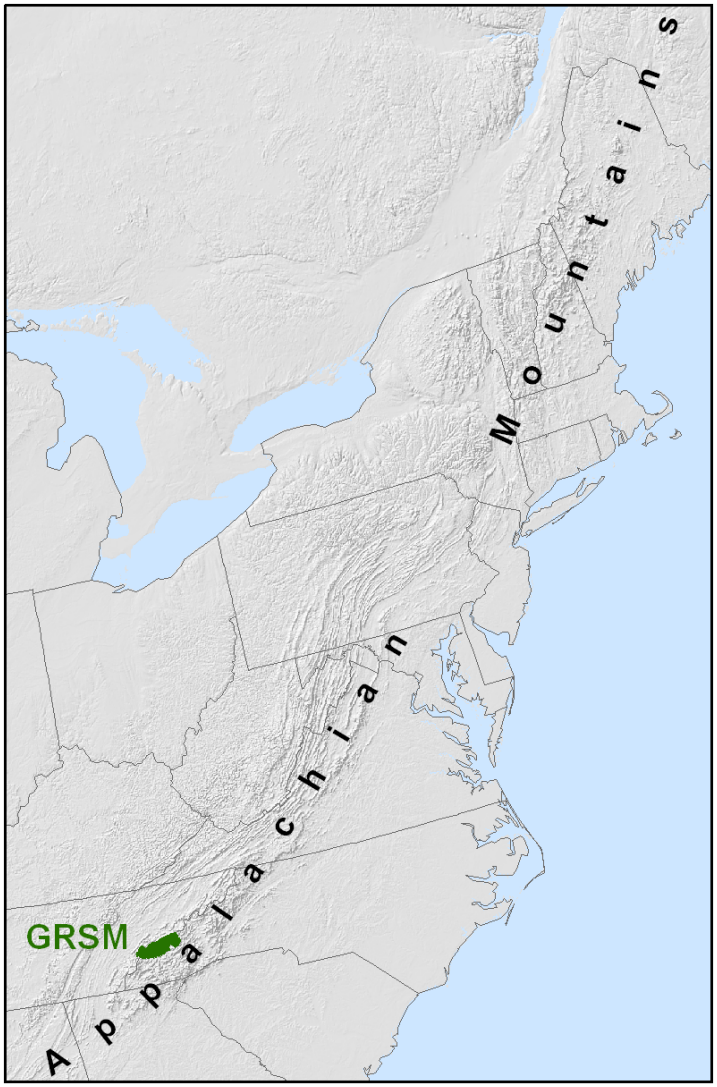

Figure 3.1: Location of GRSM in the Appalachian Mountain chain.

The GRSM is located in the Southern section of the Blue Ridge province of the Appalachian Highlands division, based on Nevin Fenneman's classic physiographic regions classification system (Fenneman, 1917). The GRSM spans over 2,000 km^2 (800 mi^2) along the Tennessee/North Carolina border. This area of the southern Appalachian Mountains is one of the oldest mountain ranges in the world, possibly 200-300 million years old (NPS, 2008).

The Smoky Mountains are some of the highest mountains in the vast Appalachian mountain chain. This wilderness of rugged terrain includes 16 peaks over 1,829 m (6,000 ft) in elevation. Elevations within GRSM range from a low of 266 m (873 ft) to the summit of Clingmans Dome at 2,025 m (6,643 ft), the third tallest peak in the Eastern United States. The high crest stretches for over 58 km (36 mi) above 1,524 m (5,000 ft) from the southwestern to the northeastern portions of the park. Local relief, the vertical rise from a mountain's base to its summit, is over 1,524 m (5,000 ft) in places. Mount Le Conte, 2,010 m high (6,593 ft), rises one vertical mile above its base, giving it the greatest local relief in the East (NPS, 2008).

The GRSM is one of the most biologically diverse temperate regions in the world. High relief combined with high humidity and abundant rainfall support an incredible array of plant life, including 1,300 native plant species (Nichols and Langdon, 2007). With 95% of the park being forested, habitat is abundant for the park’s 200 species of birds, 66 types of mammals, and 43 species of amphibians (NPS, 2008). Due to the park's wide range of habitats and ecosystems, it was designated by the United Nations as an International Biosphere Reserve in 1976 and a World Heritage Site in 1983 (Jenkins, 2007).

Trail Selection

The study area is primarily the North Carolina side of GRSM (Figure 3.2). The decision was made to restrict field work to the North Carolina side of the park due to the wealth of data

freely available from the North Carolina Floodplain Mapping Program (www.ncfloodmaps.com), including lidar-derived DEMs and lidar point data. Field work was conducted along existing hiking trails, representing two distinct areas of the park. The first area is the Appalachian Trail (A.T.) from Fontana Dam to Doe Knob in the western portion of the park. The second area follows the Cataloochee Divide in the eastern portion of the park along two trails, the Cataloochee Divide Trail and the Hemphill Bald Trail. These trails are really sections of the same physical path, and this area will be referred to as the Cataloochee Divide/Hemphill Bald Trail in this study.

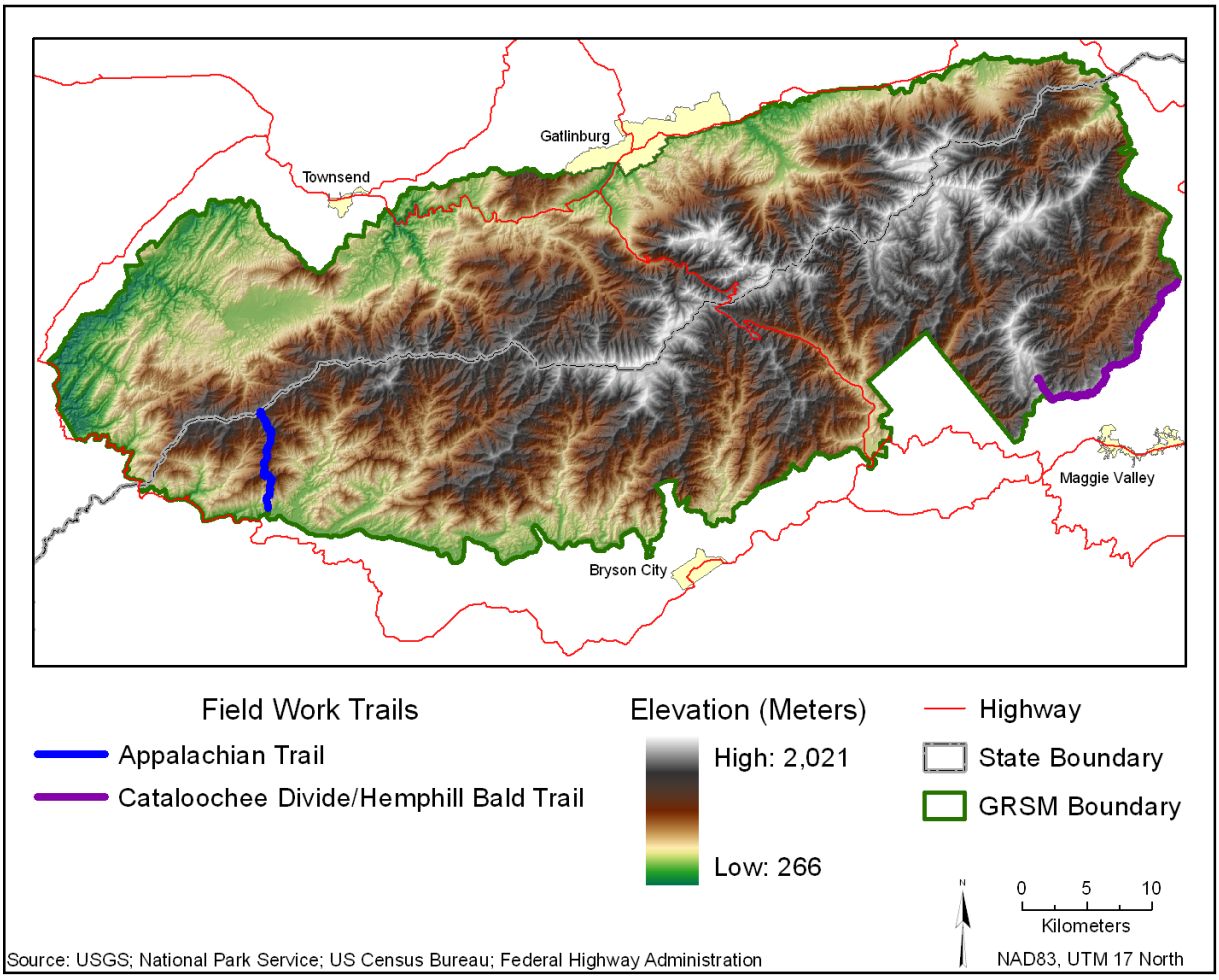

Figure 3.2: Study area, including field work trails, within GRSM.

In the choice of trails, accessibility was a consideration, so trailhead parking was important, as were suitable field sites that were not too distant, since data collection took about 1-1.5 hours at each site, limiting the distance that could be traveled on a given day. Another factor was the vegetation and potential views. Desired trails were those that included heavily forested areas and areas that were more open, such as a bald, rocky outcrop, or fire tower. The possibility for long distance views was important. Given the stated criteria, the A.T. from Fontana Dam to Doe Knob and the Cataloochee Divide/Hemphill Bald Trail were good choices.

A.T. from Fontana Dam to Doe Knob

The Fontana Dam to Doe Knob section of the A.T. begins from a trailhead (573 m, or 1,880 ft) about ¾ km northwest of Fontana Dam, which, at 146 m (480 ft) tall, is the highest dam east of the Rocky Mountains. Completed in 1944, it created Fontana Lake by damming the Little Tennessee River. This heavily forested trail trends in a south-to-north direction for about 10.0 km (6.2 mi) in length. The first section climbs steeply to the peak of Shuckstack, gaining over 610 vertical m (2,000 ft) in less than 4.8 km (3 mi). A short side trail leads to the summit of Shuckstack (1,225 m, or 4,020 ft), which has an 18.3 m (60 ft) fire tower that offers tremendous views from above the tree tops. Beyond Shuckstack the trail's grade is more gentle and climbs gradually towards forested Doe Knob (1,313 m, or 4,308 ft), where the A.T. continues northeast to begin its long traverse of the Smokies' crest.

Cataloochee Divide/Hemphill Bald Trail

The Cataloochee Divide/Hemphill Bald Trail follows the park boundary along Cataloochee Divide in a southwest-to-northeast direction. Field sites are located along a 13.7 km (8.5 mi) stretch of this trail, from Little Bald Knob at 1,676 m (5,500 ft) to the trailhead at Cove Creek Gap at 1,241 m (4,072 ft). Along this stretch, the trail remains at a generally high

elevation, ranging from a low of 1,241 m (4,072 ft) to a high of 1,695 m (5,562 ft) at Hemphill Bald. The trail is often along the narrow, forested ridge top of Cataloochee Divide. There are a few breaks in the trees that allow nice views of distant ridges. Hemphill Bald is split between private ownership and GRSM land. An area open to the public on the private side, just across the park boundary, offers sweeping, long range views to the south and east.

Site Selection

Although some field sites were known in advance, most sites were chosen in the field. Selections were based on terrain, visibility, distance from previous sites, and variety. Terrain types include summits, ridge tops, flat areas, and sloping hillsides. Several locations with open views were chosen. Sites were spaced to provide a good balance along each trail and avoid clustering. Sites were also chosen to provide variety. This included vegetation type and density, quality of views, slope, and other intangibles. Although no random or uniform sampling took place, the 15 locations chosen should be considered representative of the types of areas one would encounter on these trails (Figure 3.3). A description of each field site is listed in Table 3.1, and pictures of the sites are illustrated in Figure 3.4.

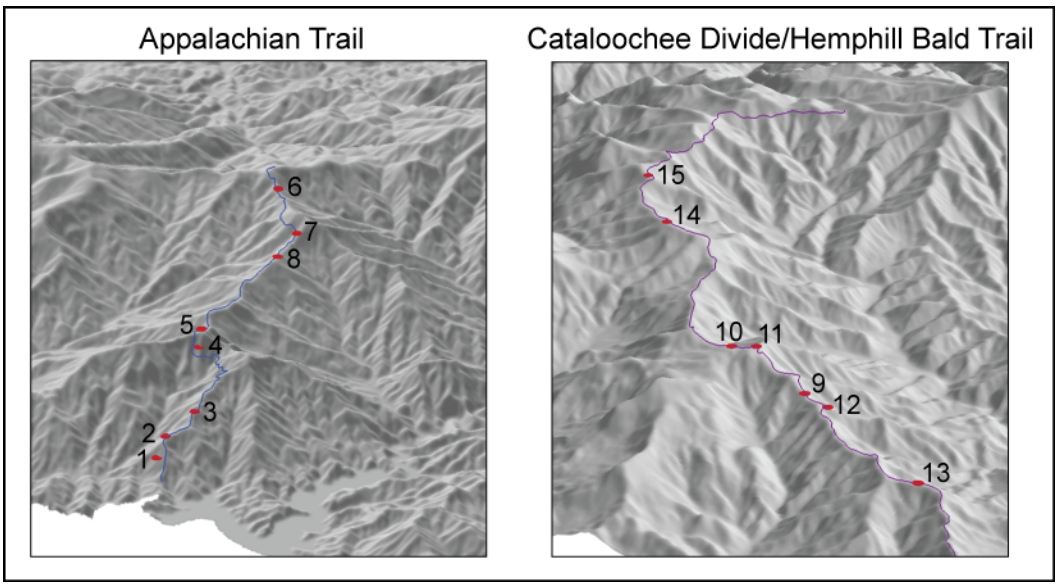

Figure 3.3: Field sites 1-8 along the A.T., and field sites 9-15 along the Cataloochee Divide/Hemphill Bald Trail.

Table 3.1: Field sites. *A.T. = Appalachian Trail; C.D./H.B. = Cataloochee Divide/Hemphill Bald.

Site	Site Name	Trail*	Elevation (m)	Terrain
1	Shuckstack Ridge 1	A.T.	692	Moderately steep hillside
2	Shuckstack Ridge 2	A.T.	821	Ridge crest
3	Shuckstack Ridge 3	A.T.	909	Ridge crest
4	Rocky Ledge	A.T.	1,098	Steep ledge with views, ~100’ in length
5	Shuckstack Summit	A.T.	1,225	Small, rocky summit with 60’ fire tower
6	Doe Knob	A.T.	1,313	Ridge crest
7	Greer Knob	A.T.	1,255	Steep hillside
8	Peak 4071	A.T.	1,232	Flat, broad ridge crest
9	Taylor's Turnaround	C.D./H.B.	1,379	Flat, broad ridge crest
10	Vegetation Tunnel	C.D./H.B.	1,510	Sloping terrain with dense, 12’ high vegetation
11	Trail Bend 1	C.D./H.B.	1,528	Flat top of small ridge
12	Trail Bend 2	C.D./H.B.	1,370	Flat top of small ridge
13	Cut Out View	C.D./H.B.	1,380	Narrow ridge crest with 11’ wide view without trees
14	Hemphill Bald	C.D./H.B.	1,695	Summit of bald, half covered in trees and half with unobstructed views
15	Little Bald Knob	C.D./H.B.	1,676	Wide ridge crest with views where trees have been cleared

Site 1

Site 2

Site 3

Site 4

Site 4 Panorama

Site 5 Ground

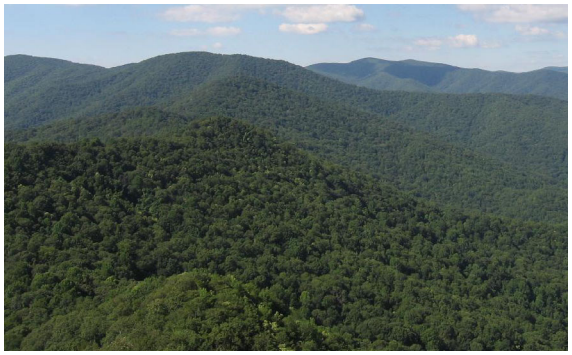

Site 5 Tower

Site 5 Tower Panorama

Site 6

Site 7

Site 8

Site 9

Site 10

Site 11

Site 12

Site 13

Site 14A

Site 14B

Site 14C

Site 14D

Site 14A Panorama

Site 15

Figure 3.4: Pictures of field sites.

CHAPTER 4: DATA AND METHODOLOGY

Elevation Data

Digital elevation data are increasingly available for the U.S. at high resolutions. An invaluable source of DEMs is the USGS NED. This is a dataset of raster DEMs served over the World Wide Web (seamless.usgs.gov) that provides seamless coverage across the U.S. at medium and, for some areas, high resolution (Gesch et al., 2002). The backbone of this multi-resolution dataset is 1 arc-second (~30 m) data, but the 1/3 arc-second NED (~10 m) is now available for the whole contiguous U.S. Currently, only a few areas of the U.S. have 1/9 arc-second (~3 m) data available from the NED (USGS, 2008). These high resolution data are available for western North Carolina, due to the lidar flown for North Carolina's Floodplain Mapping Program. Another good source of data is the North Carolina Department of Transportation (NCDOT), which makes lidar-derived DEMs available by county at 20-ft (~6 m) resolution (www.ncdot.org/it/gis).

Due to the NED being stored in the geographic reference system of latitude/longitude, the raster resolution, or post spacing, is not uniform for all areas of the country. Measures of latitude and longitude, such as degrees, vary in length, due to the shape of the earth. This is most evident with measures of longitude, which converge to a point at the poles (Longley et al., 2005). In western North Carolina, the 1 arc-second DEMs are approximately 28.5 m in resolution, the 1/3 arc-second DEMs are approximately 9.5 m, and the 1/9 arc-second DEMs are approximately 3.2 m in resolution. For the sake of convention, these DEMs will often be referred to as 30 m, 10 m, and 3 m, respectively. The NCDOT 20-ft DEMs, referred to as 6 m, are about 6.1 m in spacing.

Figure 4.1 is a comparative illustration of the grid sizes of these datasets. Figure 4.2 uses shaded relief to illustrate the loss of detail that occurs as resolution becomes coarser.

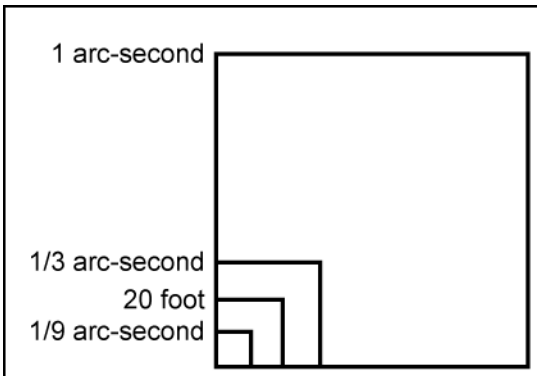

Name	Resolution (m)	Coverage Area (m^2)	Area Compared to 3.2 m
1 arc-second	28.5	812.25	79.32
1/3 arc-second	9.5	90.25	8.81
20 foot	6.1	37.21	3.63
1/9 arc-second	3.2	10.24	1.00

Figure 4.1: Comparison of DEM resolutions.

The NED Release Notes of December 2008 and the NED Spatial Metadata (ned.usgs.gov/ned/downloads.asp) indicate that the source of 1 and 1/3 arc-second NED products for North Carolina is the lidar-derived, 1/9 arc-second data. If all NED data is derived from the 3-m data, then this should be verifiable by resampling these data to coarser resolutions, since the NED Data Dictionary of February 2006 states that source data are resampled to produce the various NED products. The resampling method will matter (Lillesand et al., 2008). Cubic convolution is the method recommended to users by the USGS, as this is the method reportedly used in the production of the NED (USGS, 2007; Gesch et al., 2002). However, another USGS source states that bilinear interpolation is used to resample data, fill in missing data, and correct mismatches along seams (USGS, 2006).

The 1/9 arc-second data for Graham and Swain counties were resampled with ArcGIS, using both cubic convolution and bilinear interpolation, to match the resolution of the 1 arc-second NED. These datasets were horizontally registered to the 1 arc-second NED and compared

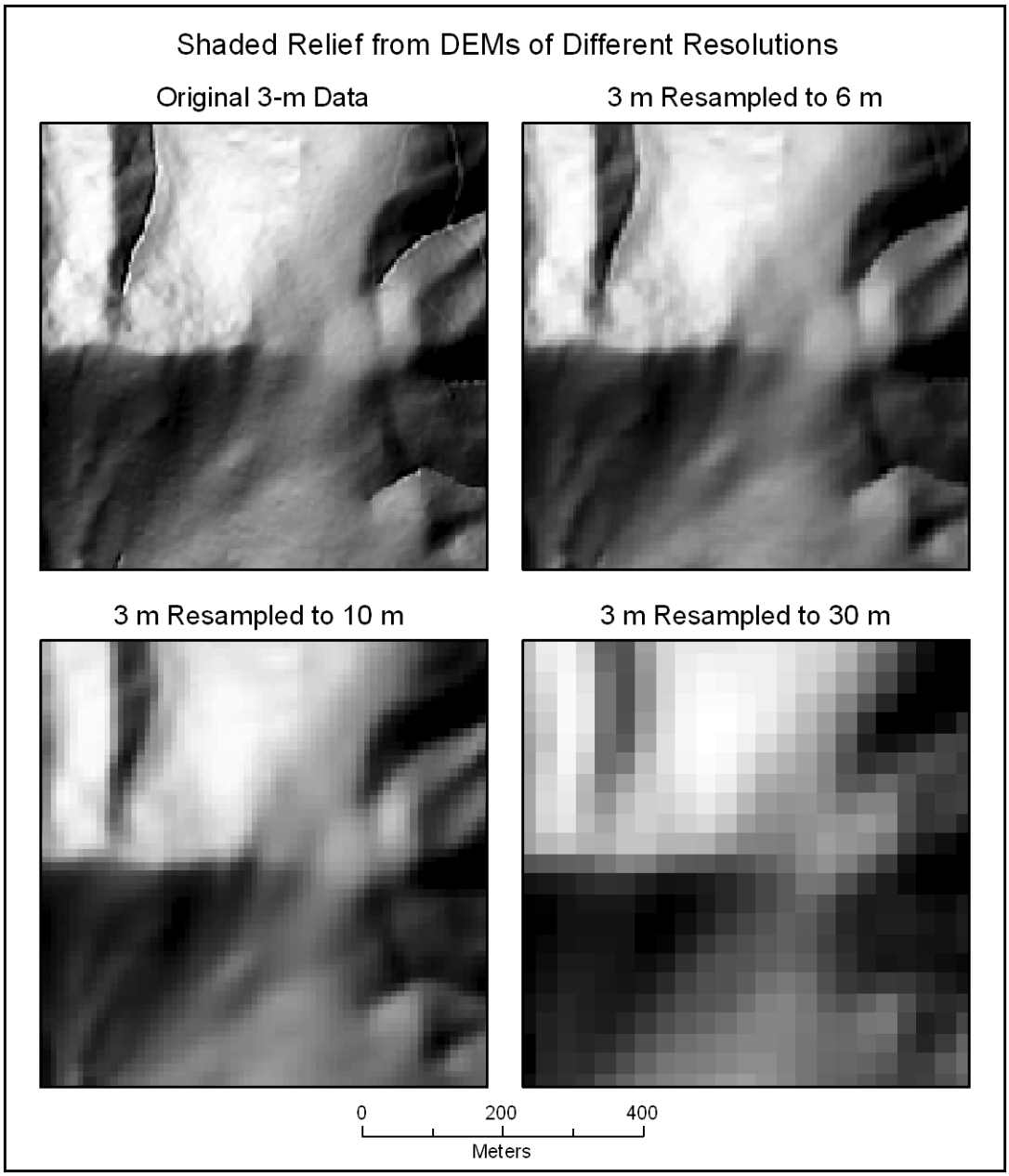

Figure 4.2: Levels of detail available with various resolutions of DEMs.

by subtracting the original DEM from the resampled DEM, e.g., [3-m DEM resampled to 30 m] – [1 arc-second NED]. The data resampled with bilinear interpolation more closely matched the 1 arc-second NED than data resampled with cubic convolution. However, differences between the resampled and 1 arc-second datasets were larger than expected (SD = 6.4 m), and spatial

autocorrelation was clearly present. A strong relationship, which was significant ($p < .001$), between aspect and the sign (positive/negative) of elevation differences also occurred throughout the data. If the 1 arc-second data was derived from a non-lidar source, such as photogrammetry, then that may explain this terrain correlation. Regardless, it seems likely that the 1/9 and 1 arc-second NED have different origins.

Due to this finding, the data source used for most studies was the 1/9 arc-second NED, which has 3-m spatial resolution (Table 4.1). Various resolutions of DEMs were utilized in numerous tests, as a type of sensitivity analysis. These coarser resolution DEMs were resampled from the 3-m data in ArcGIS with bilinear interpolation. Resolutions generated were 6 m, 10 m, and 30 m, to match the resolutions of the previously discussed datasets that are also available to users. Datasets were projected to UTM Zone 17 North, NAD83. Following the examples of Lee (1991) and Maloy and Dean (2001), TINs were generated from the various resolutions of raster DEMs in ArcGIS with a z-tolerance of 0, which is the maximum accuracy that ArcGIS can create a TIN from a raster. The TINs were utilized in several tests.

Table 4.1: Elevation data for western North Carolina.

Name/type	Spatial resolution	Accuracy	Method of acquisition	Source projection/ datums	Source
1/9 arc-second DEM/raster	3 m; resampled to 6, 10, and 30 m	+/- 7-15 m vertical RMSE, published by USGS; 3-m data is likely better	Lidar	Geographic/ NAD83 and NAVD88	USGS NED/*The National Map* Seamless Server
Bare-earth lidar/mass points	Variable density (~3+ m)	+/- 0.25 m vertical RMSE	Lidar	North Carolina State Plane/ NAD83 and NAVD88	North Carolina Floodplain Mapping Program
TIN/ vector	Variable; derived from lidar and 3-, 6-, 10-, and 30-m DEMs	Variable, depending on source and interpolation	Generated from lidar point data or rasters	Inherited from source	North Carolina Floodplain Mapping Program or USGS NED

The North Carolina 3-m data does not extend all the way to the Tennessee border, and this is the cause of the stair-step appearance of some DEMs. This is probably advantageous, because edge-matching problems were discovered in the 1/3 and 1 arc-second NED along the North Carolina/Tennessee border. These issues will not affect the data used in this thesis.

The other elevation data used in this study is bare-earth lidar data obtained from the North Carolina Floodplain Mapping Program (www.ncfloodmaps.com). The multiple lidar returns were processed and filtered so that these data are believed to have reflected from the ground. Surface interpolation tests in Chapter 6 used lidar data from Haywood County, which had been previously projected to the North Carolina State Plane coordinate system, NAD83.

Vegetation Data

Vegetation data, which were used in the study on positional errors (Chapter 7), are listed in Table 4.2. The primary source of data is the digital vegetation maps created by the Center for Remote Sensing and Mapping Science (CRMS) at The University of Georgia. The CRMS created detailed overstory and understory maps of GRSM from aerial photographs acquired in 1997 and 1998 (Welch et al., 2002). Chapter 7's study utilized maps of canopy closure that were created during this project, which was completed in 2004 (Madden et al., 2004). The other source is the National Land Cover Database 2001 (NLCD 2001), created by the federal Multi-Resolution Land Characteristics (MRLC) Consortium. It consists of tree canopy percentages and land cover at 30-m resolution from Landsats 5 and 7, with 2001 being the nominal year of data acquisition (Homer et al., 2004).

Table 4.2: Vegetation data for western North Carolina.

Name	Data type	Spatial resolution	Description	Method of acquisition	Source/Date
CRMS canopy closure	Polygons	0.5 ha minimum mapping unit	Percent of canopy closure (leaf-on)	Derived from overstory classes from 1:12,000 CIR aerial photographs	U.S. Forest Service/ October 1997-1998 (leaf-on)
NLCD 2001 Tree Canopy	Raster	30 m (1 acre minimum mapping unit)	Percent of canopy closure (leaf-on)	Landsat 5 TM, Landsat 7 ETM+, 1-m DOQQ	MRLC Consortium/2001 nominal year

Field Methods

The purpose of the field work was to observe and photographically record visibility on the ground within the study area. Field data was collected in GRSM during leaf-on conditions, July 14-17, 2008. Along the two selected trails of the study area, a hand-held digital camera, tripod, Garmin GPS V receiver, magnetic compass, a “flag” or target, notebook, small-scale topographic map (1:62,500), CRMS vegetation maps, watch, vegetation field guide, tape measure, level, and voice recorder were carried.

At each field site the tripod and camera were set up on the trail or just off the trail. The GPS unit was placed on the ground right next to the tripod, and once the unit was receiving numerous, strong signals, waypoints were saved. At each site 4 waypoints from each spot were saved, where each waypoint was an average of 30 readings. Since the GPS V unit receives, decodes, and calculates its position once every second, a 30-second average is an average of 30 readings, and the unit’s display indicates the number of readings (Wing and Eklund, 2007). Multiple GPS readings are recommended under forest canopies, due to the effects of multipath reflection (Scherzinger et al., 2001). Averaging 20-60 readings will improve precision, as the effects of extreme readings will be reduced (Oderwald and Boucher, 2003). Wing et al. (2005)

found that obtaining an average of numerous positional readings will give a more reliable estimate of the true location. Also noted were the approximate number of satellite signals received during the 30-second interval and the estimated positional error, or accuracy, of each waypoint, as displayed by the GPS V.

At each site the tripod was set to its maximum height (1.5 m), the camera was leveled on the tripod, and 360° panoramic photos were taken. Using a magnetic compass, the first photo of each series was taken facing north, with subsequent overlapping photos taken at increments in a clockwise fashion (0° to 90°… to 360°), until a full panorama had been taken. Other data collected at each site included time, weather, and a description of the terrain and vegetation.

As a source of control for assessing the accuracy of GPS coordinates, information was gathered in advance about the two National Geodetic Survey (NGS) markers that would be accessible during field work. These ground control points (GCPs), which were located near Sites 5 and 14, were found in the field, and GPS coordinates were recorded there.

Other steps were taken to collect data about vegetation density, such as shooting vertical photos and determining the visibility of a flag, suspended from branches, from various distances and directions. This was for another aspect of the study, incorporating vegetation into visibility analyses. Time did not permit this issue to be included in the study, so information about these field methods and data will not be presented.

Lab Methods

Detailed methods used in the various investigations can be found in the Data and Methodology section of each manuscript chapter. Generally, the purpose of lab work was to assess the sources of uncertainty that affect visibility analyses and evaluate their impacts. Data manipulation and GIS analyses were performed with ArcGIS. The Hawth's Analysis Tools

extension (www.spatialecology.com) proved to be very useful and was used frequently. ERDAS Imagine was used in Chapter 5 for the software comparison of viewsheds. Microsoft Excel was used often for tabulating data and generating descriptive statistics. Stata was utilized occasionally for statistical tests.

CHAPTER 5

AN ASSESSMENT OF VISIBILITY ALGORITHMS: COMPARING ESRI VIEWSHED WITH ERDAS VIEWSHED AND ESRI LINE OF SIGHT

Lockhart, D. To be submitted to *Landscape Analysis using Geospatial Tools: Community to the Globe* (M. Madden and E. Allen, editors), Springer-Verlag.

Introduction

Many GIS and image processing software packages are equipped with functions that perform visibility analyses based on elevation data, enabling the visibility of surface or near-surface features to be determined from an observer's location. Two points are intervisible if there is an unobstructed view between them, which is based on the terrain surface and the geometry between an observer and target (TEC, 2004). This is the line of sight (LoS) concept, and it answers the question as to whether a target will be visible from an observation point. A viewshed is the LoS approach applied in many directions, and it determines the entire area that will be visible from an observation point. Viewshed indicates what the vista will be like from a location (Goodchild and Lee, 1989).

There are numerous applications for visibility analysis, including visual impact assessment of new construction and development, communications tower siting, identifying scenic viewpoints, defense planning, and many others. Analyses can be performed in a host of different GIS programs, and as with any computer program, the results of analyses are determined by the coded procedures, or algorithms. Algorithms developed by different companies or individuals can generate different results even if they are designed to compute the same phenomenon (Fisher, 1993). It has been noted that visibility algorithm information is not widely published by software vendors, so users are unable to adequately understand the calculation processes or know how to improve the results (Fisher, 1993; Riggs and Dean, 2007).

Many people are undoubtedly utilizing viewshed and other visibility functions within various GIS programs. Papers have been published on the uncertainty of viewshed results, validating GIS results with field work, and creating faster algorithms (Fisher, 1991; Maloy and Dean, 2001; Izraelevitz, 2003). However, it seems that a relatively small percentage of people

who use visibility functions are questioning the results or trying to fully understand the algorithms. As an anecdote, when one reads ESRI support pages (support.esri.com), many discussions can be found on how to write scripts and work with viewshed results, but few individuals, if any, are asking questions about the validity of the algorithms and outputs. This is a concern. Even some researchers make the assumption that a commercially implemented viewshed algorithm will not affect visibility results (Yu et al., 2007). However, the field testing of commonly used commercial GIS programs by Riggs and Dean (2007) demonstrated that this is a faulty assumption, because the choice of software program does affect visibility results.

There are numerous obstacles to field checking GIS-generated visibility results. These include cost, time, inclement weather, and travel logistics, to name a few. Comparing results between software packages and/or algorithms will not assess the accuracy of any one function, but can provide a measure of agreement and inform users as to the variability between various functions, and one may logically assume that since time and money have gone into research and development of the computer procedures, more confidence should be placed in results that tend to agree (Champion, 2003). There are two routines for determining visibility in ESRI ArcGIS, the raster viewshed and the vector LoS functions (ESRI, 2002) (Figure 5.1). A viewshed algorithm is also implemented in ERDAS Imagine (Leica Geosystems, 2007).

The basic concept involved in calculating visibility is fairly simple, but its implementation is a complex function and is different across GIS platforms (Fisher, 1993; Dean, 1997). Two locations are intervisible, or visible to each other, if a straight LoS between them does not intersect the terrain at any point (Maloy and Dean, 2001). A straight LoS can be conceptualized as a ray or laser. In a computer environment, a ray between an observer and target is evaluated as it passes over the digital elevation surface. If the ray encounters

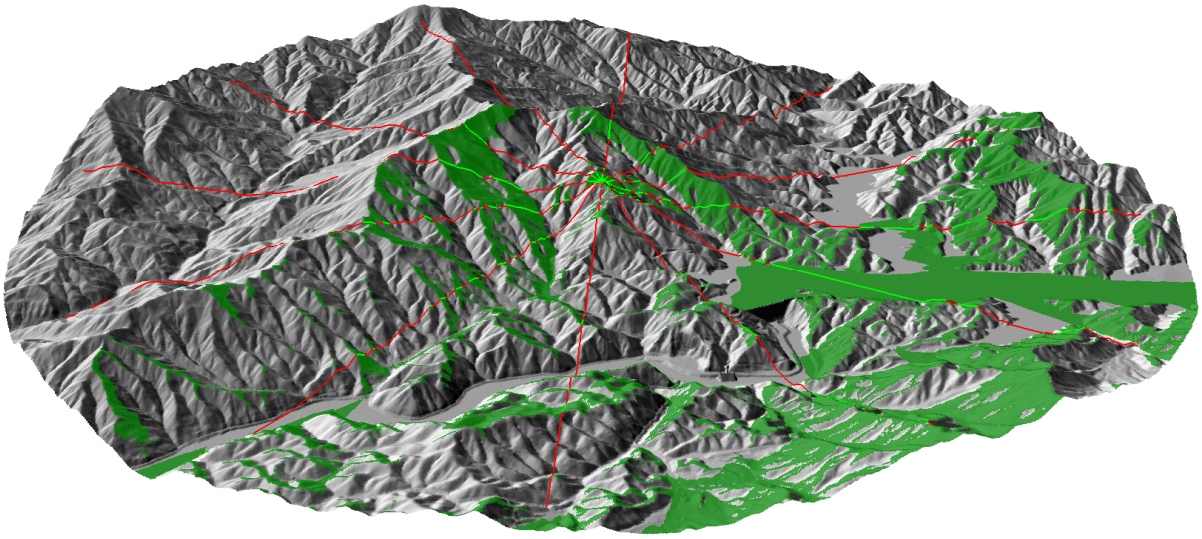

Figure 5.1: Raster viewshed and vector LoSs generated with ArcGIS in 3D perspective view. Green areas are visible and red areas are not visible.

interference from the surface before the target is reached, then the target is not visible, i.e., the target is masked (Lee and Stucky, 1998; Rana, 2003). A viewshed is an extension of the LoS concept and can be thought of as a collection of individual LoSs. Instead of only considering the visibility of a specific target or along a specific line, a viewshed considers the total area that is visible to an observer (Goodchild and Lee, 1989).

Inconsistencies in visibility results can occur when different software is used to perform the same task with the same data. Riggs and Dean (2007) reported that viewshed agreement ranged from 89% to 93% among ArcGIS, Imagine, and Idrisi. Due to this predicament, Fisher (1993) argued three main points. First, that there should be standards or benchmark datasets used to test GIS functions. This is because multiple algorithms exist for performing the same task, but differences in assumptions, coding, and implementation can lead to different results, and this reduces the confidence of users. Second, algorithms should be published, because users have a right to know how viewshed results are obtained. Third, viewsheds are fundamentally uncertain

and are not repeatable across various computer systems. Therefore, binary results (visible or not visible) are limiting and even unacceptable.

Examination of Visibility Algorithms

There are numerous, key questions with regard to how an algorithm determines visibility. The first question concerns gridded DEMs and how they are interpreted, whether as a continuous surface or as discrete cells. Another important question is the method by which an elevation surface is sampled along a line, whether one is computing a single LoS or a viewshed. A third key question is how a target location is deemed visible or not. In the case of a standard viewshed, in which results are generated in a raster format, what part(s) of the cell are evaluated? In other words, if a raster cell is determined to be visible, what exactly does that mean? Understanding these issues is crucial if visibility results are to be properly comprehended and explained.

Interpretation of Gridded DEMs

Information from the US Army Topographic Engineering Center (TEC) (2004) indicates that some algorithms treat gridded DEMs as a continuous surface, while others treat them as a collection of discrete cells. In a discrete interpretation, the whole area of each cell has a single value, like a digital image pixel, and can be conceptualized as a plateau. If treated as a continuous surface, each DEM cell value is interpreted as being the value at the cell centroid, and values in other areas of the cell are determined by interpolation from the values of the 4 nearest cells (Maune et al., 2001; Fisher, 1993). These two interpretations were described by Kidner et al. (1999) and are illustrated in Figure 5.2.

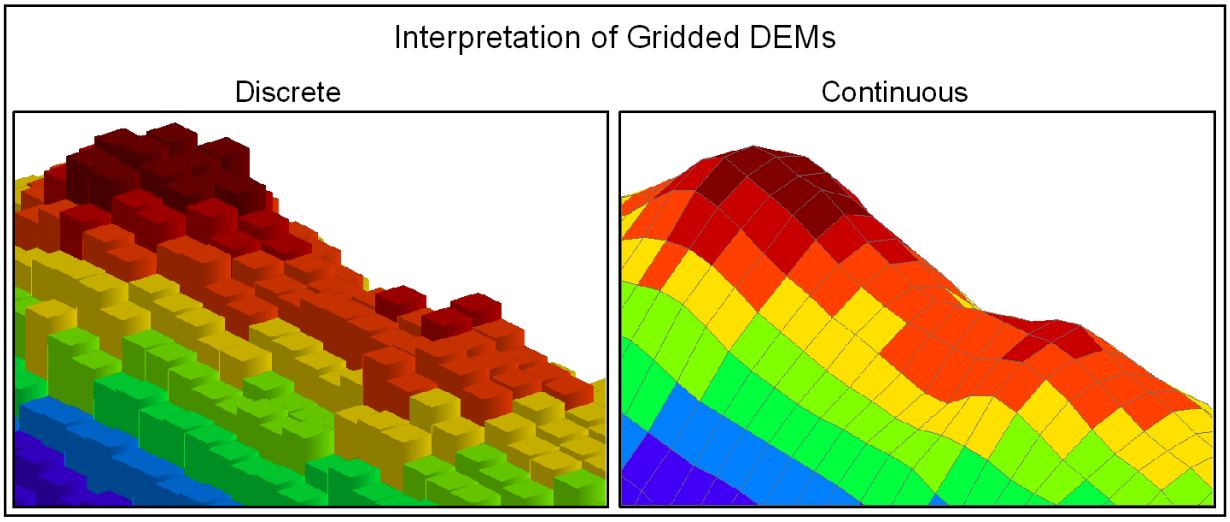

Figure 5.2: Discrete and continuous surface interpretations of a DEM grid. Adapted from Kidner et al. (1999).

Elevation Sampling

There are numerous methods in which the elevation surface can be sampled along a line. These methods involve questions of "where" and "how." "Where" is related to the discrete/continuous interpretation of a DEM grid (or even a TIN) and, more specifically, the locations of grid/LoS crossings, and "how" refers to the method of obtaining a z-value from the surface, which may involve interpolation.

One of the fundamental papers on these issues is by Yoeli (1985), who created a program named HIDE to generate intervisibility maps. In Yoeli's algorithm, elevation is sampled at intersection points, locations where a LoS crosses the DEM grid. This method is easily understood and computationally straightforward. An important aspect of this method is that distances between sampled points often vary. This is illustrated in Figure 5.3, in which the distance between points 5 and 6 is much less than the distance between points 6 and 7. The magnitude of this situation is reduced with finer resolution DEMs, but it could present problems with coarse data. At a minimum, users should be aware of this characteristic. The issue of "how"

elevation values are determined, as implemented by Yoeli, is that the z-values of intersection points are linearly interpolated between grid cell postings. For example, in Figure 5.3, the elevation of point 3 is interpolated based on grid posts A and B.

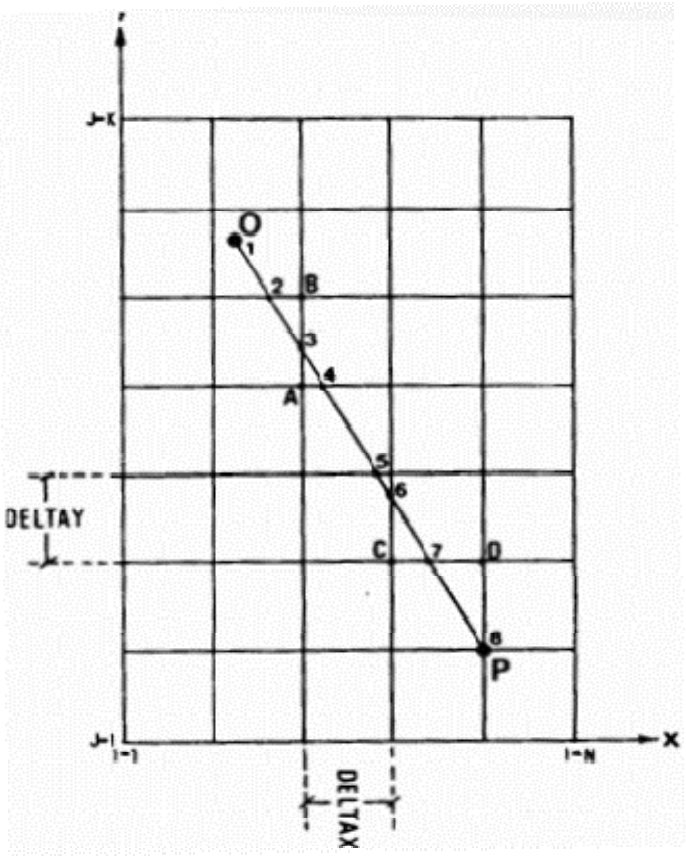

Figure 5.3: Elevation sampling along a line of sight. From Yoeli (1985).

Fisher (1993) generically describes a viewshed algorithm for a gridded DEM in two steps. The first step is detecting the planimetric location where a LoS intersects the DEM grid. Then, at this location, the DEM elevation is compared to the LoS elevation. If the DEM elevation is higher than the LoS elevation before the target location is reached, then the target is deemed not visible. Fisher describes four algorithms that treat the “where” and “how” questions differently. He refers to these as linear interpolation between grid neighbors (Yoeli, 1985), triangulation of the grid, grid constraint of the mesh, and the stepped model. The first three

methods conceptualize and treat the DEM as a continuous surface, with elevation values interpolated by various means. The fourth method, the stepped model, treats all points within a grid cell as having the same elevation, thus giving an appearance of steps between cells. This is the discrete interpretation used by some visibility functions. The four algorithms tested by Fisher (1993) yielded "striking" results because the viewsheds had a good deal of variability, with the stepped model varying greatly from the others.

Guth (2004) gave descriptive names to four algorithms discussed by Champion et al. (1995), regarding the locations of grid/LoS crossings. The names given are Nearest Posting, Grid Triangle Sides, Radial Interpolation, and Grid Square Sides, the last being Yoeli's algorithm (1985). Huss and Pumar (1997) state that a common sampling method is to determine elevations at a fixed interval along a LoS.

The "how" question, the method of obtaining a z-value from the surface, is no less complicated. If the grid is treated as a continuous surface, then the sampled z-value will depend on the interpolation scheme used. No less than ten point interpolation methods were reviewed by Kidner et al. (1999), including bilinear interpolation, bicubic interpolation, and others. Theoretically, any of these methods could be coded into a visibility algorithm.

Determining Target Visibility

In a viewshed result, what does it mean if a raster cell is deemed visible? The criteria with which a software program determines the visibility of a location is a key component to an algorithm. Fisher (1993) argued that it was only logical for viewshed targets to be cell centroids, but he acknowledged that other interpretations existed. He explained that viewsheds could be represented and computed in four ways: point-to-point, point-to-cell, cell-to-point, and cell-to-cell (Figure 5.4). The point-to-point method involves a single LoS, point-to-cell and cell-to-point

involve up to 4 LoSs, and cell-to-cell could involve as many as 16 LoS calculations before a single cell was deemed not visible.

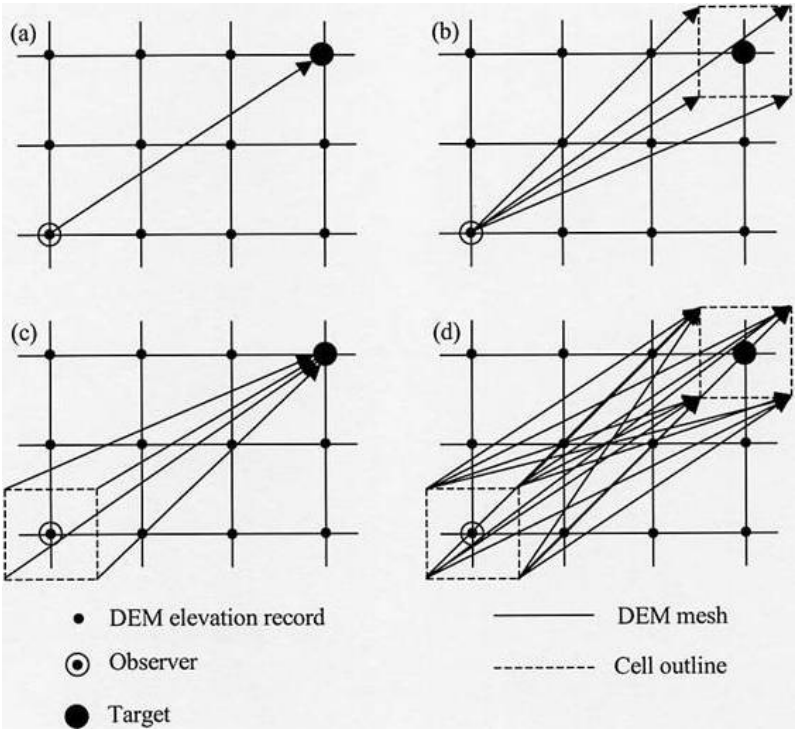

Figure 5.4: Methods of approximating observer and target locations: a) point-to-point, b) point-to-cell, c) cell-to-point, and d) cell-to-cell. From Fisher (1993).

Variations of Fisher's (1993) methods could be programmed, such as the requirement that 2, 3, or all 4 cell corners be visible in the point-to-cell method, or a target be visible from 2, 3, or all 4 cell corners in the cell-to-point method, in order for intervisibility to be determined. The point-to-point method is clearly the most computationally efficient, and this is the method employed in the ArcGIS viewshed algorithm. In this function, cell visibility is determined only by the visibility of raster cell centroids (ESRI, 2007b).

When the elevation surface is a TIN, there is no standard method for determining regions of visibility. In studies by Maloy and Dean (2001) and Riggs and Dean (2007), the same algorithm was used, and the outputs were the TIN polygons. In these studies, TIN visibility could

be evaluated with any of four different criteria. A polygon could be considered visible if the center of a TIN facet was visible, or if 1 of 3 nodes, 2 of 3 nodes, or all 3 nodes of each triangle were visible.

With the ArcGIS vector LoS function, the question concerning the analysis of the target location is straightforward, so long as the target is clearly defined. Since the target is a point, this is analogous to determining the visibility of a cell centroid. In both cases, they are 0-dimensional points.

Description of ESRI and ERDAS Algorithms

ESRI and ERDAS documentation contains limited information regarding specifics on how visibility is calculated in the respective software programs, but the ArcGIS Desktop Help provides much more useful information than the Imagine help files. Some of the most helpful information comes from TEC (2004), which gathered details on numerous software packages that perform visibility analyses.

Although the ESRI algorithms are proprietary, TEC's overview of the viewshed algorithm is that it "uses an expanding local horizon analysis of slope angles to determine visible and invisible terrain." This agrees with the ArcGIS help files, which explain the viewshed function this way: "The visibility of each cell center is determined by comparing the altitude angle to the cell center with the altitude angle to the local horizon. The local horizon is computed by considering the intervening terrain between the point of observation and the current cell center. If the point lies above the local horizon, it is considered visible" (ESRI, 2007b). The concept of horizons is explained by De Floriani and Magillo (2003). A local horizon is a location that is visible to an observer but which blocks the view of locations beyond. A hill is an example. Using the figure from De Floriani and Magillo (2003) (Figure 5.5) to illustrate the preceding

definition, point p_1 represents a local horizon. From the observer v, point q_2 lies above the local horizon and is considered visible, but point q_1 lies below the local horizon and is not visible.

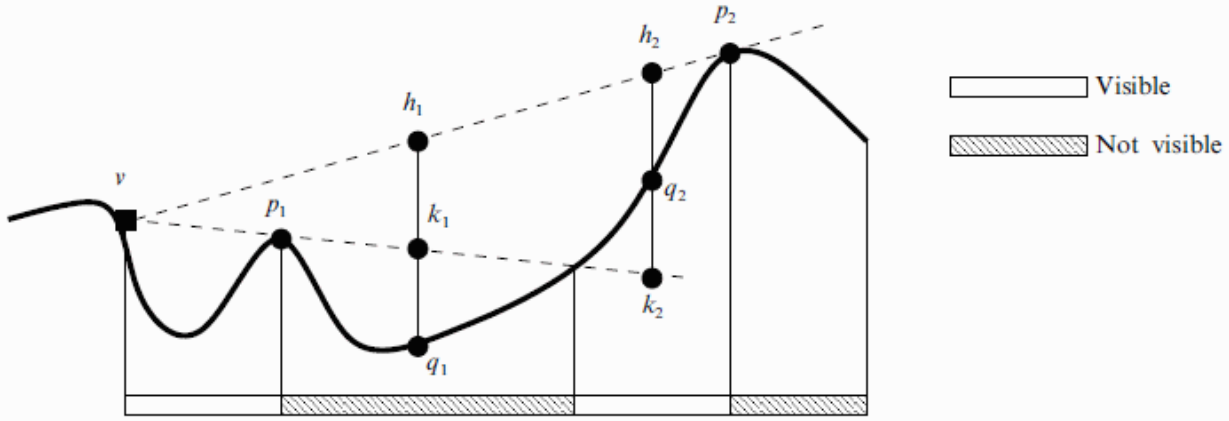

Figure 5.5: Local horizons on an elevation profile. From De Floriani and Magillo (2003).

TEC (2004) states that ArcGIS uses a different algorithm for computing viewshed and vector LoS. ArcGIS help files do not provide specifics on the vector LoS algorithm, but TEC (2004) reports that it "uses a slope angle comparison of a full profile to determine visible and invisible terrain between two point locations." The two ESRI functions appear to be performing the same task. Perhaps different algorithms are used simply because of the different inputs (lines versus points) and outputs (lines versus raster), but calculations are essentially the same.

The LoS algorithm in ArcGIS has vector line inputs and outputs. This allows a more detailed exploration of visibility, as one can create as many LoSs across a raster cell as one wishes. Viewsheds are raster data. A summary of inputs and outputs of the two algorithms is in Table 5.1. In a crude way, LoSs can be somewhat approximated in Imagine by displaying visibility as "spokes" radiating outwards from the observer, but these spokes are still raster cells. They are not true lines but only subsets of the viewshed and are limited by the DEM resolution.

Table 5.1: Inputs and outputs of the viewshed and LoS functions in ArcGIS.

Viewshed	LoS
Inputs	
▪ Elevation surface (DEM or TIN)	▪ Elevation surface (DEM or TIN)
▪ Observer's position (point)	▪ Line(s) between observer and target(s)
▪ Optional: observer and cell heights (offsets)	▪ Optional: observer and target heights (offsets)
Outputs	
▪ Raster layer	▪ Vector line(s)
▪ Indicates whether each cell is visible or not	▪ Indicates whether each target is visible or not
	▪ Visibility determined along entire length of line
	▪ Optional: obstruction point for each line

Imagine and ArcGIS documentation does not address the question of how elevations are determined between the observer and target, e.g., where elevation is sampled and whether z-values are interpolated, and if so, the method that is used. The best information comes from TEC (2004), which indicates that Imagine's viewshed algorithm treats DEM cells as discrete units (the stepped model), with each cell having a constant z-value. From this information, it is inferred that elevation is sampled at grid crossings, for sampling in between grid crossings would have no impact on the elevation profile generated and would slow down processing, with no benefit.

In contrast, the ArcGIS functions do not employ the stepped model. In ESRI algorithms, DEM elevation "is represented as a continuous surface, re-sampled using bilinear interpolation" (TEC, 2004). Each DEM cell value is interpreted as the value occurring at the cell centroid, and values in other areas are determined by interpolation from the values of the four nearest cells. Where elevation points in a DEM are sampled is still unclear, but based on other information, it can be surmised. Visibility can be calculated in ArcGIS based on TIN surfaces, and according to TEC (2004), "Profile points are calculated only at edge crossings and node locations" for TINs. This is Yoeli's (1985) method applied to a TIN, so it is assumed that the same technique is utilized for raster DEMs. Regarding how elevation is obtained from a TIN, ESRI documentation

provides no explanation, and ArcGIS provides two methods of interpolating elevation from a TIN surface, linear and natural neighbors. The assumption, based on other help files and TEC (2004), is that linear interpolation is the method used. It was tested and verified that the 3D Analyst extension uses linear interpolation, by default, when interpolating z-values from a TIN.

An understanding of observer and target heights is also essential. From all information sources reviewed, the following was gleaned regarding DEMs in ArcGIS: 1) viewshed observer height is determined by bilinear interpolation if elevation is not specified in the attribute table; 2) viewshed target (cell centroid) height is assumed to be determined by bilinear interpolation, but no information has been found to explicitly verify this assumption; 3) LoS observer height is determined by bilinear interpolation if elevation is not specified in the attribute table; and 4) LoS target height is determined by bilinear interpolation. The uncertainty of number 2 would not be an issue in the situation in which a DEM had been resampled with bilinear interpolation, because a cell centroid's elevation would be the same whether it was obtained by interpolation or not.

There is a wealth of literature about viewsheds. Although ArcGIS provides a second visibility function, the vector LoS, there is little or no literature available assessing it. In particular, there is no known literature demonstrating discrepancies between ESRI viewsheds and LoSs. Therefore, no information is available about their agreement with regards to raster and TIN data models. Given that ESRI's LoS and viewshed functions use different algorithms, a problem could arise if a target of interest is determined to be visible by one algorithm and not visible by the other. Tests can be performed to see how well they agree.

Purpose and Objectives

The overall purpose of this study is to investigate uncertainties in GIS visibility by comparing viewshed results between two software programs, and also, results between two types

of visibility algorithms implemented in the same software program. Results will provide a measure of agreement and be informative as to the variability among these various functions.

The study is split into two parts, each with a different study area, data, methods, and results. In the first part, the two visibility functions within ArcGIS, the viewshed and LoS, were compared. One objective is to gain a better understanding of how these operations work. Another objective is to determine whether the visibility of certain locations, or features, in ArcGIS is dependent on the analysis method used. To this end, examples of discrepancies are presented, to demonstrate the need for this evaluation. Systematic tests were conducted to compare the agreement between the viewshed and LoS functions with varying terrain conditions, data structures, resolutions of data, target heights, and observer positions within the landscape.

The second part of this study is a comparison of viewsheds generated from ArcGIS and Imagine. The viewshed algorithms in these two programs purportedly perform the same function, and they allow similar input parameters to be adjusted by the user. The assumption from a general GIS user's perspective is that the same inputs should give the same results, regardless of which program is used. For example, one would expect two database programs to retrieve the same data, as long as the right SQL instructions were used. Likewise, it is reasonable to expect the same results from viewshed functions implemented in different programs. The objective is to quantify viewshed agreement between ArcGIS and Imagine. Different resolutions of DEMs will be utilized to determine if agreement is sensitive to the spatial resolution of the terrain data. In both parts of this study, possible explanations for non-agreement were explored.

Data and Methodology

ArcGIS Viewshed/LoS Comparisons

No information has been encountered that documents whether discrepancies occur between ESRI's viewshed and LoS functions, so it was not known if a need existed for this type of evaluation. Therefore, some preliminary tests were conducted. The underlying assumption is that a viewshed and LoS should agree when the same target is considered. Since the viewshed algorithm evaluates a raster cell for visibility at its centroid, it follows that setting up the same centroid as an LoS target should yield the same result, so long as all inputs (elevation surface, observer position and height, target position and height, etc.) to the two functions are the same.

In the first preliminary test, a 30-m DEM in Haywood County was utilized, with the observer located at a cell centroid (Figure 5.6). A viewshed was generated. Then the same input parameters were used to generate multiple LoSs from the same observer to targets that were equally spaced. The LoSs pass through cells A, B, and C, and purposely pass through the cell centroids, since these are the focal point for classifying a cell as either visible or not visible. Under consideration are three patches of ground (1, 2, and 3), each 10 m × 10 m. Even at this close range (~30 m), there are conflicting results, and Figure 5.6 illustrates several potential problems or sources of misunderstanding.

Cell A is deemed visible by the viewshed because its centroid is visible, even though only 25% of its area is visible by LoS. Half of Cell B is visible by LoS, but the viewshed function reports that the cell is not visible. This is further complicated by the cartographic LoS output, in which it appears that the centroid is visible. Like Cell A, only 25% of Cell C's area is visible by LoS. But unlike Cell A, Cell C's centroid is apparently deemed not visible, because the cell is not visible according to the viewshed. Although the three patches (1, 2, and 3) are all completely

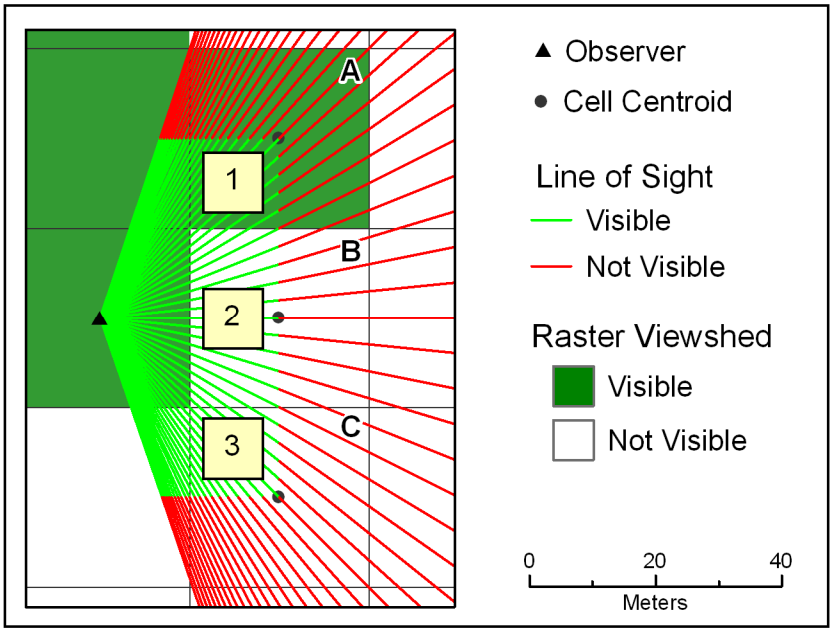

Figure 5.6: Viewshed and lines of sight.

visible by LoS, only Patch 1 would be deemed visible by the viewshed function. This indicates that the way in which a target is defined and the method used to determine its visibility can severely impact results. It would not be difficult to imagine and illustrate other scenarios that provided conflicting and confusing results.

An issue was discovered with ESRI's LoS results that could easily cause confusion and/or a misperception of results. It is first necessary to explain LoS outputs. For an LoS analysis along a single line, the result is 1 or 2 polylines. A single polyline means that the entire line is either visible or obscured, and 2 polylines mean that 1 or more segments are visible and 1 or more segments are obscured. By default, visible portions are displayed in green and non-visible are in red. In addition, data are written to the polyline attribute table. One field links the line back to the source in case there are multiple LoSs created in a batch. Two visibility fields are created, VisCode, which indicates whether a segment is visible or not, and TarIsVis, which indicates whether the target is visible or not. Values of 1 indicate visible. An optional point can be

generated that represents the first obstruction encountered along an LoS, and this obstruction point will only be generated if the target is deemed not visible (ESRI, 2007a).

The confusion could come depending on whether one consults the values written to the table, which are the actual results, or the output cartographic line. A situation can arise in which an obstruction point spatially coincides with the target. This can occur where the LoS is tangent to the elevation surface at the target, and this intersection of the LoS with the terrain becomes an obstruction point. In this case, the LoS will be displayed green, indicating visible, where it reaches the target, but the presence of an obstruction point and the values written to the table indicate that the target is not visible. Fisher (1993) came to the same conclusion when he pointed out that if the slope angle to a target and an interim height are equal, the target should be considered blocked, or masked. The important point is that one can be tempted to reach conclusions from the displayed color of the line rather than from consulting the attribute table.

There are other factors in ArcGIS that can lead people to be misled by the results. First, the quick and easy way to determine LoS is to digitize or “draw” a line over an elevation surface. This is faster than connecting point coordinates with lines and using the 3D Analyst LoS tool, but the line and associated result are much less precise. Second, the LoS generated from drawing yields only a red/green graphic; it is not a shapefile and has no associated attribute table to which results are written. Third, the cartographic representation (red/green line) of the LoS tool may disagree with the actual result that is written to the attribute table. Fourth, the creation of obstruction points is optional in the LoS tool, so it may not occur to some users to consult the attribute table since they would not see the overlap of an obstruction with the target.

As an example of potential confusion, Figure 5.7A shows two outputs from the LoS function from the same observer, Line 1 and Line 2, with Targets A and B in the middle of these

lines. The red/green rendering of the lines is the same: the surface is visible to both targets and is not visible beyond them. However, Target A is obscured and Target B is visible, according to the LoS algorithm. One would not know this if the optional obstruction points were not used, if one did not consult the attribute table, or if one simply drew the LoS to generate a graphic. The elevation profile of Line 1 (Figure 5.7B), bilinearly interpolated from a 30-m DEM, demonstrates that the viewer's LoS appears to be tangent to the surface at Target A, and this intersection with the terrain leads to a "not visible" LoS result in ArcGIS. One could argue that the result should be that Target A is visible since the LoS is tangent. But according to the ESRI LoS algorithm, this is not the case, and this could easily lead to confusion.

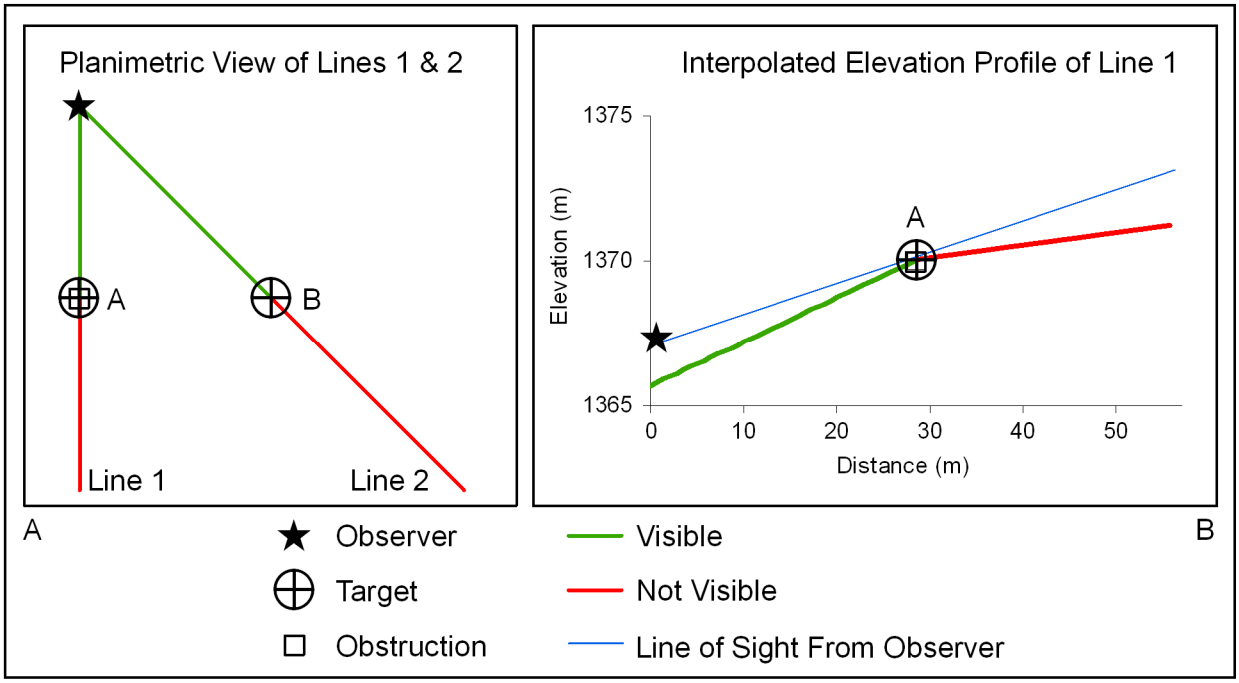

Figure 5.7: Planimetric and profile views of lines of sight.

Since horizontal distances are normally much greater than differences in the vertical direction, vertical exaggeration is needed to visualize and interpret terrain profiles. Vertical

exaggeration is the ratio of the vertical scale to the horizontal scale (Microdem, 2008). In Figure 5.7B, the vertical exaggeration is 3.

Once the possibility of confusion and discrepancies between LoSs and viewsheds was established, three sets of tests were employed to examine the agreement between viewshed and LoS results in ArcGIS. In the first set of tests, target agreement between the algorithms was quantified by setting up all viewshed-visible centroids as LoS targets. In the second set of tests, agreement over a given area was quantified along transects. In the third set of tests, elevation profiles were constructed to examine viewshed/LoS disagreements.

Systematic comparisons of the LoS and viewshed functions were undertaken in ArcGIS to explore the relationships among terrain, data structures, data resolutions, target heights, and observer positions. Visibility was tested in two areas with substantially different terrain characteristics to test whether visibility agreement was sensitive to the roughness of the terrain. Swanson (2003) reported that GIS-based visibility was less accurate in rough terrain, as assessed by field work. The two areas were circular regions 3 km in diameter (Figure 5.8). The area centered on Waypoint 709 (Site 11) in Haywood County, North Carolina, is very rugged, dominated by high ridges and steep hillsides (refer to Chapter 3). Its elevation range is 481 m with a standard deviation of 120 m, and the mean slope is 21° (based on 30-m DEM). The observer point, 709, is located on a flat bench along a ridge top. The other area of interest, on the Tennessee side of GRSM in Cades Cove, is a valley surrounded by modest hills. It has an elevation range of only 108 m with standard deviation of 16 m, and the mean slope is 4° (based on 30-m DEM). To further this test, two observer locations were utilized in Cades Cove, each having a different terrain situation. Observer A is on the valley floor and Observer B overlooks the valley from a hillside approximately 50 m above the valley.

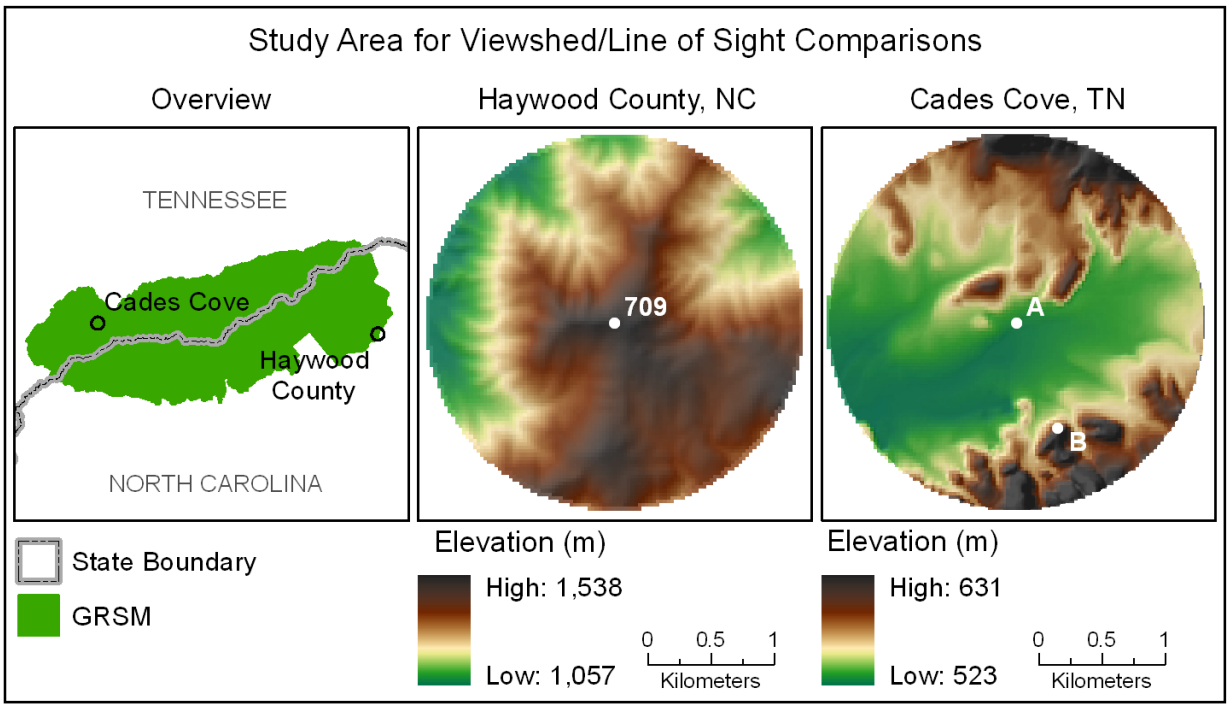

Figure 5.8: Study area for viewshed and line of sight target comparisons.

Other terrain parameters, derived from 30-m DEMs, describing these areas are given in Table 5.2. These include the bilinear interpolated elevation of the observer and the mean slope of the study area. Other parameters, based on Carlisle (2000), include relative relief, mean extremity, and texture within a 5-cell radius of the observer. Relative relief is simply the range of elevation values within the radius. Mean extremity relates the observer's elevation to its neighbors by subtracting the mean elevation of neighboring cells from the observer's cell. Texture, the range of slope values in the neighborhood, indicates terrain ruggedness. Observer A is located in a relatively homogeneous area, characterized by flat ground. It is slightly lower (0.7 m) than the average terrain surrounding it. Observer B is on a sloping hill surrounded by rugged terrain, and it rises higher than the nearby terrain by 18.5 m, affording it unobscured views to the north. Waypoint 709 is on flat ground surrounded by steep slopes. There is great relative relief in the area, and it rises above its surroundings by an average of 16.0 m.

Table 5.2: Terrain characteristics of study area.

Observer	Elevation (m)	Slope (°)	Relative Relief (m)	Mean Extremity (m)	Texture (°)
A	526.5	4	7.9	-0.7	5.4
B	573.2	4	51.4	18.5	27.7
709	1533.1	21	64.7	16.0	36.1

Tests were conducted in both areas with DEM and TIN surfaces. DEMs used were 10-m and 30-m resolution from the USGS NED (refer to Chapter 4). For Cades Cove, 10 m was the highest resolution DEM available, and it was resampled with bilinear interpolation to 30 m. For Haywood County, the source was a 3-m DEM, which was resampled with bilinear interpolation to 10-m and 30-m resolution. Following the example of Maloy and Dean (2001), a TIN was created from each DEM. This was accomplished in ArcGIS with a z-tolerance of 0, which is the maximum vertical accuracy with which TINs can be derived from DEMs in ArcGIS, and it means that the TIN will have the same elevation value as the DEM at each DEM cell centroid.

Since cell visibility in ArcGIS viewsheds is determined by cell centroids, all centroids determined to be visible by a viewshed can be set up as LoS targets. This is accomplished by extracting the binary viewshed result (0 or 1) of each cell to each cell's centroid. Selecting points with a value of 1 creates a dataset of points deemed visible by viewshed. The vector LoS function requires a line, from an observer to a target, as the input. This means the observer must be connected to every centroid as a polyline. A relatively efficient method to do this was found using the Hawth's Analysis Tools extension (www.spatialecology.com). The X,Y coordinates of the observer and all point targets were loaded into a file, and a tool was run to connect the points as polylines. The result is a single polyline shapefile, with as many lines as targets, each connecting the observer to a centroid. There were usually thousands of lines in each test. The vector LoS function was executed with the polyline shapefile and the same inputs (elevation

data, observer height, target height) as the viewshed. The methodology is illustrated in Figure 5.9.

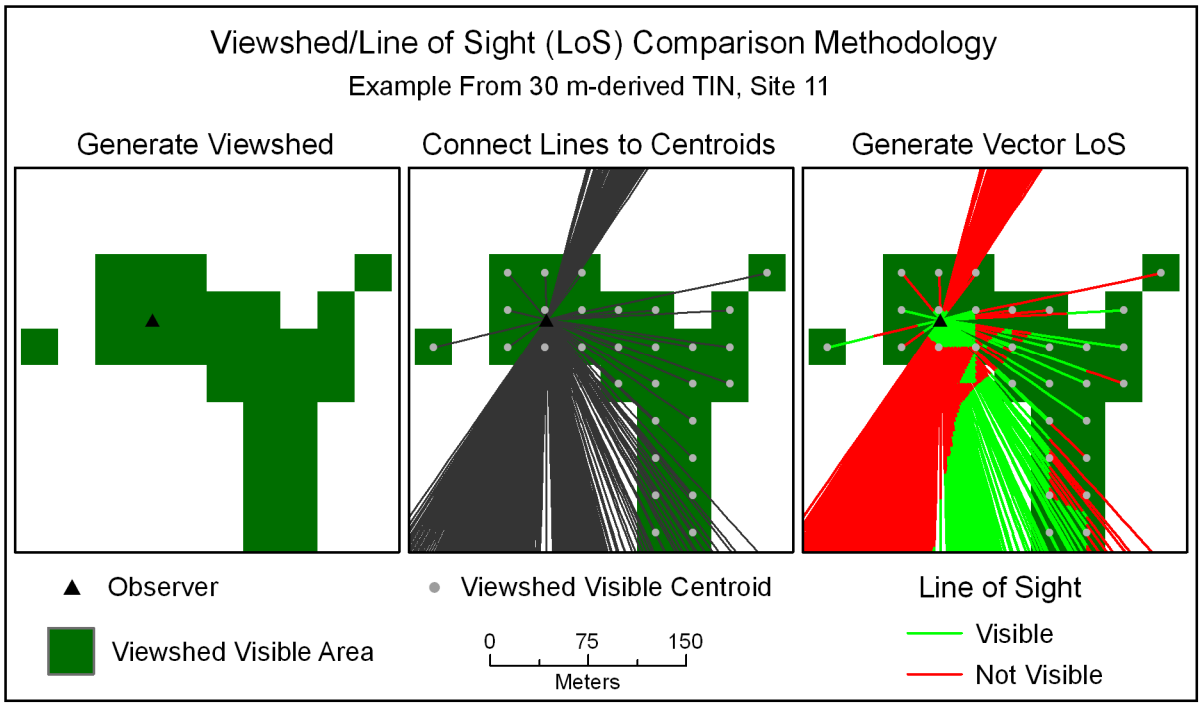

Figure 5.9: Methodology for viewshed and line of sight target comparisons.

Ideally, the two visibility functions will agree. To determine the number of visible LoS targets, the number of obstruction points was consulted, as one obstruction point is created along a LoS if a target is determined to be masked. The level of agreement was calculated as the ratio of the number of LoS-visible targets to the viewshed-visible cells, or the percentage of visible cells from the viewshed that were also visible by LoS.

(LoS-visible targets / viewshed-visible cells) × 100%

This technique does not test the accuracy of the two functions but their agreement. It was advantageous to design a test in which viewshed results are set as the standard to which LoSs are to be compared so that there would be a one-to-one relationship between targets. While the number of viewshed-visible cells is limited by the resolution of the viewshed raster defined by

the user, and these cells cannot overlap, an infinite number of LoSs could be generated within a given raster cell, thus creating a many-to-one relationship. While other comparison methods were utilized, this method was most efficient, and even in the relatively small study areas resulted in tens of thousands (50,000+) of targets from a single 10-m viewshed raster.

Target heights, or offsets above the surface, were set at 0 m (ground level), 0.1 m, and 3 m to provide information as to whether LoS/viewshed agreement is dependent on target height. In all comparisons, observer height was set at 1.5 m above the surface. This value is added to the observer's default ground elevation, which is determined by the algorithm. As mentioned, this value is found by bilinear interpolation for a DEM.

The question of how heights are obtained from a TIN surface for visibility analyses is less clear than it is for a gridded DEM. One can verify the method used to set an observer's height by testing different values for the Spot attribute (ground elevation) and OffsetA (relative observer height) and comparing viewshed results. These are two optional attributes that can be specified in the observer's point shapefile table. For example, if a particular interpolation method is used to set an observer's height by default, and ground elevation obtained by that interpolation method is 200 m, then the following three scenarios should all produce the same viewshed result: 1) specifying ground elevation of 200 m and adding an offset of 1 m; 2) specifying a ground elevation of 201 m with no added offset; and 3) adding height above the ground of 1 m to the default ground elevation. Using these procedures, it was verified that ArcGIS uses bilinear interpolation with a DEM to set an observer's height by default. However, the method that is used to determine an observer's height using a TIN could not be duplicated/verified with certainty. Various tests discovered an apparent discrepancy, with the surface z-value used by the

algorithm higher, by about 0.6-0.7 m, than the linear interpolated z-value. Given this situation, it is unknown exactly how observer height is determined from a TIN in ESRI visibility algorithms.

Not knowing how ArcGIS computes default observer heights from a TIN is concerning. This is an early indicator that there is less certainty when TINs are used for visibility. This uncertainty could surely impact results, depending on how one sets up the observer's position. It has been seen in the work of others that 2 m is often used for a person's height (Fisher, 1993; Riggs and Dean, 2007). This is slightly higher than the average person's height. But if the algorithm sets the observer approximately 0.6 m higher than the user assumes, then the effective observer height is 2.6 m (8' 6"), clearly unrealistic to represent an average person's height.

In addition to quantifying target agreement, the question of viewshed/LoS agreement can be evaluated in areas between observers and targets. Agreement across an area can be tested along transects. To do this, three tests were conducted from different areas and elevation surfaces. In each test, 10 LoS polylines were selected randomly from a previously conducted LoS test with the Microsoft Excel random number generator. For tests with a 30-m DEM and a 30-m-derived TIN, points were sampled at 15-m intervals along the selected lines, and sampling was done at 5-m intervals when the surface was a 10-m-derived TIN. Point sampling is a proxy for line length and provides an estimate of line characteristics. Locations and parameters of the tests included the 30-m DEM in Cades Cove from Observer A with target heights of 0 m, the 30-m-derived TIN in Cades Cove from Observer A with target heights of 0 m, and the 10-m-derived TIN in Haywood County with target heights of 3 m (Figure 5.10).

To perform the tests, the sampled points were overlaid on previously generated viewshed and vector LoS outputs. The visibility results (visible or not visible) from each algorithm were written to the sampled points. The data indicate the percentage of a line that is visible according

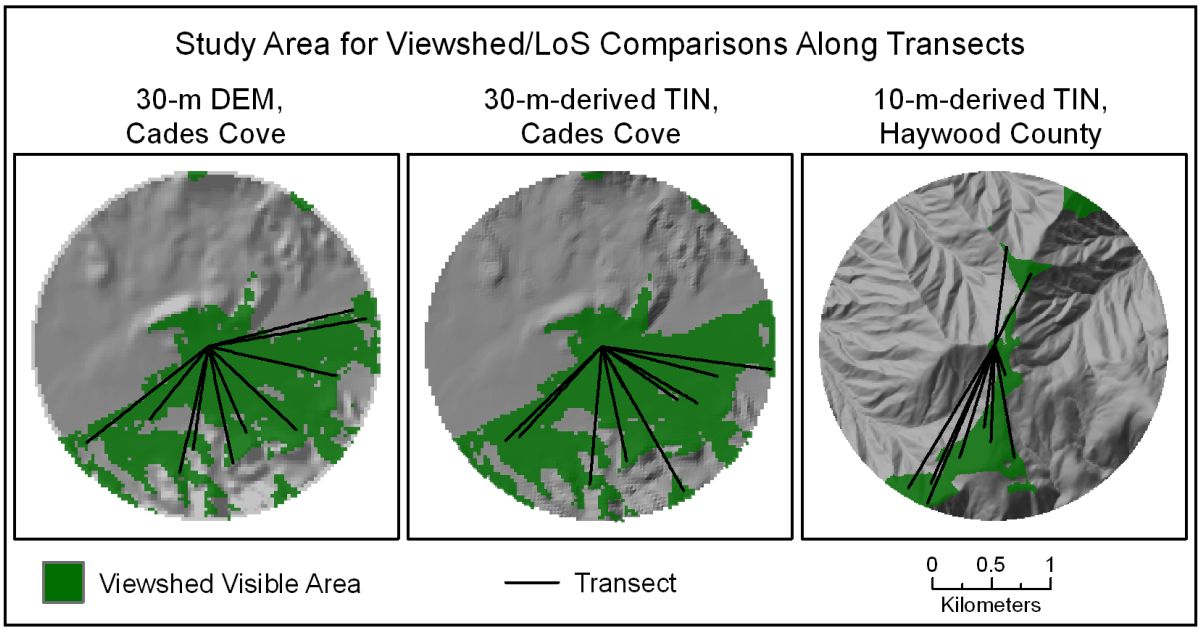

Figure 5.10: Study area for viewshed and line of sight transect comparisons.

to LoS versus the percentage that is visible according to the viewshed function. More importantly, a comparison of the data on a point-by-point basis quantifies the agreement between the two functions across the surface.

Two elevation profiles were created and utilized to probe inconsistencies in visibility results. In the first profile, the purpose is to better understand LoS/viewshed disagreement with different elevation structures. A target was selected. This target, a raster centroid, was deemed visible by the viewshed function from Waypoint 709 (Site 11) with both the 30-m DEM and 30-m-derived TIN. In these viewsheds, inputs were the same, such as observer offset (1.5 m) and target height (0.1 m). The selected centroid, set up as an LoS target with the same inputs and parameters as the viewsheds, was deemed visible with the DEM but not visible with the TIN. To investigate the inconsistencies, elevation profiles along the LoS were created from both surface models. The distance between the observer and target is 46.5 m, and points were sampled equidistantly along this line, approximately every meter, to generate 48 sample points. Elevation

was extracted to the points using bilinear interpolation from the DEM and linear interpolation from the TIN, the methods believed to be used by the LoS algorithm.

In the second profile, a viewshed/LoS discrepancy with a TIN was investigated. A target deemed visible in Cades Cove by the viewshed but not visible by the LoS algorithm was selected. Following the information from TEC (2004) about ESRI algorithms with TINs, elevation was sampled along the LoS only where a TIN edge or node was crossed. This resulted in 85 points, and in addition to the observer position, spot heights for 86 points were obtained by linear interpolation. The profile graph was used to visualize and assess the algorithm discrepancies. In both of these profile examples, disagreements and uncertainties exist concerning the visibility of certain targets. The differences must be attributed to the elevation surfaces or to algorithm differences, since the inputs in each test are equal.

ArcGIS/Imagine Viewshed Comparisons

To compare ArcGIS and Imagine viewsheds, four field sites were chosen from two areas, one in the western region of GRSM located in Swain County, Sites 1 and 3, and the other in the eastern region of GRSM in Haywood County, Sites 12 and 13 (Figure 5.11) (refer to Chapter 3). The western region is approximately a half-circle with a 30-km diameter, while the eastern region is circular, 25 km in diameter. The terrain in both areas is extremely rugged, and elevation ranges are greater than 1,000 m. Site 1 (Waypoint 616) is located along a moderately steep side hill, sloping down from northeast to southwest, and the slope is 17.6°, based on 10-m data. Site 3 (Waypoint 642) is located atop a flat ridge crest, and the slope is 6.1°. Site 12 (Waypoint 723) is situated on the top of a small ridge with a slope of 9.5°, and Site 13 (Waypoint 733) is on a flat spot of a narrow ridge crest with a 2.6° slope.

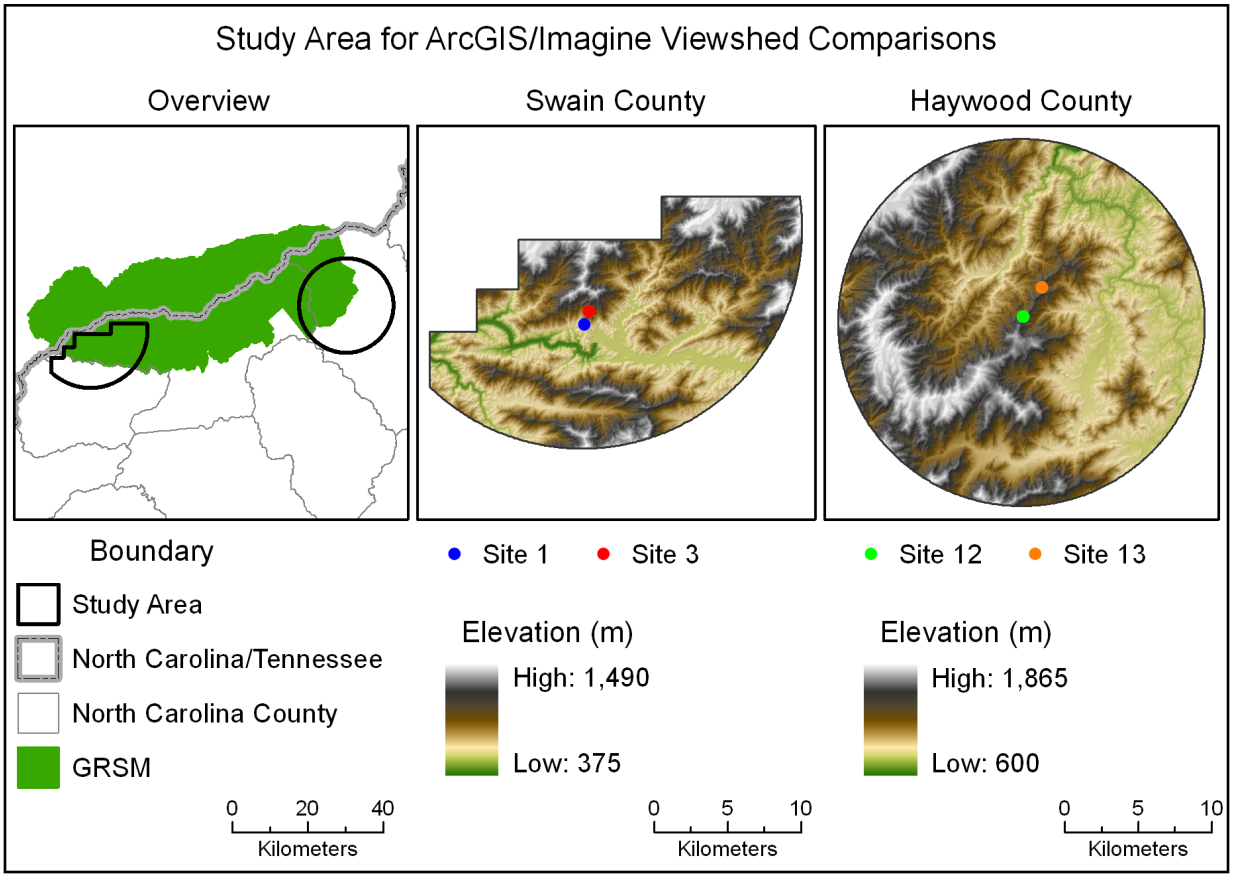

Figure 5.11: Study area for viewshed comparisons between ArcGIS and Imagine.

Elevation data of three resolutions were used: 30, 10, and 6 m. The 1/9 arc-second NED (refer to Chapter 4) was resampled to these resolutions with bilinear interpolation in ArcGIS. The 3-m data was not employed in these tests, as the large study areas made the algorithm processing time prohibitive. Identical DEMs were input into the software programs to generate the viewsheds. The common file format used was .img, since this is the native image format in Imagine and produces results identical to those of other raster formats in ArcGIS.

For viewshed comparisons between ArcGIS and Imagine, input parameters were entered as equally as possible. The field of view (360°) and range (extent of DEM) were set to be equal. The observer location is a point shapefile in ArcGIS, while Imagine accepts X,Y coordinates. These coordinates were obtained and input with high precision (tenth of a millimeter). Both

algorithms have options to use earth curvature. However, the ERDAS documentation does not provide information about the calculations implemented, so it is unknown whether the two programs have different curvature corrections. To make the software comparisons as nearly identical as possible, viewsheds were generated without earth curvature adjustments.

One of the most important, if not the biggest, issues that could lead to varying results from the two algorithms is their different interpretations of the DEM. Imagine's viewshed algorithm treats DEM cells as discrete units (the stepped model), with each cell having a constant z-value. However, ArcGIS treats DEMs as a continuous surface, with z-values determined by interpolation from the values of the four nearest cells. As a result of these different DEM interpretations, default observer heights are calculated differently in the two programs. For viewsheds in ArcGIS, the default observer height is obtained by bilinear interpolation (ESRI, 2008). In Imagine, the default observer height is the grid cell value in which the observer is located and is not interpolated. These conditions were verified in both programs. The magnitude of the differences is dependent on the DEM resolution and the nature of the topography.

Due to the different surface interpretations, relative and absolute height are often different in the two programs for the same planimetric position. Ideally, a single viewshed would be generated in each program with an observer height of 1.5 m above the ground, the relative height. But since the ground elevation is calculated differently (cell value in Imagine and interpolated value in ArcGIS), equal relative heights often result in different overall, or absolute, heights. So a viewshed comparison with the same relative heights may have observers at different absolute heights. The converse can be true, that setting observers in both programs to the same absolute height can result in observers at varying heights above the ground. For example, at Site 1 with the 30-m DEM, the default observer height in ArcGIS is 678.5 m but is

683.9 m in Imagine. Therefore, adding an observer height of 1.5 m makes the absolute height 680.0 m in ArcGIS and 685.4 m in Imagine. This same absolute height of 685.4 m in ArcGIS places the observer 6.9 m above the ground.

The methods employed by the algorithms to calculate default observer heights cannot be altered by the user. Although it seems that for point-to-point analyses, such as the viewshed, having the same relative height is most important, the matter of different absolute heights should not be completely ignored. To deal with these differences, two sets of comparisons were generated for each site/DEM combination. In the first, the same relative height (1.5 m) is used. If this resulted in the same absolute height, no further tests were needed. However, if this resulted in different absolute heights, then the greater of the two absolute heights was chosen, and a viewshed was generated from that absolute height in the remaining program. Given the 3 resolutions of DEMs tested at each site, there are 6 comparisons that can be made per site (3 with equal relative height and 3 with equal absolute height). With 4 sites, there are a total of 24 software comparisons. Since there were 3 situations where the relative and absolute heights were equal, these 24 comparisons were made possible by generating 42 viewsheds, instead of 48.

To measure the spatial agreement of viewsheds, raster viewshed values were reclassified, and the layers were overlaid and added. This facilitated the computation of several areal statistics, based on the reporting of viewshed results by Maloy and Dean (2001) and Riggs and Dean (2007): percentage of area visible only in Imagine, percentage of area visible only in ArcGIS, and percentage of area visible in both, which is the overlap or agreement (Figure 5.12). The total area used to derive these percentages is the area visible by at least one software program (Riggs and Dean, 2007). An additional measure of agreement was also calculated. Given that ArcGIS viewsheds in these tests are nearly always smaller than Imagine viewsheds,

the overlap area can be divided by the ArcGIS viewshed area. The resulting percentage reveals how much of the ArcGIS viewshed is contained within the Imagine viewshed.

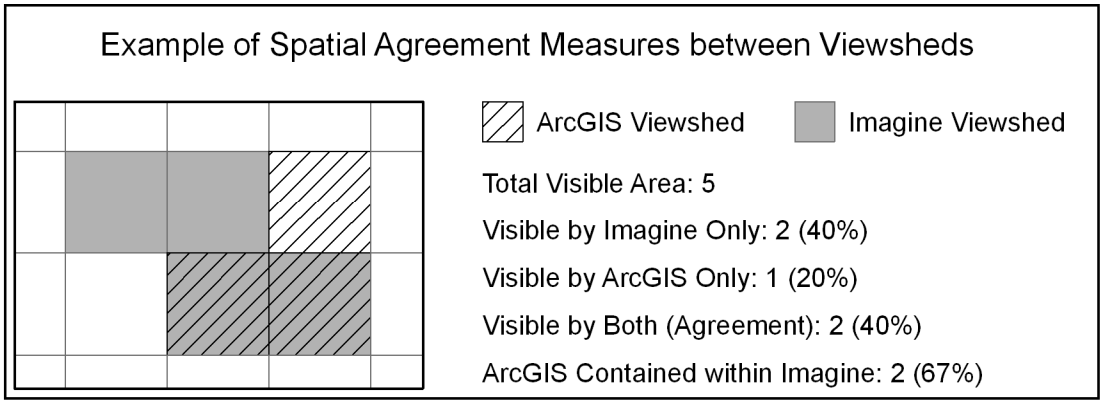

Figure 5.12: Illustration of areal statistics derived from viewshed comparisons.

Elevation profiles were created to analyze differing results between the ArcGIS and Imagine viewsheds. Two transects were created, beginning at Site 1. The observers were set at the same absolute height with the 30-m DEM. Transect 1 extended to the southwest for 382 m from Waypoint 616, and Transect 2 extended 268 m to the north (Figure 5.13). Elevation was obtained by bilinear interpolation at DEM grid crossings to simulate visibility in ArcGIS, and cell values were sampled at DEM grid crossings to simulate Imagine visibility. This resulted in 21 points along Transect 1 and 9 points along Transect 2. There are more points along Transect 1, and they are less evenly spaced, because the line cuts diagonally across the square DEM grid structure. The z-values were compared along the transects, and profile graphs were created. Viewshed results were visualized along the transects by displaying visible regions in green and non-visible regions in red.

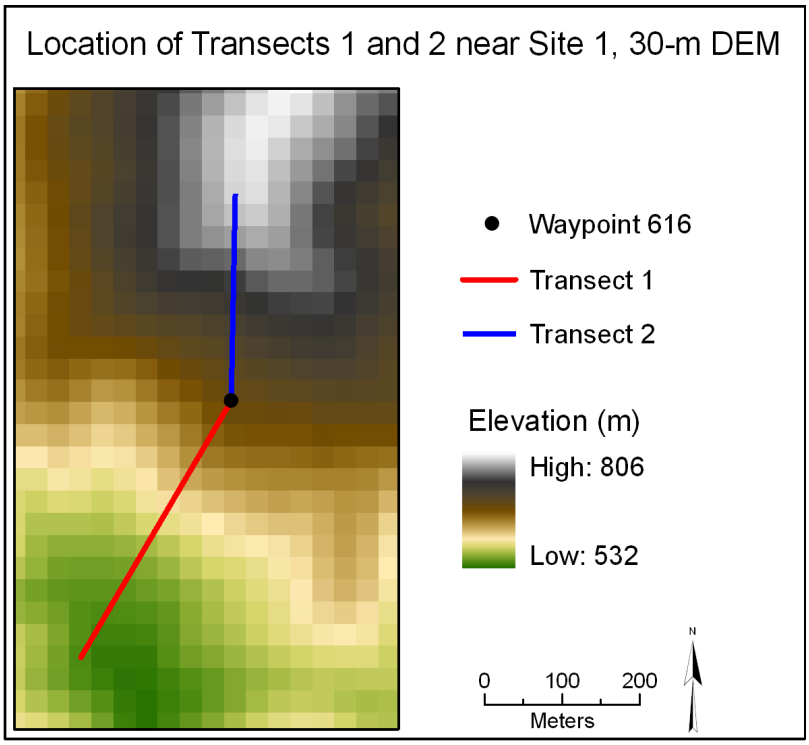

Figure 5.13: Transects used to create elevation profiles.

Results

ArcGIS Viewshed/LoS Comparisons: Agreement of Targets

The agreement of 36 viewshed and 36 LoS tests is given in Table 5.3. Included are 18 results for TINs and 18 for DEMs. From each observer location (Observers A and B in Cades Cove and Waypoint 709 in Haywood County), the level of agreement between LoS and viewshed targets was found for 3 target heights (0, 0.1, and 3 m). This was carried out for 4 elevation surfaces (10- and 30-m DEMs, 10- and 30-m-derived TINs). N is the number of cells visible by viewshed and set up as LoS targets. Initial Agreement is the agreement taken at face value, and the 0.1-m Provision is the agreement found when targets and obstruction points are within 0.1 m of each other (explained further below).

Table 5.3: Agreement of viewshed and line of sight targets. Red: < 95%; Orange: 95% to <99%.

			TIN Surface			DEM Surface		
Observer	Target Height	Res.	N	Initial Agreement	0.1-m Provision	N	Initial Agreement	0.1-m Provision
A	0.0 m	30 m	2,947	89.24%	89.24%	2,844	49.26%	99.02%
A	0.1 m	30 m	3,052	91.12%	91.12%	2,974	99.36%	99.36%
A	3.0 m	30 m	3,805	96.61%	96.61%	3,918	100.00%	100.00%
A	0.0 m	10 m	24,629	94.73%	94.73%	24,106	52.58%	99.34%
A	0.1 m	10 m	26,428	96.97%	96.97%	26,176	99.79%	99.79%
A	3.0 m	10 m	35,055	98.75%	98.75%	35,451	99.94%	99.94%
B	0.0 m	30 m	5,216	98.45%	98.50%	5,718	51.00%	99.63%
B	0.1 m	30 m	5,277	98.56%	98.56%	5,762	99.69%	99.69%
B	3.0 m	30 m	5,922	99.29%	99.29%	6,336	99.95%	99.95%
B	0.0 m	10 m	48,620	99.22%	99.23%	50,061	43.73%	99.83%
B	0.1 m	10 m	49,354	99.38%	99.38%	50,761	99.86%	99.86%
B	3.0 m	10 m	55,398	99.70%	99.70%	56,609	99.96%	99.96%
709	0.0 m	30 m	465	76.56%	76.56%	628	61.78%	99.20%
709	0.1 m	30 m	472	76.69%	76.69%	630	99.21%	99.21%
709	3.0 m	30 m	584	78.94%	78.94%	739	99.73%	99.73%
709	0.0 m	10 m	5,317	88.98%	88.98%	6,093	56.80%	99.26%
709	0.1 m	10 m	5,405	88.79%	88.79%	6,182	99.51%	99.51%
709	3.0 m	10 m	6,938	87.47%	87.47%	7,598	99.87%	99.87%

With DEMs, agreement was very high, 99% or greater, when targets were raised above the ground level, even 0.1 m, but all ground level targets had agreements of less than 62%. Since the ArcGIS default setting for target height is 0 for both LoS and viewshed functions, this could lead to a large discrepancy between the two visibility algorithms that may not be warranted if target heights are not raised at all above the ground surface.

Agreement with TINs was never as low as the lows found with DEMs. Agreement was greater than 75% in all cases. Although lifting targets slightly above the surface (0.1 m) improved agreement for TINs in all cases except for Observer 709 with the 10-m-derived TIN, the increases were not nearly as drastic as with DEMs. For each combination of observer, data resolution, and data structure, agreement improved when target height was increased. Again, the only exception occurred for Observer 709 with the 10-m-derived TIN, in which agreement

decreased slightly. However, there was no significant difference in average viewshed/LoS agreement between targets that were 0.1 m and 3 m high with TIN models. There was a significant difference ($p = .012$ for a 2-tailed test) in agreement with DEMs between 0.1-m and 3-m targets.

Agreement is higher with a DEM surface than with a TIN in 12 out of 18 sets of locations/parameters. All 6 of the greater agreements with TINs occur when the target height is 0 m. Anytime the target is raised above the surface, there is greater agreement between the LoS and viewshed functions with a DEM. The reason for low agreement with DEMs when the target was at ground level was explored. Situations were identified in which the target and obstruction points appeared to overlap. Even though ArcGIS indicates these targets are masked, I wanted to see how the statistics changed if the targets were considered visible when this occurred. If one considers a target to be visible so long as it is very close to the obstruction point, algorithm agreement from a DEM drastically improves. Even a very small circular distance of 1 decimeter increased all DEM LoS/viewshed agreements to at least 99%. These are the values in the 0.1-m Provision column. For example, if one took results at face value for Observer A with surface targets over a 30-m DEM, agreement is poor (49.26%). However, if LoS masked targets that are within 1 decimeter of their obstruction points are considered to be visible, then agreement increases to 99.02%. This pattern occurs for all tests with a ground surface target and a DEM: initial agreement ranged from 43.73% to 61.78% but improved to over 99% when provision was made for target/obstruction overlap. With this provision, viewshed/LoS agreement is always better with a DEM than a TIN in ArcGIS. Average agreement with a DEM is 99.62%, and it is 92.19% with a TIN. These differences in means are statistically significant as determined by a *t*-test ($p = .001$ for a 2-tailed test).

This provision had no real effect on TIN-based visibility agreement. TIN obstructions occurred elsewhere in the landscape. What occurred often with a TIN was that a small, dense group of obstruction points near the observer blocked many, sometimes hundreds, of distant targets (Figure 5.14). This situation was never found with DEMs.

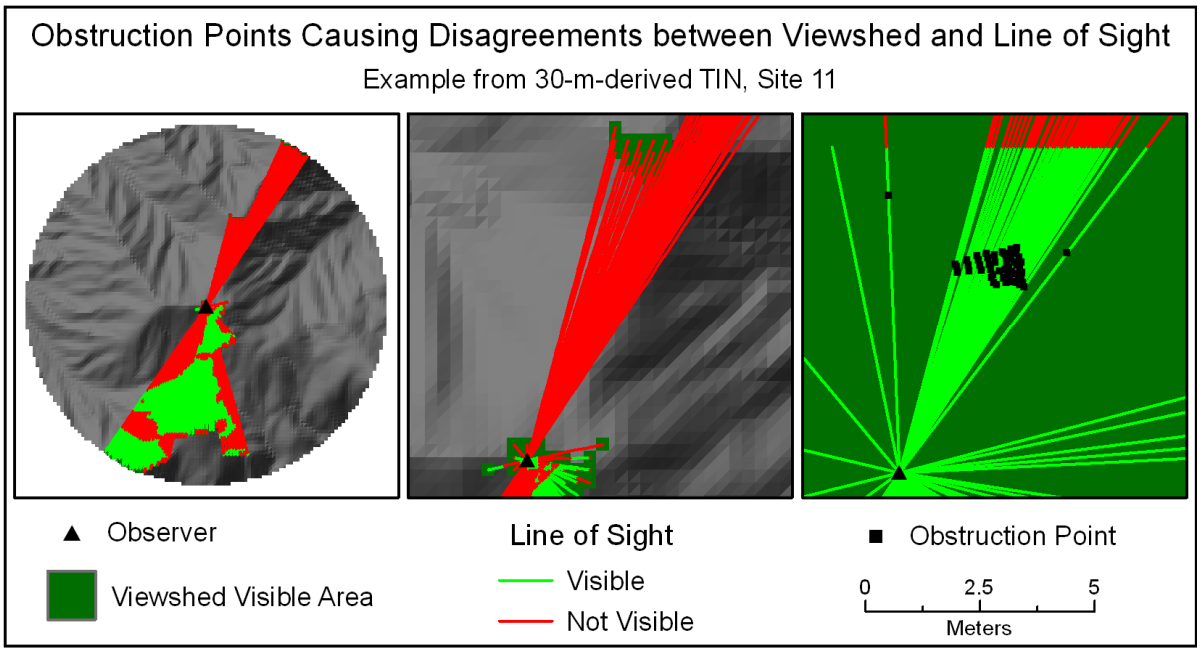

Figure 5.14: Masking of LoS targets by obstruction points near an observer with a TIN. Study area overview (left), larger scale (middle), and close-up view (right).

The resolution of the elevation models had no statistically significant effect on viewshed/LoS agreement. Overall agreement was 99.71% with 10-m DEMs and 99.53% with 30-m DEMs. Average agreement was 94.89% with 10-m-derived TINs and 89.50% with 30-m-derived TINs. Although the higher resolution data produced a higher agreement rate within each data structure, the differences were not significant at a 95% confidence level.

Agreement differed among the sites. Significant differences occurred among all three sites with the TIN, with p-values ranging from .001 to .031 for 2-tailed tests. Agreement was highest for Observer B, which overlooks the valley from a hillside, at 99.1%. Observer A, on the

valley floor, had 94.6% agreement. Observer 709, in the rugged landscape of Haywood County, averaged the lowest agreement, 82.9%. With DEMs, a significant difference ($p = .029$ for a 2-tailed test) in agreement only occurred between one pair of sites, Observers B and 709, which averaged 99.8% and 99.5% agreement, respectively.

ArcGIS Viewshed/LoS Comparisons: Agreement Along Transects

In addition to target agreement, agreement between viewsheds and vector LoSs across an area was quantified. It was found previously that the 30-m DEM in Cades Cove from Observer A, with target height = 0 m, had 49.3% initial agreement of targets and 99.0% agreement with the 1 decimeter provision (Table 5.4). Along 10 random lines, it was found that approximately 83.8% of the line lengths were deemed visible by the viewshed function, and 86.0% were visible by the LoS function. In a point-by-point comparison of the sampled points, 34 of the 720 points disagreed in visibility, a 95.3% agreement rate between the viewshed and LoS algorithms along these lines. Most disagreements occurred near viewshed boundaries (Figure 5.15). In this test, the viewshed cell size is rather large (30 m), so this is understandable, since the only area of the cell evaluated by the viewshed function is the center. This provides an example of why a viewshed boundary should be considered somewhat uncertain.

Table 5.4: Agreement of viewshed and line of sight along transects.

				Transects		
Area	Data	Target Height	Target Agreement	Viewshed Visible	LoS Visible	Viewshed/LoS Agreement
Cades Cove	30-m DEM	0 m	49.3%	83.8%	86.0%	95.3%
Cades Cove	30-m TIN	0 m	89.2%	91.3%	85.9%	92.3%
Haywood County	10-m TIN	3 m	87.5%	32.9%	33.1%	78.0%

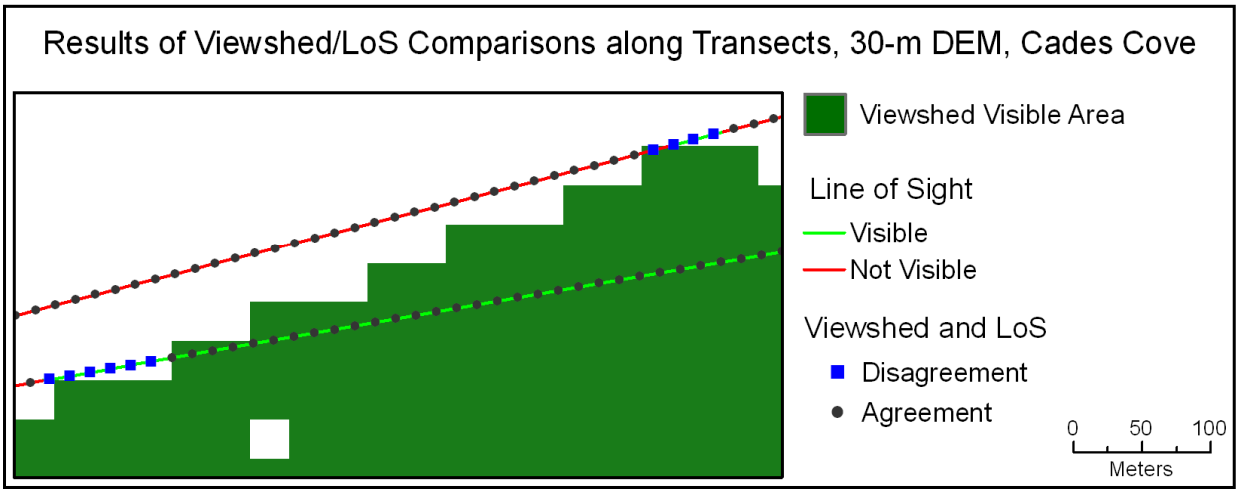

Figure 5.15: Example of viewshed/LoS disagreements near viewshed boundaries.

The 30-m-derived TIN in Cades Cove from Observer A, with target height = 0 m, had 89.2% agreement of targets (Table 5.4). Along 10 random lines, approximately 91.3% of the line lengths were visible by viewshed, and 85.9% were visible by LoS. In a point-by-point comparison of the 689 sampled points, only 53 disagreed in visibility, a 92.3% agreement rate between the visibility algorithms along these lines. This comparison method yields a slightly higher rate of agreement than comparing targets in this area.

The 10-m-derived TIN in Haywood County, with target height = 3 m, had 87.5% agreement of targets (Table 5.4). Along 10 random lines, essentially the same percentage of the lines was visible by viewshed (32.9%) and by LoS (33.1%), but they differed on a point-by-point basis. Of 1,902 points, 418 disagreed in visibility between viewshed and LoS, a 78.0% agreement rate (Figure 5.16). This is worse than the viewshed/LoS target agreement in this area.

Reasons for the relatively low level of agreement (78.0%) between the viewshed and LoS results along transects from the 10-m-derived TIN in Haywood County were explored. There was great variation in the size of the clusters of points (number of consecutive points) that disagreed. From the 10 lines there were 33 clusters. These averaged 13 points in length with a

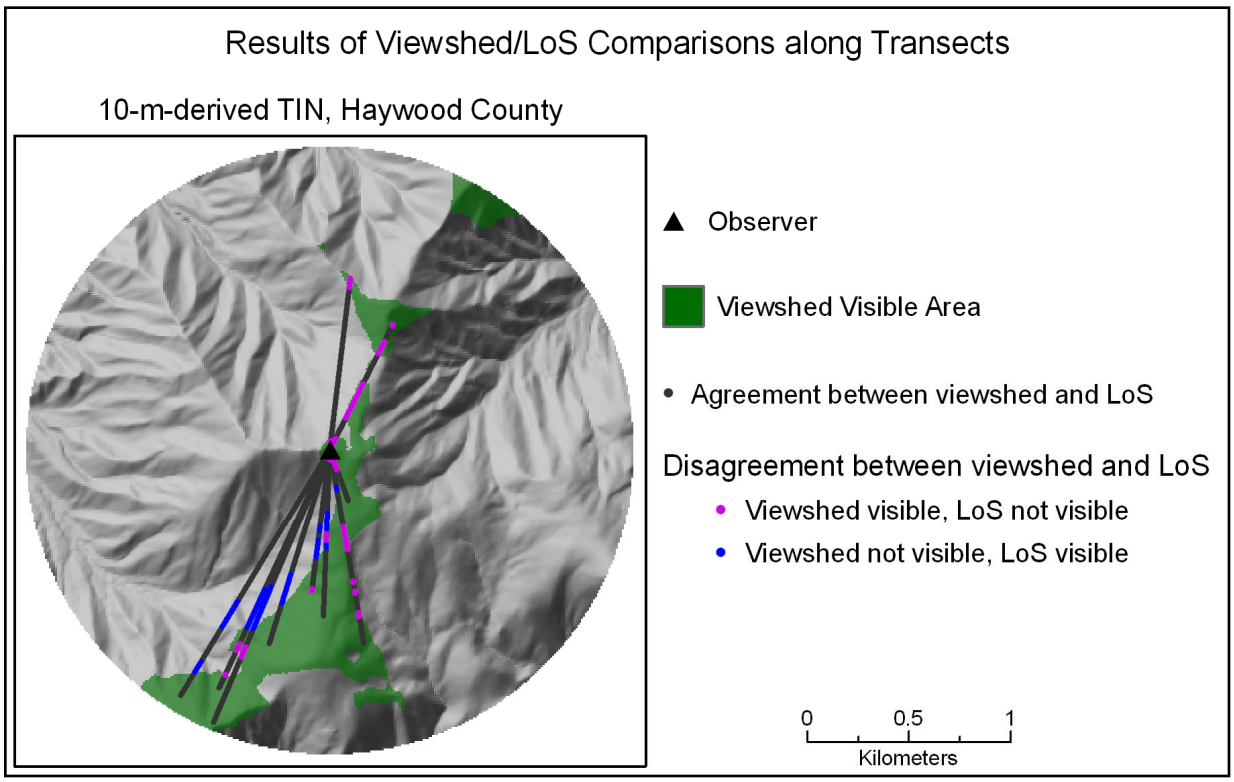

Figure 5.16: Viewshed/LoS agreement along 10 transects.

standard deviation of 12, and ranged from 2 to 46 points. Some points of disagreement occurred near viewshed boundaries, where the resolution and nature of the raster viewshed evaluation could be an explanatory factor, but many other contradicting points occurred well within or outside viewshed boundaries. There was no significant difference in elevation between the points that agreed and those that disagreed. There was a significant difference ($p<.001$ for a 2-tailed test) in mean slope, with the set of points that agreed on visibility having a steeper mean slope (20.3°) than those that disagreed on visibility (18.3°).

Disagreement can occur in two ways. Category 1 is a situation in which viewshed indicates not visible and LoS indicates visible, and in Category 2, viewshed indicates visible and LoS indicates not visible. These categories were examined. Among the 418 points that disagreed between viewshed and LoS, these categories were evenly split, 211 versus 207 points. These

categories did have a statistically significant difference ($p<.001$ for a 2-tailed test) in mean slope, with Category 1 having a steeper mean slope (19.8°) than Category 2 (16.8°). There was also a significant difference ($p<.001$ for a 2-tailed test) in elevation between the two categories, with Category 2 having a greater mean elevation (1,477.8 m) than Category 1 (1,395.7 m). On average, points of disagreement between viewshed and LoS were 139.5 m below the observer for Category 1 points and 57.4 m below the observer for Category 2 points. Thus, Category 1 points (viewshed not visible and LoS visible) are significantly lower in elevation and have steeper slopes.

ArcGIS Viewshed/LoS Comparisons: Agreement from Elevation Profiles

Elevation profiles were utilized to examine viewshed/LoS disagreement with different elevation structures. A common target, a cell centroid, was visible by the viewshed function with both the 30-m DEM and 30-m-derived TIN. This point was visible by the LoS function with the DEM but not visible with the TIN. Elevation profiles along this LoS were created from both surfaces (Figure 5.17A and B) with a vertical exaggeration of 5. Points were sampled every meter with bilinear interpolation from the DEM and linear interpolation from the TIN. Algorithm results, displayed in green and red, are represented in the graphs. The geometry of the profiles from the TIN and DEM appear very similar. After approximately 10 m, the terrain is no longer visible from the TIN due to an obstruction, and the algorithm results agree with the profile (Figure 5.17A). Although the DEM profile appears basically the same, all points along the LoS, including the target, are deemed visible by the LoS function (Figure 5.17B). The TIN LoS algorithm result appears to be more accurate, as it agrees with the profile graph.

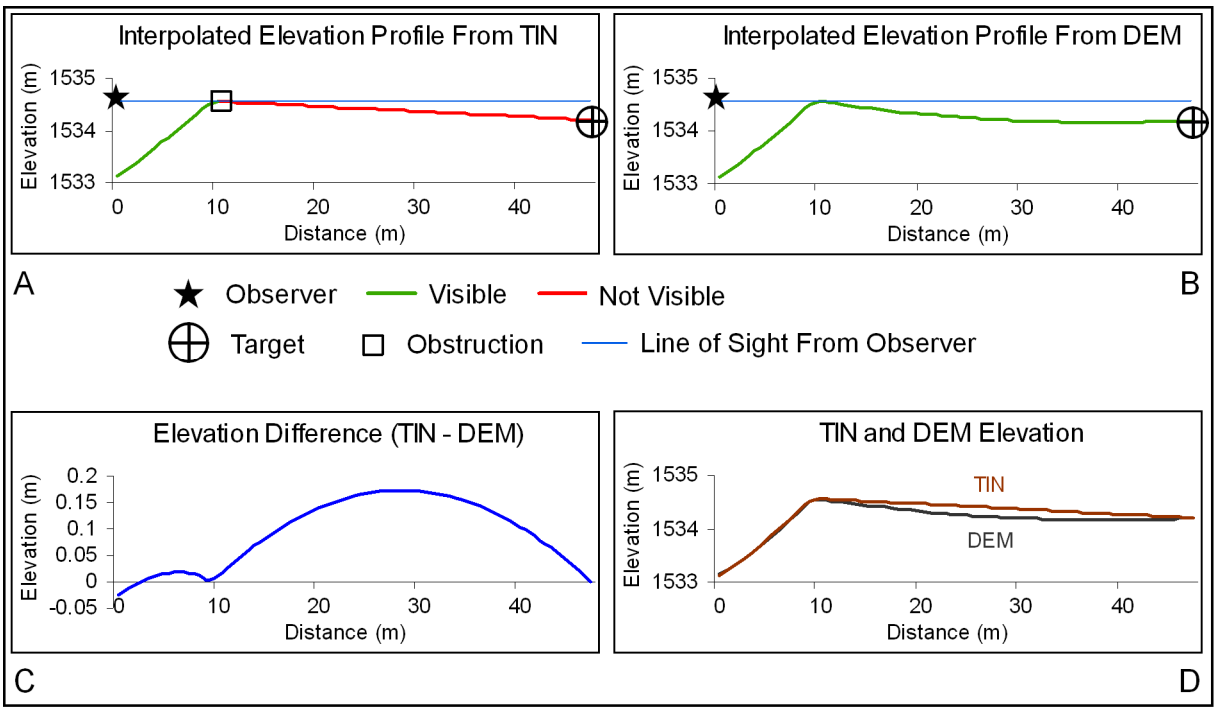

Figure 5.17: Elevation comparison of TIN and DEM along line of sight.

Elevation values from the sampled points were compared by subtracting the DEM elevation from the TIN elevation. These differences are illustrated with a vertical exaggeration of 50 in Figure 5.17C. The TIN is generally higher, but by an average of only 0.09 m, and the greatest difference is only 0.17 m. In addition, at the point where visibility is obstructed along the TIN (~10 m), the two surface models have essentially the same elevation. In Figure 5.17D, as in Figure 5.17C, it is seen that the TIN model is slightly higher, but the two surfaces are the same at the target point and at the TIN obstruction point.

The preceding test provides inconclusive results. After examining the data, it is not clear why the LoS function indicates that the target and entire length of the LoS are visible with the DEM, but the target and most of the LoS are not visible with the TIN. Since the TIN provides a higher elevation surface, one would assume that if there was a discrepancy, there would be more visibility across the TIN than the DEM, but the LoS algorithm contradicts this. Since it is thought

that the ESRI algorithms sample elevation at DEM grid crossings and TIN edges and nodes, profiles were created with this method, too, but they did not clarify the situation.

In the second elevation profile, a discrepancy existed with a TIN in which a target deemed visible by viewshed was deemed not visible by the LoS function. Elevation was sampled along the LoS only where a TIN edge or node was crossed, and z-values were obtained by linear interpolation (Figure 5.18A). These elevations were graphed, with a vertical exaggeration of approximately 11, to visualize the LoS profile (Figure 5.18B).

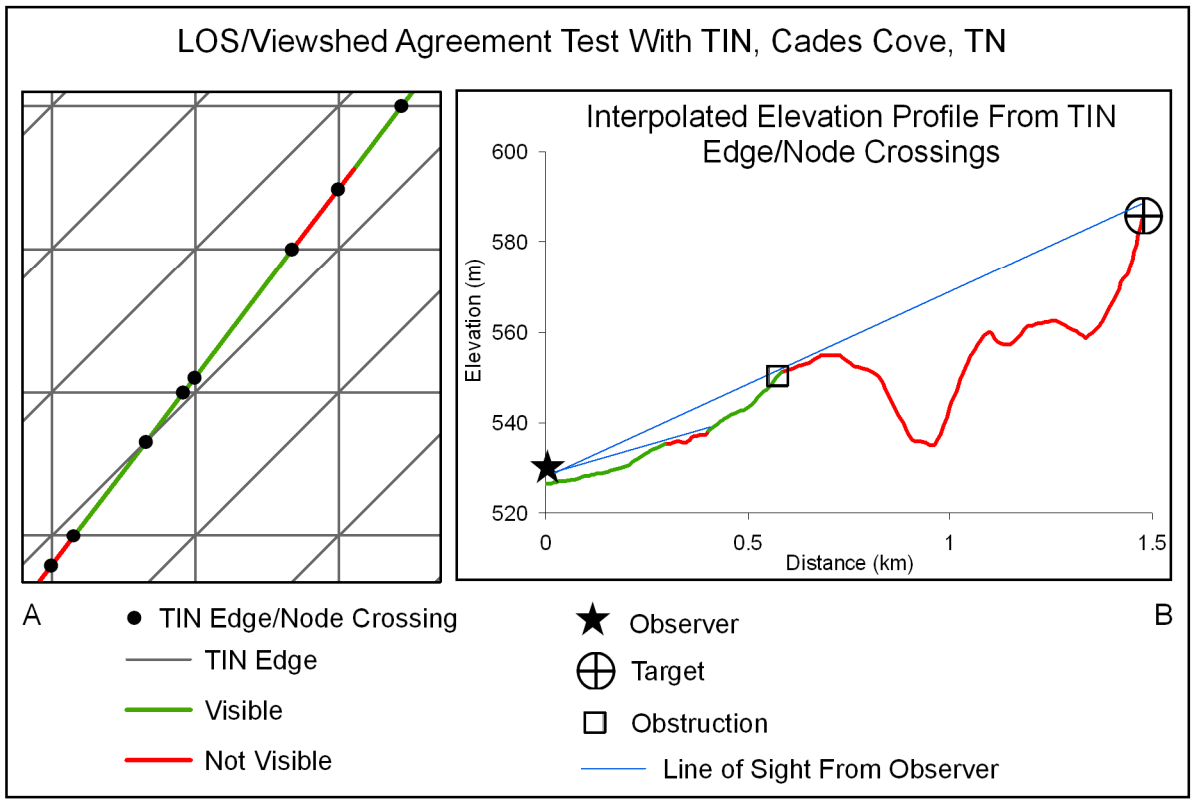

Figure 5.18: Planimetric and profile views of line of sight.

Visually, the elevation profile supports the LoS result. The terrain is masked beyond 0.6 km by a hill, and the target is not visible. The target would be visible if it were slightly higher. However, this same target, a raster centroid, was calculated as visible by the viewshed function. It is not clear why a discrepancy exists. A potentially important finding resulted from this test.

The results challenge the assertion that the vector LoS function only evaluates a TIN at edge and node crossings. It is demonstrated that visibility along the vector LoS can change in locations other than a TIN edge or node, evidenced by the changing colors of the output line in the upper right of Figure 5.18A. Therefore, it would seem that visibility is being evaluated at other locations.

ArcGIS/Imagine Viewshed Comparisons: Spatial Agreement

Viewshed parameters and resulting visible areas are presented for the 24 software comparisons in Table 5.5. For each site/DEM combination, two viewshed comparisons are available: one in which the observers in ArcGIS and Imagine were at the same relative height, and one with equal absolute heights. In 3 cases (Site 1 with the 10-m DEM, Site 3 with the 30-m DEM, and Site 12 with the 6-m DEM) these heights were identical.

To visualize the data from Table 5.5, two graphs depict the viewshed sizes from the combinations of software systems, DEM resolution, and site (Figure 5.19). Graphs are separated by whether the observers had the same relative height or the same absolute height. In each graph, 6 results are presented per site. ArcGIS and Imagine results are displayed side-by-side, in an alternating fashion, with ArcGIS in green and Imagine in red. The colors are ordered by DEM resolution: coarser resolution DEMs are less saturated and finer resolution DEMs are more saturated. Thus, to compare equal inputs in the different programs, one would compare the light green with the light red (30-m data), the medium green with the medium red (10-m data), and the dark green with the dark red (6-m data). To compare the effects of data resolution, one would compare within a color (e.g., light, medium, and dark green).

Table 5.5: Visible areas of viewshed results.

		ArcGIS			Imagine				
Site	DEM Res. (m)	Rel. Height (m)	Abs. Height (m)	Visible Area (km^2)	Rel. Height (m)	Abs. Height (m)	Visible Area (km^2)	Same Rel. Height	Same Abs. Height
1	30	1.5	680.0	17.4	1.5	685.4	19.6	✓	
1	30	6.9	685.4	23.4	1.5	685.4	19.6		✓
1	10	1.5	684.6	19.8	1.5	684.6	20.7	✓	✓
1	6	1.5	688.2	18.6	1.5	689.1	19.2	✓	
1	6	2.3	689.1	18.8	1.5	689.1	19.2		✓
3	30	1.5	897.7	37.0	1.5	897.7	40.5	✓	✓
3	10	1.5	905.0	33.0	1.5	904.8	34.5	✓	
3	10	1.5	905.0	33.0	1.7	905.0	34.6		✓
3	6	1.5	906.3	30.0	1.5	906.1	30.0	✓	
3	6	1.5	906.3	30.0	1.8	906.3	30.9		✓
12	30	1.5	1363.6	50.8	1.5	1361.2	53.2	✓	
12	30	1.5	1363.6	50.8	3.8	1363.6	60.2		✓
12	10	1.5	1363.7	49.8	1.5	1364.4	52.3	✓	
12	10	2.2	1364.4	50.8	1.5	1364.4	52.3		✓
12	6	1.5	1363.7	47.7	1.5	1363.7	49.5	✓	✓
13	30	1.5	1360.2	52.6	1.5	1363.4	76.5	✓	
13	30	4.7	1363.4	76.2	1.5	1363.4	76.5		✓
13	10	1.5	1364.9	68.9	1.5	1365.7	72.5	✓	
13	10	2.2	1365.7	70.6	1.5	1365.7	72.5		✓
13	6	1.5	1365.9	66.4	1.5	1366.6	69.8	✓	
13	6	2.3	1366.6	67.8	1.5	1366.6	69.8		✓

One observation from Figure 5.19 is that Imagine viewsheds are consistently larger than those from ArcGIS with the same input DEM. With equal relative height, all 12 of the Imagine viewsheds are larger, and with equal absolute height, 11 of the 12 Imagine viewsheds are larger. The only exception is at Site 1 with the 30-m DEM.

The effect of increasing the spatial resolution of the DEMs is to, generally, decrease the viewshed area. The mean visible area with the 30-m DEMs is 45.7 km^2, and it decreases to 44.1 km^2 with the 10-m DEMs and to 41.6 km^2 with the 6-m DEMs. However, *t*-tests found no significant differences in the overall mean visible area at a 95% confidence level among these

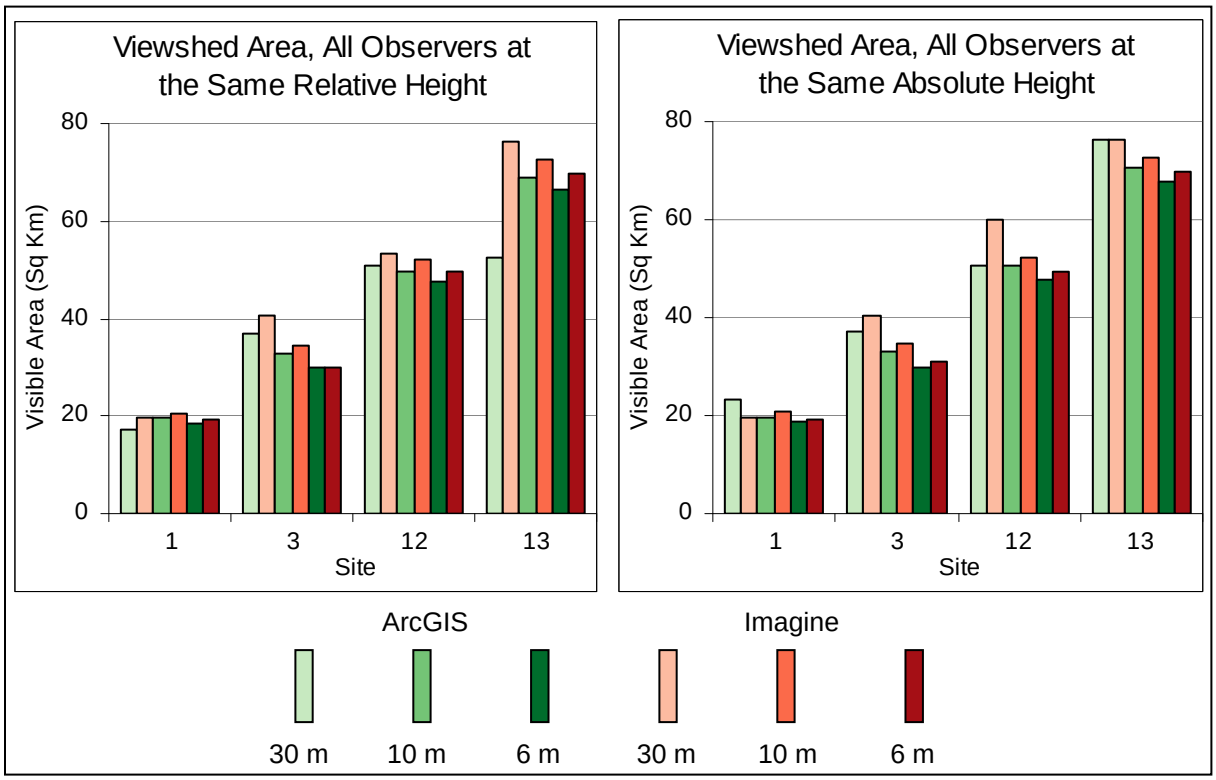

Figure 5.19: Graph of visible areas by observer height, software system, DEM resolution, and site.

DEM resolutions. When analyzed by site, only Site 3 viewsheds were significantly different by resolution, with p-values ranging from <.001 to .004 for 2-tailed tests. Mean visible area here is 38.8 km^2 with the 30-m data, 33.8 km^2 with the 10-m data, and 30.2 km^2 with the 6-m data.

ArcGIS and Imagine viewshed sizes were compared for each set of equal inputs (DEM resolution, observer location and height). The differences in visible areas are summarized by descriptive statistics in Table 5.6. Mean differences decrease as resolution increases. The largest differences and greatest range are found with the 30-m data. Although these statistics are aspatial and are not informative as to the locations or spatial agreement of the viewsheds, they do hint that higher resolution DEMs will generate more similar viewsheds in the two software programs. Viewsheds generated from observers with equal relative height have greater mean differences,

for all resolutions, than those with equal absolute height. Even though the Imagine viewsheds tend to be larger than the ArcGIS viewsheds, *t*-tests indicated no significant differences at a 95% confidence level in mean visible area with the same inputs.

Table 5.6: Differences between ArcGIS and Imagine viewshed sizes (in km^2).

	Same Relative Height			Same Absolute Height		
DEM Res. (m)	Mean (km^2)	Min (km^2)	Max (km^2)	Mean (km^2)	Min (km^2)	Max (km^2)
All	3.9	0.1	23.9	2.3	0.2	9.4
30	8.0	2.2	23.9	4.2	0.2	9.4
10	2.1	0.9	3.6	1.5	0.9	1.9
6	1.5	0.1	3.4	1.3	0.4	2.0

The average levels of spatial agreement between ArcGIS and Imagine viewsheds across the four sites are reported in Table 5.7. Areas predicted visible only by Imagine were about twice as large as those predicted only by ArcGIS, on average, which is not surprising since Imagine viewsheds are larger than those from ArcGIS. Agreement ranged from 49.4% to 94.1%, the overall average agreement between the algorithms was 86.7%, the median level of agreement was 92.3%, and 95.0% of ArcGIS viewsheds were bounded by Imagine viewsheds, i.e., the delineated Imagine viewshed areas contained 95.0% of ArcGIS viewsheds.

Table 5.7: Mean values of spatial agreement between ArcGIS and Imagine viewsheds.

DEM Res. (m)	Visible by Imagine only	Visible by ArcGIS only	Visible by Both (Agreement)	ArcGIS Contained within Imagine
All	9.1%	4.2%	86.7%	95.0%
30	16.8%	9.3%	73.9%	88.5%
10	5.6%	1.5%	92.8%	98.4%
6	4.8%	1.9%	93.3%	98.0%

Data resolution proved to be extremely important in viewshed agreement. Large increases in agreement occur with the 10-m DEMs compared to the 30-m DEMs. The average viewshed area unique to Imagine was reduced by two-thirds, and the area unique to ArcGIS dropped from

9.3% to 1.5%. Agreement increased nearly 20 percentage points, from 73.9% to 92.8%, and a *t*-test found that this difference in means was statistically significant ($p = .008$ for a 2-tailed test). By increasing DEM resolution from 30 to 10 m, the ArcGIS viewshed area contained within the Imagine viewsheds increased by 9.9 percentage points. However, increasing the resolution from 10 m to 6 m had marginal effects. Although it did improve the area of overlap by half a percentage point (92.8% to 93.3%), this difference was not statistically significant ($p = .314$ for a 2-tailed test).

The results for each site are graphically displayed in Figure 5.20. It is clear that variations in spatial agreement exist from site to site, especially with the 30-m data. The percent of visible areas unique to Imagine range from 9.1% at Site 3 to 34.5% at Site 13 with the 30-m DEM with equal relative heights, and the percent of visible areas unique to ArcGIS range from 0.6% at Site 3 to 25.2% at Site 1 with the 30-m DEM with equal absolute heights. Agreement was below 50% (49.4%) at Site 1 with the 30-m DEM with equal relative heights, and as high as 90.3% at Site 3. Measures from the 10-m and 6-m DEMs are comparable, and the results from relative and absolute heights are stable from site to site with a 10-m or 6-m DEM.

It was demonstrated in Table 5.7 that mean viewshed agreement increased as DEM resolution increased. When analyzed by observer height, greater agreement between viewshed algorithms occurred with equal absolute heights, as opposed to equal relative heights, for all three data resolutions (Table 5.8). But these differences in means are not statistically significant based on *t*-tests at a 95% confidence level.

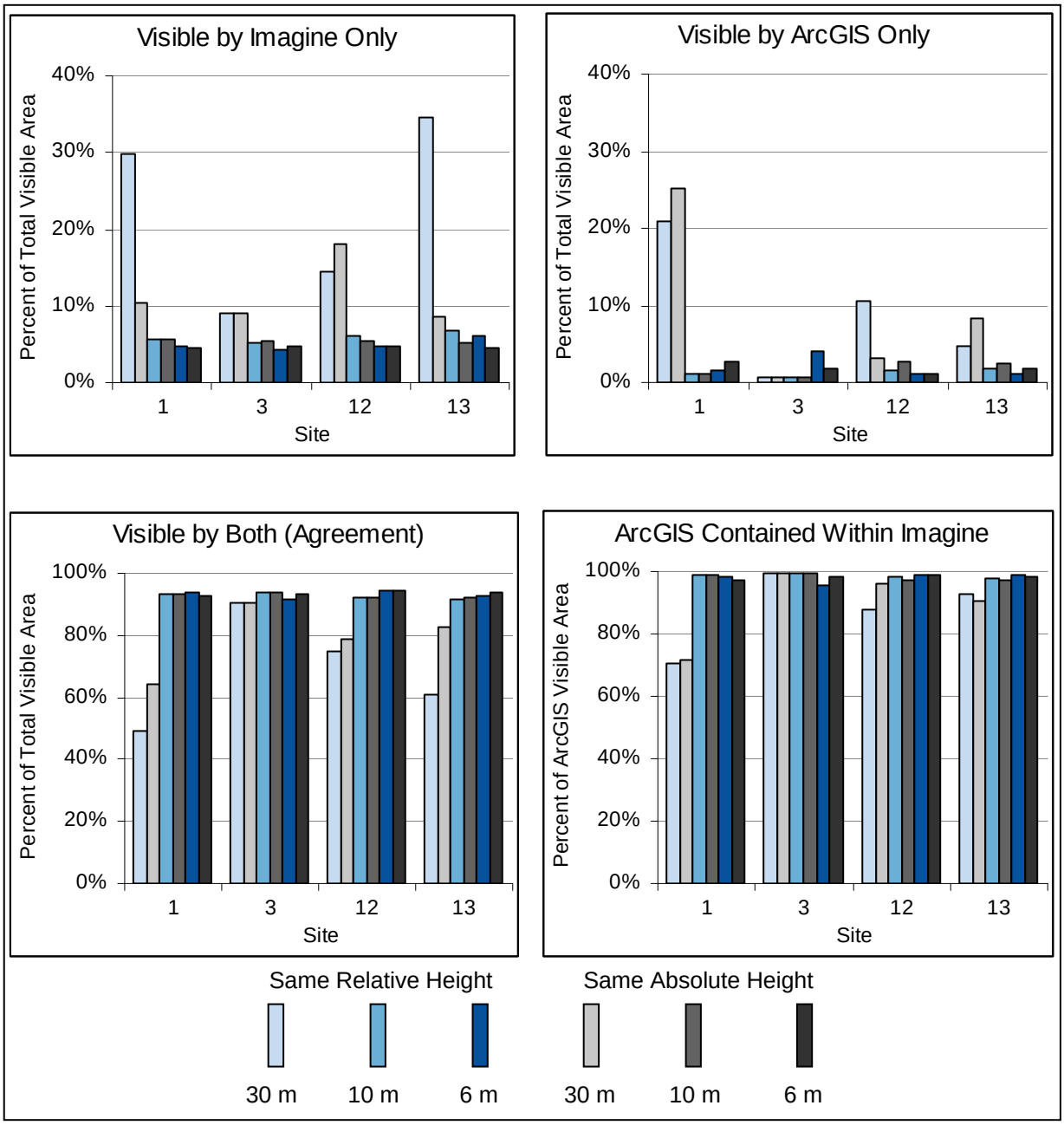

Figure 5.20: Graph of spatial agreement between ArcGIS and Imagine viewsheds.

Table 5.8: Mean values of spatial agreement by observer height and DEM resolution.

	30-m DEM		10-m DEM		6-m DEM	
	Rel.	Abs.	Rel.	Abs.	Rel.	Abs.
Visible by Both (Agreement)	68.8%	79.1%	92.7%	92.9%	93.0%	93.5%

An example of a statistically "average" 30-m viewshed comparison (Table 5.7) is provided in Figure 5.21. The viewsheds were generated in ArcGIS and Imagine from Site 12 with observers having the same relative height (1.5 m) above the ground. As seen in the main image, as well as in the secondary image, small areas of disagreement commonly occur along the borders of viewsheds. In these locations, it may be enough to just consider the viewshed boundaries as somewhat uncertain or fuzzy. However, there are large areas of disagreement that are particular to a certain software program and are not simply boundary issues. For example, west of the viewpoint is a large area predicted visible only by ArcGIS (in yellow), and there is a large area to the east that is visible only by Imagine (in light blue). These large areas of disagreement are displayed as clumps of red in the secondary image.

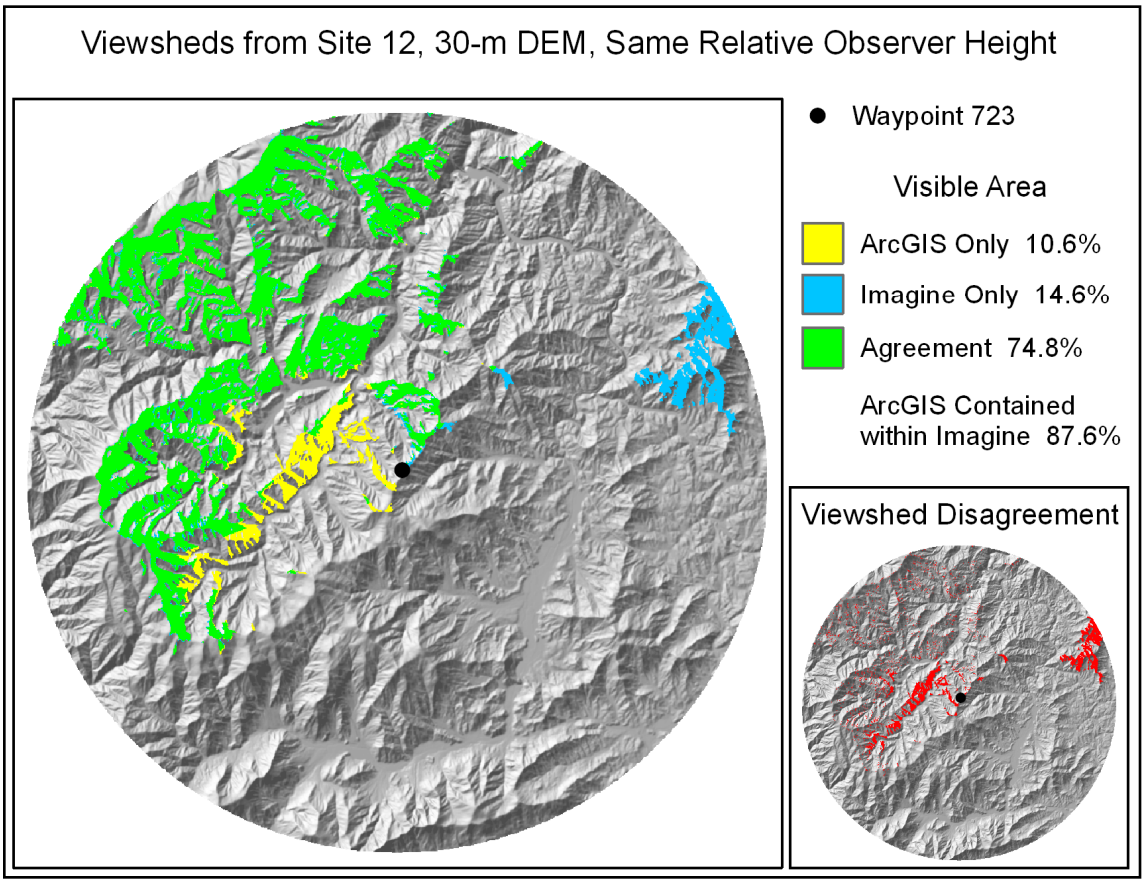

Figure 5.21: Viewshed agreement between ArcGIS and Imagine from Site 12 with a 30-m DEM.

Visibility along Transect 1, from Waypoint 616 to its end, progressed as follows: ArcGIS visible, visible by both programs, Imagine visible, not visible, ArcGIS visible, visible by both, ArcGIS visible (Figure 5.22). Visibility along Transect 2 alternated between ArcGIS-visible and visible by both programs.

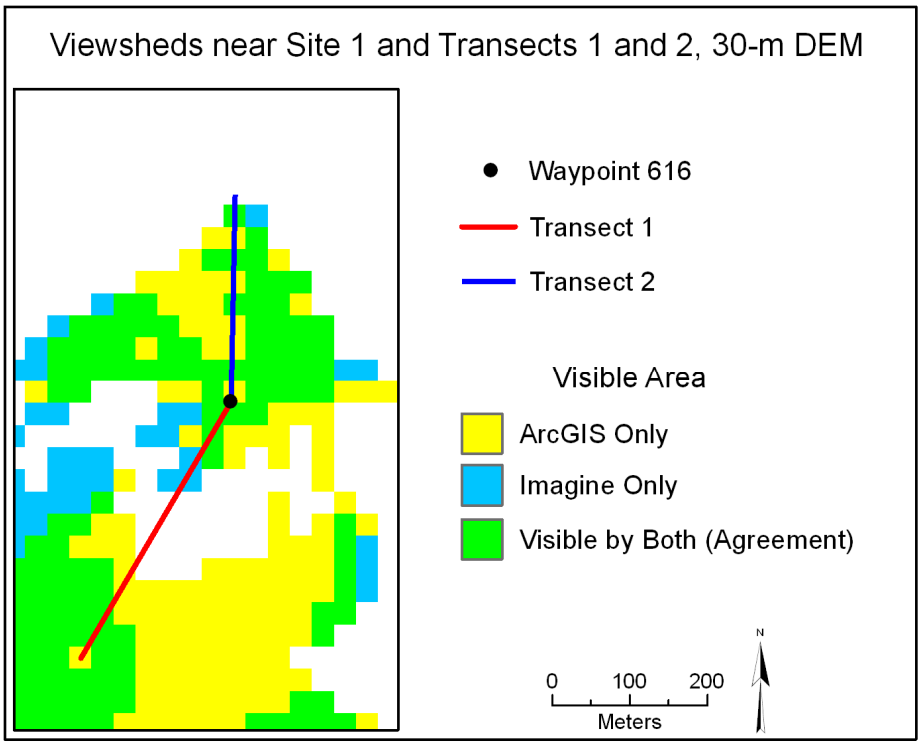

Figure 5.22: Viewshed agreement along Transects 1 and 2.

ArcGIS/Imagine Viewshed Comparisons: Agreement from Elevation Profiles

Elevation values varied, when sampled at DEM grid crossings, depending on whether the z-values were interpolated or not. Along Transect 1, the range of differences of the 21 points was 17.9 m, with the interpolated value as much as 10.1 m lower than the cell value and as much as 7.8 m higher than the cell value. On average, the two values were 3.8 m apart. The ArcGIS interpolated elevation and Imagine non-interpolated elevation values at these points are illustrated in Figure 5.23. The interpolated z-values clearly have a smoother profile along the

transect, whereas the cell values utilized by Imagine create a blocky, stepped appearance. At the 9 points along Transect 2, the range of differences was 15.8 m, and the average difference between interpolated and non-interpolated elevation was 6.6 m.

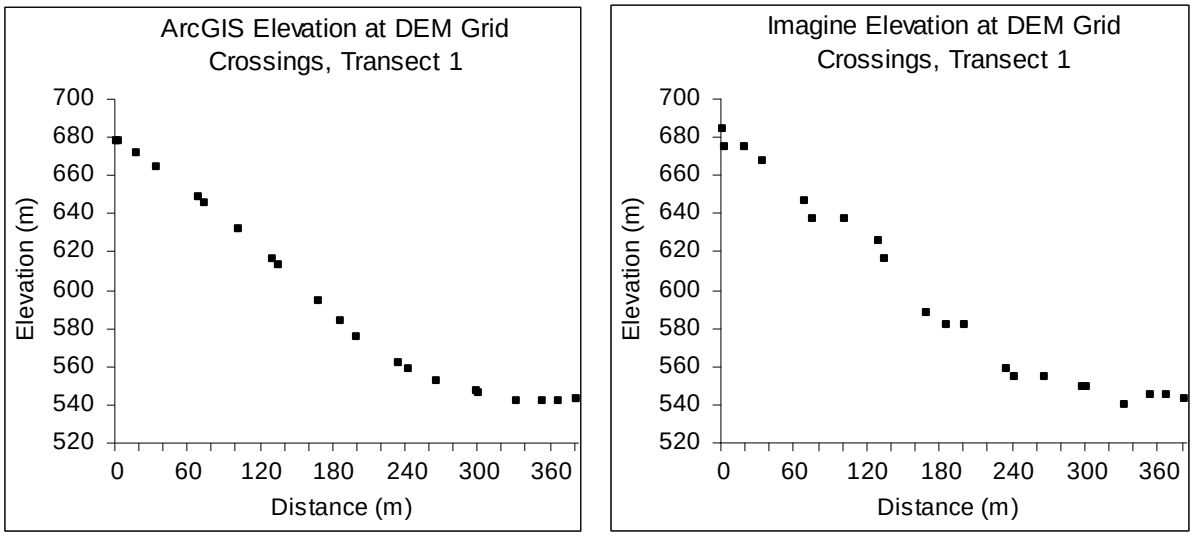

Figure 5.23: Elevation profiles along Transect 1, from ArcGIS (left) and Imagine (right).

The elevation profiles along Transect 2 simulate the line of sight from the observer across the terrain (Figure 5.24). Elevation was sampled at DEM grid crossings, according to the algorithm parameters. The discrete interpretation of the DEM in Imagine creates a stepped profile. While the geometry of the re-created ArcGIS profile and the illustrated viewshed results match, understanding the Imagine viewshed results, when examining the re-created profile, is not as clear. For example, it is surprising that the DEM cell in which the observer is located is considered not visible by the Imagine viewshed function. It is not entirely clear how each cell is evaluated for visibility.

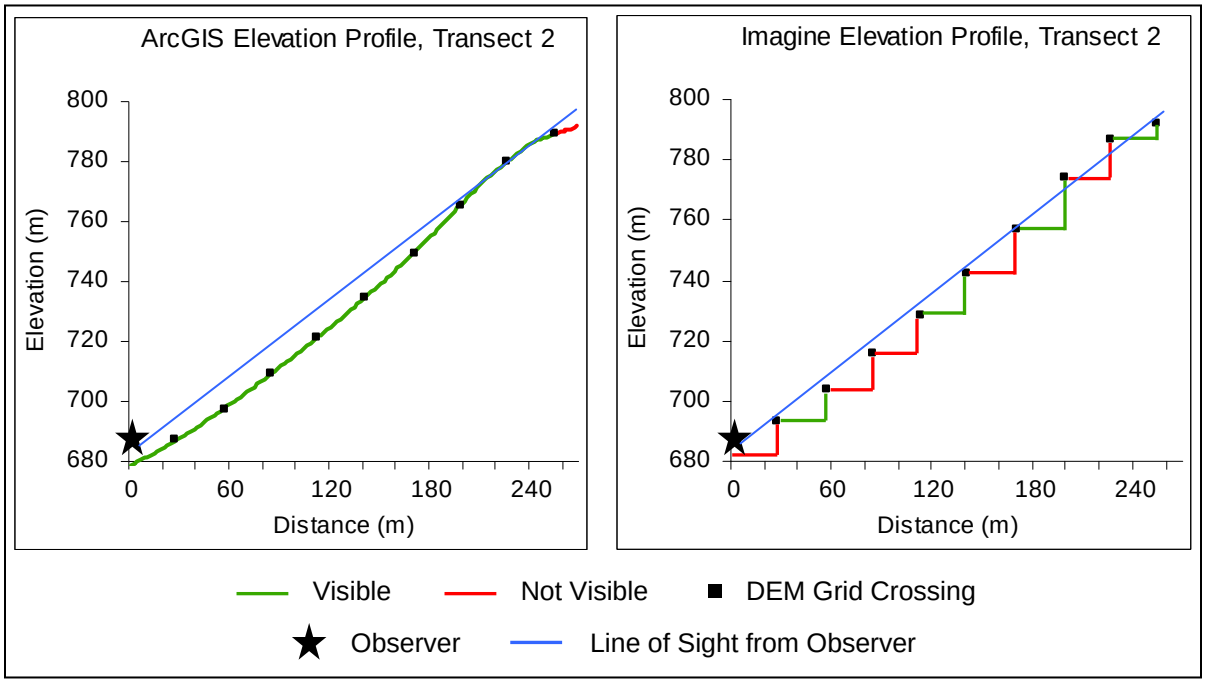

Figure 5.24: Elevation profiles and viewshed results along Transect 2, from ArcGIS (left) and Imagine (right).

Summary and Conclusions

The ESRI viewshed function is a good tool, and it has been demonstrated to be more accurate than ERDAS and IDRISI algorithms when compared to field-surveyed viewsheds (Riggs and Dean, 2007). Since LoSs are vector data, visibility can be determined at fine scales. In some circumstances this could be a disadvantage, as there are an infinite number of lines that could be drawn outwards from an observer. For visibility across a large area, the viewshed is more appropriate. Viewsheds are quicker and simpler to generate than vector LoSs, but the ArcGIS LoS output is richer in information. A summary of pros and cons is listed in Table 5.9.

The LoS function is a very nice bonus, since many GIS programs do not include a vector visibility function, but users could be misled by results if they are not fully informed. There are at least four potential pitfalls, which include: (1) the cartographic representation (red/green line)

Table 5.9: Pros and cons of the ArcGIS viewshed and LoS functions.

Viewshed	LoS
Pros	
▪ Commonly used in various applications and implemented in numerous GIS software.	▪ Vector outputs do not have the resolution constraints of raster outputs.
▪ Quick and easy: inputs are simple and easily generated.	▪ Output provides useful information: visibility along LoS and obstruction points are very helpful.
▪ Good for general visibility and OK for specific targets.	▪ Good for specific targets.
Cons	
▪ Cell visibility is somewhat arbitrarily determined.	▪ More time intensive and challenging to create precise input lines.
	▪ Not designed for general visibility.

of the LoS may disagree with the actual result that is written to the attribute table; (2) obstruction points are optional but should be standard output; (3) the easiest way to create an LoS is by digitizing, but this method is imprecise and should only be used to get a general idea about visibility; and (4) a digitized LoS is a graphic and not a shapefile, which is a serious limitation.

Visibility results can be dependent on the function used and the type of elevation data structure. If a target is above ground level, there is more uncertainty as to its true visibility if a TIN model is used, even though agreement between LoS and viewshed with TINs can be expected to be greater than 75%. There is greater agreement between the LoS and viewshed algorithms if a DEM is used, as long as two factors are accounted for. The target must be above the ground level, even by a decimeter, and one should investigate the possibility that obstructions are very near targets, which makes the masking of targets questionable. When these issues are considered, the average viewshed/LoS agreement with a DEM is 99.62%, it is 92.19% with a TIN, and these differences between the data structures are significant. Viewshed/LoS agreement with DEMs was significantly better for targets 3-m high than 0.1-m high. This is supported by the results reported by Swanson (2003), that viewshed accuracy improved with higher targets.

One potential problem with using TINs in ArcGIS is that viewshed results are rasters of square cells. This mixing of data models, at the least, means that the spatial structure of the output is different from the input.

Another factor is the method of connecting lines between the observer and LoS targets. The method used in this study was to obtain X,Y coordinates to the 4th decimal place (tenth of a millimeter) and connect the coordinates with a function in Hawth's Analysis Tools. An alternate approach was tried. The ET GeoWizards package (www.ian-ko.com), an ArcGIS utility, will connect points (100 maximum points in the free version). In the original test using Waypoint 709, the 30-m DEM, and a target height of 0 m, LoS/viewshed agreement was 61.78%. From the 240 targets that disagreed in this test, 60 were selected and connected to the observer with ET GeoWizards. The LoS function was run, and of the 60 targets, 11 (18.33%) were deemed visible and 49 (81.67%) were still not visible. Assuming these statistics would hold true for the remainder of targets, using this method of creating LoS inputs would improve viewshed/LoS agreement from 61.78% to 68.79%. Of the 49 targets that were still considered not visible by LoS, 47 (95.92%) of the obstructions occurred within 0.1 m of the target. It seems that the method of connecting points for LoS analyses does matter, but not nearly as much as whether targets are raised above the ground, and overlap of targets and obstructions still occurs. Since ArcToolbox does not have a built-in function to connect points as lines, another option would be to write Visual Basic code to perform this task.

The resolution of the elevation models had no statistically significant effect on viewshed/LoS agreement. Terrain, and the observer's position within the terrain, apparently did have a significant effect on agreement. Significant differences occurred among all three sites with TINs, and agreement was significantly different between Observers B and 709 with DEMs.

The common result was that lower agreement occurred with Observer 709 in the rugged terrain, and the highest level of agreement occurred with Observer B, overlooking the valley from a hillside. These results seem to support those reported by Swanson (2003), that viewsheds were less accurate in rough terrain. The greatest source of uncertainty in the different visibility functions was the use of a TIN model.

Other tests provided inconclusive results. Agreement between viewsheds and vector LoSs across an area were quantified along transects. This method of evaluating algorithm agreement sometimes resulted in higher levels of agreement than target comparisons, but sometimes not. Some statistically significant differences were found. Points that agreed on visibility had a steeper slope, on average, than those that disagreed on visibility. Among points that disagreed between LoS and viewshed, those deemed visible by LoS but not visible by viewshed were lower in elevation and had steeper slopes. Despite these statistically significant findings, it is not clear that any meaningful conclusions can be drawn from them. A positive result of these tests is that they provided examples of why a viewshed boundary should be considered fuzzy.

Recreating the logic of visibility through elevation profiles was used to examine viewshed/LoS disagreements. These profiles did not provide conclusive results to shed light on the reasons for disagreements. In addition, it seems that the vector LoS function does not evaluate a TIN at edge and node crossings only. If this is the case, it means that Yoeli's (1985) sampling algorithm is not used, and this adds even more uncertainty to visibility with a TIN.

This study found that the average spatial agreement between ArcGIS and Imagine viewsheds was 86.7%. These results are similar to those reported by Riggs and Dean (2007), who found the level of spatial agreement between the viewshed functions to be 89%. An additional measure used in this study, but not reported by Riggs and Dean (2007), is how much

the smaller viewsheds are contained within, or bounded by, the larger viewsheds. In these tests, 95.0% of ArcGIS viewsheds were contained within Imagine viewsheds.

Data resolution was important in viewshed agreement. Spatial agreement with 10-m data was much higher than with 30-m data, increasing from 73.9% to 92.8%, but increasing the resolution from to 6 m did not produce any significant improvements. Riggs and Dean (2007) did not explicitly report how agreement between viewshed functions varied with resolution, but they did report marked changes in viewshed accuracy with varying DEM resolutions from ArcGIS and Imagine. With the seven different resolutions tested (from 1 m to 20 m), they reported that ArcGIS accuracy ranged from 77% to 85% and Imagine accuracy ranged from 66% to 83%. Accuracy declined as resolution became coarser than 4 m, which was the resolution that most closely matched the input data.

It is not surprising that viewshed boundaries between programs may have some small disagreements on a pixel-by-pixel basis as to exactly where the visible areas are delineated. One could consider these regions to have uncertain or fuzzy boundaries. While these were encountered, more concerning were cases in which large areas of disagreement were found that were not related to simple boundary issues. These were also found by Riggs and Dean (2007), who attributed these viewshed disagreements to “fundamental differences in the viewshed algorithms used by the various software systems.” These large, non-boundary disagreements contributed to the high variability among the sites, especially with 30-m DEMs. For example, there is a low level of agreement at Site 1 with 30-m data because there is a linear region extending southeast from the observer, and north of that line are areas visible only by ArcGIS. This is a large area of disagreement. At Site 13, nearly all viewshed regions east of the observer are visible only by Imagine. There is also a linear region extending northwest from the observer,

bounding an area visible only by ArcGIS. Elevation and slope data were examined here, and the vista from the observer was simulated in ArcScene. However, it is not clear why the Imagine viewshed indicates that the region is not visible. Elevation profiles along transects seemed to verify ArcGIS viewshed results, but they were less helpful in confirming Imagine results.

There were a number of interesting observations that were found to be not statistically significant. For example, higher resolution DEMs tended to generate smaller viewsheds, and there were higher levels of agreement between ArcGIS and Imagine when observers had the same absolute heights compared with equal relative heights. This latter observation was surprising, because the assumption was that observers with the same relative height would create the more fair comparison, since viewshed calculations are based on point-to-point, or relative, elevation differences. The fact that these findings were not significant could be due to the small sample sizes. Similar data with larger sample sizes will have greater significance, so a larger study could discover whether the differences are likely to be real or are due to chance.

Given the accuracy results of ArcGIS and Imagine viewsheds reported by Riggs and Dean (2007), viewshed accuracies from various DEM sources and resolutions found by Maloy and Dean (2001), and the viewshed agreement between ArcGIS and Imagine found in this study, it would be helpful to calculate estimates to help users understand the confidence they should have in their viewshed results. The resolution and accuracy of elevation data have a tremendous impact on viewsheds. Riggs and Dean (2007) found that even small amounts of DEM error could severely decrease viewshed accuracy. As a practical example, a viewshed created from the NED 10-m DEM was only 54% accurate, as compared to the 83% accuracy of the viewshed created from the custom 10-m DEM produced by Riggs and Dean from a field survey. Maloy and Dean (2001) found that 81.5-m DEMs were less accurate than 30-m DEMs, but oversampling the 30-m

DEM to a finer resolution did not increase accuracy. Similarly, Riggs and Dean (2007) found that an optimum DEM resolution is one that most closely matches the spacing of the input data, and oversampling to a finer resolution does not improve viewshed results.

The source of the NED data used in this study is lidar. The density of lidar points in the study areas is not known but can be roughly estimated. The USGS uses the lidar data to create DEMs of approximately 3-m resolution. A single, 0.6 km^2 region in the eastern study area (Haywood County) was found to have a lidar point density of 1 point per 20.4 m^2, which would approximate a DEM with a post spacing of 4.5 m. Lidar obtained in eastern North Carolina from the same company (Fugro EarthData) that collected lidar in the study area had an average spacing of 3 m (NCFMP, 2003). Hodgson et al. (2003) used Fugro EarthData lidar for an area in North Carolina that had a spacing of 3.4 m. Thus, it can be assumed that DEMs of 3-4 m resolution closely match the lidar source data. The finest resolution used in this study (6 m) should be more accurate than the 10-m and 30-m DEMs, which have been generalized even more than the 6-m DEM.

Riggs and Dean (2007) found that ArcGIS viewsheds were more accurate, compared to field-surveyed viewsheds, than Imagine viewsheds. At the optimum spatial resolution, ArcGIS was 85% accurate and Imagine was 83% accurate. Average accuracy from the seven different resolutions used was 82% for ArcGIS and 76% for Imagine. An examination of their results indicates that Imagine decreased in accuracy faster than ArcGIS as spatial resolution became coarser. Riggs and Dean (2007) do not report the accuracy of their DEMs, but the RMSE of their TIN model was 0.28 m, which is very similar to the North Carolina lidar requirements of 0.25 m (Fugro EarthData, 2006). The study areas in GRSM are just as rugged, if not more so, than the

area surveyed by Riggs and Dean (2007). Therefore, the accuracy of ArcGIS viewsheds in GRSM are likely less than 85% accurate, on average, and Imagine less than 83% accurate.

Based on these comparisons of accuracy and agreement, one could adopt some guidelines for estimating viewshed accuracy. A DEM of high accuracy, such as one derived from lidar, will be most accurate when its resolution most closely matches the density of its source. Lower resolution DEMs will generate less accurate viewsheds. One could assume that ArcGIS viewsheds will be 85% accurate or less, and Imagine viewsheds 83% accurate or less, with a highly accurate DEM. With DEMs derived from more traditional means (photogrammetry, contours, etc.), accuracy may be only 50-60%, based on the finding by Maloy and Dean (2001) and Riggs and Dean (2007). As resolution becomes more coarse, Imagine viewsheds will drop off in accuracy more than ArcGIS viewsheds. With a lidar-derived 10-m DEM, Imagine viewsheds may drop to 76% accurate, and ArcGIS may drop to 83% accurate, approximately. Overall, agreement between the two programs can vary from around 70% to over 90%.

The ArcGIS visibility functions are useful tools with many options. This study found that ArcGIS viewshed and LoS results often have a high level of agreement (85+% agreement in 75% of cases), but discrepancies do exist. This study also found that the average spatial agreement between Imagine and ArcGIS viewsheds was 86.7%. It is hoped that software vendors will provide more thorough documentation on the details of their visibility algorithms, so that users will be able to more effectively interpret results, understand limitations, and provide interested parties with an estimate on the accuracy of the results.

CHAPTER 6

THE EFFECTS OF INTERPOLATION TECHNIQUES AND DATA MODELS ON VIEWSHEDS

Lockhart, D. To be submitted to *Landscape Analysis using Geospatial Tools: Community to the Globe* (M. Madden and E. Allen, editors), Springer-Verlag.

Introduction

Data describing the surface of the earth can be represented and stored in a variety of digital models or structures. Elevation data can be stored as contour lines of equal elevation, a uniformly spaced horizontal grid of elevation values as a raster digital elevation model (DEM), irregularly spaced mass points, or contiguous, non-overlapping triangles as a triangulated irregular network (TIN) (Maune et al., 2001a; Kidner et al., 2000).

The two basic data models used for visibility analyses are the raster DEM and vector TIN. A model is a representation of an unknown reality, and multiple representations or models can exist (Goovaerts, 1997). Models simplify reality. This may be necessary for several reasons. The attribute of interest may be extremely complex, and methods of recording or representing it accurately may not be feasible with current technology. An attribute, such as elevation, is a continuous phenomenon that could theoretically be measured at any point. Since points are 0-dimensional, it is impossible, practically, to sample every point within a given area. Even an elevation data model that covers a whole area, such as a TIN or DEM, has values recorded at specific points (nodes or posts) within said area. These models are considered as continuous fields, since they do provide values for any location within a given area, but the underlying data are really discrete measurements (Longley et al., 2005; Fisher and Tate, 2006).

Point data can be used to create a continuous surface representing elevation (Franke, 1982). When a DEM is generated from lidar mass points, the surface must be interpolated (Lloyd and Atkinson, 2002; Su and Bork, 2006). This is akin to an estimation or prediction. Watson (1992) refers to interpolation as “an informed estimate of the unknown.” In the interpolation of an elevation surface, sample points are points with a measured z-value. The sample points are used to estimate the elevation at locations that do not have measured z-values (Yilmaz, 2007).

These sample points can be regularly spaced, irregularly spaced, or have any other spatial pattern. This depends on the methods and technologies that are used to sample elevation. One could obtain z-values in the field at regular or irregular intervals with GPS. Regularly or irregularly spaced samples can be obtained with photogrammetry. Lidar and radar systems generate irregularly spaced points (Maune et al., 2001a).

The data structures of DEMs and TINs are fundamentally different. A DEM is a raster model of uniformly sized square cells (Longley et al., 2005). This is a very common model for publicly available digital elevation data. The DEM structure has appeal because it is simple, but it may not realistically represent the terrain. There is some mismatch since the earth's surface is not composed of square cells, although this problem can be reduced with DEMs of finer spatial resolution (smaller cells). A DEM is composed of cells that may reflect an average elevation, elevation at the cell centroid, or elevation at one of the grid corners. This is a complication, and in fact, the raster model can store two disparate types of data. The first is the pixel interpretation, in which a raster cell is considered to represent a single value, as in a traditional land use/land cover map. The DEM may be interpreted as a group of discrete cells, with elevation treated as homogeneous in each pixel (Figure 6.1). The second interpretation of a raster cell is the lattice, in which a raster value represents an attribute at a specific location, such as the cell centroid or grid corner. In this continuous, or surface, interpretation of a DEM, elevation is considered as heterogeneous in each pixel, with the potential for a different value at any specific point in a cell (Maune et al., 2001a; Riggs and Dean, 2007; Wise, 2000; Kidner et al., 1999). These different interpretations can lead to problems, as various software functions make different assumptions and treat raster data differently. For example, viewshed algorithms implemented in GIS programs may treat DEMs differently and produce varying results (Fisher, 1993).

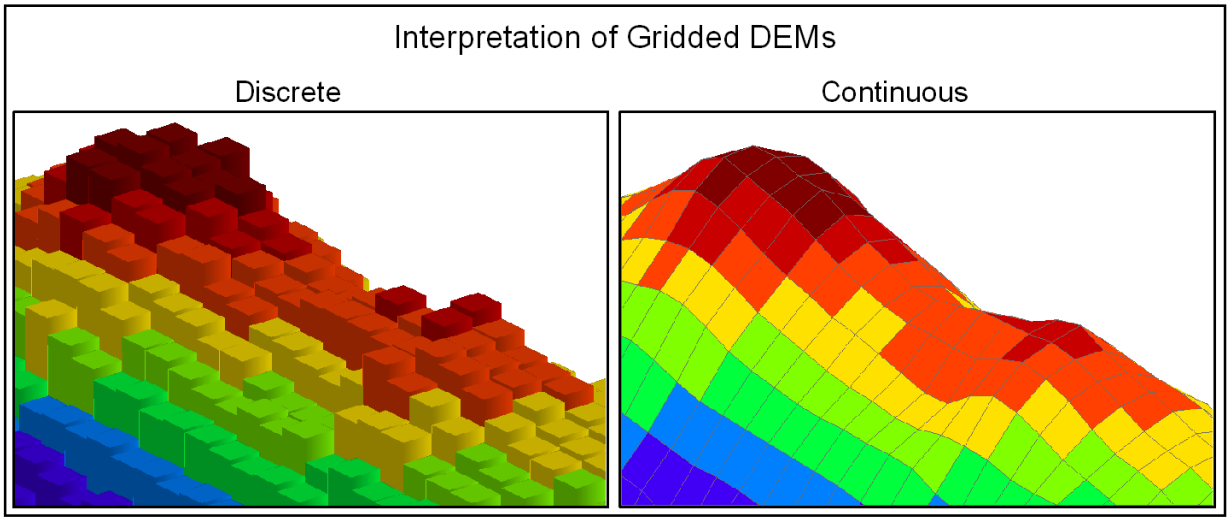

Figure 6.1: Discrete and continuous surface interpretations of a DEM grid. Adapted from Kidner et al. (1999).

A TIN is a vector model of contiguous triangles developed by Peucker et al. (1978) that relies on Delaunay triangulation. The TIN structure is made up of nodes (triangle vertices), edges (triangle sides), and facets (the triangle planes). A TIN's facet is cast at an angle in 3D space (Maloy and Dean, 2001). Thus, different points on a TIN facet may have different elevations while the TIN surface is assumed to be homogeneous in terms of slope and aspect. The topology of the original TIN structure is maintained by nodes storing information about neighboring nodes (Peucker et al., 1978). Other methods of storing topology exist, as well (Kidner et al., 2000). Storing this information requires overhead, but many have theorized that the TIN structure is superior to a raster model for various representations and analyses, including viewsheds (De Floriani et al., 1994; Dean, 1997; Maloy and Dean, 2001).

One of the major differences in the creation of a TIN versus a DEM is that irregularly spaced input points are retained in the TIN structure and become TIN nodes, but a DEM "loses" these explicit points in the interpolation process. The spacing and distribution of point samples, ideally, would depend on the nature of the terrain. An area with little variation requires relatively

few points to represent the changing ground, but an area with rough topography requires more points to accurately model the terrain (El-Sheimy et al., 2005). Especially important are ridge lines and peaks in a mountainous region (Goodchild and Lee, 1989). The TIN structure is considered to be advantageous when an elevation model is created from mass points from a source such as lidar, because the location of the inputs is retained (Maune et al., 2001a).

It is well known that interpolation methods will produce different elevation surfaces (Franke, 1982; Yang and Hodler, 2000). Many GIS packages offer multiple interpolation routines for creating DEMs (Yilmaz, 2007). Interpolation methods can be deterministic or probabilistic. Deterministic models estimate a single value at an unsampled location and do not consider the potential error of that estimate. Probabilistic, or geostatistical, models do not simply estimate a single value, but provide a probability distribution of possible values (Goovaerts, 1997). Kriging, named for Danie Krige (1951), is a geostatistical method, while inverse distance weighted (IDW) and natural neighbor (NN) are deterministic methods.

One of the first computerized interpolation methods was IDW, developed by Donald Shepard at Harvard University in 1967 and implemented in the SYMAP computer program (Chrisman, 2006). IDW uses weighted averages from surrounding points (Longley et al., 2005). The weight applied to any nearby sample point is inversely related to the distance between the sample and the location of interest, the location where a value is to be estimated. Weight decreases as distance increases, so a closer value will have more influence on the estimated value than a point that is farther away (Doucette and Beard, 2000). The weighting can be controlled by selecting a weighting power, or weighting exponent (e.g., inverse distance *squared*). The greater the exponent, the less influence distant points will have (Yilmaz, 2007). Although this is a straightforward interpolation method, it is not the most recommended technique for elevation

data because it can result in a dimpled surface or “bulls-eyes” on surface and contour maps (Yang and Hodler, 2000; Maune et al., 2001a; Kienzle, 2004).

Natural neighbor interpolates elevation with a weighting technique based on area (Yilmaz, 2007). This method finds the closest neighboring points, the natural neighbors. From a Delaunay triangulation of input points, the location of interest determines its Voronoi neighbors, or closest surrounding nodes. These are the natural neighbors. Only immediate neighbors have any weight, and the weighting of each neighbor is based on the area of overlap between its Voronoi polygon and the estimated point’s polygon, proportional to the overlapping of other neighbors’ polygons with the estimated point’s polygon (Maune et al., 2001a).

Kriging is a technique that incorporates spatial correlation into the weighting of nearby values (Maune et al., 2001a). Advantages of this method are that it is not as arbitrary as some interpolators because the weights are based on the spatial data itself, estimates are unbiased, and confidence levels of the estimates can be determined, to name a few (Oliver and Webster, 1990). Weights are obtained by fitting the best line through a semivariogram (Lloyd and Atkinson, 2006). The semivariogram is a graph of points, in which each point represents a pair of input data (e.g., 2 lidar points). The y-axis is the elevation difference and the x-axis is the distance between the points in each point pair (Longley et al., 2005). The line of best fit, a non-linear curve, is the model that represents the spatial correlation of the input data (ESRI, 2007a). There are many types of kriging (simple, universal, cokriging, disjunctive, etc.), but ordinary kriging is well suited for elevation data (Oliver and Webster, 1990; Maune et al., 2001a).

The literature is replete with studies of the accuracy of various surface interpolation methods, but there is no single method that is the “best” for all situations (Lam, 1983; Doucette and Beard, 2000; Fisher and Tate, 2006). Lloyd and Atkinson (2002) found that kriging

produced a more accurate DEM from lidar than the IDW method, but Su and Bork (2006) reached the opposite conclusion – a DEM derived from lidar by IDW had a lower RMSE than interpolation by kriging. Yang and Hodler (2000) noted that kriging accuracy was "only marginally better" than IDW, in terms of global accuracy measured by RMSE. Kriging did outperform IDW in terms of relative accuracy, which describes the spatial distribution of error, as kriging errors were more evenly distributed and IDW errors were more spatially concentrated (Yang and Hodler, 2000). Some believe that TINs are superior to DEMs. Gong et al. (2000) found that in rough terrain, triangulation methods are preferred to DEM interpolation. Yilmaz (2007) derived surface models from points and reported that triangulation was less accurate than kriging but slightly more accurate than IDW, and natural neighbor was the least accurate of these four methods.

One application that is dependent on terrain representation is the viewshed function. Tests have been conducted using various data structures, resolutions of data, and other variables (Dean, 1997; Kidner et al., 2001; Riggs and Dean, 2007). Inconsistent results have not been unusual. Since different interpolation techniques produce different elevation datasets, a function such as the viewshed, which is a first derivative of elevation data, will certainly be affected (Ervin and Steinitz, 2003). This study does not attempt to answer the question as to which data structure or interpolation method is superior, but provides an example of how choices made in the creation of an elevation model can impact viewshed and other elevation derivatives.

Purpose and Objectives

This study is essentially a demonstration. It is a likely, real world scenario that one has lidar data (or other point data) that needs to be converted into an elevation model such as a TIN or DEM. GIS software, such as ArcGIS, provides multiple options for generating a DEM. The

purpose of this study is to examine how the choices of data structure or interpolation method affect the resulting elevation surface. The objective is to evaluate the implications of these choices through viewsheds.

Bare earth lidar points in an area of rough, mountainous terrain are transformed into the two main elevation data structures used in viewsheds, the TIN and DEM. DEMs are generated with three commonly used interpolation methods from a standard GIS package using default settings to simulate typical GIS users. Then three types of statistical assessments are utilized to compare the resulting elevation models. The effects of the data structures and interpolation schemes are examined by creating and comparing viewsheds generated from these models. It is beyond the scope of this work to exhaustively explain the construction of elevation models and the various interpolation methods available. Readers are recommended to refer to El-Sheimy et al. (2005), Oliver and Webster (1990), Watson (1992), Franke (1982), Lam (1983), Goovaerts (1997), or other works.

Data and Methodology

A dense network of bare earth lidar points were acquired from the North Carolina Floodplain Mapping Program (www.ncfloodmaps.com) for a small area in Haywood County around Site 11, along the eastern border of GRSM (Figure 6.2) (refer to Chapter 3). The study area size is 604 m east-west and 1,021 m north-south, or approximately 0.6 km^2. This area has nearly 200 m of vertical relief (elevation of the lidar points range from 1,344.23 to 1,540.55 m, and data was converted to m from its original format in ft measured to 2 decimal places). The mean elevation is 1,468.1 m, but the z-values have a bimodal distribution. The terrain is rugged, with a mean slope of 19.5°, and slopes are as steep as 57.3° (derived from a 3-m DEM with kriging).

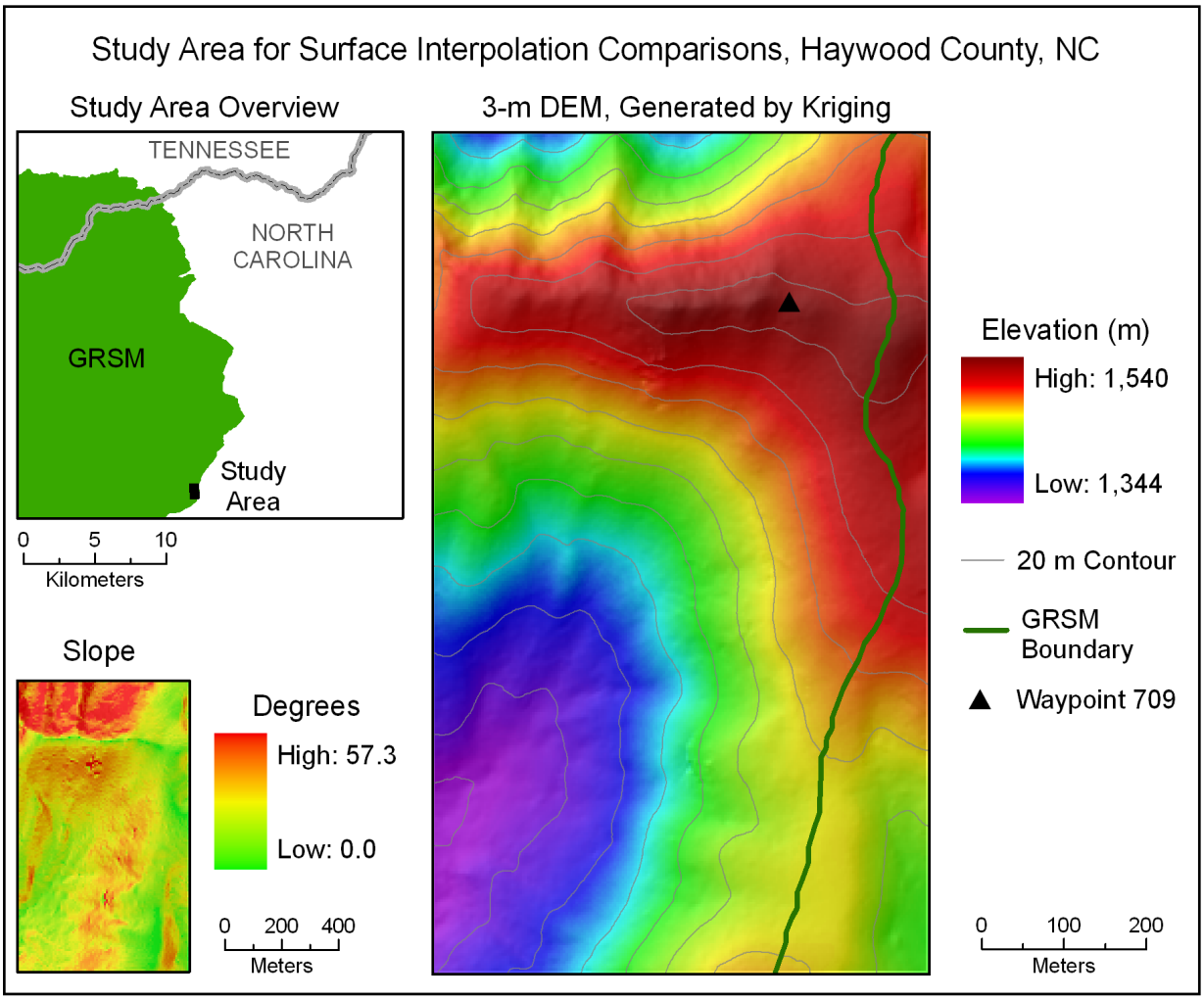

Figure 6.2: Study area.

There are 30,183 lidar points in the study area, which averages to 1 point per 20.4 m^2. The point density varies and is not uniform (Figure 6.3). Although lidar mass points tend to be irregularly spaced by the nature of the technology, some large areas with few or no points (voids) are obvious in Figure 6.3. One reason for these voids is that during data processing, it may be determined that certain lidar returns are from features above the ground, i.e., the lidar pulse did not reach the ground. These data are removed from the bare earth dataset (NCFMP, 2003). To quantify the point density, a grid was created that covered the study area. Each cell of the grid is 10 m per side, so that each cell is 100 m^2 in area (Figure 6.3). The Hawth's Analysis Tools

extension was utilized to count the number of lidar points within each cell. Density ranged from 0 to 18 lidar points per 100 m^2, with a mean of 4.9 per 100 m^2.

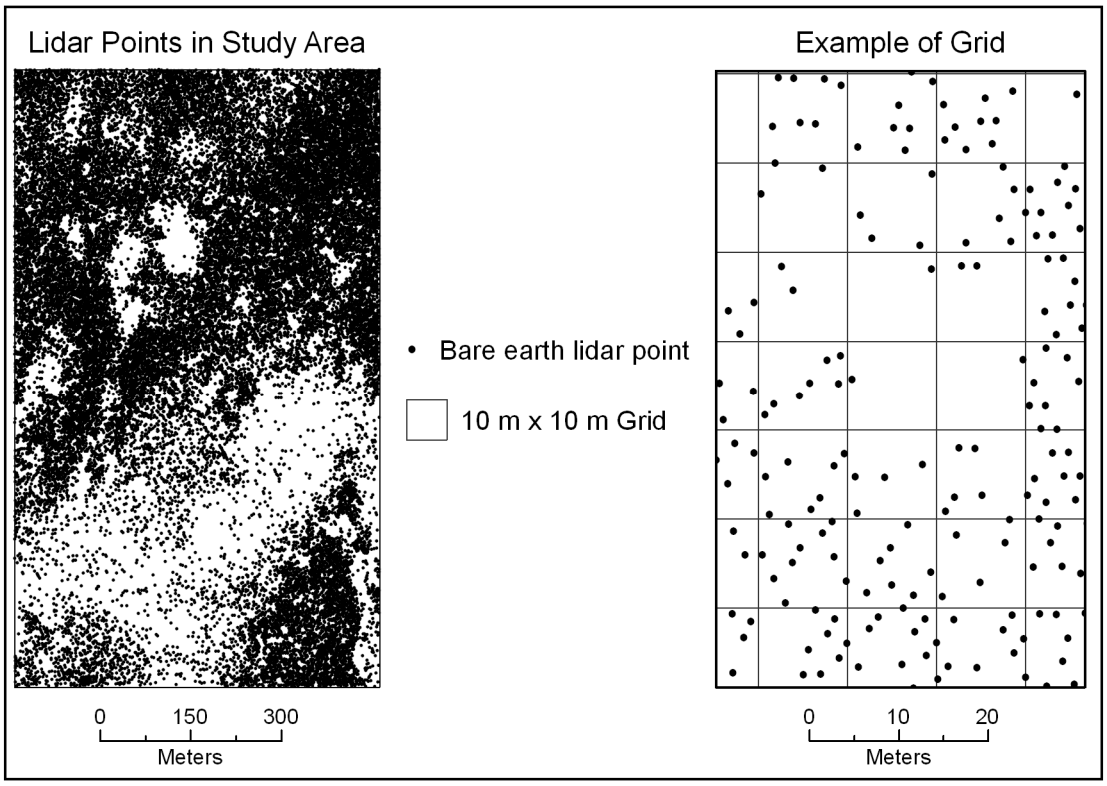

Figure 6.3: Distribution of lidar points in the study area.

A TIN and three DEMs were created from the lidar points in ArcGIS (Figure 6.4). Spatial resolution of the DEMs is 3 m. This spacing was chosen because it is known that the USGS uses this lidar data to generate the 1/9 arc-second NED DEMs, which are approximately 3 m in resolution (refer to Chapter 4). The DEM interpolation methods were IDW, kriging, and NN. All parameters used were the ArcGIS defaults. For IDW, these defaults were 12 points in the search radius and an exponent of 2; for kriging, the defaults were ordinary kriging with a spherical semivariogram model and a 12 point search radius; and for NN, no parameters are selected by the user.

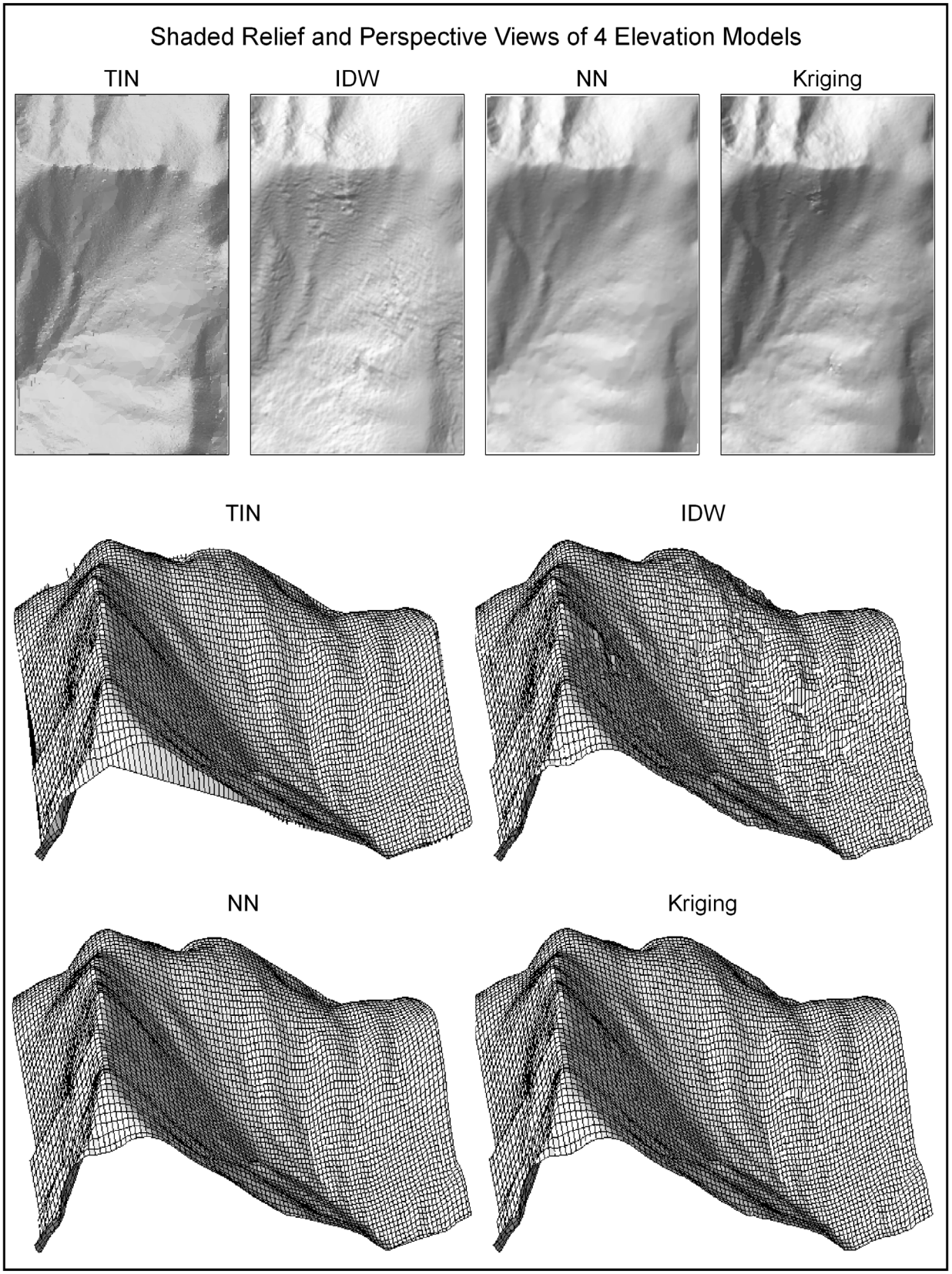

Figure 6.4: Shaded relief planimetric and wire-frame perspective views of elevation models. Perspective views are vertically exaggerated by a factor of 3 for visualization purposes.

The importance of visualizing elevation data and assessing interpolation results by graphical appearance has been promoted by Franke (1982), Wood and Fisher (1993), and Yang and Hodler (2000). A visual examination of the 4 elevation models (Figure 6.4) reveals some differences in surface morphology. There are some notable differences among the models in the upper portion of the south-facing slope of the prominent east-west ridge. Overall, the NN model appears the most smooth, and the IDW model appears the least smooth and most different from the other models.

Three types of statistical assessments were used to compare the resulting elevation models. The first method directly compares all raster pixels of the three DEMs. This was accomplished by simply overlaying the rasters and using raster math to subtract the z-values of one DEM from another (Hirano et al., 2003). This procedure creates a "difference" image. All raster pixels were correctly registered and required no shifting. This process produced three difference images: 1) IDW minus NN; 2) IDW minus Kriging; and 3) Kriging minus NN.

It is assumed that the largest differences between models will occur in areas of the lowest input point density, since the interpolation functions are performing more guesswork where there are fewer data. This assumption is logical and is related to research that found that higher point density led to more accurately interpolated DEMs (Gong et al., 2000). To determine if there is a correlation between source point density and elevation model differences, the grid of 10-m squares was utilized. The raster difference images were converted to vector data, and the values were written to each 10 m × 10 m grid cell with Hawth's Analysis Tools. Since the square polygons of the two layers are of different sizes (3 m versus 10 m), an area weighted mean option in Hawth's Analysis Tools was used to derive a difference image value for each 10-m cell based on the area of the overlapping polygons. Each 10-m grid cell then had data on lidar point

density and a value from each of the three difference images. Difference image values were transformed to absolute values, which indicate the magnitude of difference between each DEM pair. Pearson's correlation coefficients were then calculated in Microsoft Excel between lidar point density and the magnitude of DEM differences for each difference image.

The other two methods used different types of point datasets to compare elevations from the raster and TIN models. Bare earth lidar points are the first type. In the Delaunay triangulation, the input elevation points become TIN nodes, but these input locations and values have no special significance after the DEM has been interpolated (Figure 6.5). The z-values of the TIN nodes are equal to the original z-values of the lidar points. To find the DEM elevation at these points, the raster values were extracted to these 30,183 points using bilinear interpolation. Differences in values among the data models were calculated. The resulting statistics are indicators of how well the interpolation processes retain the source values. This is an approach similar to validation, except that in validation some of the input data is withheld in the interpolation process to determine how well the interpolation estimates elevation at the location of the withheld points (Maune et al., 2001a). In the method used in this study, results will indicate how much the interpolation processes altered the z-values at the input points.

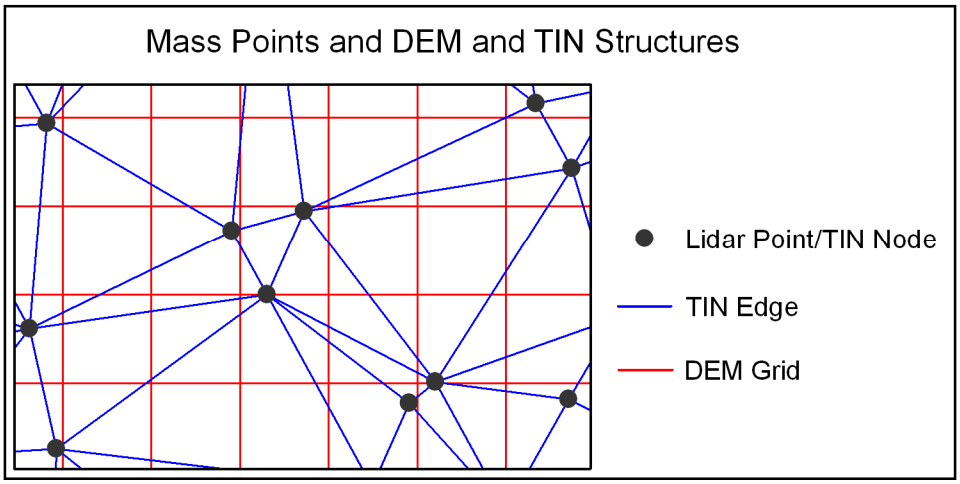

Figure 6.5: Example of mass points and elevation model structures.

The second type of point dataset for surface model comparisons is a point sample along a transect. Transect elevations from various DEMs can provide a quantitative measure, as well as a visual assessment (through profile graphs), of height variability among datasets (Hirano et al., 2003). Elevation comparisons at the input lidar points are mute regarding what happens between the source points, but sample points along transects can provide this information. Two transects were created that passed through areas of various lidar point density, and both lines traversed areas of relatively great elevation change (Figure 6.6). Points were sampled along each line every 10 m, resulting in 71 points along Transect 1 and 84 points along Transect 2. Elevation values were extracted to the points from DEMs by bilinear interpolation and by linear interpolation from the TIN. To test for correlation between point density and elevation model differences, the 10-m grid was employed. The point density value of each grid square was added to sample points along the transects via a spatial join. Elevation values at the sample points were compared among the four data models by subtracting z-values of one model from another. This resulted in six model comparisons (TIN minus IDW, TIN minus Kriging, TIN minus NN, IDW minus Kriging, IDW minus NN, and Kriging minus NN). The relationship between point density and the magnitude of elevation difference was then calculated by Pearson's correlation coefficient.

Once the elevation models were compared, viewsheds were generated in ArcGIS with the models from Waypoint 709, with an observer height of 1.5 m above the ground. These viewsheds demonstrate the impact that different interpolation methods and data structures can have on the viewshed function, even over a relatively short distance and small area.

Due to varying levels of viewshed agreement in the southern region of the study area, a third transect was created, from Waypoint 709 to the southern region, to investigate the cause of disagreement in this area. The line is 801.5 m long. This transect was used to examine the line of

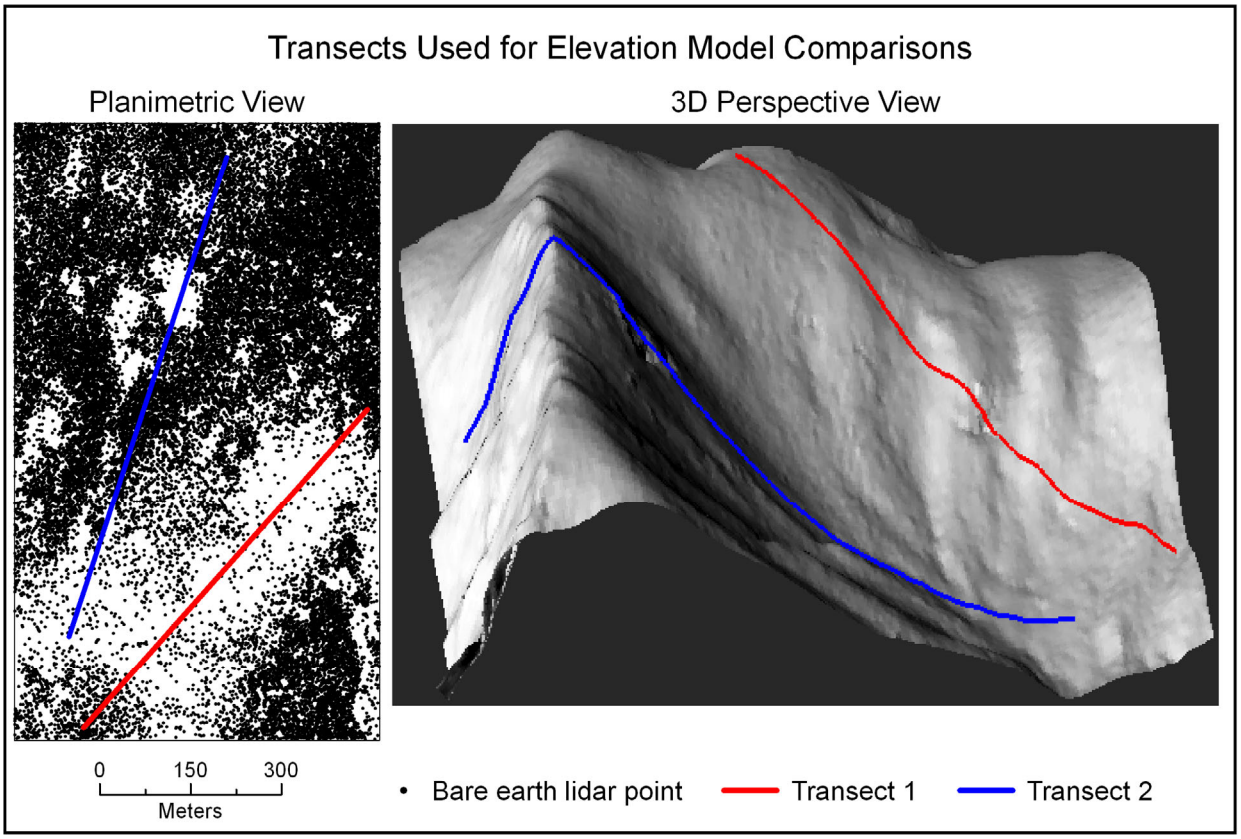

Figure 6.6: Location of transects within the study area. Perspective view is vertically exaggerated by a factor of 3 for visualization purposes.

sight (LoS) from the observer along the four elevation surfaces by creating elevation profiles from each surface. Based on the information available, it is assumed that the ArcGIS viewshed algorithm samples elevation where the LoS crosses a part of the elevation structure, as in the method described by Yoeli (1985). This would occur at TIN edge and node crossings and DEM grid crossings (Fisher, 1993; Huss and Pumar, 1997). Points were created with Hawth's Analysis Tools at all locations where these crossings occurred. This resulted in 322 points from the TIN and 257 points from the DEMs. Elevation values from the TIN and DEMs were extracted to the points with linear and bilinear interpolation, respectively, and the viewshed result (visible or not visible) was extracted to the points.

Results

Difference Images

Three difference images were created by directly comparing each of the three DEMs with one another (Figure 6.7). Pixel values of one DEM, representing elevation, were subtracted from another DEM, producing three difference images: 1) IDW – NN; 2) IDW – Kriging; and 3) Kriging – NN.

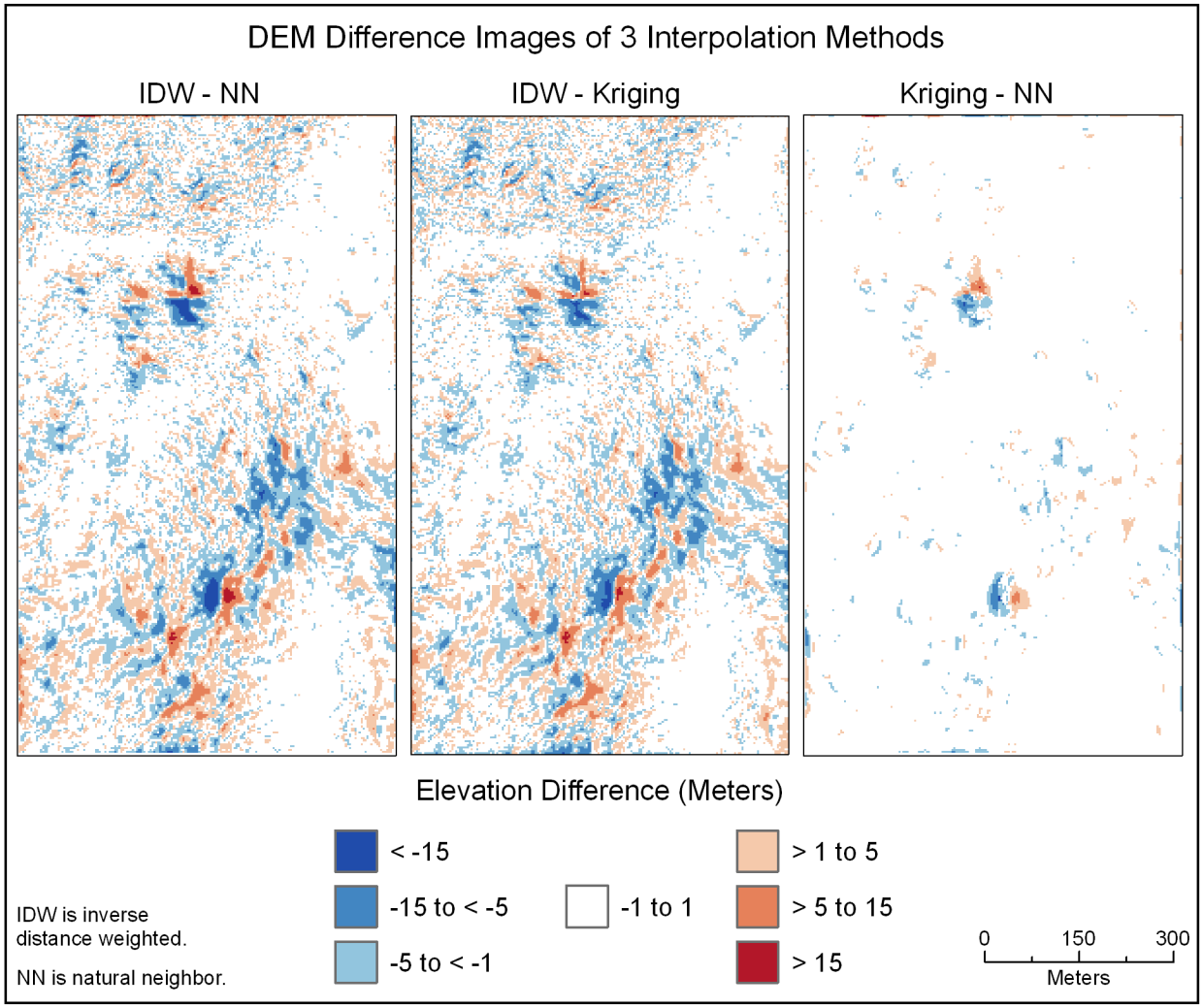

Figure 6.7: Difference images of the three interpolation model comparisons.

Statistics from the difference images are indicators of how much any two DEMs vary from one another on a pixel-by-pixel basis (Table 6.1). The DEMs that are most different are the IDW and NN. These models differ by as much as 33 m in a particular location. The IDW – NN image has the greatest range of values (62.81 m), the mean that is furthest from 0 (-0.12 m), and the greatest dispersion as measured by standard deviation (2.47 m). The negative mean difference indicates that, on average, the IDW z-values are lower than NN values by 0.12 m. The data approximates a normal distribution, with 96.8% of values falling within 2-sigma of the mean (~ -5 to 5 m). The other difference images have similar statistical properties, though less extreme. The IDW – Kriging image falls in the middle of the three comparisons, in terms of its range, mean, and standard deviation, although its mean and standard deviation are comparable to the IDW – NN image. The two models that are most similar are the Kriging and NN DEMs. The mean difference is essentially 0 (-0.01 m), standard deviation is small (0.73 m), indicating that few values are very far from the mean, and this difference image has the smallest range. However, there are some individual pixels that do vary quite a bit between these two models, as the maximum difference is greater than 27 m.

Table 6.1: Statistics from the difference images.

	Min	Max	Mean	SD
IDW – NN	-33.39	29.42	-0.12	2.47
IDW – Kriging	-28.82	20.84	-0.11	2.20
Kriging – NN	-19.02	27.11	-0.01	0.73

The statistical results (Table 6.1) are reflected in the cartographic depiction of the difference images (Figure 6.7). The IDW – NN and IDW – Kriging images are very similar in spatial pattern and type of difference (positive versus negative). The Kriging – NN image has

much more white displayed, and this confirms the low standard deviation value by illustrating that the majority of differences are less than 1 m in magnitude.

From a visual assessment of the difference images, it appears that regions of large differences tend to occur in areas of low lidar point density. This was confirmed by statistical analysis. Correlation coefficients were calculated between lidar point density and the magnitude of DEM differences, and all correlation coefficients were significant ($p<.001$ for a 2-tailed test). The weakest relationship between input point density and DEM differences occurred with the Kriging – NN image, which had a correlation of -0.16. This is not too surprising since the Kriging and NN interpolations generated the DEMs that were most similar, so their differences were not that great originally. The association of point density with IDW/NN differences was moderately strong, with a correlation of -0.44. The strongest correlation, -0.48, was between point density and IDW/Kriging differences. Although none of these relationships are extremely strong, and point density alone would not make a very reliable predictor of model variability, statistically significant relationships do exist, and they confirm the assumption that interpolated surfaces tend to agree more where there are more input data and greater differences between models occur where input data are less dense.

Another method of examining the data is through exploratory data analysis. Geovisualization allows one to interact with geographic data, and it assists in the search for trends (MacEachren and Kraak, 2001). An example is Figure 6.8, in which the IDW – NN differences are mapped to show both the magnitude (distance from horizontal plane) and the type (positive or negative by color) of difference. This provides a 3D representation of how differences between models vary spatially. In a GIS environment, the data can be rotated, tilted, etc. for exploration. This approach is related to the 3D residual error maps demonstrated by Yang

and Hodler (2000), in which the absolute values of point-based relative errors were used to generate accuracy maps as surfaces.

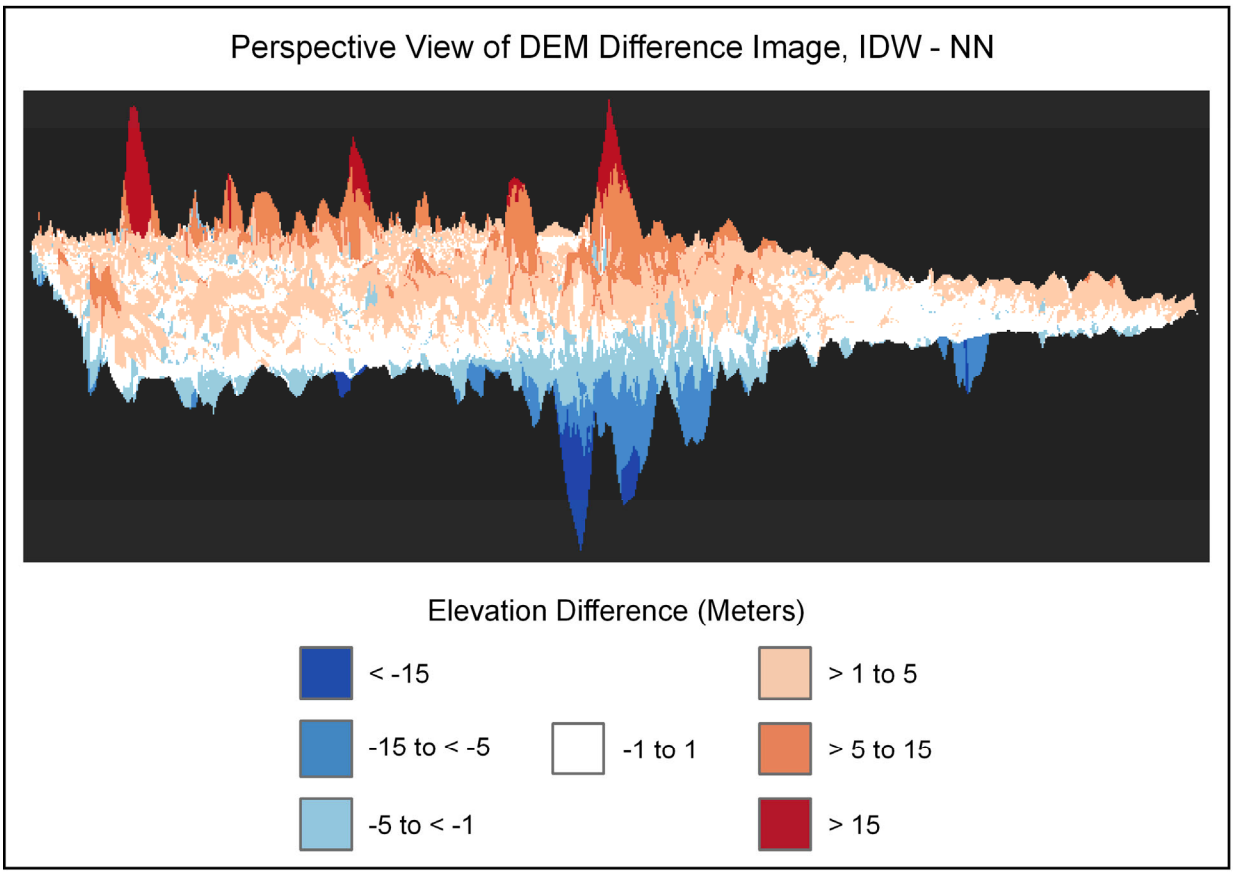

Figure 6.8: 3D rendering of IDW – NN image. Elevation differences are exaggerated by a factor of 5 for visualization purposes.

DEMs Versus TIN Nodes/Input Lidar Points

The 30,183 lidar points were the inputs used by the three interpolation functions to create the DEMs. During TIN creation, the points became TIN nodes. DEM elevations were extracted to the 30,183 points, and the elevation differences between the DEMs and the TIN nodes were calculated.

Vertical RMSE is normally used as a measure of accuracy (Maune et al., 2001b). This analysis is not an accuracy assessment *per se*, since the comparison does not involve an

independent source of data, but the results are informative as to how close the DEM values are to the source values after interpolation. Standard deviation is reported instead of RMSE, since the mean is essentially 0 for all three DEMs, and standard deviation equals RMSE when the mean is 0 (Fisher and Tate, 2006) (Table 6.2). The interpretation of standard deviation is that if the data are normally distributed, and they are, then approximately 68% of all values will occur within +/- 1 standard deviation. For example, 68% of the differences between the interpolated elevation and the source elevation are between -0.19 m and 0.19 m for the IDW DEM.

Table 6.2: Statistics from the comparison of DEM values with input values.

	Min	Max	Mean	Absolute Mean	SD
IDW	-1.39	2.17	< 0.01	0.13	0.19
NN	-1.29	0.95	< 0.01	0.07	0.11
Kriging	-1.16	0.89	< 0.01	0.07	0.10

A visual examination of the results found edge effects with the NN model. Thirty-five of the 36 points with variations greater than 1 m between the NN model and the input lidar points occurred along the edge of the study area. These data were excluded, and the descriptive statistics of Table 6.2 do not include these points.

The greatest variability at the source points occurred with the IDW DEM, as measured by range (-1.39 m to 2.17 m), absolute mean (0.13 m), and standard deviation (0.19 m). The mean often balances out between positive and negative values, as in these comparisons, in which the mean is very close to 0. The absolute mean is useful because it expresses the magnitude of average difference between values. For example, z-values of the IDW model differ from the input z-values, or TIN nodes, by 0.13 m, on average. The NN model performed second best, and the Kriging model most closely matches the input data. It had the smallest range and standard

deviation. The NN model was comparable to the Kriging model, and these two had the same absolute mean difference from the TIN node elevations.

Transects

Points were sampled every 10 m along two transects that passed through areas of various lidar point density and elevation characteristics (Table 6.3). Transect 2 traversed areas with a higher mean density and a greater variation of density. This transect also covered a greater range of elevation.

Table 6.3: Lidar density and terrain characteristics along transects.

	Lidar Point Density (per 100 $m^{2)}$				Elevation (m) from TIN			
	Min	Max	Mean	SD	Min	Max	Mean	SD
Transect 1	0	8	1.1	1.8	1387.4	1519.3	1444.1	44.7
Transect 2	0	14	4.8	4.1	1359.6	1539.7	1434.4	59.6

Statistics were generated from the elevation values at the sample points for six model comparisons (Table 6.4). The IDW interpolated model differs the most from the other three models. The greatest variations in range, absolute mean, and standard deviation along both transects involve the IDW DEM (IDW – NN, IDW – Kriging, and TIN – IDW). Differences are greater along Transect 1 than Transect 2. On average, IDW DEMs differ from the other models by ~1 m and ~0.6 m along Transects 1 and 2, respectively, as measured by the absolute mean difference. The average range of elevation differences between IDW and other models is 12.61 m along Transect 1 and 11.13 m along Transect 2. The maximum difference at any point is 8.10 m between the TIN and IDW models along Transect 1. On average, the standard deviation between IDW and other models is 1.81 and 1.25 m for Transects 1 and 2, respectively.

Table 6.4: Data model elevation comparison at transect sample points.

	Transect 1					Transect 2				
	Min	Max	Mean	Absolute Mean	SD	Min	Max	Mean	Absolute Mean	SD
IDW – NN	-7.93	5.04	0.01	1.04	1.88	-6.42	5.52	-0.08	0.60	1.37
IDW – Kriging	-7.23	4.85	0.05	0.98	1.66	-5.41	4.06	-0.11	0.47	1.02
TIN – IDW	-4.67	8.10	0.02	1.03	1.88	-5.49	6.48	0.09	0.62	1.37
TIN – Kriging	-0.43	2.06	0.06	0.15	0.32	-3.50	2.43	-0.02	0.18	0.57
Kriging – NN	-2.03	0.52	-0.04	0.15	0.33	-2.37	3.52	0.03	0.15	0.55
TIN – NN	-0.16	0.38	0.02	0.07	0.10	-0.43	0.39	<0.01	0.06	0.10

The two models that are most similar are the NN DEM and the TIN. Along both transects, a total of 155 points, z-values were different by 0.43 m at most. Values from both transects are normally distributed, with 147 out of 155, or 94.8%, of values within +/- 2-sigma of the mean (-0.19 to 0.21). Differences between the Kriging model and the TIN and NN models were basically mirror images for Transect 1. Range was ~2.5 m. The Kriging model was normally lower in elevation than either the TIN or NN models. In the Kriging/TIN and Kriging/NN comparisons, the absolute mean differences (0.15 m) are equal, and the standard deviations (0.32 versus 0.33 m) are nearly identical. These model comparisons are also mirror images for Transect 2, although there is more variability, or greater differences in the model comparisons, along Transect 2 than Transect 1. The range in the Kriging/TIN and Kriging/NN comparisons was ~6 m. Unlike Transect 1, the Kriging model was normally higher in elevation than either the TIN or NN models. The absolute mean differences (0.18 versus 0.15 m) and standard deviations (0.57 versus 0.55 m) are very similar in the Kriging/TIN and Kriging/NN comparisons.

On a point-by-point basis along each transect, the correlation was found between lidar point density and the absolute elevation difference for the six model comparisons. Correlation was not extremely high along Transect 1, ranging from -0.20 to -0.32, but 5 of the 6 correlations

were statistically significant at a 95% confidence level with a 2-tailed test (p-values ranged from .007 to .049). The negative correlation confirms the assumption that greater elevation differences between models were found with lower point density, while smaller elevation differences coincided with higher density. Correlations were higher along Transect 2, ranging from -0.25 to -0.40, and all were statistically significant with a 2-tailed test (p-values ranged from <.001 to .021).

Impact on Viewsheds

Differences among elevation models generated from the same source data were quantified in Tables 6.1, 6.2, and 6.4. Can these differences, attributed to different data structures and interpolation methods, affect viewsheds over a relatively short range? Viewsheds were created from the four elevation surfaces from Waypoint 709, and all other inputs were identical. The TIN model generated the smallest viewshed, by far (Table 6.5). It predicts a visible area of approximately half the extent of the DEM viewsheds. DEM results are similar, with the Kriging model generating the largest viewshed.

Table 6.5: Viewshed area (in m^2) from the four data models.

	TIN	IDW	NN	Kriging
Visible Area (m^2)	24,630.8	44,000.1	46,005.9	47,895.3

A visual analysis of the four viewsheds illustrates that the viewshed areas are very similar in the northern part of the study area (Figure 6.9). In the east central region, the TIN predicts no visible area, while the three DEMs predict areas as visible, although they disagree slightly as to the exact boundary. In the southern region of the study area, the TIN predicts the smallest visible area. The DEMs predict a much larger visible area, and again, the exact boundary is slightly different with each model.

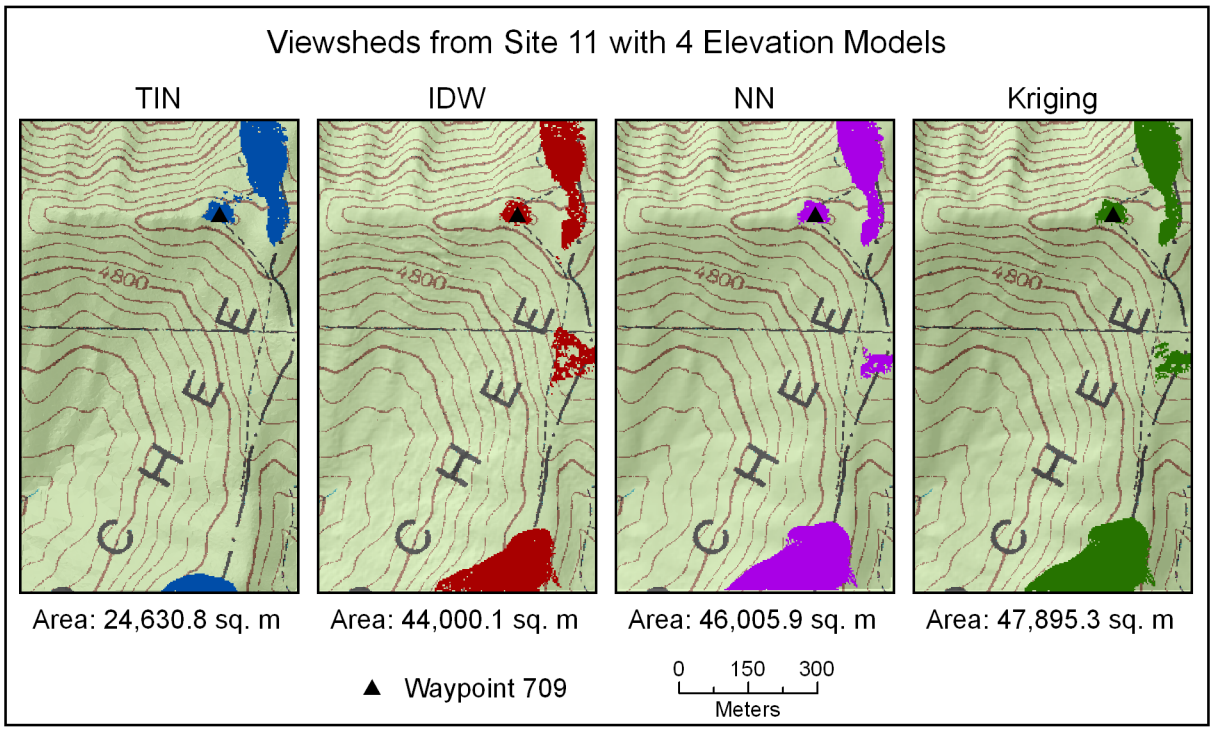

Figure 6.9: Viewsheds generated from the four elevation models, superimposed on a 1:24,000 scale Digital Raster Graphic.

Another way of visualizing these four viewsheds is to overlay them. A probable viewshed was created by adding the rasters together (Figure 6.10). Visible areas that are common to all four viewsheds have 100% agreement, while areas predicted visible by only one of the four models represent 25% agreement. These levels of confidence, or agreement, are cartographically represented with a sequential color ramp. One would have less confidence in areas of lighter green and more confidence in areas of darker green. Most of the area in the northern region is dark green, representing full agreement. In the east central region, agreement is from 25 to 75%. In the southern region, there is 100% agreement for a small area and less overlap towards the west, north, and east. The area where all viewsheds agree is 19,679.4 m^2, and this accounts for 35.8% of the total area predicted visible from any of the four waypoints, and 70.8% is visible by at least three of the four viewsheds.

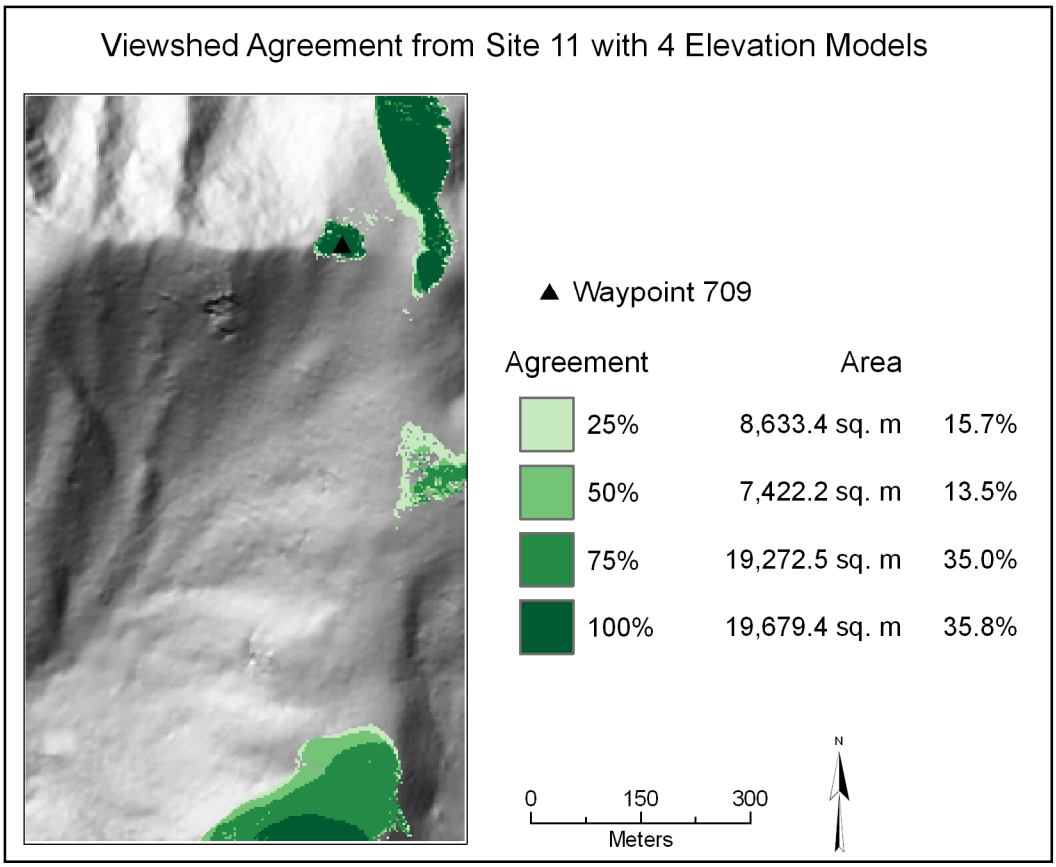

Figure 6.10: Probable viewshed from the four elevation models.

To investigate the viewshed disagreements in the southern region, elevation was sampled from the four elevation models at TIN edge and DEM grid crossings along Transect 3 (Figure 6.11). There are 8 sample points where the viewsheds disagree. At the first of these points, only the Kriging model predicts a visible surface. At the other 7 points, the Kriging and NN models predict the surface to be visible, but the IDW and TIN models predict it to be masked.

A comparison between the IDW and Kriging models illustrates the differences in elevation and possible explanations for visibility differences. A graph of the full profile does not immediately reveal the cause of viewshed differences that occur approximately 675 m away from the observer (Figure 6.12A). The IDW model is higher in elevation than the Kriging model at 7 of the 8 points in question (Figure 6.12B). This seems to contradict the viewshed results,

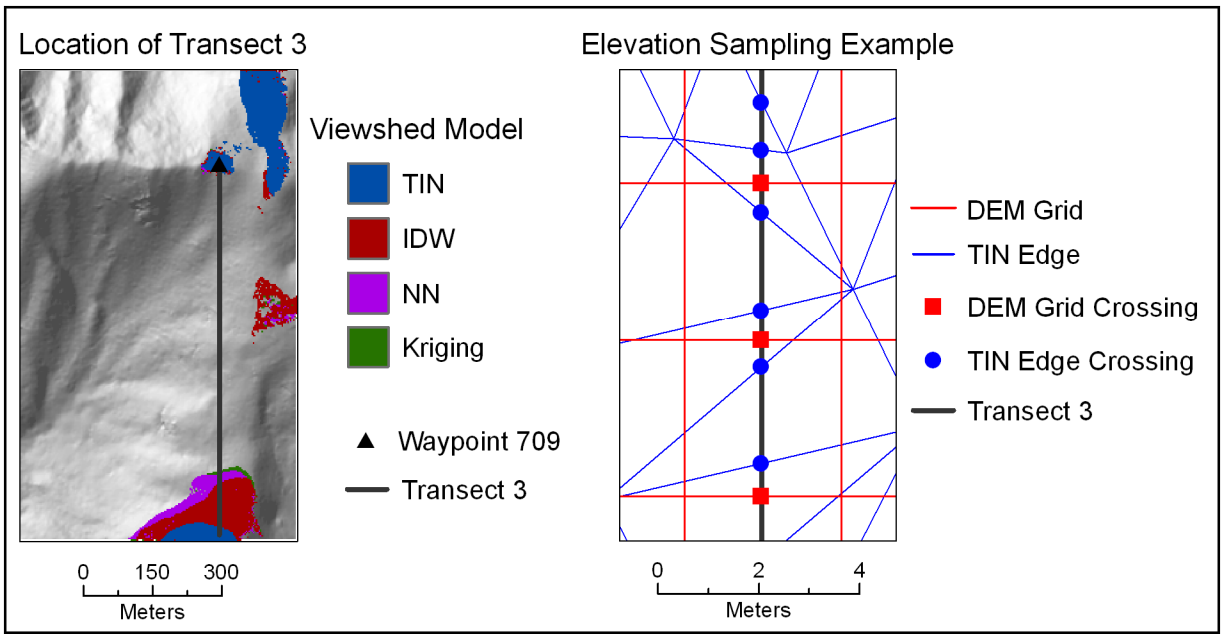

Figure 6.11: Location of Transect 3 within the study area and an example of elevation sampling at TIN edge and DEM grid crossings.

since a higher surface is more likely to be visible than a lower surface. And the differences in observer height with the different elevation models are small, but in fact, the IDW model is 0.15 m higher than the other models.

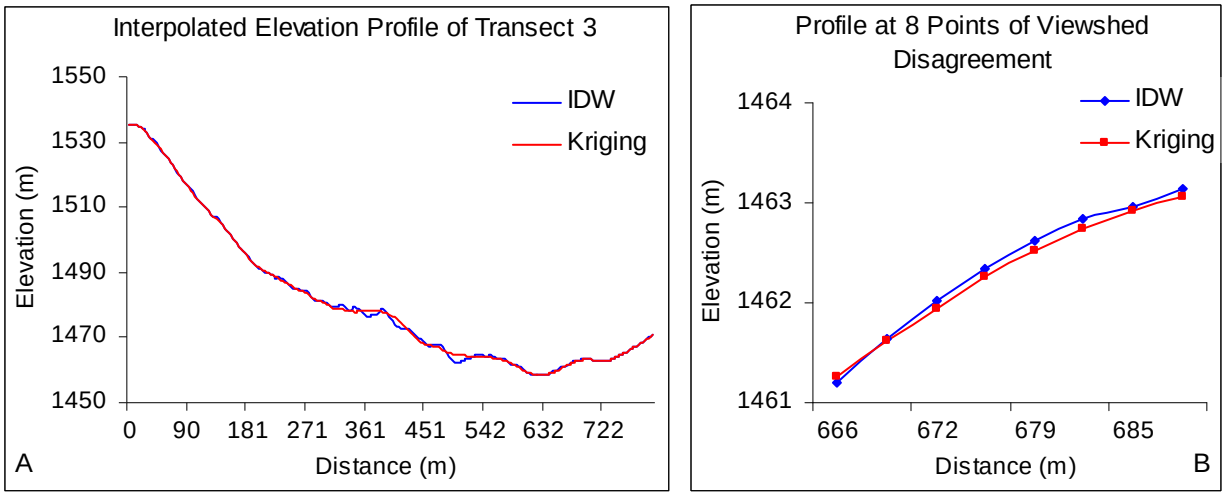

Figure 6.12: Full profile of Transect 3 (A) and profile of the points of viewshed disagreement (B) for the IDW and Kriging DEMs.

Upon further inspection, the full profile indicates that the cause of the viewshed differences in the southern region may be due to elevation differences near the observer, and not in the southern region itself. An elevation profile of the differences between the IDW and Kriging models near the observer illustrates that approximately 24 and 39 m away from the observer, the IDW model is more than 0.3 m higher than the Kriging model (Figure 6.13). The most plausible explanation for the viewshed differences is that these small elevation differences close to the observer impact what can be seen hundreds of meters away, as the higher IDW surface changes the sight angle of the observer.

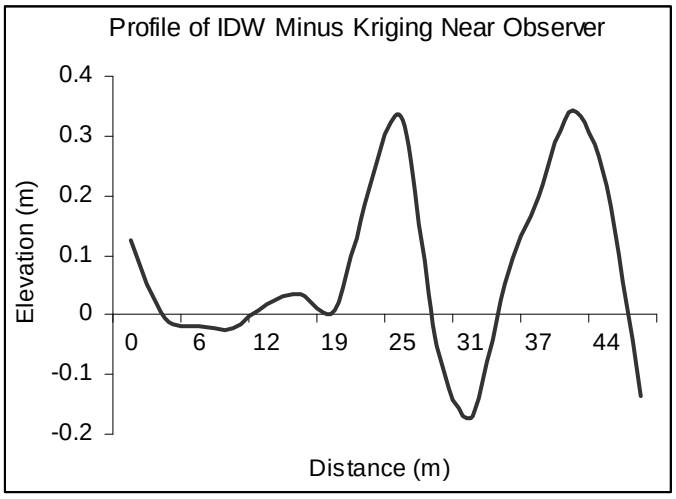

Figure 6.13: Profile of differences near the observer between IDW and Kriging DEMs.

Summary and Conclusions

Based on results of the three methods of elevation model comparisons (difference images, variability at input points, and transects), the IDW interpolation seems the poorest choice. This confirms the recommendation from Maune et al. (2001a), the findings of Lloyd and Atkinson (2002), and a visual inspection of the data. The IDW DEM was a part of the difference images that had the greatest variations. The greatest altering of the input z-values during interpolation occurred with the IDW DEM. Along transects, the IDW model differed the most

from the other three models. A user who chooses this type of interpolation in a mountainous region will be working with an elevation model that likely varies greatly from other interpolated models.

The NN and Kriging interpolated models are more similar to one another and are better choices for elevation data. These models demonstrated relatively little variation in the difference image. The Kriging model most closely matched the input lidar data. These results confirm those of Lloyd and Atkinson (2002), who stated that kriging produced a more accurate DEM from lidar data than the IDW interpolation method. Along transects, the most similar models were the NN DEM and the TIN. This is not surprising, since both models are based on similar underlying structures and methods, the Voronoi diagram and Delaunay triangulation. If one is interpolating surface models for large areas with dense point data, then processing time could be a consideration. A similar amount of time was required to create the IDW and NN models, but the Kriging model took approximately 20 times longer to generate. Since the NN and Kriging models were relatively similar, the NN model could be the more practical choice in some cases.

The assumption that larger differences between elevation models will occur in areas with low input point density was confirmed by tests with the difference images and transects, and this finding complements that of Gong et al. (2000). Although correlation was only moderately strong, nearly all associations were statistically significant at a 95% confidence level. Elevation differences among models were greater along Transect 1 than Transect 2, and this is likely due to Transect 1 having a lower mean point density.

The main question of this study is whether the type of data structure or interpolation method chosen by a user can substantively impact a viewshed over a small area. The answer is yes, these choices can have an important impact and could certainly add to viewshed uncertainty.

Any of these schemes could be chosen in the course of one's work, and each model is a valid representation. Many GIS users may not have the time, ability, or inclination to compare interpolation results. Wood and Fisher (1993) point out that users often do not even know what they should be concerned with regarding the quality of their data.

In this study, the TIN model generated a much smaller viewshed than the DEMs. The DEM viewsheds are similar to one another, and the Kriging model generated the largest viewshed. An investigation into a specific region of viewshed disagreement between the IDW and Kriging models found that disagreements hundreds of meters away from the observer were caused by very small elevation differences (~0.3 m) near the observer. It appears that these small differences changed the LoS angle of the observer. This finding is supported by the results of Riggs and Dean (2007). They report that even small DEM errors can substantially reduce viewshed accuracy.

The use of the probable viewshed is very useful in the scenario presented here (Fisher, 1992; Fisher, 1994). It allows a user to see the effects that interpolation and data model choices have on viewsheds. Since testing the accuracy of elevation data is not always feasible, the probable viewshed is a method that gives users a sense of the confidence they can have in their results.

A direction for future research would be to perform tests similar to those discussed with multiple resolutions of DEMs. The resolution chosen for this study was 3 m in order to mimic the 1/9 arc-second NED. Riggs and Dean (2007) found that the most accurate viewsheds were generated from a DEM with a resolution that most closely matched the average spacing of the input point data. The mean lidar density in the study area was 1 point per 20.4 m^2, which translates to a 4.5-m DEM. Other resolutions could also be generated, and tests could be

conducted to determine whether viewshed agreement increased or decreased substantially with varying DEM resolutions.

CHAPTER 7

THE IMPACT OF GPS POSITIONAL UNCERTAINTY ON VIEWSHEDS

Lockhart, D. To be submitted to *Landscape Analysis using Geospatial Tools: Community to the Globe* (M. Madden and E. Allen, editors), Springer-Verlag.

Introduction

The ubiquity of the Global Positioning System (GPS) has revolutionized mobile mapping and field-based data collection, for geographers and non-geographers alike. Like a worldwide radio station, people can tune in to determine their geographic location at the flip of a switch.

The term GPS refers to the U.S. global navigation satellite system (GNSS). This was the world's first fully operational GNSS. It was funded and developed by the U.S. Department of Defense, and its military name is NAVSTAR. The first experimental satellite was put into orbit in 1978, but it was not until 1995 that a full constellation was operating. The constellation consists of 24+ satellites approximately 20,000 km above the earth's surface. The satellites are configured in six orbital planes, with four satellites in each plane. While only 24 satellites are necessary for continuous, worldwide coverage, extra satellites are in orbit to provide backup in case there is a failure. The satellites are not in geostationary orbit, so their relative positions are constantly changing (Rizos, 2002).

GPS satellites have four very accurate atomic clocks, and satellites know their orbital position, or ephemeris, from data sent to them from the GPS control segment, which is made up of numerous ground stations that monitor satellite activities (Rizos, 2002). The satellite transmits a signal with its location and time at a known, constant speed, the speed of light. With each satellite at a different distance from the receiver, and signals traveling at identical speeds, the receiver's antenna detects signals with different times (precise time that signal left the satellite), which are a function of their distance away. The GPS unit compares the time the signal was received to the encoded time and calculates the difference. This difference in time can then be converted to a distance (rate × time = distance). With at least four of these signals decoded and calculations performed, the receiver can estimate its own location (Abidin, 2002).

GPS receivers are common consumer items today, at least in the U.S. They are used in recreational activities like hiking, hunting, and biking. GPS is a frequently used navigational tool in boats, commercial trucks, personal automobiles, emergency response vehicles, and aircraft. Various types of scientists, surveyors, and others who work in the field use GPS to determine locations of interest. The U.S. military, the original intended user, is heavily dependent on GPS.

A great feature of GPS is that so long as one can lock on to enough satellites, geographic location can be determined in all weather conditions, whether it is day or night. In addition, there is no limit to the number of users who can access the satellite signals. But for the GPS-computed geographic coordinates to be valuable, users must have some idea about the accuracy of the coordinates. A few commonly confused, key terms need to be defined. Accuracy refers to how close a measurement is to the "truth" or some value accepted as true. Precision is the degree to which measurements cluster together, i.e., how repeatable the values are (Maune et al., 2001). It is important to note that these properties may or may not coincide. A bias in measurements may be caused by systematic errors in the system, causing values to be skewed in a particular way (Figure 7.1).

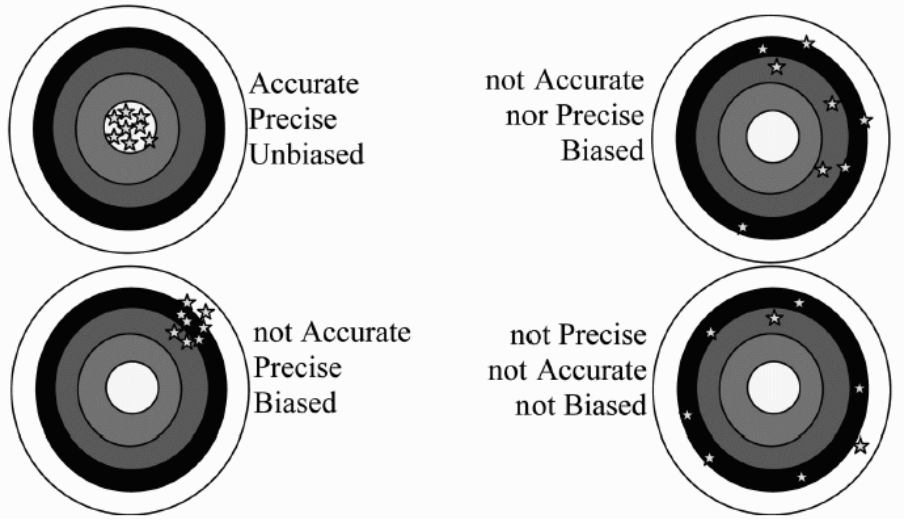

Figure 7.1: Accuracy, precision, and bias. From Fisher (2009).

Errors are mistakes or deviations from true values. Systematic errors follow a regular pattern and may indicate a problem with the measurement equipment. Random errors are unpredictable but tend to cancel each other out if the number of measurements is large enough (Shi, 2009).

Numerous factors can impact the accuracy of GPS coordinates, including the user's environment and the spatial distribution of GPS satellites relative to the user. Measurement errors can stem from signal biases and random errors (Arnaud and Flori, 1998). Examples of biases are atmospheric effects, satellite ephemeris, and satellite clock error. These biases can be accounted for and corrected. Errors that cannot be accounted for include receiver clock error and multipathing (Rizos, 2002; Deckert and Bolstad, 1996). Multipath errors occur when GPS signals reflect off surrounding objects before reaching the receiver. This is a problem in areas covered by dense vegetation and urban settings with buildings (Abidin, 2002).

GPS-estimated positional error, or simply error, is the horizontal distance between a GPS receiver’s computed location and its true location. The direction of the error is not considered (Oderwald, 2003). It can be thought of as the radius of a circle of error. Without differential corrections, typical GPS accuracy is about 10-20 m (Shi, 2009). Differential corrections can reduce GPS errors in the field by utilizing a reference receiver to account for and correct errors that are common to both receivers (Lillesand et al., 2008). In the U.S., the Federal Aviation Administration provides real-time differential corrections for free via the Wide Area Augmentation Service (WAAS). Officially, WAAS provides 7.6-m horizontal accuracy at a 95% confidence level, but actual results are usually even better than this (Lachapelle et al., 2002).

GPS receivers are often categorized as survey-, mapping-, or consumer-grade. Survey-grade receivers are the most expensive ($8,000+), most accurate (cm-level accuracy), and have

the most options. Mapping-grade units are in between, typically costing several thousand dollars and having accuracies of a few meters. Consumer-grade receivers cost a few hundred dollars (or less), have fewer features, and are typically accurate to within 10 m or less. The Garmin GPS V is an example of a consumer-grade GPS receiver (Wing and Eklund, 2007).

An empirical study of the Garmin GPS V demonstrated that its average horizontal accuracy over a range of canopy closure conditions is 3.5 m, and its computed location is within 6.5 m of the true location 95% of the time, while its average accuracy under dense canopy is 4.7 m with a 9.5-m, 95% confidence estimate (Wing et al., 2005).

GPS receiver manufacturers report the accuracy of their products with various measures that have different meanings. The GPS V display indicates the accuracy for each horizontal position, and this accuracy is expressed as 2dRMS (personal written communication, Garmin Support, Oct. 24, 2008). A 2dRMS (two-distance root mean square) specification indicates that approximately 95% (2-sigma) of computed x,y coordinates will be within the distance of the receiver's stated accuracy from true X,Y coordinates (Plackner, 1998). This can be considered a 95% confidence estimate or probability (Stombaugh and Clement, 1999). For example, if the receiver indicates 6-m accuracy at a given time/location, there is only a 5% chance that the true horizontal position is more than 6 m away from the receiver's computed x,y position.

It is postulated that the variability of GPS coordinates, especially those obtained in areas of dense tree cover and high ridges, could affect GIS analyses that are heavily dependent on these point coordinates. An example is the viewshed function. Huss and Pumar (1997) found that viewsheds are sensitive to horizontal position in rugged terrain because a change of position alters the geometry between an observer and nearby ground features or obstacles. Although the DEM used in their tests was of coarse resolution (100 m post-spacing), relocating an observer to

the nearest grid cell (100 m away), which had the same elevation, caused the visible area to be reduced by 75%.

Purpose and Objectives

Since consumer-grade GPS receivers are commonly used in various types of field work, relying on the GPS coordinates can introduce uncertainty into some calculations and analyses. For example, visibility may be based on a viewshed generated from point coordinates obtained by GPS. The purpose of this study is to assess the precision and accuracy, where possible, of GPS positions and to quantify the uncertainty of viewsheds that can result from GPS coordinate variability. The relationship between GPS-stated accuracy, precision, and tree cover will be calculated for all 15 field sites, and GPS positions will be evaluated against ground control points (GCPs) at two sites to determine their accuracy. The role of GPS variability and digital elevation model (DEM) resolution in viewshed agreement will be quantified for three select sites, and probable viewsheds will demonstrate various levels of agreement as an alternative cartographic output to a single viewshed map.

Data and Methodology

Field work was conducted at 15 field sites in Great Smoky Mountains National Park (GRSM) in western North Carolina (refer to Chapter 3). While the precision of GPS data was computed for all sites, the uncertainty of viewsheds due to GPS variability was conducted at three sites (1, 3, and 5), and GPS accuracy could only be assessed at Sites 5 and 14 (Figure 7.2). For viewsheds, the maximum extent was limited to a semi-circular area 30 km in diameter. The source data was the 1/9 arc-second USGS NED, which was resampled using bilinear interpolation in ArcGIS to 6, 10, and 30 m (refer to Chapter 4). Viewsheds were not generated from the 3-m data in light of the lengthy processing time required. Due to edge-matching

problems found in other NED data near the Tennessee border, and the fact that the 1/9 arc-second data coverage is incomplete along the border, the DEMs were clipped, resulting in the stair-step appearance of the study area's boundary (Figure 7.2). The total size of this area of interest is 297.6 km^2.

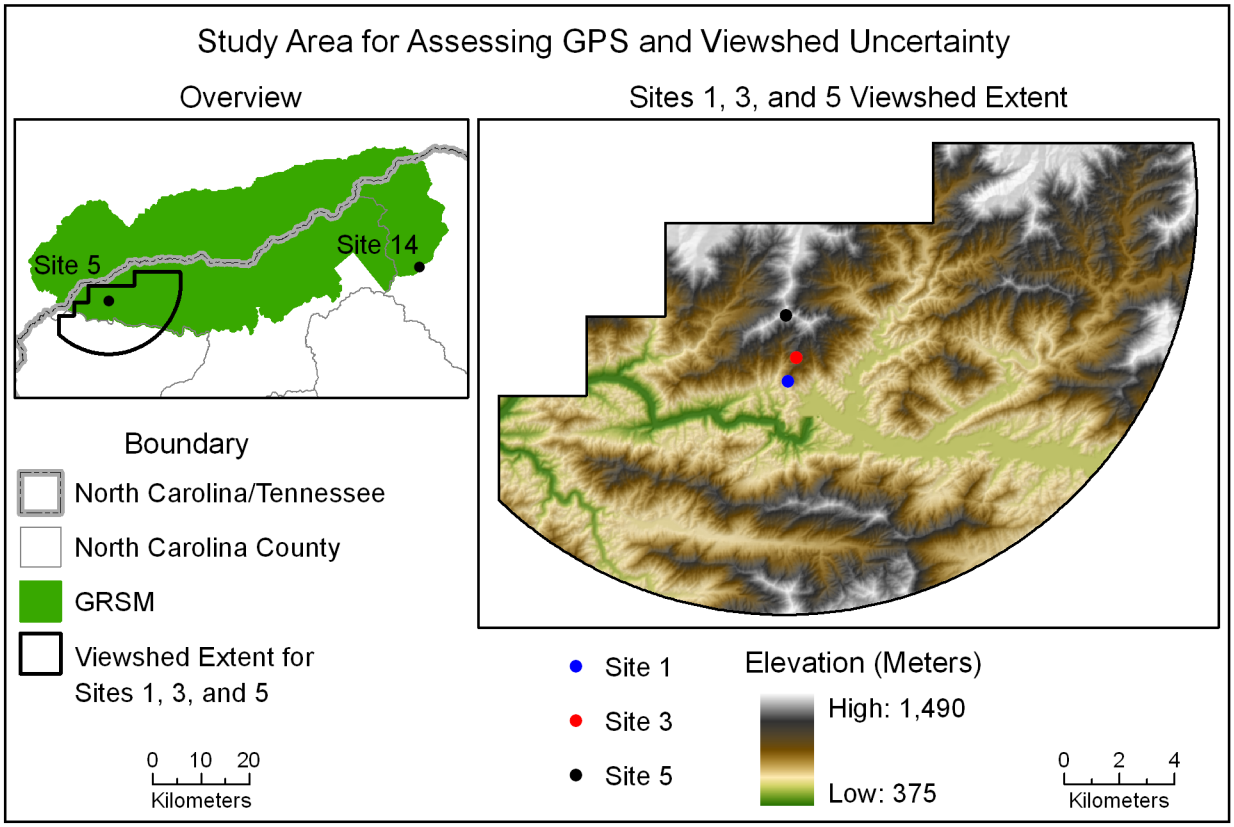

Figure 7.2: Study area.

Due to the potential for signal shading and multipath reflection under forest canopies, it is best to take multiple GPS readings (Scherzinger et al., 2001). During field work, four x,y,z points were acquired by the GPS V for the exact same ground location at each field site, and each waypoint was an average of 30 readings. Acquiring multiple observations from the same location has the effect of improving precision due to the averaging of observations over time (Oderwald, 2003; Rizos, 2002). Research has also demonstrated that more readings at a site

increase accuracy (Deckert and Bolstad, 1996; Wing et al., 2005). An assessment of GPS accuracy was performed from data at Sites 5 and 14, which coincided with the locations of National Geodetic Survey (NGS) markers. These two NGS GCPs, Permanent Identifier FB2620 and FB2478, are horizontal control stations with X,Y coordinates given to the third decimal place in the UTM coordinate system (mm precision). The Z-values at these GCPs are of lower quality but are accurate within 1 m (NGS, 2008). The GCP X,Y,Z coordinates were compared with the four x,y,z GPS coordinates to calculate horizontal and vertical RMSE values.

Due to the effects of multipathing, it is common for GPS units to deliver more accurate (closer to the truth) and more precise (more repeatable) coordinate measures in areas free of thick vegetation cover (Deckert and Bolstad, 1996). Other than at Sites 5 and 14, which had NGS GCPs, it is not possible to truly assess the accuracy of the GPS coordinates. However, the precision of coordinates can be calculated and correlated with the GPS unit's reported accuracy, or error, and these, in turn, may be tested for a relationship with tree cover to find associations that may help in estimating accuracy.

To calculate GPS precision, the Euclidean distance among the four x,y coordinates at each field site was found with Hawth's Analysis Tools, yielding a distance matrix of six values for each site (Figure 7.3). Descriptive statistics of precision were calculated for all sites. For waypoints collected in the field, the stated accuracy indicated by the GPS unit's display, as well as the number of satellite signals received, were recorded on paper and integrated into the database afterwards. The receiver's stated accuracy is illustrated in Figure 7.3 as the radius of a 95% confidence buffer.

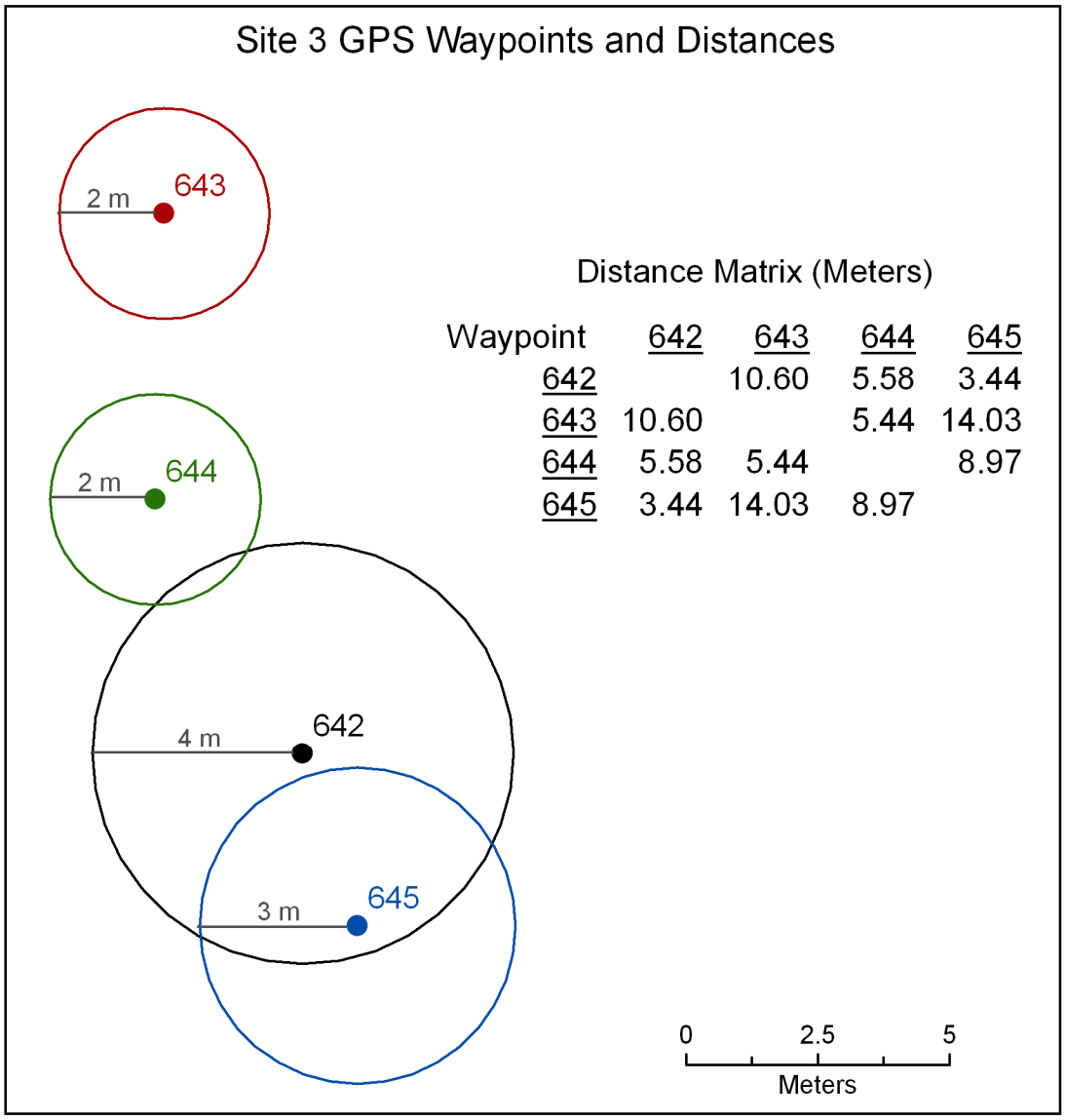

Figure 7.3: Site 3 GPS waypoints, stated accuracy circles, and distances between points.

Two independent sources of vegetation data were used, the MRLC Consortium NLCD 2001 Tree Canopy and the UGA CRMS GRSM leaf-on percent canopy datasets (refer to Chapter 4). Tree cover values from both datasets were extracted to all GPS waypoints. NLCD canopy is ratio data. CRMS canopy is ordinal data, with four categories representing canopy cover: class 1 (0%-25%), class 2 (>25%-50%), class 3 (>50%-75%), and class 4 (>75%-100%) (Madden et al., 2004). CRMS polygons are grouped into ordered categories, so polygons can be differentiated

between classes (class 1 versus class 2) but not within classes (e.g., a polygon in class 1 cannot be said to have higher or lower canopy cover than another class 1 polygon). These are considered weak-ordered ordinal data, and the appropriate test for relationships between the NLCD and CRMS data is the Pearson chi-square statistic (Wong and Lee, 2005). To make the data compatible for this test, the NLCD values were converted to the same four classes used by CRMS (0%-25%, >25%-50%, >50%-75%, >75%-100%).

A linear regression model was created for the number of satellite signals and the GPS-reported accuracy for all waypoints. The association between GPS-reported accuracy, precision, and tree cover was calculated for all 15 field sites. GPS-reported accuracy and precision were correlated with Pearson's correlation coefficient. The associations of GPS-reported accuracy and precision with the NLCD data were found with Pearson's correlation coefficient.

Viewsheds from the four waypoints for Sites 1, 3, and 5 were generated in ArcGIS and compared in order to determine the impact of GPS variability. Since true geographic positions are normally unknown when working in the field, each GPS waypoint is considered a valid location for "Site X." Site 3 is located atop a relatively flat ridge crest, and the average slope of the terrain at its four waypoints is 6.1°, based on 10-m data. The GPS coordinates of the four waypoints at Site 3 are the second least precise of all 15 field sites. The closest pair of coordinates is 3.44 m apart, the furthest is 14.03 m apart, and the average distance between each pair of points is 8.01 m (Figure 7.3). Viewsheds were generated with 30-, 10-, and 6-m DEMs. Figure 7.4 illustrates the Site 3 waypoints and error circles superimposed on these resolutions of DEMs, showing how points can fall into different grid cells of the same DEM, and thus have different z-values, due to horizontal uncertainty and various spatial resolutions of data.

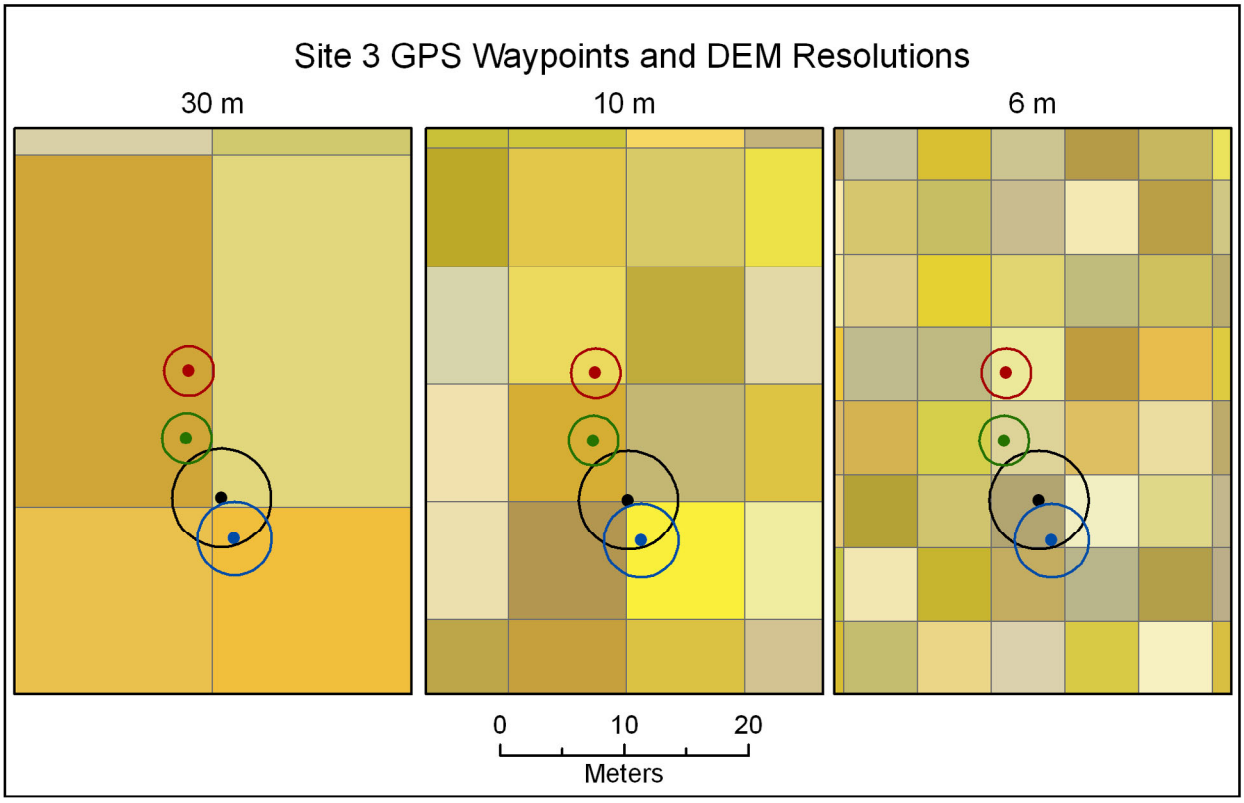

Figure 7.4: Site 3 GPS waypoints and error circles superimposed on 30-, 10-, and 6-m DEMs. Pixel colors are for visualizing different cells only; they do not represent elevation values.

Site 1 is located along a moderately steep side hill, sloping down from northeast to southwest. The average slope of the terrain at its four waypoints is 17.6°, based on 10-m data. The GPS-calculated positions of the four waypoints at Site 1 are more compact than those of Site 3 (Figure 7.5). The closest pair of coordinates is 3.30 m apart, the furthest is 10.77 m apart, and the average distance between each pair of points is 7.37 m. All viewsheds from Sites 1 and 3 were generated with the same relative height above the ground, 1.5 m.

Site 5 is located on the peak of Shuckstack, a prominent mountain rising above Fontana Lake. Coordinates collected from the fire tower, 18.3 m above the ground, have about as much variability as those from Site 1. The maximum distance between any pair of points is 10.01 m.

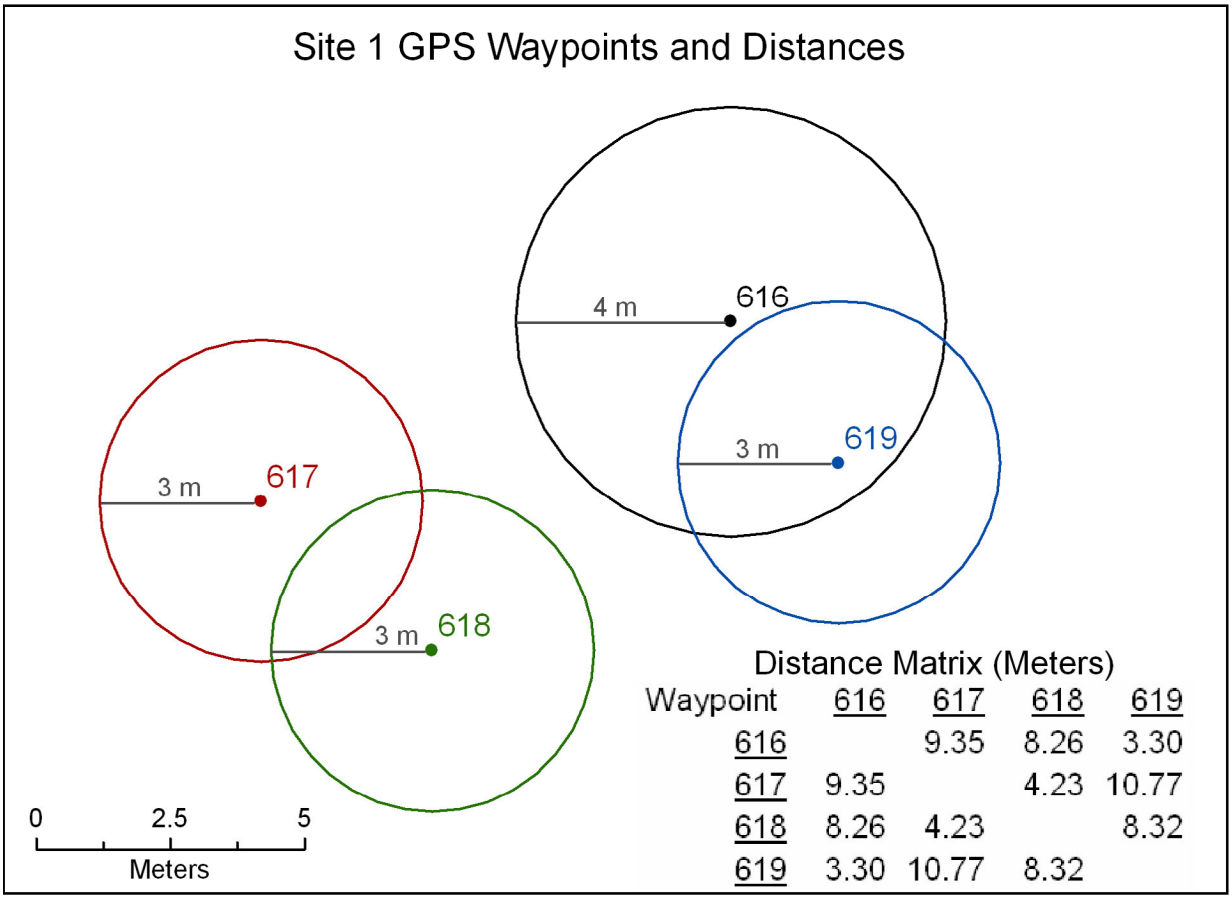

Figure 7.5: Site 1 GPS waypoints and error circles.

Results

GPS Accuracy and Precision

The GPS accuracy assessment was performed with NGS GCPs at Sites 5 and 14. During the time of GPS data acquisition, 11 satellite signals were received at Site 5 and 9 were received at Site 14. Planimetric accuracy was comparable but slightly better at Site 14. The horizontal RMSE was 3.1 m at Site 5 and 2.4 m at Site 14. At the same time, average GPS-reported accuracy was 2.8 m for Site 5 and 2.3 m for Site 14. Vertical RMSE was lower than horizontal RMSE: 1.8 m for Site 5 and 2.1 m for Site 14. These RMSE values represent a 1-sigma, or 68%, confidence estimate.

Among all waypoints, 2dRMS accuracy reported by the GPS V ranged from 2 to 10 m, with a median of 3 m and a mean of 3.5 m (Figure 7.6). Mean reported error, grouped by field site, ranged from a low of 2.0 m at Sites 13, 14A, 14B, and 14D to a high of 7.8 m at Site 10. The mean number of satellite signals received, grouped by site, ranged from a low of 5.0 at Site 2 to a high of 11.3 at Site 5. The overall average was 8.0 satellites. For each waypoint, GPS-reported horizontal accuracy was plotted against the number of satellite signals received (Figure 7.6). As expected, more satellite signals led to lower reported errors, or higher accuracy. In this regression model, the number of satellites accounts for 33% of the variability in reported accuracy, and this r^2 value is statistically significant ($p<0.001$) for the 138 waypoints tested.

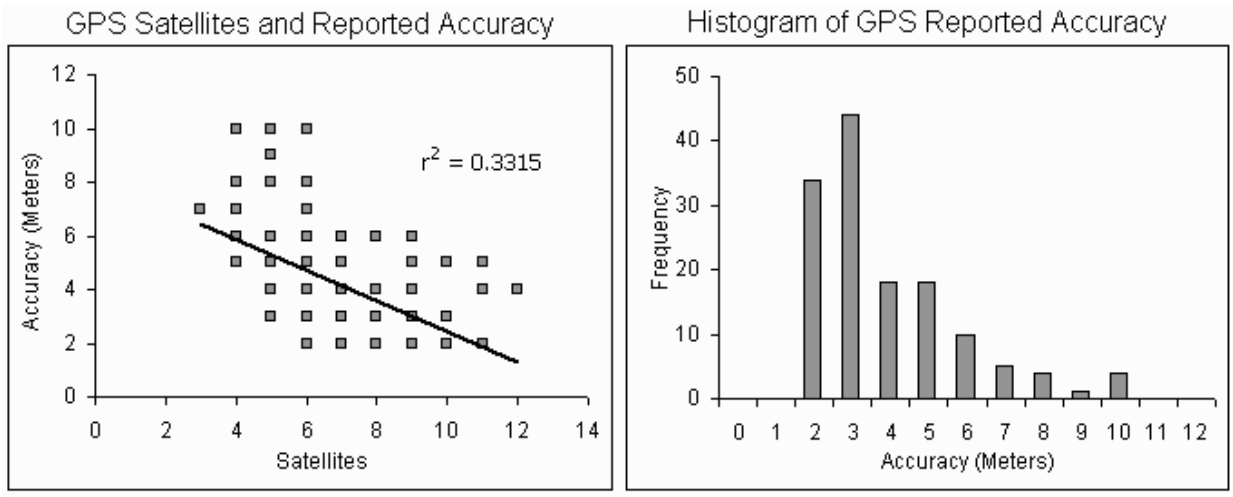

Figure 7.6: Scatterplot and linear regression of satellite signals with GPS-reported accuracy (left) and histogram of GPS-reported accuracy (right).

GPS precision is found by examining the compactness of waypoints. Overall, the mean distance between each pair of points at the field sites is 4.5 m, with a standard deviation of 2.3 m. There is much variation among the sites. The mean distance between pairs of points is lowest (0.6 m) at Site 14C and highest (12.2 m) at Site 6. The greatest distance between any two points at a site is 21.5 m at Site 6, with variability greater than 33 m when the error circles are included.

The closest two points at Site 6 are 6.0 m apart. At the GCPs of Sites 5 and 14, precision is higher than the 4.5-m average. The mean distance between pairs of points at Site 5 is 3.1 m. Point coordinates are extremely compact at the Site 14 GCP, with a mean of 0.5 m. Here, the most dispersed points are only 0.8 m apart.

GPS-reported accuracy correlates moderately well with the previously discussed precision statistics for data grouped by site. Correlation (r) was 0.50 between reported accuracy and the mean distance between point pairs, and correlation was 0.48 for reported accuracy and the standard deviation of point pairs. These correlations are not overwhelmingly strong, although they are both significant for a 2-tailed test at a 95% confidence level ($p<.038$). If the GPS-reported accuracy was "true," one might expect higher correlations. If the indicated accuracy is poor at a site, one assumes that the receiver cannot obtain a good fix on its position, and that other coordinates obtained there might vary widely. If the reported accuracy is very good at a site, indicating small estimated positional errors, then multiple readings should be spatially compact, with short distances between pairs of coordinates, and an association greater than 0.50 should result. This result calls into question the 2dRMS, or 95% confidence estimate, of the GPS V's reported accuracy.

As discussed, Site 14C's coordinates are the most precise, while Site 6 has the least precise coordinates. The GPS-reported 95% confidence estimate seems reasonable for Site 14C, but not for Site 6 (Figure 7.7). Given that the four GPS coordinates were obtained from the same location, the little overlap among the four error circles at Site 6 makes suspect the claim that each circle has a 95% chance of containing the true location. More evidence against the truthfulness of the 95% confidence intervals originates from Sites 5 and 14. Of the four error circles at Site 5,

only one encompasses the NGS GCP, and just two of the four error circles at Site 14 encompass the GCP.

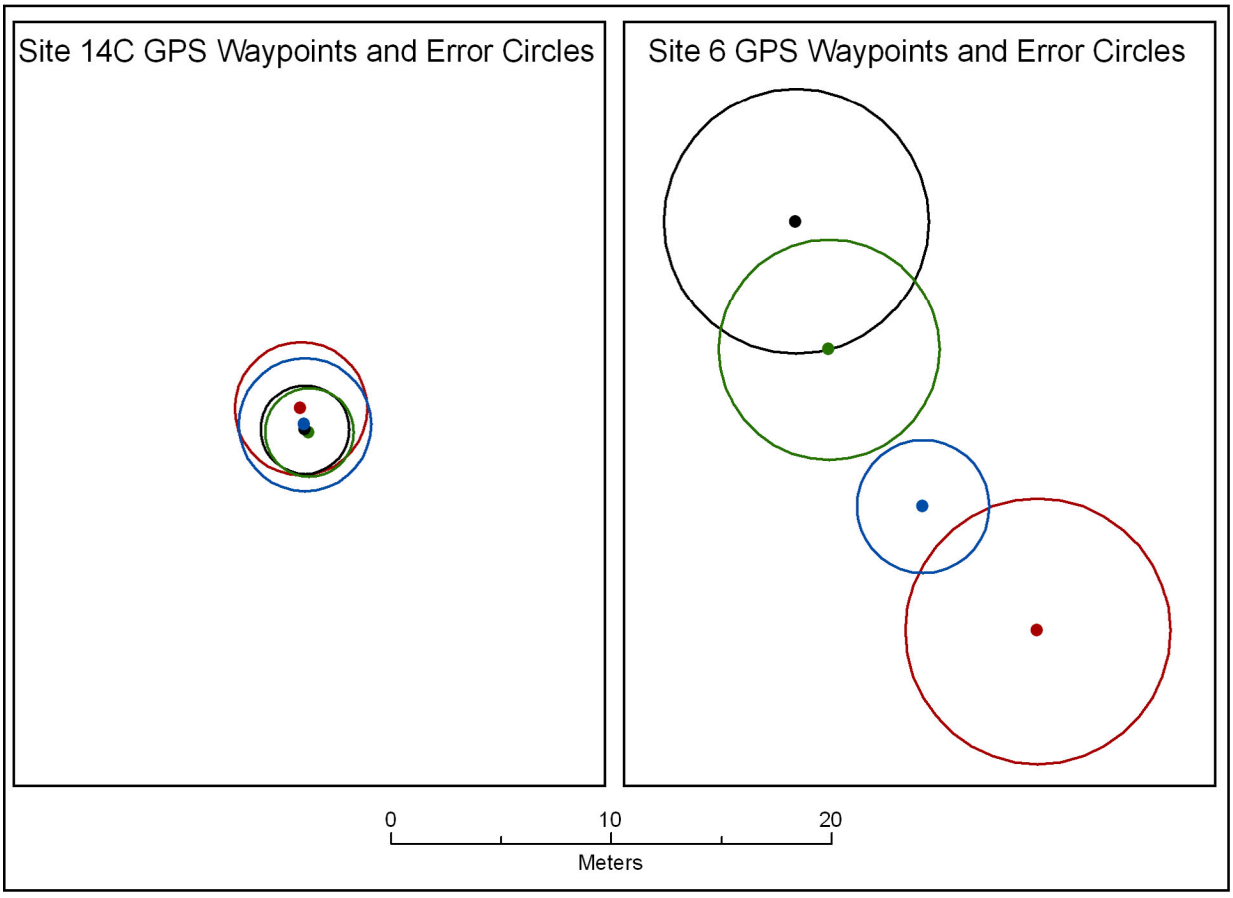

Figure 7.7: Precision and reported error of GPS coordinates at Sites 14C and 6.

Canopy cover data was analyzed for all waypoints. Average cover according to the NLCD data was 67.9%. However, most values were either very low or very high. Twenty locations (26.3%) had 0% tree cover, meaning totally exposed, and 52 (68.4%) had greater than 89% tree cover. According to the CRMS data, only four waypoints (5.3%) were located in the lowest class, while the rest were evenly split between class 3 and class 4 at 47.4%. To compare the two datasets, NLCD values were converted to the same four classes used by CRMS. The data

are summarized by field site in Figure 7.8. It can be seen that NLCD data estimates more extreme cover (very low and very high) than CRMS data.

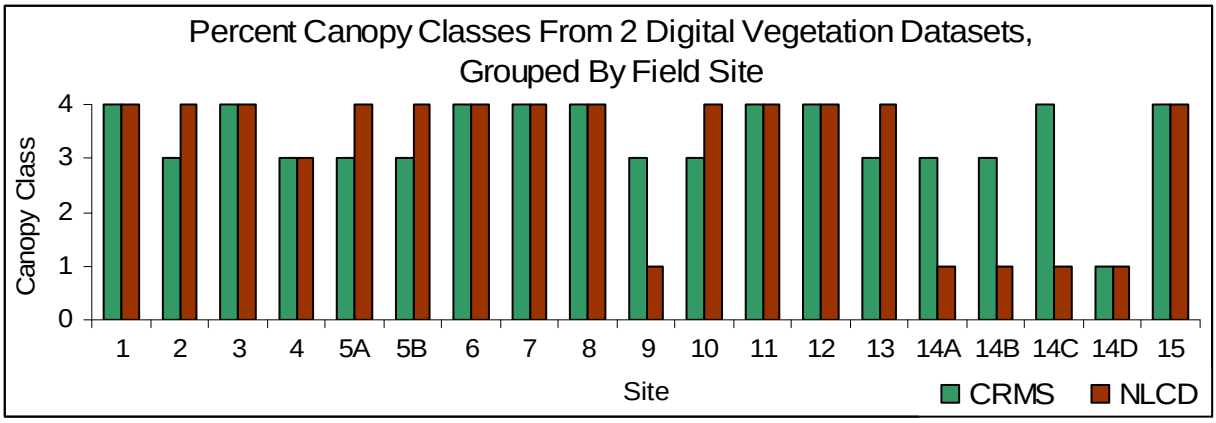

Figure 7.8: Field site canopy cover classes from NLCD 2001 Tree Canopy and CRMS GRSM leaf-on percent canopy datasets.

The relationship between the two canopy datasets at waypoints was evaluated with the chi-square statistic. The resulting statistic is 22.3, which is statistically significant ($p < .001$), indicating a correlation between the data. These datasets agree fairly well, except for two sites. At Site 14, where the locations are not under trees in reality, CRMS data predicts moderate cover while the NLCD correctly identifies no cover. At Site 9, CRMS data correctly identifies moderate cover while the NLCD incorrectly indicates no cover. These discrepancies do not reflect negatively on the vegetation data, for both of these sites are located at boundaries between forest and clearings, and this level of precision is well beneath the minimum mapping units of the canopy data.

There is a moderate relationship between GPS-reported accuracy and NLCD data. Summarized by site, the correlation coefficient is 0.50. This is statistically significant ($p = .030$ for a 2-tailed test) and indicates that the GPS receiver reported more confidence in its x,y location where there was less tree cover.

The relationship of coordinate precision with NLCD data is stronger than that of reported accuracy with NLCD data. The correlation of tree canopy with the mean distance between each pair of points at the field sites is 0.63, which is statistically significant ($p = .004$ for a 2-tailed test). This means there is a tendency for sites with less tree cover to have more compact GPS-derived coordinates than those under dense canopy.

Site 3 Viewsheds

A good deal of variation in the sizes of computed viewsheds is apparent from the waypoints of Site 3. This can be seen by viewing each row of Table 7.1, where the viewshed area is given for each DEM across the four waypoints. The bilinearly interpolated elevation of the observer, which is used by ArcGIS in generating the viewsheds, is also given for each point. With the 30-m DEM, viewshed areas vary by as much as 6.8 km^2. There is less variation in viewsheds derived from the 10-m data, but the greatest range (8 km^2) comes from the 6-m DEM.

Table 7.1: Visible area (in km^2), DEM elevation (bilinearly interpolated, in m), and ranges in visible area (in km^2) for Site 3 waypoints.

	Waypoint ID								
	642		643		644		645		Area
DEM Res.	Area	Elev.	Area	Elev.	Area	Elev.	Area	Elev.	Range
30 m	36.9	896.2	30.1	897.4	30.2	896.9	36.9	895.7	6.8
10 m	32.8	903.5	28.5	903.2	32.1	903.5	32.9	903.1	4.4
6 m	29.8	904.8	21.8	904.0	28.2	904.7	29.6	904.6	8.0
Area Range	7.1	8.6	8.3	6.6	3.9	7.8	7.3	8.9	

Data from Table 7.1 is displayed graphically in Figure 7.9, and a pattern is apparent. Waypoints 642 and 645 have the largest and most similar viewsheds, in terms of size, which is not surprising since they are located only 3.44 m apart (Figure 7.3). Waypoint 643 consistently has the smallest viewsheds, and is located the furthest north. Viewsheds from Waypoint 644 fall in between. All of these differences in visible area across waypoints are due to different

horizontal positions, as calculated by GPS, but the most distant points, 643 and 645, are only 14 m apart.

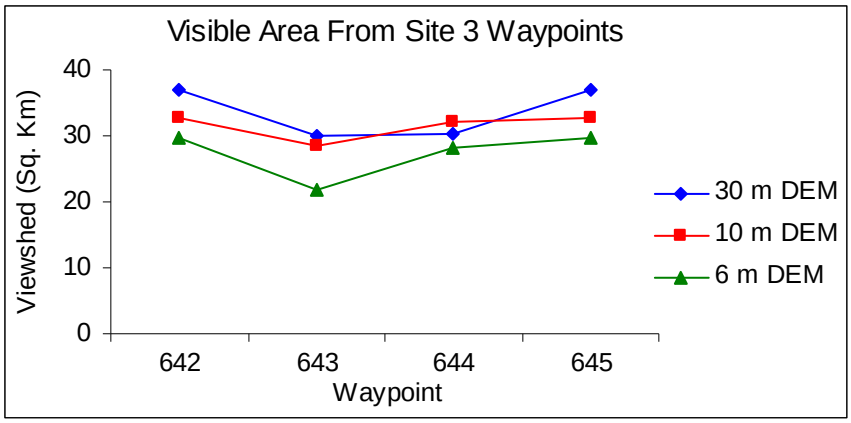

Figure 7.9: Viewshed area for three resolutions of DEMs from Site 3 waypoints.

Viewshed sizes differ from one resolution of DEM to another from the same waypoint (Table 7.1). Looking down each waypoint column at the three DEMs, it is clear that from the exact same observer location, different predicted viewsheds result from DEMs having different resolutions, even when the DEMs are all resampled with the same method from the same source data. The greatest variability occurs from Waypoint 643, where predicted viewsheds varied by 8.3 km^2, and the least variability (3.9 km^2) occurs from Waypoint 644. The average viewshed range at Site 3 attributable to DEM resolution is 6.7 km^2, about the same average range that is attributable to different horizontal positions (6.4 km^2). The general pattern seen in Figure 7.9 is that the higher resolution data tend to generate smaller viewsheds.

Viewsheds from the four waypoints of Site 3 with the 30-m DEM are illustrated in Figure 7.10. Overlays can be used to create a probable viewshed, where one would have more confidence that areas of greater agreement more likely reflect reality. Viewshed agreement is cartographically represented with a sequential color ramp, indicating regions covered by only one viewshed (25%), two viewsheds (50%), three viewsheds (75%), or all four viewsheds (100%

agreement). The area where all viewsheds agree is 29.1 km^2, and this accounts for 77.2% of the total area predicted visible from any of the four waypoints. Since the true location where the GPS waypoints were collected is unknown, and the probable viewshed takes this uncertainty into account, a conservative estimate of the true viewshed would be the region with 100%, or even 75%, overlap.

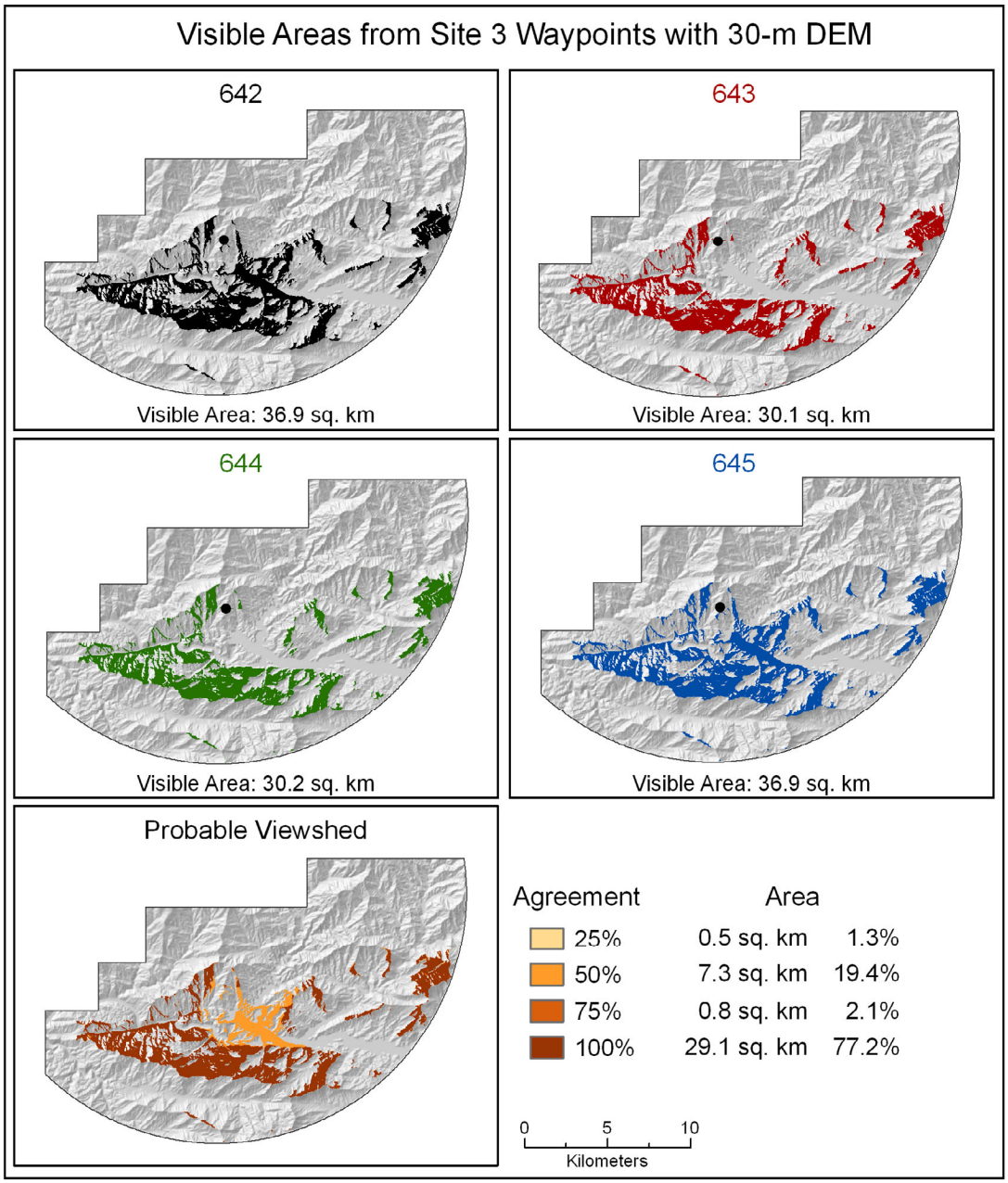

Figure 7.10: Viewsheds from Site 3 waypoints with 30-m DEM.

Site 1 Viewsheds

Viewsheds from Waypoints 616-619 at Site 1 show much less variability than those from Site 3 (Table 7.2). Very consistent results are obtained across the waypoints with 10-m and 6-m DEMs. The most variability occurs with the 30-m DEM. The greatest difference (5.9 km^2) is between Waypoints 616 and 619, which is surprising since these locations are the closest to each other, only 3.3 m apart.

Table 7.2: Visible area (in km^2), DEM elevation (bilinearly interpolated, in m), and ranges in visible area (in km^2) for Site 1 waypoints.

	Waypoint ID								
	616		617		618		619		Area
DEM Res.	Area	Elev.	Area	Elev.	Area	Elev.	Area	Elev.	Range
30 m	17.3	678.5	19.9	675.0	21.6	675.1	23.2	678.3	5.9
10 m	19.7	683.1	19.6	681.1	19.8	680.8	19.8	682.4	0.2
6 m	18.5	686.7	18.7	685.0	18.8	684.8	18.4	685.7	0.4
Area Range	2.4	8.2	1.2	10.0	2.8	9.7	4.8	7.4	

DEM resolution has less effect at Site 1 than Site 3. The greatest viewshed range occurs from Waypoint 619, where predicted viewsheds varied by as much as 4.8 km^2, and the least variability (1.2 km^2) occurs from Waypoint 617 (Table 7.2). The average viewshed range at Site 1 attributable to DEM resolution is 2.8 km^2, slightly more than the average range that is attributable to different horizontal positions (2.2 km^2). The pattern seen in Figure 7.11 is that the 6-m data again predict smaller viewsheds than the 10-m data. The 30-m data predict the smallest viewshed from Waypoint 616 and the largest viewsheds from the remaining three waypoints.

The probable viewshed from the four waypoints with the 30-m data is in Figure 7.12. Of the total area predicted visible from any of the waypoints, 91.5% is visible by at least three of the four waypoints. This represents a high level of agreement. GPS variability has little effect upon viewsheds at Site 1, and there is even greater viewshed agreement with the 10-m and 6-m DEMs.

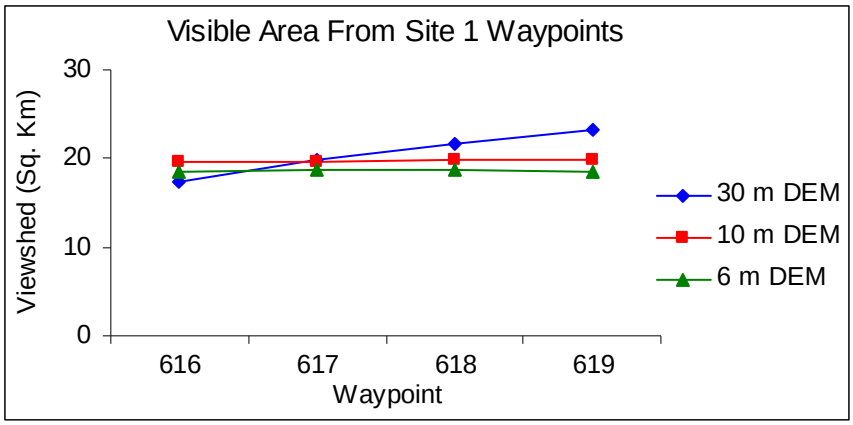

Figure 7.11: Viewshed area for three resolutions of DEMs from Site 1 waypoints.

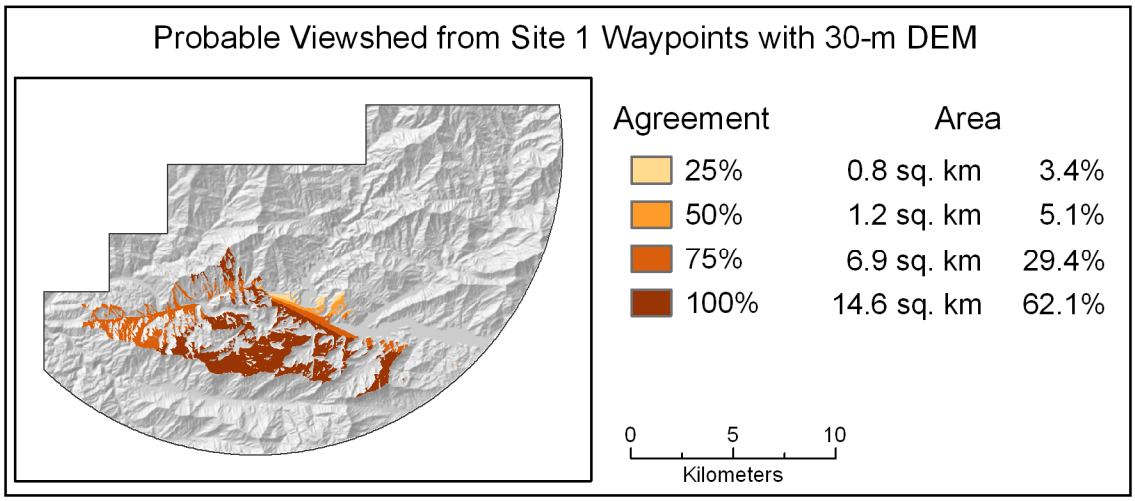

Figure 7.12: Probable viewshed from Site 1 with 30-m DEM.

Site 5 Viewsheds

In contrast to Site 1, Site 5 viewsheds with the 30-m DEM are nearly identical (Table 7.3). This occurs even though the waypoints from Site 5 have about as much horizontal variability as those from Site 1. From the four waypoints, viewsheds range from 83.0 to 83.2 km^2, a difference of just 0.2 km^2. When the viewsheds are overlaid, 96.3% of the total area predicted visible from any of the waypoints is visible from all four waypoints. The GPS uncertainty has almost no effect on viewshed agreement. This very high level of agreement

occurs because the viewshed was generated with the observer positioned 18.3 m above the ground surface to simulate the vista from the fire tower at Site 5, which is where Waypoints 657-660 were obtained. The viewpoints are clear of any nearby ground interference, and visibility from that height hardly varies over a 10-m horizontal distance.

Table 7.3: Visible area (in km^2), DEM elevation (bilinearly interpolated, in m), and range in visible area (in km^2) for Site 5 waypoints.

	Waypoint ID								
	657		658		659		660		Area
DEM Res.	Area	Elev.	Area	Elev.	Area	Elev.	Area	Elev.	Range
30 m	83.0	1212.8	83.2	1213.5	83.2	1213.6	83.1	1213.2	0.2

Summary and Conclusions

For a consumer-grade receiver, the WAAS-enabled Garmin GPS V performed well in terms of positional accuracy in a heavily forested, mountainous setting. Validated at two GCPs that coincided with field sites, its horizontal RMSE was 2.4 m under open skies (Site 14) and 3.1 m under thin canopy cover (Site 5). Converting these values to the National Standard for Spatial Data Accuracy specifications, published in 1998 by the Federal Geographic Data Committee (Maune et al., 2001), horizontal accuracy was 4.2 m at the 95% confidence level under open skies and 5.4 m at the 95% confidence level under thin canopy cover. These results are comparable to those of Wing et al. (2005), who found the GPS V's accuracy to be 4.8 m with a 95% confidence estimate under open skies and 6.8 m at the 95% confidence level under moderate canopy (40-50% cover). The mean distance between the four GPS coordinates at Site 5 was 3.1 m, and the precision was very high at Site 14, with a mean distance of 0.5 m. In this latter situation, the recorded GPS coordinates were very compact, but some type of bias kept them from being centered directly on the GCP.

As expected, more satellite signals led to higher accuracy reported by the GPS receiver's display when calculating point coordinates. In a regression model, the number of satellites accounts for 33% of the variability in reported accuracy, so this could serve as a rough guide for users to estimate how accurate their readings might be, based on how many satellites they expect to be visible at a certain time and place. The accuracy displayed by the GPS unit correlates moderately well with precision statistics measured at the sites ($r = 0.50$), but one might expect the relationship to be stronger if the GPS-reported accuracy was true. This statistical finding, as well as a visual review of point distributions and error circles at sites, calls into question the 2dRMS, 95% confidence estimate of the GPS V's displayed accuracy. Results of this study demonstrate that the accuracy indicated by the display should not be taken too literally, but only regarded as a guide.

Tree cover from two digital vegetation datasets, NLCD 2001 and CRMS GRSM layers, was compared for the field sites and a statistically significant correlation was found. One difference between the datasets is that NLCD data provide more extreme estimates of cover (very low and very high) than the CRMS data. There is a moderate association between GPS-reported error and NLCD canopy data ($r = 0.50$), and there is a stronger relationship between GPS precision among coordinates and NLCD data ($r = 0.63$). This confirms the assumption and results of previous investigations that locations with less tree cover will have more precise, and possibly more accurate, GPS coordinates than those under thick canopy (Deckert and Bolstad, 1996; Wing et al., 2005).

Viewshed uncertainty based on the variability of GPS coordinates was evaluated at three sites. It was demonstrated at Site 3 that horizontal differences of only 14 m can have an important impact on GIS-generated viewsheds, and various resolutions of DEMs can affect

results differently. The higher resolution data tended to predict smaller viewsheds. The average viewshed range at Site 3 attributable to DEM resolution is about the same average range that is attributable to GPS variability.

Viewsheds from waypoints at Site 1 exhibited less variability than those from Site 3. Surprisingly, the greatest viewshed difference occurred between waypoint coordinates that are only 3.3 m apart. This is consistent with the research of Huss and Pumar (1997), who found that viewsheds are site-specific and that horizontal positional changes can have significant effects on viewsheds. DEM resolution also had less effect at Site 1 than Site 3. The average viewshed range at Site 1 attributable to DEM resolution is slightly more than the average range that is attributable to different horizontal positions. Like Site 3, higher resolution data generally predicted smaller visible areas.

Waypoints from the Site 5 fire tower have about as much variability as those from Site 1, but the 30-m viewsheds are nearly identical. Since the viewpoint is 18.3 m above the ground surface, there is no nearby terrain interference, and the horizontal position differences have very little impact on visibility. This demonstrates that ground obstructions near an observer are the main cause of viewshed uncertainty due to positional variations.

In summary, these results attest to the fact that even if multiple GPS coordinates computed from the same location are very precise and have high accuracy as reported by the GPS receiver, the true location is still unknown. Even small horizontal differences between GPS waypoints, and a point's short distance from the true location, can have a surprisingly large impact on GIS-generated viewsheds. The amount of impact is dependent on the nearby terrain, the height of the observer above the ground, and the spatial resolution of the elevation data.

Users predicting visibility from a location with an uncertain position should generate viewsheds from numerous positions surrounding the estimated location. Viewsheds should be generated from multiple GPS coordinates obtained at a given site. If one can estimate the predicted error circles, viewsheds could even be generated outside those circles, as those areas are not guaranteed to encompass the true location. Due to various biases, multiple coordinates obtained by a consumer-grade GPS that are very repeatable may still be far enough from the true location that relying on those coordinates alone, and not considering surrounding locations, may result in misleading viewsheds. Creating probable viewsheds will help in visualizing the uncertainty and in identifying areas of high and low agreement and confidence.

CHAPTER 8

EVALUATING A 3D VISUALIZATION TOOL FOR QUANTITATIVE VISIBILITY ANALYSIS

Lockhart, D. To be submitted to *Landscape Analysis using Geospatial Tools: Community to the Globe* (M. Madden and E. Allen, editors), Springer-Verlag.

Introduction

There are a variety of parties who have an interest in visibility. Applications abound, including landscape planning and architecture, communications tower siting, identifying scenic viewpoints, planning of defense installations, and visibility of new construction, to name a few. Many geographic information systems (GIS) are equipped with analysis functions that provide visibility results in a straightforward manner (Wang et al., 2000). ArcGIS provides three methods for determining the visibility of surface or near-surface features. These techniques include two algorithms, the viewshed and the line of sight (LoS), and 3D visualizations within ArcScene.

The term "viewshed" originated with the U.S. Forest Service in the 1970s (Ervin and Steinitz, 2003). The first computerized viewshed application, named VIEWIT, was developed by the Forest Service's Pacific Southwest Forest and Range Experiment Station in 1968 (Amidon and Elsner, 1968). In a GIS environment, a ray between an observer and target is evaluated as it passes over the digital elevation surface. If the ray encounters interference from the surface, then the two points are not visible to each other (Rana, 2003). This is the general procedure used by both the viewshed and LoS functions.

The viewshed is the most widely used visibility method. It has been implemented in a number of commercial, academic, and military software packages (Fisher, 1993; Riggs and Dean, 2007). Published research on numerous technical issues and applications of viewsheds is abundant (Goodchild and Lee, 1989; Fisher, 1991; Huss and Pumar, 1997; Llobera, 2007). Quick and easy, one only needs to provide an elevation surface (normally a gridded DEM, but some software allows a TIN) and an observer's position to find all the areas in the extent of the dataset that are visible. The output is a raster layer that indicates whether each cell is visible or not.

Unlike the viewshed, the LoS algorithm in ArcGIS is primarily a vector data function. LoS determines the visibility of a specific point target, as well as visibility along the straight LoS between the observer and target. As inputs, it takes an elevation surface (DEM or TIN) and one or more polylines, along which visibility is determined. The output is one or more vector lines with a continuous, linear record indicating either visible or not visible. Whether the specified target, the end point of the line opposite the observer, is visible is also an output. While many lines may be included and processed together, more time is needed to create these lines, so this procedure is more time intensive for a user than the viewshed.

ArcScene is the 3D viewing application that is part of ESRI's ArcGIS 3D Analyst extension. It allows users to create perspective views and scene fly-throughs (ESRI, 2002). It is a medium-priced visualization tool that lacks some of the complexity and functionality of higher-end packages such as Visual Nature Studio, but offers good capabilities in an interface that is relatively intuitive for those with prior experience with ESRI products (Appleton and Lovett, 2009). ArcScene is also readily available to the GIS community, whereas specialized visualization programs are less common and more expensive.

Computerized landscape visualizations began in the 1970s (Ghadirian and Bishop, 2008). Visualizations are utilized to communicate complex information, and the fields of scientific visualization and geovisualization are evolving rapidly (Wang et al., 2006). Geovisualization, according to MacEachren and Kraak (2001), "integrates approaches from visualization in scientific computing, cartography, image analysis, information visualization, exploratory data analysis, and geographic information systems to provide theory, methods, and tools for visual exploration, analysis, synthesis, and presentation of geospatial data." Appleton et al. (2002) outlined three categories of geovisualization: image draping, in which data layers are draped over

a 2.5D or 3D terrain representation, photorealistic rendering, in which a more realistic landscape simulation is created with vegetation and other landscape features, and virtual worlds, which are primarily interactive in nature.

Both urban and forestry applications are drivers of current geovisualization research. Visualizations are believed to improve forest research and management (Wang et al., 2006). Wisconsin uses a 3D forest visualization system that enables users to create photorealistic landscape renderings of current and possible future states of the forests (Stoltman et al., 2004). Due to the complexities of urban environments, creating photorealistic 3D models of cities is a great challenge. However, there is a need for these visualizations in the fields of urban planning and tourism (Haala and Kada, 2009).

The move towards 3D visualizations has been accompanied by a realization of the need for new tools to expand visibility algorithms. Ervin and Steinitz (2003) pointed out that there are limitations of the traditional GIS viewshed and that new 3D visibility capabilities are needed. Bishop (2003) expressed the same sentiment, arguing that the “essentially two-dimensional approach” of GIS visibility algorithms is insufficient in areas with many vertical elements. He advocated advancing to a 3D-based visibility approach. Winterbottom and Long (2006) combined GIS viewsheds with virtual reality in an archaeological study. Viewsheds were used to define minimum and maximum visible areas, while virtual reality provided rich visualizations of the landscape. A new tool was created for ArcGIS named the Viewsphere by Wang et al. (2006). This tool's intended use is to quantify 3D visibility in an urban environment. The Viewsphere differs from the traditional viewshed in that it calculates the visible volume instead of just surface or near-surface features. It determines vertical viewing, e.g., building facades, and not just horizontal visibility. Yu et al. (2007) also developed a 3D approach to visibility in with

ArcGIS' 3D Analyst (ArcScene). Their objective was to expand viewsheds to quantify visibility from high-rise buildings.

ArcScene is but one of numerous programs and modules that provide the capability of creating perspective views of terrain and landscapes with GIS data. With ERDAS Imagine's VirtualGIS, one can create 3D terrain renderings, drape imagery and vector data, and navigate and fly-through the virtual environment (Leica Geosystems, 2007). MICRODEM can create perspective views, and it allows draped imagery and fly-throughs (MICRODEM, 2005). There are specialized, high quality visualization programs like Visual Nature Studio that offer a rich suite of tools for creating photorealistic landscape simulations (3D Nature, LLC, 2008). This program is considered one of the best for integrating geographic data and creating visualizations at multiple scales (Wang et al., 2006). However, it was pointed out by Appleton et al. (2002) that "with capability comes complexity."

Although it was not specifically designed for the purpose of determining visibility like the viewshed or LoS functions, perspective views within ArcScene can be used to simulate a landscape vista, and therefore, visibility. ArcScene is a visualization tool and lacks many analytical functions. This is not unusual. Visualization tools are not designed to provide quantitative or statistical analyses of data (Gahegan, 1999). Whether ArcScene can be used for quantitative analyses is a worthwhile question. Gahegan (1999) states that the utility of visualization is difficult to assess because results gleaned from visualization cannot be compared to other methods. However, in this study, visualization results *can* be compared to other methods.

This study was inspired by the work of Germino et al. (2001), the only type of research encountered that compares 2D versus 3D visibility with ESRI software. They used ArcInfo 7.1.1

to determine visibility with two methods. The first technique was a planimetric simulation (2D) with the viewshed algorithm, and the second method was a panoramic or perspective simulation (3D) with a surface drape. They compared panoramic photographs, the ground truth, with both planimetric and perspective views in ArcInfo to quantify viewsheds and visible landcover classes.

Their approach was unique but required multiple steps. Planimetric (2D) visibility was computed by running the viewshed routine with 30-m DEMs. The viewshed was overlaid with GAP landcover to determine visible landcover. For perspective (3D) visibility, the observer's position, height, and other inputs were set equal to the viewshed inputs, and landcover was draped over the DEMs. The observer's view of the landscape was captured as an image and subsequently converted to a polygon coverage. Then the relative areas of each visible landcover class were calculated. This process was repeated to obtain a 360° panoramic view from each observer location. The percent of visible landcover classes for each observer location was compared between the 2D and 3D views to determine the agreement of these two methods in quantifying visible landcover.

Perspective landcover visibility was validated with field-based panoramic images. A video camera, set up at 1.5 m above the ground, recorded a 360° panoramic view of the landscape, and still images were extracted and stitched together into a panoramic image. Landcover classes were digitized from the image, converted to polygons, and the relative areas of the visible landcover classes were calculated. These results were compared to the 3D draped image results to assess the accuracy of the 3D perspective view.

In addition to comparing visible landcover, the extent of 2D and 3D views were compared, based simply on the delineated viewsheds. Test points were digitized at specific

distances (2, 5, 15, 25, or 50 m) either inside or outside the planimetric viewshed. These test points were draped over the DEM and counted. The percent of points that were correctly visible or correctly invisible was calculated, with the assumption that all points within the 2D viewshed would be visible and no points outside the 2D viewshed would be visible in the 3D view if the 2D and 3D simulations agreed perfectly.

Germino et al. (2001) found good agreement between the planimetric and perspective visible areas. Test points that were far (50 m) from the boundary of the 2D delineated viewsheds had 100% agreement. As the distance between test points and viewshed boundaries decreased, agreement decreased. For example, at a 2-m distance agreement was between 75% and 80%. It appears that agreement between 2D and 3D visibility was higher for points that were digitized inside of the viewshed, as opposed to outside, but detailed results were not published. Germino et al. (2001) speculated that a higher resolution DEM would have resulted in better agreement.

The 3D perspective view of landcover created in ArcInfo proved to be very accurate, as assessed by field data. There was only about 2% of error in the estimates of the visible area of each landcover class. Even though the boundaries of 2D and 3D visible areas agreed well, the agreement of these two methods in quantifying visible landcover was poor. The landcover discrepancies were mainly due to slope differences in the study area (Wyoming). For an observer on the ground, the viewshed algorithm is suitable for quantifying the land areas covered by various types of vegetation, but this result may be different from an observer's experience of the visible landscape in the field. In a perspective view, one will find the terrain and landcover more noticeable if it is at more of a perpendicular angle to one's line of sight, e.g., a hill rising up in front of an observer. However, flat ground that is more parallel to one's line of sight will be less noticeable, and will be experienced or seen as making up less of the visible area. These effects

can be heightened if different types of vegetation occur in areas of different slope, such as tall trees on sloped hills versus shrubs in a flat valley. Perspective distortions can also occur due to distance, in which landcover closer to an observer will appear larger and make up a higher percentage of the view than an equally sized patch of ground that is farther away. Consequently, Germino et al. (2001) found perspective views to be better at describing visible landcover.

There are various techniques for determining visibility in a landscape. The approach taken in this project is to use both a traditional viewshed algorithm and 3D visualizations. This is similar to the methods employed by Germino et al. (2001). The third technique available in ArcGIS, the LoS algorithm, will also be utilized, but to a lesser degree.

Observer and target heights can be adjusted in perspective views and in some viewshed algorithms, as in ArcGIS. An investigation related to that of comparing 2D and 3D visibility is the effect of altering these heights, or offsets. Increasing observer and target heights in a viewshed analysis should increase the visible area. Raised targets may become visible even when the surface is not visible. For example, beyond the crest of a hill the top of a tower may be seen even when its base is obscured by the hill. Field validation of viewshed accuracy, using several software programs, indicated that accuracy improved from ~94% to ~97% with a 1-m DEM when the visibility of higher targets (1.6 m versus 1 m) was considered (Swanson, 2003).

Purpose and Objectives

The purpose of this project is to compare visibility with the ArcGIS 3D Analyst extension between the planimetric viewshed algorithm (Viewshed_3d command) and the perspective view of ArcScene. Software-related issues should not be a factor since all processing is done within the same software package and version, ArcGIS 9.2. The specific questions focus on the accuracy of the geometry within ArcScene. How geometrically accurate are the 3D

visualizations within ArcScene? Are they a viable alternative to the viewshed or LoS algorithms for determining visibility? Can this visualization tool be used for quantitative analyses?

The assumption is that visibility results from the algorithms should agree with visibility observed within ArcScene. Visibility of specific, identifiable, near-surface features based on viewsheds were compared with the visibility of the same features in ArcScene. The objective is to quantify this level of agreement. Different resolutions of raster DEMs and DEM-derived TINs were utilized to determine if agreement is sensitive to the data structure and/or spatial resolution of the underlying terrain data, and tests were performed in two regions with markedly different terrain characteristics and relative observer positions to determine if these factors impact visibility agreement. It is assumed that if agreement varies, it will be lower in rugged terrain, as Swanson (2003) reported that GIS-based visibility was less accurate in rough terrain, as validated by field work.

Another objective is to analyze the effects of modifying observer and target heights on visibility. A case study quantified the impacts on viewsheds by systematically altering these parameters.

Data and Methodology

Viewshed/visualization tests were conducted in two areas, where the terrain and the observer's position within the terrain were very different (Figure 8.1). These areas were chosen to test whether visibility agreement was sensitive to the roughness of the terrain and the relative position of the observer. The first area is a circular region 6 km in diameter centered on Waypoint 709 (Site 11) in Haywood County, North Carolina (refer to Chapter 3). This area is very rugged, dominated by high ridges and steep hillsides. Its elevation range is 698 m (873 m to 1571 m) with a standard deviation of 160 m, and the mean slope is 21° (based on a 30-m DEM).

The observer location is high, relative to the surrounding terrain, located at 1,534 m on a flat bench along a ridge top. The second area is a circular region 3 km in diameter located in Cades Cove, on the Tennessee side of GRSM. This is a low lying valley surrounded by modest hills. Its elevation range is only 108 m (523 m to 631 m) with a standard deviation of 16 m, and the mean slope is 4° (based on a 30-m DEM). The observer location is on the valley floor, low in relation to the surrounding terrain at just 526 m. The Cades Cove study area is smaller than the Haywood County area because enlarging the Cades Cove area would only encompass additional rugged terrain, and the purpose was to utilize flat land to compare results in different types of terrain.

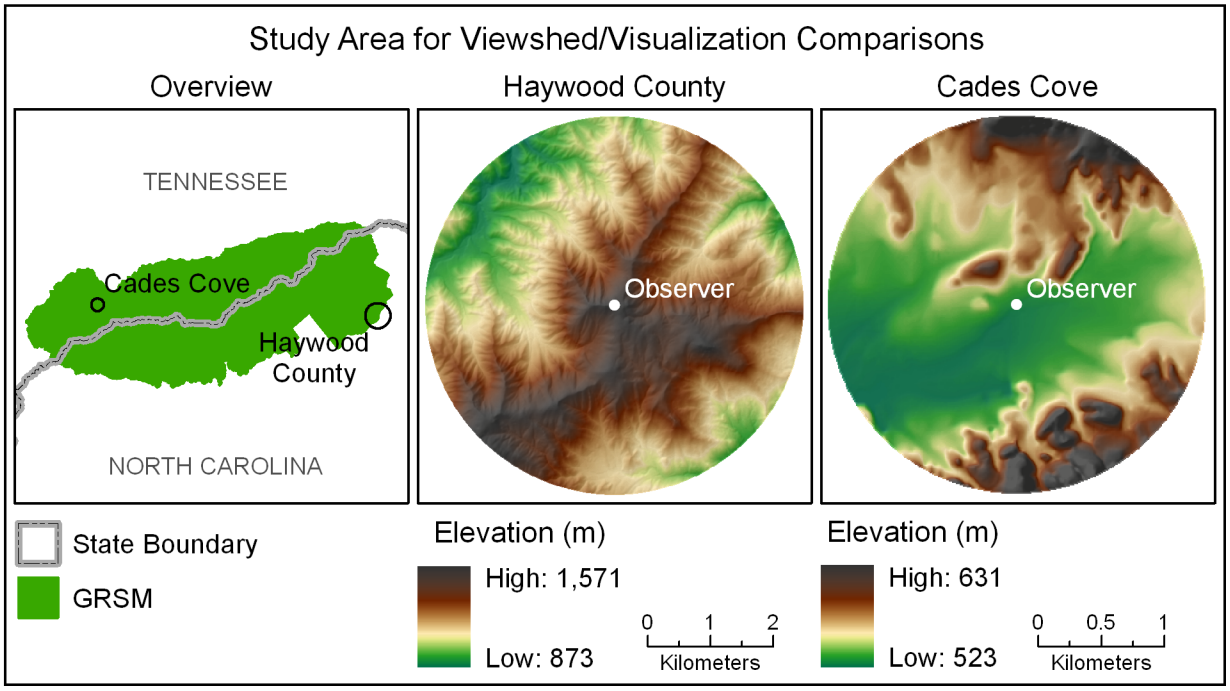

Figure 8.1: Study area for 2D/3D visibility comparisons.

The elevation data utilized was of the highest resolution available in each area, subsequently resampled to lower resolutions for comparisons. In Haywood County, the USGS 1/9 arc-second NED DEM, which is approximately 3 m in resolution, was resampled to 6 m, 10 m, and 30 m (refer to Chapter 4). Tests were conducted with all four resolutions of data. The

highest resolution DEM available for Cades Cove is the 1/3 arc-second NED, which is approximately 10 m in resolution. This was resampled to 30 m.

Maloy and Dean (2001) created triangulated irregular networks (TINs) from DEMs in their viewshed accuracy tests, and Lee (1991) described various methods of deriving TINs from gridded DEMs. Thus, TINs were created from the 6-m, 10-m, and 30-m Haywood County DEMs in ArcGIS with z-tolerance = 0. This is the maximum vertical accuracy with which TINs can be derived from DEMs in ArcGIS, and it means that the TIN will have the same z-value as the DEM at the centroid of each DEM cell (ESRI, 2007). The 3-m DEM could not be converted to a TIN with 0 z-tolerance due to a limit reached on the maximum number of data points. This is an example of a GIS limitation in performing terrain analysis. TINs were created from the 10-m and 30-m Cades Cove DEMs with 0 z-tolerance.

The study area for analyzing the effects on viewsheds of altering observer and target heights is a semi-circular region, 30 km in diameter, in the southwestern portion of GRSM (Figure 8.2). The observer is Waypoint 642 at Site 3 (refer to Chapter 3). The data for generating viewsheds was the 1 arc-second USGS NED, with a spatial resolution of approximately 30 m (refer to Chapter 4).

To evaluate viewshed uncertainty in an algorithm versus visualization approach, using different terrain data types and resolutions, a scenario was created to simulate a real-world application involving feature visibility in a landscape. Germino et al. (2001) digitized test points both inside and outside of planimetric viewsheds, then draped the test points over an elevation surface to compare the number of points predicted to be visible with a viewshed with those actually visible in a 3D perspective view. Following this example, and improving upon this methodology, square features representing buildings were created instead of points. Each

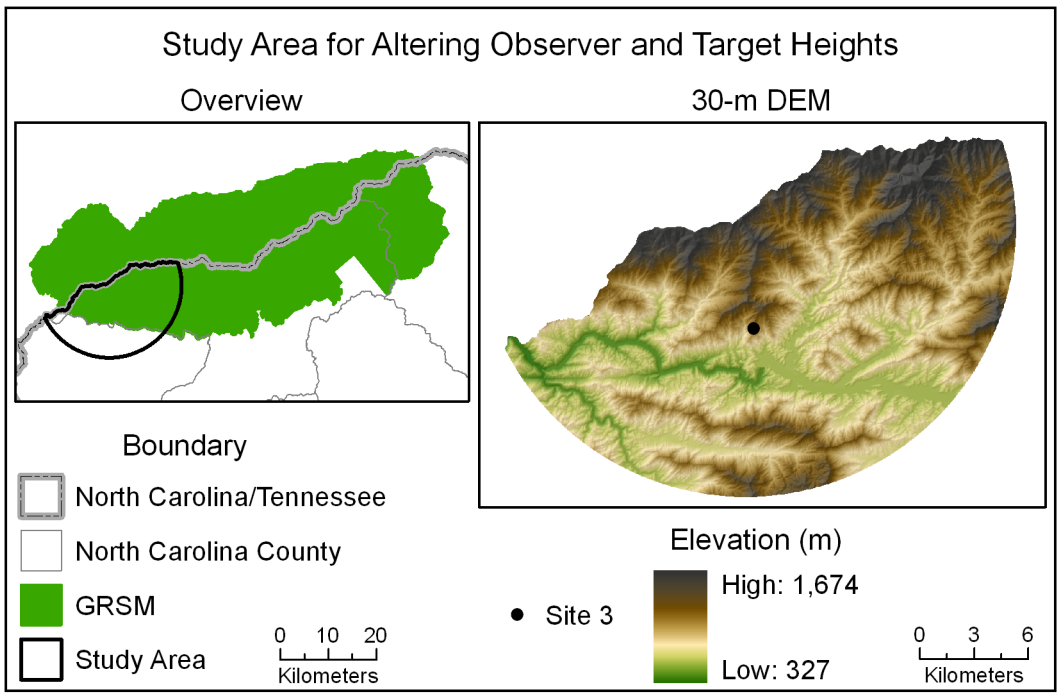

Figure 8.2: Study area for differing observer and target heights.

"building" measured 20 m × 20 m, representing the size of a large house of approximately 4,300 square feet.

In the Haywood County study area, 200 buildings were created, randomly distributed throughout the area. Viewsheds were generated in ArcGIS from the four resolutions of DEMs and three TINs. Relative observer height was 1.5 m above the surface for DEMs, which approximates a person's height. All grid cells within the study area were considered to be raised 5 m above the surface when they were evaluated for visibility. This does not negatively impact surrounding cells, but counts a cell as visible if a feature within it, with a height of 5 m, could be seen. This 5-m target height was used to simulate a building approximately one story tall.

A different method of creating/placing buildings was used in Cades Cove. A 300-m grid was laid over the area, and then one building was placed randomly within each grid. This is a

stratified random sampling method. Viewsheds were generated in ArcGIS from the two resolutions of DEMs and two TINs. Target heights were 5 m to simulate one story buildings.

Due to uncertainties in ascertaining the default observer height from a TIN in the viewshed algorithm, a previously found offset (~0.6 - 0.7 m) was used to adjust observer heights. In the DEM test, constant relative heights (1.5 m) and varying absolute heights were used. By default, the viewshed function determines observer surface elevation by bilinear interpolation. Absolute elevation will vary based on the DEM resolution, since the elevation models are different, even though they originated from the same source data. In the TIN test, it was only possible to use constant absolute heights with varying relative heights. This is due to the way in which observers must be set in ArcScene for a faithful comparison, which is explained further in this section.

Once viewsheds were generated, they were intersected with the building polygons. The criterion for determining building visibility is whether any part of the building falls within the viewshed. Based on the 10-m DEM in Haywood County, the observer's surface elevation was 1,535.2 m and elevations of visible buildings ranged from 1,090.1 m to 1,512.2 m, with a mean of 1,365.8 m and a standard deviation of 110.3 m. For Cades Cove, the observer's surface elevation was 526.5 m and elevations of visible buildings ranged from 524.0 m to 592.8 m, with a mean of 538.4 m and a standard deviation of 16.6 m. This illustrates the differences in terrain and relative position of the observer to the buildings. In Haywood County, all visible buildings were below the observer, while in Cades Cove, most visible buildings were above the observer.

To test the agreement of building visibility between the planimetric viewshed and the perspective view, the relevant data were loaded into ArcScene. This included the elevation model, observer (point layer), viewshed layer, all buildings, and all buildings within the

viewshed. Parameters that could be controlled in ArcScene were set equal to those used in the viewshed algorithm for fidelity in comparison. Rendering of all layers, including DEMs, was set to the highest quality possible. Base heights were based on the elevation model, with raster resolution equal to that of the DEM surface. No vertical exaggeration was employed. Thus, to the extent that a user can control the geometric properties, there was no generalization or exaggeration of the data layers. Finally, building polygons were extruded 5 m above the surface (Figure 8.3).

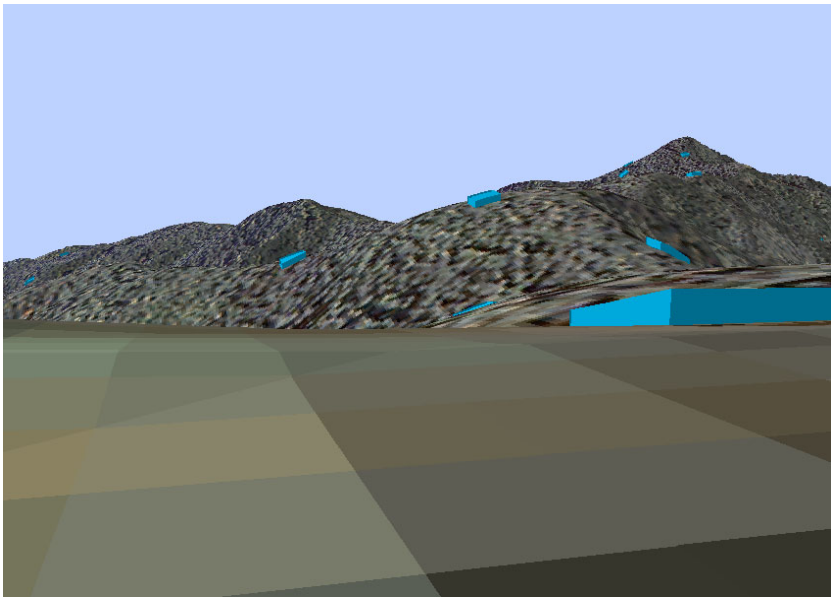

Figure 8.3: 3D view in ArcScene of Haywood County. Buildings from Test 1 and 2-m NAIP imagery are draped over a 10-m-derived TIN.

A shortcoming of ArcScene is that it does not provide an out-of-the-box tool for setting the observer position with precision (one can only click a location), so Rick Smith (University of Georgia Geography Ph.D. student) created a tool with Visual Basic to do this. The tool enables the observer's X,Y,Z position to be entered via a dialog box or based on values in the observer's attribute table. Horizontal positions are straightforward. Observer heights vary, depending on the elevation data structure used and the resolution. With DEM-based viewsheds, bilinear

interpolation is the method used for obtaining an observer's surface elevation, and this z-value can be easily determined. A viewing height of 1.5 m was then added to the observer's surface elevation. These two heights summed together give the observer's total or absolute elevation. For 2D/3D comparisons based on DEMs, the same relative observer height (1.5 m) is used, but absolute height varies for each resolution of DEM. For example, in Haywood County, absolute elevation was as follows: 3-m DEM: 1,535.2 + 1.5 = 1,536.7 m; 6-m DEM: 1,535.3 + 1.5 = 1,536.8 m; 10-m DEM: 1,535.2 + 1.5 = 1,536.7 m; 30-m DEM: 1,533.9 + 1.5 = 1,535.4 m. The important fact is that for each 2D/3D test with a specific resolution of DEM, the observer was at identical heights. Thus, relative height was 1.5 m and absolute observer elevation was 1,536.7 m for the viewshed and visualization with the 3-m DEM, and relative height was 1.5 m and absolute elevation was 1,535.4 m for the viewshed and visualization with the 30-m DEM. The test is the 2D versus 3D visibility with a given DEM; with the same inputs, they should have 100% agreement.

To ensure that 3D views with a TIN had the same observer height as their 2D viewshed counterparts, constant absolute observer heights had to be used. This means that from one TIN to another, relative observer heights differed. A spot elevation is required for setting up the vista in ArcScene. Because there is uncertainty from previous tests as to exactly how the observer height is determined in the viewshed algorithm if the absolute elevation is not specified, the same absolute height was specified for each TIN. The value selected ensured that each observer was at least 1.5 m above the surface. This is noted but does not present a problem, as the direct comparison is not between TIN/DEM viewsheds, but on the level of agreement between 2D and 3D visibility with a given surface type and resolution. In every test, 2D and 3D visibility should

agree, because all the inputs (elevation surface, observer location and elevation, building location and elevation) in each 2D/3D comparison are equal.

Once the vista was set up in ArcScene, the observer was rotated, obtaining a complete, 360° panoramic view of the landscape (Figure 8.4). Visible buildings were manually counted and missing or extra buildings were identified by their unique ID. Buildings predicted visible from the viewshed were portrayed in blue, while buildings predicted not visible from the viewshed were portrayed in pink. If the perspective view agrees with the viewshed algorithm, then all buildings deemed visible from the algorithm should be visible in the 3D landscape, and no building deemed invisible should be seen in ArcScene. In other words, all blue buildings should be seen and no pink buildings should be seen. Note that 20 m × 20 m buildings can be seen in perspective view in ArcScene even at the edge of the area of interest.

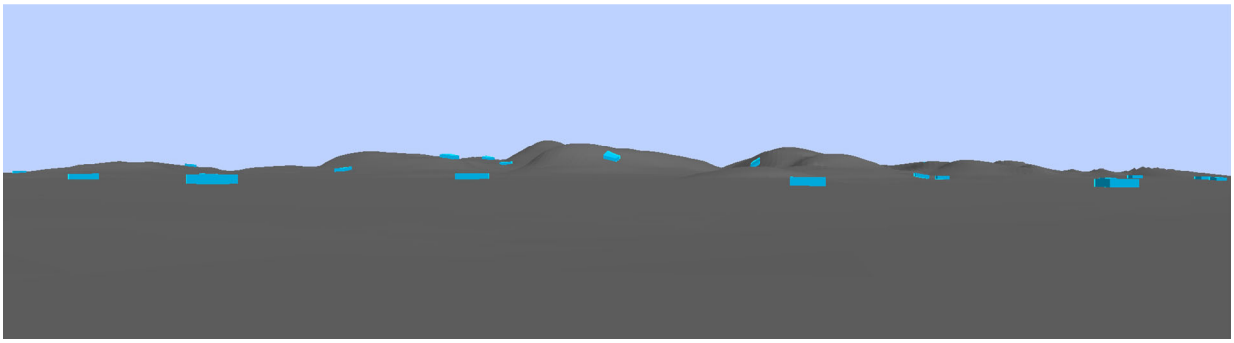

Figure 8.4: Multiple landscape vistas from ArcScene stitched together to give a view from southeast to southwest of terrain and buildings, Cades Cove, 10-m-derived TIN.

For Haywood County, the methodology was repeated so that two full tests were conducted, with two independent sets of randomly placed buildings. Results were combined to create statistical averages. Only one test was conducted in Cades Cove, but this was supplemented by comparing viewshed and visualization results with visibility from the vector LoS algorithm. For the LoS function, each building deemed visible by the viewshed was set up

as a target, equal inputs and parameters were used, and the visibility of each building centroid (or other visible point if the centroid was not visible by the viewshed) was determined by LoS.

To quantify the impact that various observer and target heights have on visible areas, observer and target heights were altered in 42 viewsheds generated in ArcGIS. Target heights used were 0 m (the ground surface), 1.5 m, 5 m, 10 m (2-3 story building height), 15 m, 20 m (fire tower height), and 50 m (cell tower height). Observer heights were 1.5, 5, 10, 15, 20, and 50 m. The visible areas predicted by the 42 viewsheds were compared. To determine whether observer height or target height had the greatest impact on the visible area, an ordinary least squares multivariate regression analysis was conducted.

Results

2D/3D Comparison - Haywood County

The visibility agreement between viewsheds and visualizations in Haywood County is given in Table 8.1 for DEMs and Table 8.2 for TINs. The variability in viewshed area is also given. For DEM-based viewsheds, the 30-m DEM predicted the smallest visible area and the 6-m DEM predicted the largest area. The situation is reversed for TIN-based viewsheds, with the 30 m-derived TIN predicting the largest visible area and TINs derived from the 6-m and 10-m DEMs predicting the smallest area.

The meaning of the tables is explained, using the 10-m DEM in Test 1 in Table 8.1 as an example. According to the viewshed function, 15 buildings are at least partially visible to the observer. In the 3D view of ArcScene, 14 of these 15 buildings (93%) are visible; 1 building is not able to be seen in perspective view. There were 5 buildings visible in ArcScene that were not predicted to be visible by the viewshed function. Summarizing from the standpoint of the

Table 8.1: Visibility agreement with DEM, Haywood County.

DEM resolution (m)	3	6	10	30
Viewshed area (sq. km)	2.6	2.7	2.5	1.9
Test 1				
Buildings visible in 2D	23	21	15	11
Buildings visible in 2D that were visible in 3D	23	21	14	11
Percent of buildings visible in 2D that were visible in 3D	100%	100%	93%	100%
Buildings visible in 3D that were not visible in 2D	0	1	5	2
Test 2				
Buildings visible in 2D	24	24	23	18
Buildings visible in 2D that were visible in 3D	24	24	21	18
Percent of buildings visible in 2D that were visible in 3D	100%	100%	91%	100%
Buildings visible in 3D that were not visible in 2D	0	1	1	0
Average				
Buildings visible in 2D	23.5	22.5	19.0	14.5
Buildings visible in 2D that were visible in 3D	23.5	22.5	17.5	14.5
Percent of buildings visible in 2D that were visible in 3D	100%	100%	92%	100%
Buildings visible in 3D that were not visible in 2D	0.0	1.0	3.0	1.0

viewshed function and borrowing from remote sensing terminology, there was 1 error of omission in ArcScene and 5 errors of commission.

Results from Tests 1 and 2 with the DEMs are very similar. All buildings predicted visible with the viewshed were visible in ArcScene with 30-m, 6-m, and 3-m DEMs. With the 10-m DEM, 1 building from Test 1 and 2 buildings from Test 2 should have been visible in ArcScene but were not. It should be noted that these 3 buildings had very small cross sections, as only a portion of the buildings were within the viewshed. Overall results indicate that from the 10-m DEM, 92% of buildings visible from the viewshed were visible in perspective view. All other DEMs had 100% of buildings visible. One could consider these as confidence estimates. “Extra” buildings, those outside the planimetric viewshed but visible in ArcScene, occurred an

Table 8.2: Visibility agreement with TIN, Haywood County.

DEM resolution (m) of TIN source	3	6	10	30
Viewshed area (sq. km)	NA	2.9	2.9	4.0
Test 1				
Buildings visible in 2D	NA	25	25	29
Buildings visible in 2D that were visible in 3D	NA	24	21	13
Percent of buildings visible in 2D that were visible in 3D	NA	96%	84%	45%
Buildings visible in 3D that were not visible in 2D	NA	2	2	7
Test 2				
Buildings visible in 2D	NA	26	25	40
Buildings visible in 2D that were visible in 3D	NA	24	24	22
Percent of buildings visible in 2D that were visible in 3D	NA	92%	96%	55%
Buildings visible in 3D that were not visible in 2D	NA	0	2	6
Average				
Buildings visible in 2D	NA	25.5	25	34.5
Buildings visible in 2D that were visible in 3D	NA	24.0	22.5	17.5
Percent of buildings visible in 2D that were visible in 3D	NA	94%	90%	51%
Buildings visible in 3D that were not visible in 2D	NA	1.0	2.0	6.5

average of 1 time with the 30-m and 6-m DEMs. An average of 3 extra buildings occurred with the 10-m data. Only the 3-m DEM had perfect agreement between 2D and 3D visibility.

Agreement between the visibility methods was not as high with TINs. The 30-m-derived TINs were especially poor, with only about half (51%) of buildings visible in viewsheds being visible in perspective view. There was also an average of 6.5 buildings visible in ArcScene that were outside the viewshed extent. Agreement improved with the TINs derived from higher resolution data, with the 6-m-derived TIN averaging 94% of buildings in viewsheds visible in ArcScene and only 1 extra building visible in ArcScene.

An example of extra buildings is illustrated in Figure 8.5, which shows both a 2D and 3D view of the same area. Five buildings in this area are considered. Buildings A, B, and C, in blue, are predicted visible by the viewshed algorithm and are visible in ArcScene. There is a

discrepancy in the pink buildings. Buildings D and E are predicted by the viewshed to be invisible, but they are certainly visible in the 3D view.

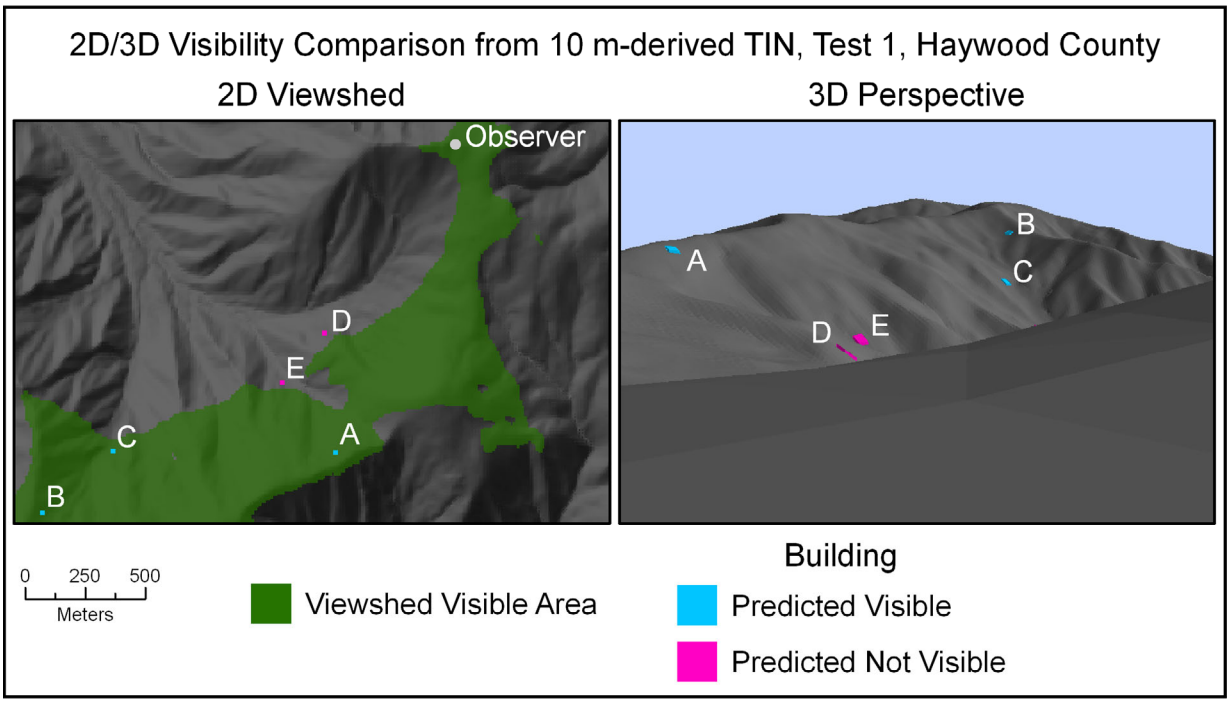

Figure 8.5: Visibility comparison in Haywood County, showing agreement of Buildings A, B, and C, but disagreement of Buildings D and E.

2D/3D Comparison - Cades Cove

Agreement between viewsheds and visualizations in Cades Cove was better with the 10-m than the 30-m DEM (Table 8.3). No extra buildings were seen with the 10-m data, and 95% of buildings within the viewshed were visible in ArcScene. The 30-m DEM had 1 extra building and 90% of algorithm-predicted buildings were visible in ArcScene. These 90% and 95% agreements could have been higher with a different placement of buildings. It was discovered that a few buildings were blocked by others. But this happens in real life, so this was a good simulation and example of how a feature predicted visible by a viewshed may be masked by other features in the environment. Vector LoS results agreed very well with the viewsheds. With

the 30-m DEM, 39 of 40 (98%) buildings were visible with the LoS function, and 38 of 39 (97%) buildings were visible by LoS with the 10-m DEM.

Table 8.3: Visibility agreement with DEM, Cades Cove.

DEM resolution (m)	3	6	10	30
Viewshed area (sq. km)	NA	NA	3.41	3.37
Test 1				
Buildings visible in 2D	NA	NA	39	40
Buildings visible in 2D that were visible in 3D	NA	NA	37	36
Percent of buildings visible in 2D that were visible in 3D	NA	NA	95%	90%
Buildings visible in 3D that were not visible in 2D	NA	NA	0	1

In Cades Cove, all buildings within the viewsheds were visible in ArcScene with TINs (Table 8.4). The 10-m-derived TIN only had 1 extra building, while there were 3 extra buildings with the 30-m-derived TIN. However, the vector LoS function did not agree as well with viewsheds and visualizations with the TINs as with the DEMs. For the 10-m-derived TIN, only 30 of 39 (77%) buildings within the viewshed were visible with LoS. This is demonstrated in Figure 8.6, in which a number of discrepancies are apparent in the southwestern portion of the study area. These are recognized by the red lines connecting to the blue buildings. Results were better with the 30-m-derived TIN, in which 33 of 37 (89%) buildings within the viewshed were visible with LoS.

Table 8.4: Visibility agreement with TIN, Cades Cove.

DEM resolution (m) of TIN source	3	6	10	30
Viewshed area (sq. km)	NA	NA	3.42	3.32
Test 1				
Buildings visible in 2D	NA	NA	39	37
Buildings visible in 2D that were visible in 3D	NA	NA	39	37
Percent of buildings visible in 2D that were visible in 3D	NA	NA	100%	100%
Buildings visible in 3D that were not visible in 2D	NA	NA	1	3

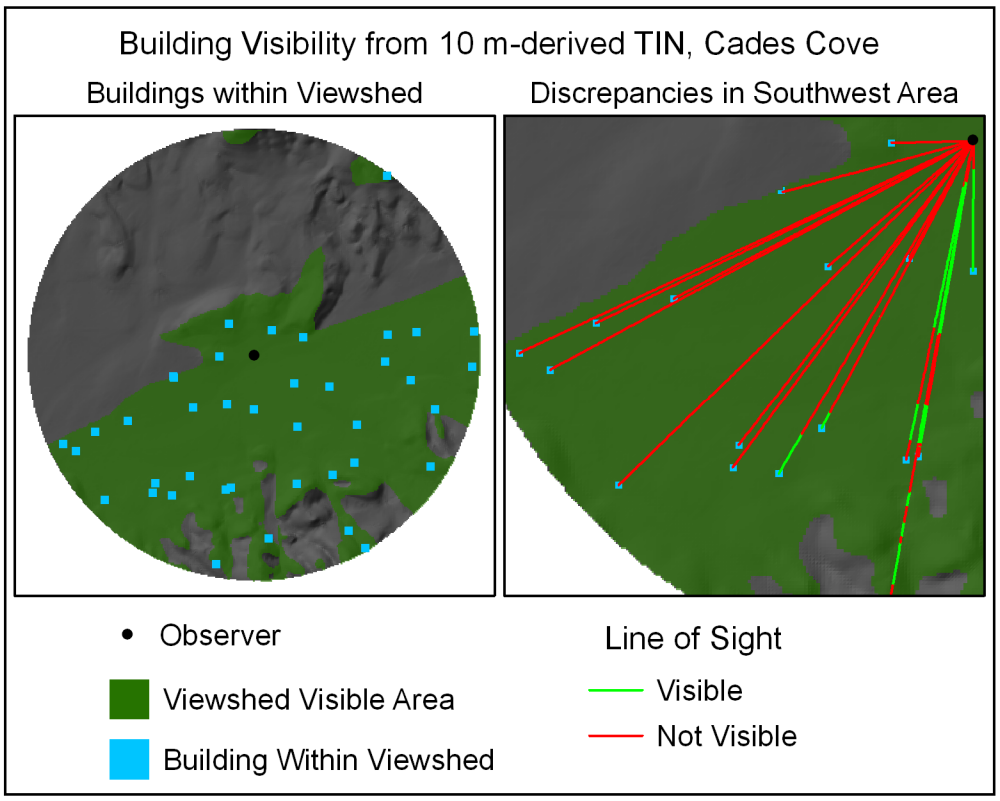

Figure 8.6: Viewshed and line of sight comparison, Cades Cove.

Observer and Target Heights

Clearly, the extent of visible areas increased as observer and target heights above the surface increased (Figure 8.7). For a given observer height, the increase in viewshed area is basically linear with an increase in target height. For a given target height, the difference in visible area is much greater when the observer height increases by 3.5 m from 1.5 to 5 m, as compared to when observer height increases by 5 m from 5 to 10, 10 to 15, or 15 to 20 m.

A multivariate regression analysis was used to determine whether observer height or target height had the strongest impact on the visible area. As expected, a very high degree of the variability in visible area is accounted for by the two predictor variables ($r^2 = 0.93$). Although both parameters are significant ($p < .001$), target height's greater beta coefficient (0.85 versus 0.46 for observer height) indicates that in this linear model, for this landscape and viewer

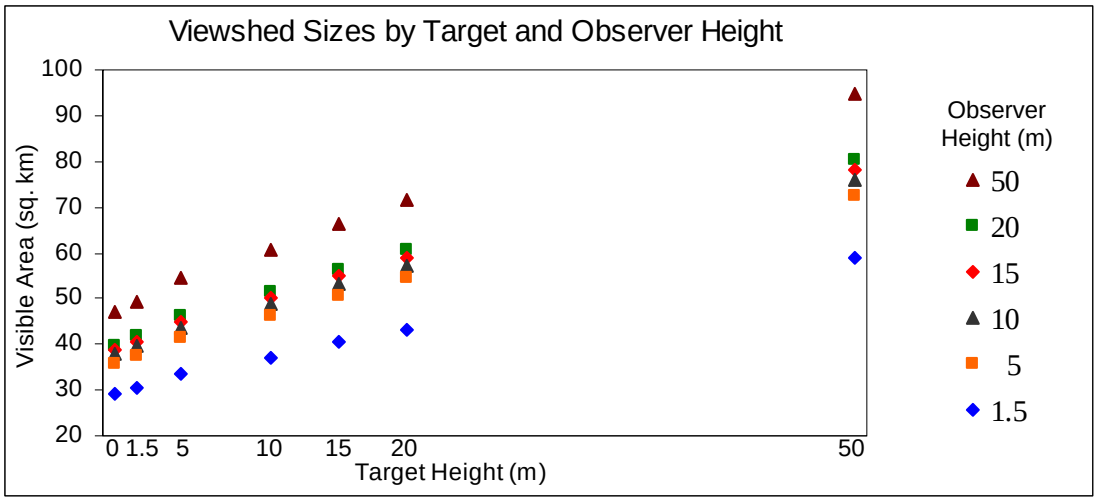

Figure 8.7: Relationship of target and observer heights with visible area.

position, target height has a greater effect than observer height on the size of the visible area. This is confirmed by the matrix of Table 8.5, which compares viewshed area by the matched combinations of target and observer offset. In this matrix, 12 of the 15 largest viewsheds occur with the target being raised, as opposed to the raising of the observer.

Table 8.5: Visible area (km^2) by target and observer heights (m). Bold indicates larger viewshed.

	Observer Offset					
Target Offset	1.5	5	10	15	20	50
1.5	30.4	**37.7**	**39.5**	**40.7**	41.8	49.3
5	33.3	41.5	43.6	44.9	46.2	54.5
10	37.1	**46.4**	48.8	50.2	51.6	60.8
15	40.4	**50.7**	**53.3**	54.9	56.4	66.4
20	**43.3**	**54.5**	**57.4**	**59.0**	60.6	71.4
50	**58.8**	**72.6**	**75.9**	**78.0**	**80.2**	94.9

To illustrate the effects of increasing target heights above the surface, a portion of the viewsheds generated from Site 3 were superimposed (Figure 8.8). One can see the increasing extent of visible areas when target heights are raised.

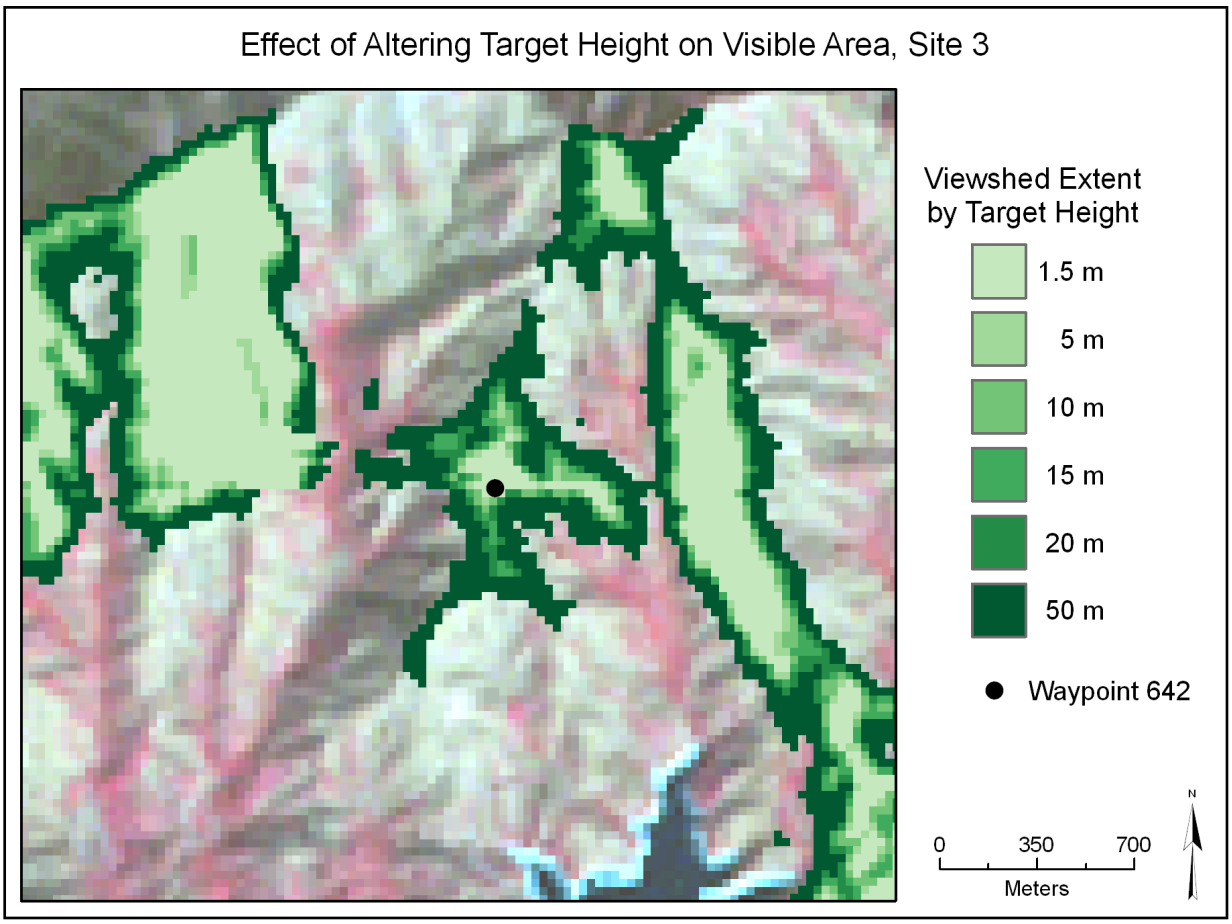

Figure 8.8: Portion of viewsheds from Site 3 illustrating more extensive visible areas with increasing target heights, superimposed on color infrared Landsat image.

Summary and Conclusions

This study used randomly distributed square features to represent buildings, similar in area and height to large houses. The number of houses predicted visible from an observer's location was determined by a viewshed algorithm. The same data were used to set up a 3D visualization, with the buildings extruded above the surface to the same height used by the viewshed function. A quantitative assessment of building visibility was made between the viewshed and visualization methods. Multiple tests were conducted to consider different elevation data structures, data resolutions, and terrain characteristics.

When considering whether features within the viewshed are visible in the visualization, 90% or greater agreement is usually attained. All DEMs in Haywood County had 100% agreement except the 10-m DEM, which averaged 92%. Agreement was lower with TINs, averaging less than 95% agreement in Haywood County. The 30-m-derived TIN fared poorly, with scarcely half of the features within the viewshed visible in ArcScene. This TIN also had the greatest number of extra buildings visible in ArcScene that were outside the predicted viewshed. Most other terrain data had few extra buildings, but DEMs performed better than TINs in this respect. The overall trend with both DEMs and TINs was for higher levels of agreement with higher resolution elevation data. The 3-m DEM was the best performing elevation model in Haywood County, the only one with perfect agreement in all measures. The 10-m DEM was an anomaly. It is not clear why, but it had the worst results of the DEMs in Haywood County.

In the flatter terrain of Cades Cove, agreement was higher. This result is corroborated by Swanson (2003), who found that viewshed accuracy decreased in rougher terrain. With TINs, all buildings within the viewshed were visible in the visualization, and a small number of extra buildings were visible. DEMs had fewer extra buildings than TINs, and 2D-visible buildings were seen in ArcScene 90%-95% of the time. Vector LoSs agreed well with viewsheds based on DEMs, but not as well with TIN-based viewsheds and visualizations. This is consistent with other tests that have found lower agreement between the viewshed and LoS functions with TINs than DEMs.

Agreement between 2D and 3D visibility was slightly better in Cades Cove than in the rugged terrain of Haywood County. This was somewhat surprising, because an observer standing on the ground could easily have his view of distant buildings blocked by intervening buildings where there is little vertical relief, as in the flat valley floor of Cades Cove. While the viewshed

would predict the distant buildings to be visible, they would be masked in the perspective view. This did occur, but agreement was still worse in Haywood County. More extensive testing would need to be conducted to make confident statements about the effects of the terrain characteristics, since only one 2D/3D comparison was performed in Cades Cove.

This study did confirm the speculation by Germino et al. (2001) that higher resolution elevation models would result in better agreement. It also affirms their finding of good agreement between the planimetric and perspective visible areas. They reported lower levels of agreement in cases where the test points were close to the viewshed boundaries. Although this type of analysis was not conducted in this study, it was observed that numerous buildings that were sources of disagreement were located very near the delineated viewshed boundary.

A few questions remain regarding the work of Germino et al. (2001). For comparing visible areas, they used digitized points. Since points have no size, by definition, it would be interesting to know how large they were rendered in the perspective view. An advantage of this current study is that simulated buildings (cubes) were used. In the 3D view, the size of the cubes remains accurate and proportional, in relation to the observer. A building that is close appears large, and a distant building appears small. In addition, Germino et al. do not state the distances that the test points were located from the observer. To validly observe the points in perspective view, they could not be long distances away, but the fact that they were points could complicate the situation. In the current study, the furthest buildings were less than 3 km away. This is an area for future study or research, to determine the relationship between an object's size and the maximum distance it can be detected.

There are several limitations to this study and these methods. It is beyond the scope of this project to state which visibility method is most accurate, the visualization, the viewshed

function, or the LoS function. However, due to the success of Germino et al. (2001) in quantifying landcover from perspective views, and other inconsistencies found between the viewshed and LoS algorithms, especially when TINs are used, it is theorized that most discrepancies found in this study are probably due to issues with the viewshed function, and not the geometry of the ArcScene simulations. It is a limitation that perspective views in a GIS program are not effective over long distances, and features must be distinguishable and large enough to be detected at a given range. Another issue is that setting up visualizations and manually counting features is much more time consuming than generating viewsheds. It should also be noted that 3D perspective views are dependent on a computer's graphics card, screen resolution, and memory capacity. Due to this, they inherently entail more uncertainty. With these caveats, this study found that ArcScene visualizations are a viable alternative to the viewshed or LoS algorithms for determining visibility. In most cases, 90% agreement can be attained, and higher resolution elevation data tends to yield high levels of agreement.

Regarding the effects of observer and target heights, for this study area and observer location, as target height was increased, the area visible to the observer increased linearly. For a constant target height, elevating the observer a short distance above ground level opened up the view more than raising the observer the same distance from a height that was already a good deal above the ground. Similar results have been found in other studies of this thesis. It occurs because the main view-obstructing obstacle is the nearby terrain for one who is standing on the ground. If one is already high above the surface, such as in a fire tower, then nearby terrain features are not a hindrance, and rising even higher in the air has little effect on what can be seen. It was also found in this study that target height had a greater effect than observer height on the size of the visible area.

CHAPTER 9

THE EFFECTS OF EARTH CURVATURE ON VIEWSHEDS

Lockhart, D. To be submitted to *Landscape Analysis using Geospatial Tools: Community to the Globe* (M. Madden and E. Allen, editors), Springer-Verlag.

Introduction

Few people still believe that the earth is flat. However, it is often treated as such when working with geographic data in GIS. Essentially, the earth has the shape of an ellipsoid. In practice, working with a spherical coordinate system is more problematic than using a rectangular coordinate system (Bossler, 2002). It can be advantageous to simplify and represent the curved earth as a flat plane.

A map projection is the representation of a portion, or all, of the curved earth surface as a flat plane (Snyder, 1987). Summarizing the creation of a map projection, one of three types of developable surfaces (cylinder, cone, or plane) is placed over a reference globe and the globe's graticule is projected onto the developable surface. Then the surface is flattened into a plane, and the location of earth features on this plane is the map projection (Slocum et al., 2008).

It is very important to note that all map projections result in some type of distortion. Various projections will have different types and amounts of distortions, and the main categories of distortions are area, shape, scale, direction, and distance. Distortions depend on the extent of the area of interest and the specific projection used (Habib, 2002).

Two of the most commonly used planar coordinate systems in the U.S. are the State Plane Coordinate System and the Universal Transverse Mercator (UTM) Coordinate System. In the state of North Carolina, these systems use different projections, although both are conformal. Conformality means that a projection preserves shape and true direction (Colvocoresses, 1997). The UTM system is based on the Transverse Mercator projection, with the whole world divided into 60 zones, each being 6° in longitude (Bossler, 2002). The UTM system is one of the world's most popular systems, and it has been heavily used in the U.S. It was adopted for use by the US Army in 1947 and the North Atlantic Treaty Organization (NATO) in the mid-1950s, and the

USGS began using it frequently in 1973 (Snyder, 1987; Colvocoresses, 1997). The Transverse Mercator projection is a cylindrical projection, with lines of true scale occurring in a north-to-south direction. The State Plane Coordinate System was developed in the 1930s by the Coast and Geodetic Survey (Snyder, 1987). The North Carolina State Plane Coordinate System is based on the Lambert Conformal Conic projection, with lines of true scale occurring in an east-to-west direction. Snyder (1987) pointed out that the USGS uses both Transverse Mercator and Lambert Conformal Conic projections.

One practical difference is that Transverse Mercator distortions occur in an east-to-west direction, while Lambert Conformal Conic distortions occur in a north-to-south direction (Bossler, 2002). Thus, states greater in extent in an east-to-west direction use the Lambert Conformal Conic projection in the State Plane Coordinate System, and states that are predominantly north-to-south use the Transverse Mercator projection in the State Plane Coordinate System (Snyder, 1987). UTM distortions within a zone are greatest near the zone's eastern and western boundaries, and North Carolina State Plane distortions are minimal north-to-south, due to the two standard parallels of latitude (Bossler, 2002). Although the State Plane Coordinate System is more accurate than the UTM system, planimetric error for UTM data is only 3-4 m at a zone's boundary (Thomas Jordan, personal communication, August 2008).

The impact of various coordinate systems and map projections is that distortions – errors – are introduced into data when transformations between systems/projections take place. When source data are in geographic latitude/longitude coordinates, such as the USGS NED, and the data are projected, an interpolation process takes place. DEM interpolation shifts grid points in east-to-west and north-to-south directions by variable distances (Franklin and Guth, 2005). Latitude and longitude at a particular location, when transformed into a planar coordinate

system, may result in X,Y coordinates that are slightly “off the mark,” or inaccurate. A feature’s shape or its relation to other features may be modified, depending on the projection.

Coordinate system/map projection choices are made for various reasons in the real world. Decisions may be made for convenience, when one just uses the system that the data were in when it was delivered. They may be practical decisions, when all the data for a project must be in a predetermined system. A choice may be made out of habit, so that the system that one is familiar with or normally uses is chosen. The decision may be made to minimize certain undesirable results and maximize the accuracy of a particular characteristic, such as area. Choices can be made thoughtlessly, especially with modern GIS software that makes the underlying coordinate systems transparent to the user.

It is not unusual for GIS viewshed functions to require DEMs to be in a square grid, and this necessitates that data be in a coordinate system such as UTM (Franklin and Guth, 2005). For this thesis, the decision was made at the outset to use the UTM coordinate system. This was based on the fact that UTM is commonly used and widely accepted, is fairly accurate even near the edge of a zone, existing CRMS data for GRSM was already in UTM, and data outside North Carolina (Tennessee and North Georgia) was to be used to a limited extent.

Is it possible that the choice of map projection could seriously affect geospatial analyses such as viewsheds? According to Franklin and Guth (2005), the errors introduced by shifting grid points during interpolation between a latitude/longitude and a rectangular coordinate system can affect visibility computations significantly. The greatest impacts will occur in rugged, mountainous terrain (Franklin and Guth, 2005). This raises the question as to whether, or by how much, viewshed results would differ if data were in the North Carolina State Plane Coordinate

System. At most, viewsheds are considered over a small portion of a state, such as western North Carolina, and UTM data are still very accurate near its zone boundaries.

Another factor to consider is whether a GIS visibility algorithm can model the curvature of the earth and the refraction of light by the atmosphere. These factors may be important over long distances (Yoeli, 1985). Ervin and Steinitz (2003) state that earth curvature must be considered in visibility analyses over long distances, as just one meter of difference has the potential to be crucial in some circumstances. Fisher, in 1993, pointed out that these issues are normally ignored by viewshed algorithms, but are important because they "cause direct lines-of-sight to be different from the actual lines viewed along." Riggs and Dean (2007) state that GIS developments since that time have incorporated these effects, but not adequately, since GIS documentation does not cite studies that have validated the implemented adjustments. Their opinion is that "this makes it impossible for a casual user of these systems to assess the accuracy of the results they produce."

Important, early work on these issues was conducted by Yoeli (1985). He explains that due to earth curvature, a specific point will be observed at a lower sight angle than if the earth was flat. This is illustrated in Figure 9.1, in which the observer views the peak at a higher angle across a flat earth and a lower angle across the curved earth. In the case of a feature with great vertical relief, such as a mountain or tower, the lower regions will be below the horizon and will not be visible in reality. This also is illustrated in Figure 9.1. With a planar model of the earth, the whole mountain is visible, but on the curved earth the lower portions of the mountain are below the horizon and obscured. These observations can only be realized in a computer program if there are corrections for earth curvature.

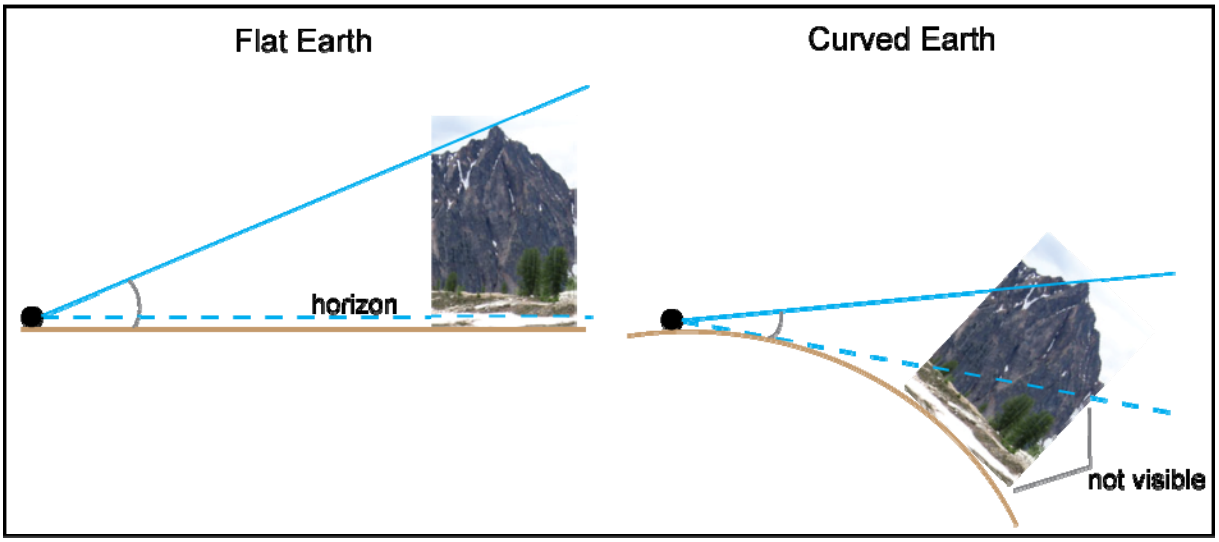

Figure 9.1: Effects of earth curvature on visibility. Adapted from Yoeli (1985).

Yoeli (1985) also points out that under normal atmospheric conditions, refraction causes an object to appear higher than it really is. Thus, a mountain peak will be seen by the observer at a higher angle (Figure 9.2).

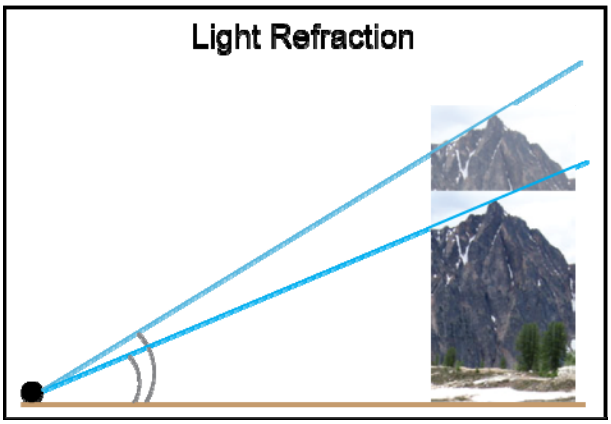

Figure 9.2: Normal effects of light refraction. Adapted from Yoeli (1985).

When working with elevation data under the assumption of a flat earth, the elevations of targets considered for visibility need to be adjusted. Yoeli (1985) explains that to adjust target elevations, curvature effects must be subtracted from, and refraction effects must be added to, a

target's original elevation. The effects of curvature should be minimal over short distances and should increase as the distance from the observer increases.

Earth curvature can be accounted for in viewshed analyses in both ArcGIS and Imagine. The formula used by Imagine is not published, but adjustments in ArcGIS factor in both earth curvature and refraction using the formulas put forth by Yoeli (1985) (ESRI, 2008a). In this formula, the impact of earth curvature is 7.7 times greater than the impact of refraction.

$$\text{Corrected elevation (km)} = \text{elevation (km)} - [0.87 * (\text{distance}^2 \text{ (km)} / \text{earth diameter (km)})]$$

or

$$\text{Corrected elevation (m)} = \text{elevation (m)} - \text{distance}^2 \text{ (km)} * 0.0683$$

Purpose and Objectives

The purpose of this study is to investigate earth curvature, and its impacts on visibility, in two ways. The first technique is to project DEMs of varying spatial resolutions into commonly used map projections and coordinate systems. Determining whether these different alterings of the data can seriously affect viewshed results is the first objective. Research with quantitative results addressing this specific issue has not been found. The second objective is to ascertain the distance at which earth curvature becomes an important factor for viewshed analyses and necessary corrections should be applied. Although adjustments for earth curvature have been addressed, the circumstances in which it is crucial is not widely discussed in the literature or software documentation.

Data and Methodology

The study area is located in western North Carolina near the western boundary of UTM Zone 17. Even at the UTM zone boundary, horizontal error (~3-4 m) is smaller than the size of 1 grid cell of the finest resolution DEM in these tests (6 m), or about 1/9 the size of the coarsest

resolution DEM cell (30 m). The source DEM was the 1/9 arc-second USGS NED (~3-m resolution) obtained in geographic coordinates of latitude/longitude (refer to Chapter 4). It was projected to UTM Zone 17 North and North Carolina State Plane (SP) using standard transformation procedures in ArcGIS. Any errors incurred in this process are less than half a pixel (ESRI, 2008b). All horizontal datums were NAD83. The NED DEM was resampled to create 6-, 10-, and 30-m DEMs using bilinear interpolation.

Projecting and resampling DEMs alters the elevation models. The result is that even with DEMs of the same resolution that originated from the same source, elevation at a given point may be different if the DEMs are in different coordinate systems/projections. To evaluate how much the elevation models differ, a north-to-south transect, 2 km in length, was created. The transect was projected into the two coordinate systems, sample points were created at 15-m intervals, and elevation values were obtained at the points with bilinear interpolation from a 30-m DEM in UTM and in SP, yielding 134 spot elevations that were compared (Figure 9.3).

Two field sites were used to investigate the effects of coordinate system/projection choices (Transverse Mercator and Lambert Conformal Conic projections) on viewsheds, Sites 4 and 9. Site 4 (Waypoint 646), in the western portion of GRSM, is along a steep, rocky ledge, approximately 30 m in length (refer to Chapter 3). Average slope within a 3-cell radius of Waypoint 646, based on the 30-m DEM, is 33.5°. Viewsheds from this site were generated over a large area (2,908 km^2). Site 9 (Waypoint 692), in the eastern portion of GRSM, is located on a gently sloping ridge crest. Average slope within a 3-cell radius of Waypoint 692 is 19.0°, and viewsheds were generated over a smaller, circular region with a 25-km diameter (491 km^2) (Figure 9.3).

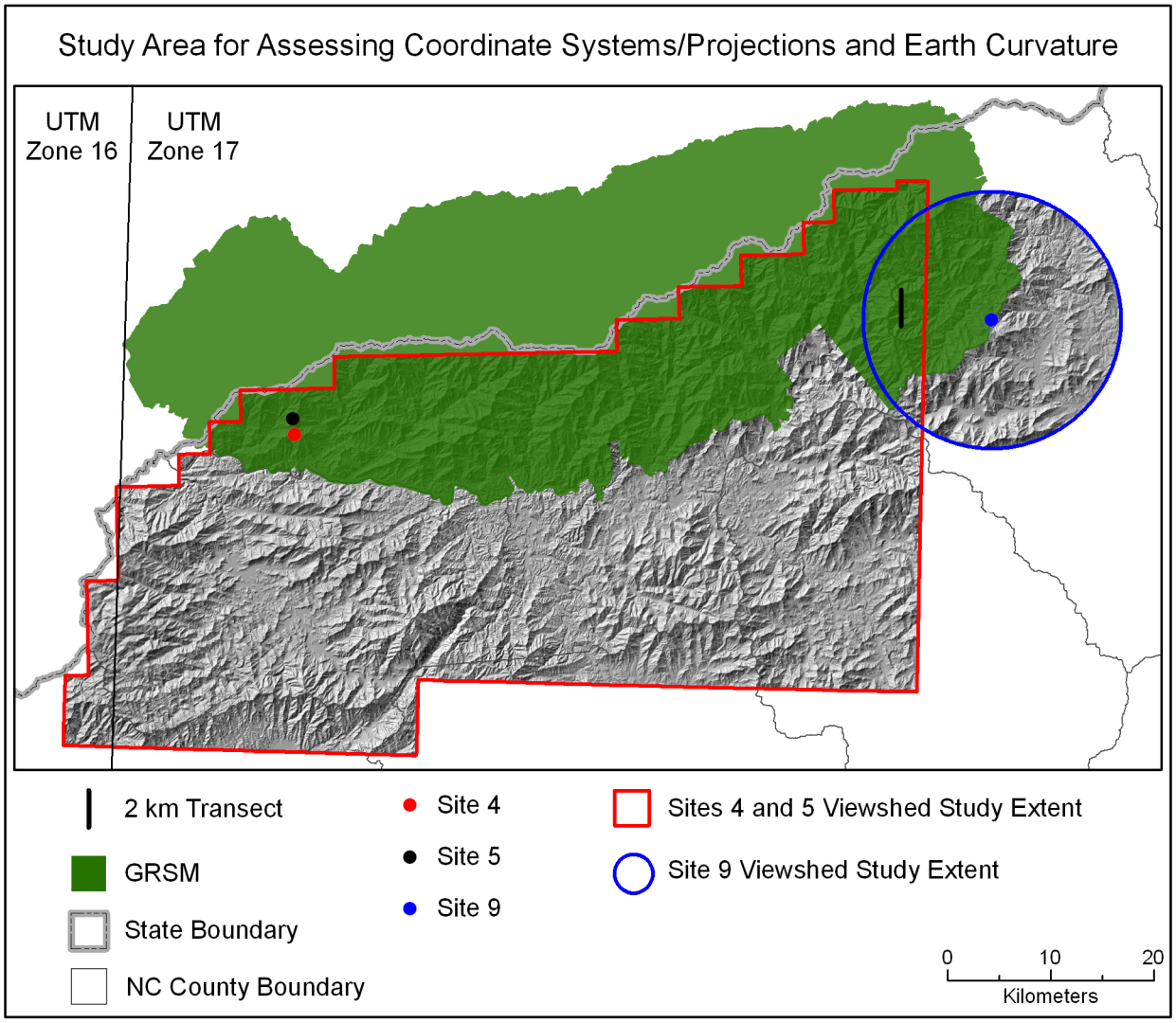

Figure 9.3: Study area for evaluating the impacts of earth curvature on viewsheds.

Since projection distortions and alterations are inevitable, these can affect the observer's height in a viewshed analysis, if the algorithm default parameters are used. To compensate, viewsheds were generated and comparisons were performed in two ways regarding the height of the observer: 1) equal absolute height, and 2) equal relative height above the surface. The ArcGIS viewshed function, by default, obtains the observer's elevation by bilinear interpolation. Interpolated elevation for each observer was determined for each DEM resolution, projection, and waypoint combination. For absolute height, an elevation slightly higher (~1-2 m) than the

highest interpolated elevation of all resolutions/projections was chosen for the observer, to ensure the observer is above the surface in all cases. For relative height, the observer's height was set at 1.5 m above the interpolated elevation for that point. Thus, scenario #1 places all observers at a site at exactly the same elevation, but they may be at different heights above the ground surface (Figure 9.4). Scenario #2 places all observers at a site at exactly the same height above the ground surface, but they may be at different elevations above the datum.

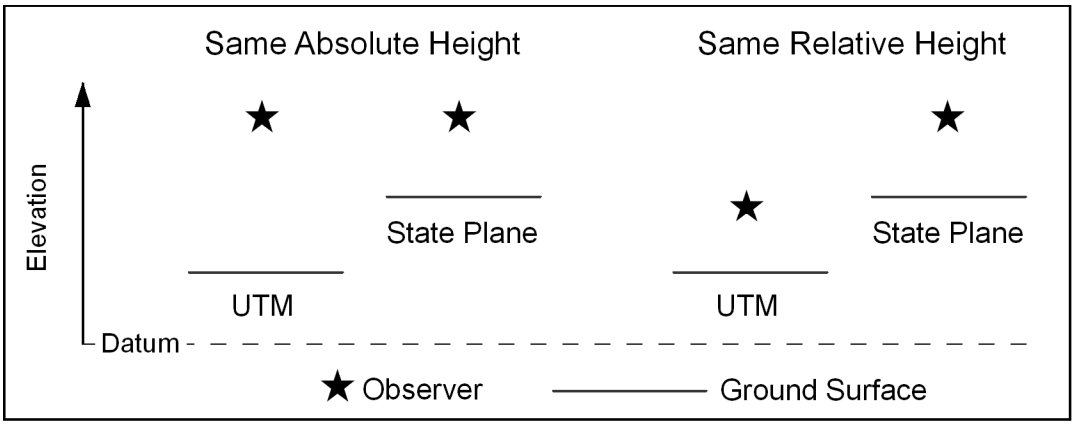

Figure 9.4: Illustration of absolute and relative heights of observers.

The reason for testing with both scenarios is to recognize that with different projections, the underlying DEMs are not the same. If a user sets an absolute height, then the observer's relative height above the surface will vary from projection to projection. This method could even set an observer below ground if one is not careful. Often, height above the surface is set, but this can result in varying absolute elevations from projection to projection, and this may not make sense if the height of a feature, such as a mountain peak, is known.

Twelve viewsheds were generated from both sites (4 and 9) for a total of 24 viewsheds. These were generated with combinations of DEM projection, resolution, and observer height. This allows an assessment of the effects of one parameter, projection or resolution, while the other is held constant. For example, differences attributable only to projections can be found for

each DEM resolution and observer height, and differences attributable only to DEM resolution can be found for each projection and observer height combination.

Another test was devised to quantify the effects of earth curvature and refraction on viewsheds. This test was conducted at Site 4 (Waypoint 646) and Site 5 (Waypoint 657). Viewsheds were generated in ArcGIS over a large area, the extent illustrated in Figure 9.3. At both sites, using a 30-m and 10-m DEM, a viewshed was computed with curvature and refraction adjustments while another viewshed ignored these adjustments. All other inputs were identical. This yielded 4 viewsheds at each site and 8 viewsheds total. To analyze the difference between each pair of viewsheds (e.g., Site 4, 30-m DEM with adjustments versus Site 4, 30-m DEM without adjustments), 3-km buffers, or distance bands, were created around the waypoint (Figure 9.5). Distance zones were used by Germino et al. (2001) in evaluating viewsheds. The purpose is to assess the differences in viewsheds in relation to the proximity of the observer, i.e., whether differences occur close to, or far away from, the observer. Zones extended as far as land was visible, which was 48 km from the observer for Site 4 and 60 km for Site 5. Viewsheds were converted to polygons, and the Hawth's Analysis Tools extension was used to summarize the visible area within each buffer. Within each buffer, the visible area was compared between adjusted and non-adjusted viewsheds. Non-adjusted viewsheds are always larger, so the difference was found by subtracting the adjusted viewshed area from the non-adjusted area. This difference was converted to a percentage by dividing the difference by the non-adjusted area, in order to adjust for the varying visible areas within each band. The resulting percentage expresses the difference in visible area per distance band due to earth curvature and refraction, with a higher percentage simply meaning greater disagreement.

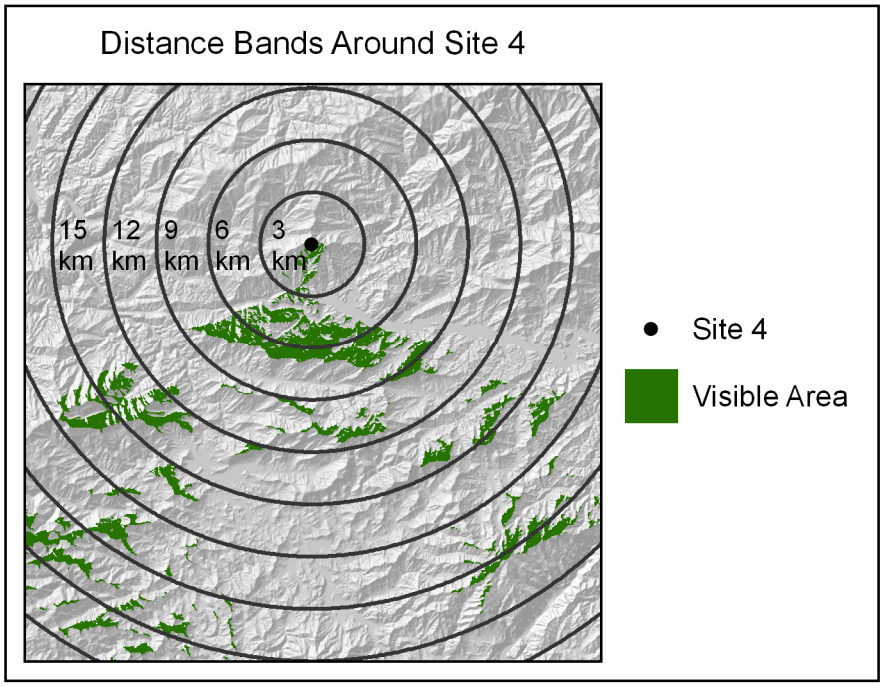

Figure 9.5: Example of distance bands, or zones, around an observer.

The amount of adjustment to a target's height to correct for curvature and refraction is given by Yoeli's formulations. Using these formulas, which are implemented in ArcGIS, the effects were simulated for an observer at sea level of a target mountain peak 1,000 m high across a range of distances from 3 to 102 km. This amount of vertical relief can easily be found in GRSM and other parts of western North Carolina. The example quantifies the corrections that should take place in the viewshed algorithm.

Results

Elevation Differences Due to Different Projections

The elevation models in different coordinate systems/projections varied little, although the presence of any difference may be a surprise to some users. The maximum difference among the 134 points was 2.34 m and the mean absolute difference was less than 1 meter (0.75 m). UTM data was, on average, 0.16 m higher than State Plane data, but the difference was not significant at a 95% confidence level. The elevation differences along the transect, computed as

UTM elevation minus State Plane elevation, are plotted in Figure 9.6, with UTM elevation as a backdrop. There may be some correlation between the terrain and the elevation differences, but more analysis is needed to claim this with any certainty.

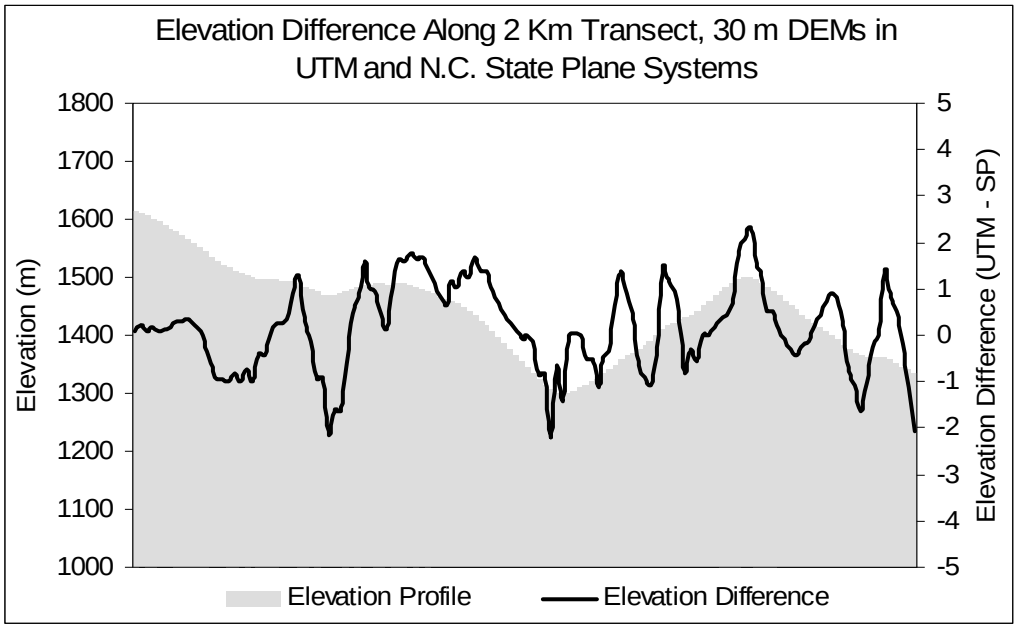

Figure 9.6: Sampled elevation differences between coordinate systems (black) plotted on top of terrain representation in UTM system (gray).

Viewshed Differences Due to Different Projections

Areas predicted visible by the 24 viewsheds are given in Table 9.1. Each row of the table allows for a comparison between systems/projections. The six comparisons at Site 9 have an average viewshed size difference of 4.6 km^2. The largest difference was 16.5 km^2 for the 30-m data with equal relative height, and the second largest difference was also with the 30-m data, but with equal absolute height. Average viewshed size difference at Site 4 was much less, 1.5 km^2. The largest difference was 7.0 km^2 for the 6-m data with observers at the same absolute height, but the other five differences were very small, less than 0.8 km^2. The average size difference for

both sites combined was 3.0 km^2. In 9 of 12 (75%) instances, viewsheds were larger with State Plane than UTM data.

Table 9.1: Size of visible areas (in km^2) from Sites 9 and 4 generated from 30-m, 10-m, and 6-m DEMs in UTM and North Carolina State Plane coordinate systems, with two methods of defining observer height.

				Visible Area (km^2)	
		Observer		Coordinate System	
Site	DEM Res.	Same Absolute Height	Same Relative Height	UTM	State Plane
9	30 m		1.5 m	27.7	44.2
9	30 m	1369 m		58.5	62.9
9	10 m		1.5 m	44.2	44.7
9	10 m	1369 m		48.7	51.9
9	6 m		1.5 m	50.3	50.5
9	6 m	1369 m		39.8	42.8
4	30 m		1.5 m	78.1	78.7
4	30 m	1098 m		100.0	100.8
4	10 m		1.5 m	73.3	73.5
4	10 m	1098 m		80.2	80.2
4	6 m		1.5 m	74.1	74.0
4	6 m	1098 m		73.3	66.3

The data in Table 9.1 are illustrated graphically in Figure 9.7. In comparing the Site 9 viewsheds from the same absolute elevation (UTM Abs versus SP Abs), their sizes differ little, and they consistently decrease in size as DEM resolution increases. Viewsheds from the same relative height (UTM Rel and SP Rel) increase in size as DEM resolution increases, the opposite of their absolute elevation counterparts.

As previously mentioned, the only major viewshed difference at Site 4 due to projection was absolute observer elevation with the 6-m DEM. Viewshed size generally decreased as DEM resolution increased.

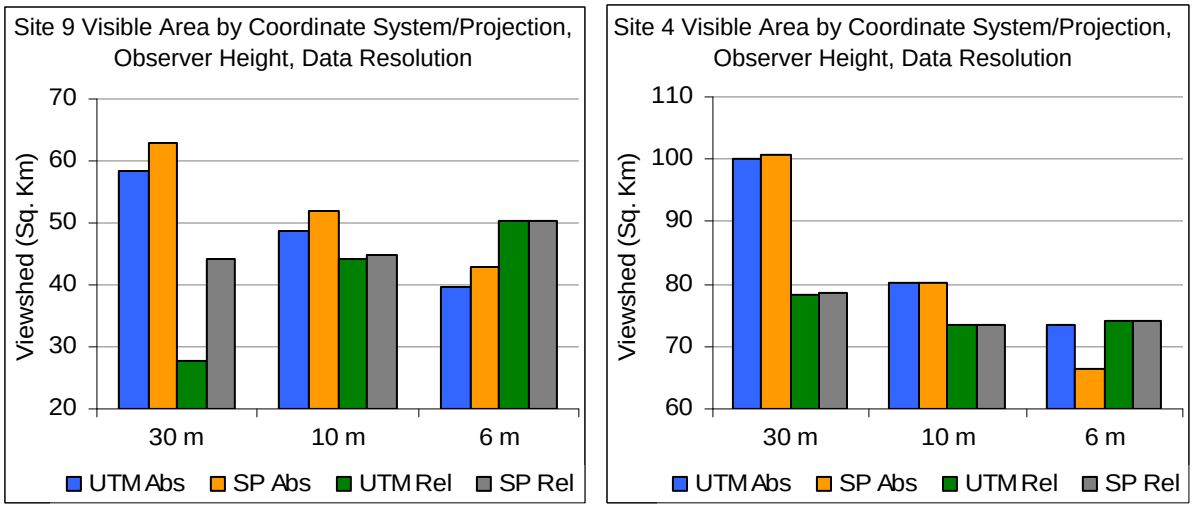

Figure 9.7: Viewshed sizes for Sites 9 and 4 with different coordinate systems/projections, observer height, and DEM resolution.

Viewshed Differences Due to Earth Curvature and Atmospheric Refraction

The distance at which earth curvature and refraction effects become important for visibility analyses was tested at two field sites with 30-m and 10-m DEMs. Four viewsheds that did not account for curvature were compared with four viewsheds that did account for curvature. Concentric zones of 3 km were used to compute the difference in visible area between corresponding viewsheds. The difference was converted to a percentage of disagreement. These percentages were graphed over the distance bands (Figure 9.8).

The data support the known fact that earth curvature affects visibility more at greater distances from the observer. This is illustrated by higher percentages of disagreement at greater distances. Visually, the trend is not linear, which is expected. The differences should be inconsequential at close range and become much larger with increasing distance. The trends appear similar to exponential growth. The data were subjected to exponential regression, and it was found that an exponential function fits the data well. All four models are significant ($p<.001$) and have r^2 values from 0.84 to 0.94, meaning that 84-94% of the variability in the percentage

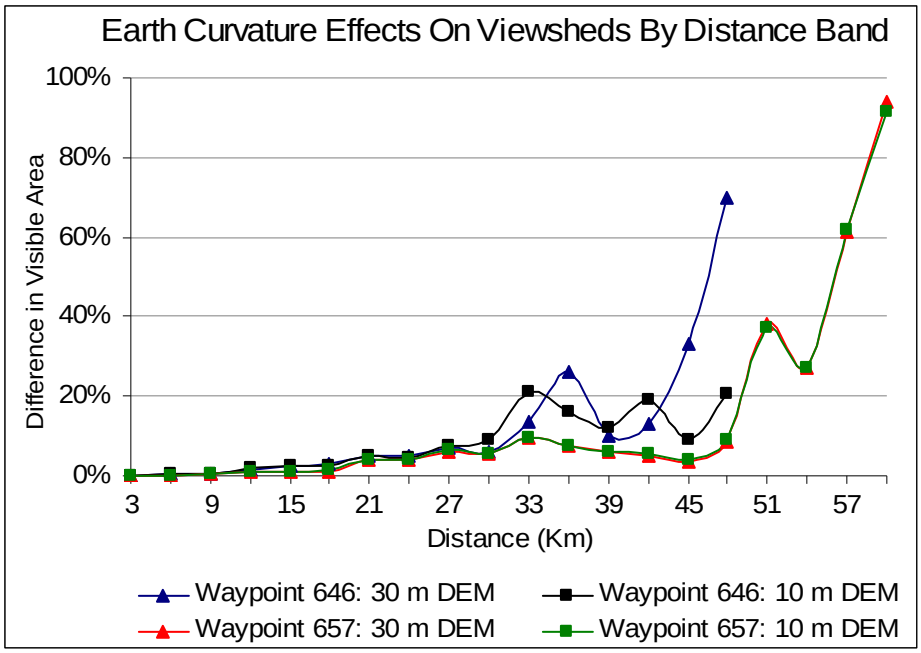

Figure 9.8: Difference in visible area by distance band due to earth curvature and refraction for Sites 4 and 5 with 30- and 10-m DEMs.

difference is explained by the distance from the observer. For 3 of the 4 pairs of viewsheds, a 5% difference is reached at 24-27 km, and a 5% difference is reached at 18-21 km for the other pair.

This is not claimed to be a statistically robust test. It is an example from four pairs of viewsheds and results cannot be extrapolated to all situations. The position of the observer and the nature of the terrain can obviously vary widely from place to place. However, a few general observations can be made for the viewsheds tested. First, for viewsheds extending less than 20 km from the observation point, employing earth curvature and refraction corrections made little difference. Second, at greater distances, such as 30+ km, not using corrections resulted in viewsheds being overestimated by 10-20% or more. Third, although these trends are not without variations, one should assume that not correcting for earth curvature will cause viewsheds to be overestimated more as distance increases from the observer.

The uncorrected elevations and those corrected for earth curvature and refraction, using Yoeli's formula, are illustrated for an observer at sea level of a target mountain peak 1,000 m high across a range of distances from 3 to 102 km (Figure 9.9).

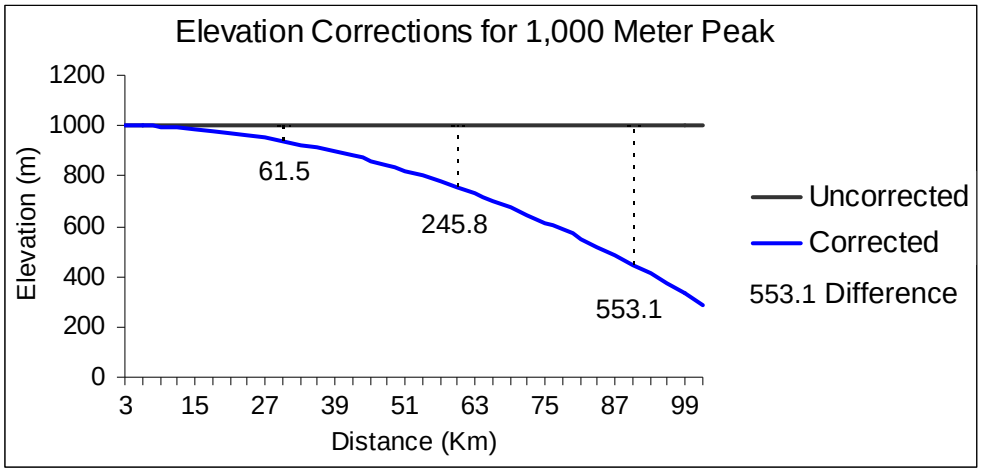

Figure 9.9: Needed elevation adjustments to correct for earth curvature and refraction over a range of distances.

The needed adjustments increase with distance. This can be seen in Figure 9.9, where the corrected elevation curve is relatively flat at close range, but the slope becomes steeper at greater distances from the observer. The difference between corrected and uncorrected elevation at 30 km is 61.5 m, 245.8 m at 60 km, and 553.1 m at 90 km. This demonstrates that over the 30-km intervals, the needed adjustments are increasing. Across the first 30-km interval the adjustment is 61.5 m, but the increase in adjustments from 30 to 60 km is 184.3 m, and the increase in adjustments from 60 to 90 km is 307.3 m. What this means is that if the 1,000 m peak is 90 km from the observer, then a visibility algorithm should consider it to be 446.9 m high. Otherwise, its visibility will be overestimated if its uncorrected elevation of 1,000 m is used.

Examples of this overestimation are given from Waypoint 646 at Site 4. With a 30-m DEM, viewshed area is 83.3 km^2 with uncorrected elevation and 78.7 km^2 using corrections.

With a 10-m DEM, viewshed area is 77.5 km^2 without adjustments and 73.5 km^2 using adjustments. In these two examples, viewsheds would be overestimated by 4.6 and 4.0 km^2, respectively, if corrections for earth curvature and refraction were not used.

Summary and Conclusions

The elevation models projected into UTM and North Carolina State Plane coordinate systems varied little. Measured along a 2-km transect, the maximum elevation difference was 2.34 m, the mean absolute difference was 0.75 m, and UTM data was 0.16 m higher, on average, than State Plane data.

Viewshed sizes depend on many factors, including the location of an observer and the nature of the terrain. The effects of different projections on viewsheds are variable. The results from Sites 9 and 4 indicate that for the areas of interest, the choice of UTM or State Plane and its associated projection usually has a small effect on visible area, but in some cases it has a large effect. In 75% of cases, viewsheds were larger with State Plane than UTM data. DEM resolution was an important factor in viewshed size, and the overall trend was a decrease in visible area as DEM resolution increased.

The distance at which earth curvature and refraction effects become important was tested. As expected, visibility is impacted more at greater distances from the observer, and the trend is exponential. In these tests, applying adjustments made little difference for distances less than 20 km. At distances of 30+ km, not using corrections caused viewsheds to be overestimated by 10-20% or more.

Earth curvature and refraction effects increase with distance, so larger errors in visibility computations will occur with distance if adjustments are not applied. The amount of necessary adjustment was quantified with the example of a 1,000-m peak. Adjustments are ever increasing

with distance, and at 90 km from an observer, the peak should be considered to be 446.9 m by a visibility algorithm. If uncorrected, visibility will be greatly overestimated at long distances.

CHAPTER 10: RESULTS AND CONCLUSIONS

Discussion of Results

A number of tests were performed to assess factors that impact the consistency and accuracy of visibility analyses in readily available GIS and image processing software. Special attention was paid to typical input data and software/algorithm choices. Results of each of the six research objectives are restated and summarized below.

1) *Perform field work in Great Smoky Mountains National Park (GRSM) to observe and photographically record visibility from the perspective of an observer on the ground, using field site locations determined by the Global Positioning System (GPS).*

No major problems were encountered conducting the field work. Travel time was about four hours to the GRSM trailheads from Athens. Field work involved four days of backpacking and one overnight backcountry camp. To perform the various field tests and collect data, approximately 20 lbs of extra gear was carried. Over the four days, 47.4 km (~30 mi) were hiked. Although the Cataloochee Divide/Hemphill Bald Trail was relatively flat and only gained 454 m (~1,500 ft) in elevation over a great distance, the A.T. climbs steeply from Fontana Dam and gains 610 m (2,000 ft) in less than 4.8 km (3 mi). Overall, the A.T. gained 740 m (2,425 ft) along the stretch where field work was conducted. Temperatures were mild for July, in the 70s, and humidity was high, but there was no rain, which would have caused a delay. Bears were encountered multiple times, as close as 15 m (50 ft), but it was fire ants that proved more troublesome.

There was a variety of terrain along these footpaths, both steep and flat, and trail tread was in fine shape, as the trails are popular, frequently used, and well maintained. Thick vegetation occasionally posed a challenge, as some work was conducted slightly off trail, and the Smokies are rich in plant life. Numerous good viewpoints were found with long-range views, and photographs were taken that recorded the visibility. The Shuckstack fire tower (18.3 m, or 60 ft) provided the best views, but one with a fear of heights would not be eager to climb to the top (Figure 10.1).

Figure 10.1: Shuckstack fire tower.

The challenges mentioned in conducting field work represent a justification for using GIS to perform visibility analyses. Field work involves time, expenses, logistical planning, and some physical effort. Although computer-based work entails its own set of challenges, it is usually performed in a more comfortable environment with more flexibility (e.g., a rain shower won't halt one's progress). Regarding technology in the field, the Garmin GPS V had little difficulty acquiring satellites under the canopy and performed satisfactorily in terms of repeatability of measurements and accuracy (refer to Objective 4, below).

2) *Evaluate the performance and products of different visibility algorithms and software programs. Two visibility algorithms within ESRI ArcGIS, the Viewshed and Line of Sight functions, are compared to determine whether the visibility of certain locations or features in ArcGIS is dependent on the analysis method used. Viewshed results are also compared between ArcGIS and ERDAS Imagine to quantify the agreement between these programs.*

The vector LoS and the raster viewshed algorithms within ArcGIS have their advantages and disadvantages. The viewshed is simpler and quicker to use, but the LoS output provides more information, such as a continuous record of visibility along a line, in addition to target visibility, and the location where visibility is blocked. More time is needed for users to become acquainted with using the LoS function, however, and there are potential pitfalls. These include the possibility that the cartographic outputs can disagree with the results written to the attribute table, obstruction points are optional but should be a standard output, and the easiest method to create an LoS is imprecise and is only a graphical output and not "hard" data.

Preliminary testing found numerous examples of discrepancies between ESRI's LoS and viewshed functions. To quantify the agreement, raster cell centroids that were deemed visible by the viewshed algorithm were set up as targets and evaluated by the LoS algorithm. This study found that viewshed and LoS results usually have a high level of agreement, e.g., 85+% agreement in 75% of cases, and 98+% agreement occurred 53% of the time. However, discrepancies can exist, and visibility with ArcGIS is dependent on the analysis method used. An issue was found with DEM surfaces: target and obstruction points appeared to overlap if the target was at ground level. This could lead to algorithm agreements being quite low (~40-60%), but raising the target, even slightly (0.1 m), increased agreement to over 99%. Agreement was

always greater than 75% when TIN surfaces were used, but the average TIN agreement, 92%, was lower than algorithm agreement with DEMs, 99%, and these differences were significant.

The resolution of the elevation data was not a significant factor in viewshed/LoS agreement, but the nature of the terrain, and the observer's position within the terrain, did have a significant effect on agreement. The highest rate of algorithm agreement was found from an observer situated on a hillside overlooking a flat valley, while the lowest level of agreement was found with an observer on a ridge top in an area of very rugged slopes. This result is related to the report by Swanson (2003), that GIS-based visibility is less accurate in rough terrain, as validated by field work. The greatest source of uncertainty in the different visibility functions was the use of a TIN model. Disagreements between the viewshed and LoS functions were investigated with elevation profiles. These profiles did not provide conclusive results, but cast some doubt as to whether the assumed elevation sampling method is, in fact, used.

Viewshed agreement between ESRI ArcGIS and ERDAS Imagine was evaluated with three resolutions of DEMs at four sites with rugged terrain. The average spatial agreement of viewsheds was 86.7%, and agreement ranged from 49.4% to 94.1%. These results are in line with those reported by Riggs and Dean (2007), who found 89% agreement between the programs. ArcGIS viewsheds were consistently smaller in area than those from Imagine, and 95.0% of ArcGIS viewsheds were contained within the bounds of Imagine viewsheds. Although it was common for areas of disagreement between the programs to occur along viewshed boundary zones, there were also situations in which large areas of disagreement were not related to simple boundary issues. These were also found by Riggs and Dean (2007). Possible causes of viewshed disagreements were explored with 3D perspective views and elevation profiles, but these methods did not provide a confirmation of Imagine results.

Data resolution was an important factor in viewshed agreement. The spatial agreement of viewsheds with 10-m data was much higher than with 30-m data, increasing from 73.9% to 92.8%. But increasing the resolution from 10 m to 6 m did not produce any significant improvements. Riggs and Dean (2007) reported marked changes in viewshed accuracy with varying DEM resolutions from ArcGIS and Imagine. They reported that ArcGIS accuracy ranged from 77% to 85% with seven different resolutions tested, and Imagine accuracy ranged from 66% to 83%. They found that viewsheds were most accurate at the DEM resolution that most closely matched the input point data.

3) *Create triangulated irregular networks (TINs) and raster digital elevation models (DEMs) with various interpolation techniques from bare-earth, lidar point data. Examine the implications of data structure and interpolation choices through the generation of viewsheds.*

Lidar point data was interpolated to create four elevation models: one TIN and three DEMs using inverse distance weighted (IDW), natural neighbor (NN), and kriging. Three methods were used to compare the generated elevation models, including difference images, variability at input points, and transects. Results indicated that the IDW model was the poorest choice, which agrees with Maune et al. (2001) and Lloyd and Atkinson (2002). Overall, the IDW DEM differed most from the other models. The NN and Kriging DEMs were relatively similar to one another. The Kriging model most closely matched the values at the TIN nodes. The most similar models along transects were the NN DEM and the TIN, which was not surprising since both models are based on similar underlying structures and methods (Voronoi diagram and Delaunay triangulation). Statistically significant correlations were found that verified the work of Gong et al. (2000), as well as the logical assumption, that larger differences between elevation models will occur in areas with low input point density.

This study found that choices of data structure and interpolation method can have a substantial impact on viewsheds and add to viewshed uncertainty. Any of the elevation models chosen would be a valid representation of the terrain, but the TIN model generated a much smaller viewshed than the DEMs, about half as large, while the DEM viewsheds were similar to one another. It was found that viewshed disagreements hundreds of meters away from the observer were caused by very small elevation differences (~0.3 m) near the observer. These results were supported by Riggs and Dean (2007), who reported that even small DEM errors can substantially reduce viewshed accuracy. In the case of this study, small differences in the surfaces substantially altered generated viewsheds.

4) *Demonstrate the uncertainty of viewsheds that can result from GPS variability by assessing the precision and accuracy, where possible, of field-collected GPS coordinates. Find the relationship between GPS-stated accuracy, precision, and tree cover.*

The accuracy of the Garmin GPS V was assessed at two GCPs. These GCPs were NGS horizontal control stations, and four GPS point coordinates were obtained at these stations, with only a minute delay in between, and each point coordinate was an average of 30 readings. The computed horizontal RMSE was +/-2.4 m (4.2 m, 95% confidence level) under open skies and +/-3.1 m (5.4 m, 95% confidence level) under thin canopy cover. These values are comparable to those of Wing et al. (2005). Four point coordinates were obtained at each field site, with each coordinate being an average of 30 readings. The distances between the four point coordinates obtained at each site were calculated to determine the precision, or repeatability, of GPS coordinates. The precision statistics correlated moderately well with the accuracy displayed by the GPS unit ($r = 0.50$), and more satellite signals led to higher accuracy as reported by the GPS receiver's display ($r^2 = 0.33$). However, it was expected that a higher correlation would exist

between precision and GPS-reported accuracy, and GPS-reported accuracy was overestimated compared to the accuracy computed at the GCPs. Where the computed 95% confidence level was 4.2 m at Site 14, the GPS-reported 95% confidence level was 2.3 m, and at Site 5 the computed value was 5.4 m but the GPS reported 2.8 m with 95% confidence. These results suggest that the accuracy indicated by the display should not be taken too literally, but should only be regarded as a guide.

A statistically significant correlation was found at the field sites between NLCD 2001 and CRMS GRSM tree cover data. There is a moderate association between GPS-reported error and NLCD canopy data ($r = 0.50$), and the relationship is even stronger between GPS variability (precision) and NLCD canopy cover ($r = 0.63$). This confirms the general assumption and results of previous investigations that locations with less tree cover will have more precise, and possibly more accurate, GPS coordinates than those under thick canopy (Deckert and Bolstad, 1996; Wing et al., 2005).

Viewshed uncertainty based on the variability of GPS coordinates was evaluated at three sites. It was demonstrated at Site 3 that horizontal differences of only 10.6 m can have an important impact (difference in visible area of 8 km^2) on GIS-generated viewsheds. Viewsheds from waypoints at Site 1 exhibited less variability than those from Site 3, but, surprisingly, the greatest viewshed difference (5.9 km^2) occurred between waypoint coordinates that were only 3.3 m apart. This is consistent with the research of Huss and Pumar (1997), who found that viewsheds are site-specific and that horizontal positional changes can have significant effects on viewsheds. Viewsheds from the Site 5 coordinates, obtained at the top of a fire tower, are nearly identical. This is because the observer was 18.3 m above the ground surface, and nearby terrain

interference is not a factor, demonstrating that ground obstructions near an observer are the main cause of viewshed uncertainty due to positional variations.

In summary, these results attest to the fact that even if multiple GPS coordinates computed from the same location are very precise and have high accuracy as reported by the GPS receiver, the true location is still unknown. Even small horizontal differences between GPS waypoints, and a point's short distance from the true location, can have a surprisingly large impact on GIS-generated viewsheds. The amount of impact is dependent on the nature of the nearby terrain and the height of the observer above the ground.

5) *Determine whether 3D visualizations are a viable alternative to visibility algorithms by comparing the visibility of randomly distributed features between the ArcGIS viewshed function and the perspective view of ArcScene. Quantify the level of agreement and assess ArcScene for its suitability as a quantitative, visibility analysis tool.*

The visibility of randomly distributed features, simulating buildings, was assessed by a viewshed algorithm and by 3D visualization. When considering whether features within the viewshed are visible in the visualization, 90% or greater agreement was normally attained in this study.

Agreement between the visibility methods was slightly better in the flat terrain of Cades Cove than in rugged Haywood County. This result is corroborated by field work that indicated that GIS-based viewshed accuracy decreased in rougher terrain (Swanson, 2003). All buildings within the TIN-based viewshed were visible in perspective view, and a small number of "extra" buildings were visible, whereas DEMs had fewer extra buildings than TINs, but agreement of viewshed-visible buildings observed in ArcScene was slightly lower at 90-95%.

Agreement in Haywood County was better with DEMs than TINs. The overall trend with both DEMs and TINs was for better agreement from higher resolution elevation data. The 3-m DEM was the only elevation model with perfect agreement in all measures in Haywood County. On average, at least 92% of viewshed-visible buildings were observed in perspective view from all DEM resolutions, with 100% agreement occurring with three of the four resolutions. Agreement was lower from TINs, with 6- and 10-m-derived TINs averaging less than 95% agreement, and the 30-m-derived TIN barely averaged 50% agreement. Regarding extra buildings visible in ArcScene that were outside the predicted viewshed, DEMs outperformed TINs in rugged terrain.

This study affirms the findings of Germino et al. (2001) of good agreement between the 2D and 3D visible areas. It also confirmed their speculation that higher resolution elevation models would result in better agreement. Due to the success of Germino et al. (2001) in quantifying landcover from perspective views, and inconsistencies found between the viewshed and LoS algorithms, especially with TINs, it is theorized that most discrepancies found in this study are probably due to issues with the viewshed function, and not the geometry of the ArcScene simulations. It is noted that there are major limitations of computer-generated perspective views. One is that they have limited effectiveness over long distances. Setting up the visualizations and manually counting features is much more time consuming than generating viewsheds. There are other factors that add to uncertainty when utilizing 3D perspective views for quantitative visibility analyses, such as computer graphics cards, screen resolution, and memory capacity. However, this study found that ArcScene visualizations are a viable alternative to the viewshed or LoS algorithms for determining visibility over a short distance or small area.

6) *Discover whether commonly used map projections and coordinate systems can seriously affect viewshed results. Investigate the distance at which earth curvature becomes an important factor for viewshed analyses.*

Three resolutions of DEMs obtained in geographic coordinates of latitude/longitude were projected to the UTM coordinate system (Transverse Mercator projection) and North Carolina State Plane coordinate system (Lambert Conformal Conic projection). Viewsheds from two sites found that the choice of these different systems and projections usually has only a small effect on visible area. However, in 2 of the 12 comparisons, visible area differed greatly, by 7.1 km^2 in one case and 16.5 km^2 in another. In 75% of cases, viewsheds were larger, by an average of 3.3 km^2, with State Plane than UTM data. The overall trend was a decrease in visible area with finer resolution DEMs, but these differences were not statistically significant.

The distance at which earth curvature and light refraction effects become important was tested. As expected, visibility is impacted more at greater distances from the observer, and the trend is exponential. In these tests, applying adjustments made little difference for distances less than 20 km. At distances of 30+ km, not using corrections caused viewsheds to be overestimated by 10-20% or more.

Summary of Results

Visibility uncertainty due to elevation data structure and resolution was assessed in several of the studies, which were mostly performed in areas of steep, mountainous terrain.. Overall, these two factors are often very important contributors to visibility uncertainty. When these inputs change (e.g., alternate from a DEM to a TIN, or from a 30-m DEM to a 6-m DEM), visibility results often change substantially. The agreement between the viewshed and LoS functions in ESRI ArcGIS was significantly better with DEMs (99%) than TINs (92%).

Resolution of the elevation data was not a significant factor in these algorithm comparisons. However, DEM resolution was important in viewshed agreement between ArcGIS and ERDAS Imagine. The average spatial agreement of viewsheds was 86.7%, but it varied by resolution, being 92.8% with 10-m data and only 73.9% with 30-m DEMs. No significant improvements were gained by using 6-m data. Increasing the spatial resolution of the DEMs, with both software programs, had the tendency to decrease the viewshed area, but these differences were not significant except for one site, which indicated significantly smaller viewsheds with higher resolution DEMs.

This study found that choices of data structure and interpolation method used to create surface models from point data can have a substantial impact on viewsheds and add to viewshed uncertainty. Any of the elevation models created could be chosen as a valid representation of the terrain, but the TIN model generated a viewshed that was much smaller in extent than the DEMs.

It was demonstrated that viewsheds can be impacted by the uncertainty of observer positions due to GPS variability, and higher resolution DEMs generally predicted smaller visible areas. At one of the Site 3 waypoints, the 6-m viewshed was only 72% as extensive as the 30-m viewshed, and the average viewshed range from the four Site 3 waypoints attributable to different DEM resolutions is 6.7 km^2. At Site 3, horizontal differences of only 10.6 m had an important impact (difference in visible area of 8 km^2) on GIS-generated viewsheds. These results attest to the fact that even if multiple GPS coordinates computed from the same location are very precise and have high accuracy as reported by the GPS receiver, the true location is still unknown. Even small horizontal differences between GPS waypoints, and a point's short distance from the true location, can have a surprisingly large impact on GIS-generated viewsheds. The amount of impact is dependent on the nature of the nearby terrain and the height

of the observer above the ground, because ground obstructions near an observer are the main cause of viewshed uncertainty due to positional variations.

Various resolutions of DEMs and TINs were used to assess visibility by a viewshed algorithm and by 3D visualization. In flat terrain, agreement between the visibility methods was comparable between DEMs and TINs. In steep terrain, greater agreement was found between the visibility methods with DEMs than TINs, and the overall trend with both DEMs and TINs was for better agreement from higher resolution elevation data. The 3-m DEM was the best performing elevation model, the only one with perfect agreement, and the worst performing model was the 30-m-derived TIN. This study found that ArcScene visualizations are a viable alternative to the viewshed or LoS algorithms for determining visibility for distances up to 3 km and areas up to 28 km^2.

Viewsheds generated from three resolutions of DEMs in two different projections were compared. As found in other tests, non-significant decreases in visible area occurred with finer resolution DEMs. As to the circumstances in which corrections for earth curvature and refraction should be used, applying adjustments made little difference for distances less than 20 km, but for distances of 30+ km, not using corrections caused viewsheds to be overestimated by 10-20% or more.

Throughout the various tests, a trend emerged that indicates that the use of TIN models leads to more uncertainty. Perhaps, as suggested by Maloy and Dean (2001) and Riggs and Dean (2007), the problem is not with the data model itself, but rather with the way visibility algorithms evaluate intervisibility across a TIN surface. Regardless, DEMs appear to be the better data model for visibility analyses, and higher resolution DEMs are recommended. Higher resolution data tend to generate less variability and better agreement.

This should not imply that higher resolution data are always better. It was seen in this study that viewshed agreement between ArcGIS and Imagine improved drastically with 10-m data compared to 30-m data, but 6-m data did not provide significant improvements. Maloy and Dean (2001) reported that oversampling data to a finer resolution actually decreased viewshed accuracy. Riggs and Dean (2007) found that the most accurate viewsheds were generated from a DEM with a resolution that most closely matched the average spacing of the input point data used to construct the DEM. In addition, data volume and computation time can be issues for viewshed analyses over large areas with high resolution data. The NED DEMs are 32-bit, floating point rasters. For an area of 491 km^2, which is roughly 50% larger than Clarke County, or about the size of Oconee County, Georgia, a 30-m DEM requires 4 MB of disk space, 10-m data requires 33 MB, 6-m data uses 81 MB, and a 3-m DEM requires 270 MB of storage space. Viewshed computation time with these DEMs, on a PC with a 1.8 GHz Intel Pentium M processor with 1.5 GB of RAM, was 6 seconds, 39 seconds, 93 seconds, and 313 seconds (5 minutes, 13 seconds), respectively. If one was generating viewsheds with high resolution data for a large region, such as all of western North Carolina, storage space (several GBs) and processing time (1 hour or more) could be serious considerations, and these factors must be weighed.

With many companies and agencies utilizing computer-based visibility analyses for many types of applications, it is important that decision makers have an understanding of the factors that can introduce uncertainty into visibility results. This thesis has sought to demonstrate several of these factors and quantify their potential effects. Issues that have been discussed previously by others were researched, and new questions were raised and investigated. As a result of this study, it is recommended that high confidence should not be placed in “typical” visibility analyses. However, the nature of the question or application matters.

The low viewshed accuracies reported by Maloy and Dean (2001) and Riggs and Dean (2007) were computed by overlaying GIS-generated viewsheds with field-surveyed viewsheds, and the areas of overlap and disagreement were calculated between the delineated viewsheds. This is a sound methodology, but it may be a more stringent technique, yielding lower accuracies, than many applications require. For example, if one simply wants to know whether a mountain is visible from a certain location, that person may not care about the exact, delineated visible parts of the mountain, but only that a portion of it can be seen. Field-surveyed and GIS-generated viewsheds could disagree quite a bit as to the precise visible boundaries, and agreement between the two viewsheds might be low, but they could still agree that part of the mountain is visible, which may be adequate information for the situation.

With that caveat, field-tested viewsheds were not extremely accurate (85% maximum), even from a custom-created DEM of high accuracy in a relatively small study area (7.28 ha) with very little vegetation and no man-made surface features (Riggs and Dean, 2007). These researchers found that ArcGIS produced more accurate viewsheds than ERDAS Imagine or Clark Labs' Idrisi. The ArcGIS viewshed function is not difficult to use and has numerous options, so its use is recommended. As wonderful as the USGS DEMs are, Riggs and Dean (2007) found that a standard USGS 10-m DEM produced results that were only 54% accurate. These results are similar to those of Maloy and Dean (2001). Lidar-derived DEMs should provide more accurate results, but these are only available for limited areas. A DEM should be most accurate when its resolution most closely approximates the density of its source data, which is often unknown to users, unfortunately. Generalizing DEMs to lower resolutions will result in faster computed, but less accurate, viewsheds. With standard USGS 10- and 30-m DEMs, users should expect accuracy to be less than 75%, conservatively, and an average of 50-60% may be

more realistic in rugged terrain or if the observer's position is not known with great certainty. In an urban or heavily vegetated area, traditional GIS-generated viewsheds over long distances may be of little value if the observer cannot move freely or rise above the nearby obstructions.

Conclusions and Future Work

Considering the decades that computer-based visibility analyses have been conducted and researched, relatively little work has been done to field-verify GIS viewsheds. Notable exceptions include Dean (1997), Maloy and Dean (2001), Riggs and Dean (2007), and the US Army Topographic Engineering Center's Line of Sight Technical Working Group (Swanson, 2003; Swanson, 2004), which has concluded its work. Numerous examples of potential barriers to performing field work have already been discussed. In addition, one may be tasked to determine visibility for regions far away, where travel is not an option. This is a great advantage of GIS-generated viewsheds and the World Wide Web: one can determine visibility for virtually any location in the U.S. without ever leaving the office. The tradeoff is that the accuracy of the results cannot be verified. It can be very time consuming and difficult to verify visibility, much more challenging than clicking buttons in a GIS program. If extensive regions are under consideration, then specific targets have the potential to be verified in the field, such as whether a particular peak or other notable feature can be seen from a certain location, but delineating the entire visible area with accuracy and precision is beyond current means.

One of the biggest issues is that most viewsheds are generated with bare earth data. In a mountainous setting, this type of data might work well above tree line or in areas with little vegetation, but results would not accurately reflect actual visibility on the ground for most of the Appalachians, especially the Southern Appalachians, which are heavily forested and do not have a true tree line, only scattered bald mountains. Llobera asserted in 2007 that the main weakness

of current visibility techniques is the difficulty of incorporating vegetation. These two areas, including vegetation in visibility analyses and validating their accuracy, is the direction of my future work on this subject. These issues must be addressed for visibility analyses to be reliable and applicable in more real-world scenarios.

REFERENCES

Introductory and Concluding Material (Chapters 1-4, 10)

Abidin, H., 2002. Fundamentals of GPS signals and data, *Manual of Geospatial Science and Technology* (J.D. Bossler, editor, J.R. Jensen, R.B. McMaster, and C. Rizos, associate editors), Taylor & Francis, London, U.K., pp. 95-113.

Agnes, M., and D.B. Guralnik, 2006. *Webster's New World College Dictionary,* Fourth edition (M. Agnes and D.B. Guralnik, editors), Wiley Publishing, Cleveland, Ohio, 1716 p.

Agumya, A., and G.J. Hunter, 2002. Responding to the consequences of uncertainty in geographical data, *International Journal of Geographical Information Science,* 16(5):405-417.

Amidon, E.L., and G.H. Elsner, 1968. Delineating landscape view areas...a computer approach, USDA Forest Service, Research Note PSW-180, Pacific Southwest Forest and Range Experiment Station, Berkeley, California.

Arnaud, M., and A. Flori, 1998. Bias and precision of different sampling methods for GPS positions, *Photogrammetric Engineering & Remote Sensing*, 64(6):597-600.

Coren, S., L.M. Ward, and J.T. Enns, 2004. *Sensation and Perception,* Sixth edition, John Wiley & Sons, New York, N.Y., 598 p.

De Floriani, L., P. Marzano, and E. Puppo, 1994. Line-of-sight communication on terrain models, *International Journal of Geographical Information Science*, 8(4):329-342.

Dean, D.J., 1997. Improving the accuracy of forest viewsheds using triangulated networks and the visual permeability method, *Canadian Journal of Forest Research*, 27:969-977.

Deckert, C., and P.V. Bolstad, 1996. Forest canopy, terrain, and distance effects on global positioning system point accuracy, *Photogrammetric Engineering & Remote Sensing*, 62(3):317-321.

Doucette, P., and K. Beard, 2000. Exploring the capability of some GIS surface interpolators for DEM gap fill, *Photogrammetric Engineering & Remote Sensing*, 66(7):881-888.

El-Sheimy, N., C. Valeo, and A. Habib, 2005. *Digital Terrain Modeling: Acquisition, Manipulation, and Applications,* Artech House, Boston, Massachusetts, 270 p.

Enns, J.T., 2004. *The Thinking Eye, the Seeing Brain: Explorations in Visual Cognition*, W.W. Norton and Co., New York, N.Y., 464 p.

Ervin, S., and C. Steinitz, 2003. Landscape visibility computation: necessary, but not sufficient, *Environment and Planning B: Planning and Design*, 30:757-766.

Fenneman, N.M., 1917. Physiographic subdivision of the United States, *Proceedings of the National Academy of Sciences of the United States of America*, 3(1):17-22.

Fisher, P.F., 1991. First experiments in viewshed uncertainty: the accuracy of the viewshed area, *Photogrammetric Engineering & Remote Sensing*, 57(10):1321-1327.

Fisher, P.F., 1992. First experiments in viewshed uncertainty: simulating fuzzy viewsheds, *Photogrammetric Engineering & Remote Sensing*, 58(3):345-352.

Fisher, P.F., 1993. Algorithm and implementation uncertainty in viewshed analysis, *International Journal of Geographical Information Systems*, 7(4):331-347.

Fisher, P.F., 1994. Probable and fuzzy models of the viewshed operation, *Innovations in GIS: Selected Papers from the First National Conference on GIS Research UK* (M.F. Worboys, editor), Taylor & Francis, London, UK, pp. 161-175.

Fisher, P.F., 1995. An exploration of probable viewsheds in landscape planning, *Environment and Planning B: Planning and Design*, 22:527-546.

Fisher, P.F., and C. Farrelly, 1997. Spatial analysis of visible areas from the Bronze Age cairns of Mull, *Journal of Archeological Science*, 24:581-592.

Fisher, P., 1998. Improved modeling of elevation error with geostatistics, *GeoInformatica*, 2(3):215-233.

Fisher, P.F., and N.J. Tate, 2006. Causes and consequences of error in digital elevation models, *Progress in Physical Geography*, 30(4):467-489.

Fisher, P., 2009. The representation of uncertain geographical information, *Manual of Geographic Information Systems* (M. Madden, editor), American Society for Photogrammetry and Remote Sensing, Bethesda, Maryland, pp. 235-264.

Franke, R., 1982. Scattered data interpolation: tests of some methods, *Mathematics of Computation*, 38(157):181-200.

Franklin, K.B., and P.L. Guth, 2005. The effects of DEM re-interpolation on viewshed computations, *Proceedings of the Sixth International Conference on Military Geology and Geography*, 19-22 June 2005, University of Nottingham, UK.

Gahegan, M., 1999. Four barriers to the development of effective exploratory visualisation tools for the geosciences, *International Journal of Geographical Information Science*, 13(4):289-309.

Germino, M.J., W.A. Reiners, B.J. Blasko, D. McLeod, and C.T. Bastian, 2001. Estimating visual properties of Rocky Mountain landscapes using GIS, *Landscape and Urban Planning*, 53(1):71-83.

Gesch, D., M. Oimoen, S. Greenlee, C. Nelson, M. Steuck, and D. Tyler, 2002. The national elevation dataset, *Photogrammetric Engineering & Remote Sensing*, 68(1):5-11.

Gesch, D.B., 2007. The national elevation dataset, *Digital Elevation Model Technologies and Applications: The DEM Users Manual*, Second edition (D.F. Maune, editor), American Society for Photogrammetry and Remote Sensing, Bethesda, Maryland, pp. 99-118.

Gong, J., Z. Li, Q. Zhu, H. Sui, and Y. Zhou, 2000. Effects of various factors on the accuracy of DEMs: an intensive experimental investigation, *Photogrammetric Engineering & Remote Sensing*, 66(9):1113-1117.

Goodchild, M.F., and J. Lee, 1989. Coverage problems and visibility regions on topographic surfaces, *Annals of Operations Research*, 18:175-186.

Habib, A., 2002. Coordinate transformations, *Manual of Geospatial Science and Technology* (J.D. Bossler, editor, J.R. Jensen, R.B. McMaster, and C. Rizos, associate editors). Taylor & Francis, London, U.K., pp. 27-49.

Holmes, K.W., O.A. Chadwick, and P.C. Kyriakidis, 2000. Error in a USGS 30-meter digital elevation model and its impact on terrain modeling, *Journal of Hydrology*, 233:154-173.

Homer, C., C. Huang, L. Yang, B. Wylie, and M. Coan, 2004. Development of a 2001 national land-cover database for the United States, *Photogrammetric Engineering & Remote Sensing*, 70(7):829-840.

Huss, R.E., and M.A. Pumar, 1997. Effect of database errors on intervisibility estimation, *Photogrammetric Engineering & Remote Sensing*, 63(4):415-424.

Izraelevitz, D., 2003. A fast algorithm for approximate viewshed computation, *Photogrammetric Engineering & Remote Sensing*, 69(7):767-774.

Jenkins, M.A., 2007. Vegetation communities of Great Smoky Mountains National Park, *Southeastern Naturalist*, 6(Special Issue 1):35-56.

Kidner, D.B., A.J. Sparkes, M.I. Dorey, J.M. Ware, and C.B. Jones, 2001. Visibility analysis with the multiscale implicit TIN, *Transactions in GIS*, 5(1):19-37.

Kidner, D.B., J.M. Ware, A.J. Sparkes, and C.B. Jones, 2000. Multiscale terrain and topographic modelling with the implicit TIN, *Transactions in GIS*, 4(4):379-408.

Kienzle, S., 2004. The effect of DEM raster resolution on first order, second order and compound terrain derivatives, *Transactions in GIS*, 8(1):83-111.

Kyriakidis, P.C., A.M. Shortridge, and M.F. Goodchild, 1999. Geostatistics for conflation and accuracy assessment of digital elevation models, *International Journal of Geographical Information Science,* 13(7):677-707.

Lachapelle, G., S. Ryan, and C. Rizos, 2002. Servicing the GPS user, *Manual of Geospatial Science and Technology* (J.D. Bossler, editor, J.R. Jensen, R.B. McMaster, and C. Rizos, associate editors). Taylor & Francis, London, U.K., pp. 201-215.

Lam, N.S., 1983. Spatial interpolation methods: a review, *The American Cartographer,* 10(2):129-149.

Lee, J., 1991. Comparison of existing methods for building triangular irregular network models of terrain from grid digital elevation models, *International Journal of Geographical Information Systems,* 5(3):267-285.

Lee, J., and D. Stucky, 1998. On applying viewshed analysis for determining least-cost paths on digital elevation models, *International Journal of Geographical Information Science,* 12(8): 891-905.

Lillesand, T.M., R.W. Kiefer, and J.W. Chipman, 2008. *Remote Sensing and Image Interpretation*, Sixth edition, John Wiley & Sons, New York, N.Y., 756 p.

Llobera, M., 2007. Modeling visibility through vegetation, *International Journal of Geographical Information Science*, 21(7):799-810.

Lloyd, C.D., and P.M. Atkinson, 2002. Deriving DSMs from LiDAR data with kriging, *International Journal of Remote Sensing*, 23(12):2519-2524.

Longley, P.A., M.F. Goodchild, D.J. Maguire, and D.W. Rhind, 2005. *Geographic Information Systems and Science*, Second edition, John Wiley & Sons, West Sussex, U.K., 517 p.

Madden, M., R. Welch, T. Jordan, P. Jackson, R. Seavey, and J. Seavey, 2004. *Digital vegetation maps for the Great Smoky Mountains National Park,* URL: http://www.crms.uga.edu/nps/grsm/GRSM_Final_Report.pdf, Center for Remote Sensing and Mapping Science, Department of Geography, University of Georgia, Athens, Georgia (last date accessed: 20 November 2008).

Maloy, M.A., and D.J. Dean, 2001. An accuracy assessment of various GIS-based viewshed delineation techniques, *Photogrammetric Engineering & Remote Sensing*, 67(11):1293-1298.

Marlin, D.A., 1992. *Digital Terrain Evaluation Study,* Hughes Aircraft Co., Advanced Systems Planning, Los Angeles, California.

Maune, D.F., 2001. Appendix B, *Digital Elevation Model Technologies and Applications: The DEM Users Manual* (D.F. Maune, editor), American Society for Photogrammetry and Remote Sensing, Bethesda, Maryland, pp. 471-500.

Maune, D.F., S.M. Kopp, C.A. Crawford, and C.E. Zervas, 2001. Introduction, *Digital Elevation Model Technologies and Applications: The DEM Users Manual* (D.F. Maune, editor), American Society for Photogrammetry and Remote Sensing, Bethesda, Maryland, pp. 1-34.

Nackaerts, K., G. Covers, and J.V. Orshoven, 1999. Accuracy assessment of probabilistic visibilities, *International Journal of Geographic Information Science*, 13(7):709-721.

Nichols, B.J., and K.R. Langdon, 2007. The Smokies all taxa biodiversity inventory: history and progress, *Southeastern Naturalist*, 6(Special Issue 1):27-34.

NPS (National Park Service), 2006. Air quality, Great Smoky Mountains National Park Management Folio #2, URL: http://www.nps.gov/grsm/naturescience/upload/air%20quality.pdf, Great Smoky Mountains National Park, Gatlinburg, Tennessee (last date accessed: 19 June 2008).

NPS (National Park Service), 2008. Great smoky mountains national park (U.S. national park service), URL: http://www.nps.gov/grsm, National Park Service, Washington, D.C. (last date accessed: 16 June 2008).

O'Rourke, K.K., 1992. Digital Terrain Database Resolution and Accuracy Analysis (DTDRAA), AD-B163471, Pacific Sierra Research Corporation, Los Angeles, California.

Oderwald, R.G., and B.A. Boucher, 2003. GPS after selective availability: How accurate is accurate enough?, *Journal of Forestry*, 101(4):24-27.

Ogburn, D.E., 2006. Assessing the level of visibility of cultural objects in past landscapes, *Journal of Archaeological Science*, 33(3):405-413.

Paternoster, A., 2007. Vision science and the problem of perception, *Cartographies of the Mind: Philosophy and Psychology in Intersection* (M. Marraffa, M. De Caro, and F. Ferretti, editors), Springer, Dordrecht, the Netherlands, pp. 53-64.

Peucker, T.K., R.J. Fowler, J.J. Little, and D.M. Mark, 1978. The triangulated irregular network, *Proceedings of the ASP Digital Terrain Models (DTM) Symposium*, 9-11 May, St. Louis, Missouri (American Society of Photogrammetry, Bethesda, Maryland), pp. 516-540.

Rana, S., 2003. Fast approximation of visibility dominance using topographic features as targets and the associated uncertainty, *Photogrammetric Engineering & Remote Sensing*, 69(8):881-888.

Riggs, P.D., and D.J. Dean, 2007. An investigation into the causes of errors and inconsistencies in predicted viewsheds, *Transactions in GIS*, 11(2):175-196.

Rizos, C., 2002. Introducing the global positioning system, *Manual of Geospatial Science and Technology* (J.D. Bossler, editor, J.R. Jensen, R.B. McMaster, and C. Rizos, associate editors). Taylor & Francis, London, U.K., pp. 77-94.

Sander, H.A., and S.M. Manson, 2007. Heights and locations of artificial structures in viewshed calculation: how close is close enough?, *Landscape and Urban Planning*, 82:257-270.

Scherzinger, B., J. Hutton, and M. Mostafa, 2001. Enabling technologies, *Digital Elevation Model Technologies and Applications: The DEM Users Manual* (D.F. Maune, editor), American Society for Photogrammetry and Remote Sensing, Bethesda, Maryland, pp. 337-366.

Shi, W.(J.), 2009. Spatial data quality and uncertainty, *Manual of Geographic Information Systems* (M. Madden, editor), American Society for Photogrammetry and Remote Sensing, Bethesda, Maryland, pp. 201-224.

Sobol', I.M., 1994. *A Primer for the Monte Carlo Method*, CRC Press, Boca Raton, Florida, 107 p.

Sorensen, P.A., and D.P. Lanter, 1993. Two algorithms for determining partial visibility and reducing data structure induced error in viewshed analysis, *Photogrammetric Engineering & Remote Sensing*, 59(7):1149-1160.

Su, J., and E. Bork, 2006. Influence of vegetation, slope, and lidar sampling angle on DEM accuracy, *Photogrammetric Engineering & Remote Sensing*, 72(11):1265-1274.

Swanson, R., 2003. Line-of-sight algorithm/viewshed results against field data, Line of Sight Technical Working Group Meeting, 5 June 2003, URL: http://www.agc.army.mil/operations/programs/LOS/20030605/Viewshed%20Evaluation6-5-03.ppt, US Army Topographic Engineering Center, Alexandria, Virginia (last date accessed: 27 October 2008).

Swanson, R., 2004. Line-of-sight field and terrain data available from TEC and overview of TEC line-of-sight application and algorithm validation methodology, Line of Sight Technical Working Group Meeting, 1 December 2004, URL: http://www.tec.army.mil/operations/programs/LOS/20041201/6-%20Test%20Data%20Set.ppt, US Army Topographic Engineering Center, Alexandria, Virginia (last date accessed: 28 December 2008).

USGS (U.S. Geological Survey), 2006. National Elevation Dataset, URL: http://ned.usgs.gov/Methodology.asp, U.S. Geological Survey, Reston, Virginia (last date accessed: 28 December 2008).

USGS (U.S. Geological Survey), 2007. The national map seamless server, National Elevation Data (NED) FAQ, URL: http://seamless.usgs.gov/faq/ned_faq.php, U.S. Geological Survey, Reston, Virginia (last date accessed: 23 May 2008).

USGS (U.S. Geological Survey), 2008. NED release notes, December 2008, National Elevation Dataset, URL: http://ned.usgs.gov/downloads/documents/NED_Release_Notes_Dec08.pdf, U.S. Geological Survey, Reston, Virginia (last date accessed: 21 January 2009).

Wang, J., G.J. Robinson, and K. White, 2000. Generating viewsheds without using sightlines, *Photogrammetric Engineering & Remote Sensing*, 66(1):87-90.

Watson, D.F., 1992. *Contouring: A Guide to the Analysis and Display of Spatial Data*, Pergamon Press, Oxford, 340 p.

Wechsler, S.P., and C.N. Kroll, 2006. Quantifying DEM uncertainty and its effect on topographic parameters, *Photogrammetric Engineering & Remote Sensing*, 72(9):1081-1090.

Welch, R., M. Madden, and T. Jordan, 2002. Photogrammetric and GIS techniques for the development of vegetation databases of mountainous areas: Great Smoky Mountains National Park, *ISPRS Journal of Photogrammetry and Remote Sensing*, 57(1-2):53-68.

Wing, M.G., and A. Eklund, 2007. Performance comparison of a low-cost mapping grade global positioning system (GPS) receiver and consumer grade GPS receiver under dense forest canopy, *Journal of Forestry*, 105(1):9-14.

Wing, M.G., A. Eklund, and L.D. Kellogg, 2005. Consumer-grade global positioning system (GPS) accuracy and reliability, *Journal of Forestry*, 103(4):169-173.

Winterbottom, S.J., and D. Long, 2006. From abstract digital models to rich virtual environments: landscape contexts in Kilmartin Glen, Scotland, *Journal of Archaeological Science*, 33:1356-1367.

Wood, J., and P.F. Fisher, 1993. Assessing interpolation accuracy in elevation models, *IEEE Computer Graphics and Applications*, 13(2):48-56.

Yilmaz, H.M., 2007. The effect of interpolation methods in surface definition: an experimental study, *Earth Surface Processes and Landforms*, 32:1346-1361.

Yoeli, P., 1985. The making of intervisibility maps with computer and plotter, *Cartographica*, 22(3):88-103.

Yu, S.M., S.S. Han, and C.H. Chai, 2007. Modeling the value of view in high-rise apartments: a 3D GIS approach, *Environment and Planning B: Planning and Design*, 34(1):139-153.

Ziadat, F.M., 2007. Effect of contour intervals and grid cell size on the accuracy of DEMs and slope derivatives, *Transactions in GIS*, 11(1):67-81.

Chapter 5

Carlisle, B.H., 2000. The highs and lows of digital elevation model (DEM) error: developing a spatially distributed DEM error model, *Proceedings of the 5th International Conference on GeoComputation*, 23-25 August 2000, University of Greenwich, U.K., URL: http://www.geocomputation.org/2000/gc999/gc999.htm (last date accessed: 3 January 2009).

Champion, D., 2003. Which LOS algorithm should be used as a standard?, Line of Sight Technical Working Group Meeting, 5 June 2003, URL: http://www.agc.army.mil/operations/programs/LOS/20030605/BestAlgorithm.ppt, US Army Topographic Engineering Center, Alexandria, Virginia (last date accessed: 28 December 2008).

Champion, D.C., K.G. Pankratz, and L.A. Fatale, 1995. The effects of different line-of-sight algorithms and terrain elevation representations on combat simulations, *TRAC-WSMR-TR-95-032(R)*, US Army TRADOC Analysis Center, White Sands Missile Range, New Mexico, 118 p.

De Floriani, L., and P. Magillo, 2003. Algorithms for visibility computation on terrains: a survey, *Environment and Planning B: Planning and Design*, 30(5):709-728.

Dean, D.J., 1997. Improving the accuracy of forest viewsheds using triangulated networks and the visual permeability method, *Canadian Journal of Forest Research*, 27:969-977.

ESRI (Environmental Systems Research Institute), 2002. ArcGIS 3D Analyst: three-dimensional visualization, topographic analysis, and surface creation, ESRI White Paper, URL: http://www.esri.com/library/whitepapers/pdfs/arcgis_3d_anal.pdf, Environmental Systems Research Institute, Redlands, California (last date accessed: 19 May 2009).

ESRI (Environmental Systems Research Institute), 2007a. How line of sight (3D Analyst) works, ArcGIS 9.2 Desktop Help, URL: http://webhelp.esri.com/arcgisdesktop/9.2/index.cfm?topicname=how_line_of_sight_(3d_analyst)_works, Environmental Systems Research Institute, Redlands, California (last date accessed: 4 February 2009).

ESRI (Environmental Systems Research Institute), 2007b. Visibility (3D Analyst), ArcGIS 9.2 Desktop Help, URL: http://webhelp.esri.com/arcgisdesktop/9.2/index.cfm?topicname=visibility_(3d_analyst), Environmental Systems Research Institute, Redlands, California (last date accessed: 4 February 2009).

ESRI (Environmental Systems Research Institute), 2008. How viewshed works, ArcGIS 9.2 Desktop Help, URL: http://webhelp.esri.com/arcgisdesktop/9.2/index.cfm?topicname=how_viewshed_works, Environmental Systems Research Institute, Redlands, California (last date accessed: 15 January 2009).

Fisher, P.F., 1991. First experiments in viewshed uncertainty: the accuracy of the viewshed area, *Photogrammetric Engineering & Remote Sensing*, 57(10):1321-1327.

Fisher, P.F., 1993. Algorithm and implementation uncertainty in viewshed analysis, *International Journal of Geographical Information Systems*, 7(4):331-347.

Fisher, P.F., and C. Farrelly, 1997. Spatial analysis of visible areas from the Bronze Age cairns of Mull, *Journal of Archeological Science*, 24:581-592.

Fugro EarthData, 2006. Using lidar as a model for floodplain mapping, URL: http://earthdata.com/pdfs/FCT_Projects_STW-NC.pdf, Fugro EarthData, Inc., Leidschendam, the Netherlands (last date accessed: 6 February 2008).

Goodchild, M.F., and J. Lee, 1989. Coverage problems and visibility regions on topographic surfaces, *Annals of Operations Research*, 18:175-186.

Guth, P.L., 2004. The geometry of line-of-sight and weapons fan algorithms, *Studies in Military Geography and Geology* (D.R. Caldwell, J. Ehlen, and R.S. Harmon, editors), Kluwer Academic Publishers, Dordrecht, the Netherlands, pp. 271-285.

Hodgson, M.E., J.R. Jensen, L. Schmidt, S. Schill, and B. Davis, 2003. An evaluation of LIDAR- and IFSAR-derived digital elevation models in leaf-on conditions with USGS Level 1 and Level 2 DEMs, *Remote Sensing of Environment*, 84(2):295-308.

Huss, R.E., and M.A. Pumar, 1997. Effect of database errors on intervisibility estimation, *Photogrammetric Engineering & Remote Sensing*, 63(4):415-424.

Izraelevitz, D., 2003. A fast algorithm for approximate viewshed computation, *Photogrammetric Engineering & Remote Sensing*, 69(7):767-774.

Kidner, D., M. Dorey, and D. Smith, 1999. What's the point? interpolation and extrapolation with a regular grid DEM, *Proceedings of the 4th International Conference on GeoComputation*, 25-28 July 1999, Fredericksburg, Virginia, URL: http://www.geovista.psu.edu/sites/geocomp99/Gc99/082/gc_082.htm (last date accessed: 19 January 2009).

Lee, J., and D. Stucky, 1998. On applying viewshed analysis for determining least-cost paths on digital elevation models, *International Journal of Geographical Information Science*, 12(8): 891-905.

Leica Geosystems (Leica Geosystems Geospatial Imaging, LLC), 2007. IMAGINE VirtualGIS® product description, URL: http://gi.leica-geosystems.com/documents/pdf/IMAGINEVirtualGISProductDEscription.pdf, Leica Geosystems Geospatial Imaging, LLC, Norcross, Georgia (last date accessed: 20 May 2009).

Maloy, M.A., and D.J. Dean, 2001. An accuracy assessment of various GIS-based viewshed delineation techniques, *Photogrammetric Engineering & Remote Sensing*, 67(11):1293-1298.

Maune, D.F., S.M. Kopp, C.A. Crawford, and C.E. Zervas, 2001. Introduction, *Digital Elevation Model Technologies and Applications: The DEM Users Manual* (D.F. Maune, editor), American Society for Photogrammetry and Remote Sensing, Bethesda, Maryland, pp. 1-34.

MICRODEM, 2008. Vertical exaggeration, MICRODEM Help files, URL: http://www.usna.edu/Users/oceano/pguth/website/microdem.htm, U.S. Naval Academy, Annapolis, Maryland (last date accessed: 3 February 2009).

NCFMP (North Carolina Floodplain Mapping Program), 2003. LIDAR and digital elevation data, North Carolina Floodplain Mapping Program Fact Sheet, URL: http://www.ncfloodmaps.com/pubdocs/lidar_final_jan03.pdf, State of North Carolina, Raleigh, North Carolina (last date accessed: 25 February 2008).

Rana, S., 2003. Fast approximation of visibility dominance using topographic features as targets and the associated uncertainty, *Photogrammetric Engineering & Remote Sensing*, 69(8):881-888.

Riggs, P.D., and D.J. Dean, 2007. An investigation into the causes of errors and inconsistencies in predicted viewsheds, *Transactions in GIS*, 11(2):175-196.

Sorensen, P.A., and D.P. Lanter, 1993. Two algorithms for determining partial visibility and reducing data structure induced error in viewshed analysis, *Photogrammetric Engineering & Remote Sensing*, 59(7):1149-1160.

Swanson, R., 2003. Line-of-sight algorithm/viewshed results against field data, Line of Sight Technical Working Group Meeting, 5 June 2003, URL: http://www.agc.army.mil/operations/programs/LOS/20030605/Viewshed%20Evaluation6-5-03.ppt, US Army Topographic Engineering Center, Alexandria, Virginia (last date accessed: 27 October 2008).

TEC (US Army Topographic Engineering Center), 2004. Line-of-sight (LOS) compendium, version 1.0, Line of Sight Technical Working Group document, URL: http://www.agc.army.mil/operations/programs/LOS/LOS%20Compendium.doc, US Army Topographic Engineering Center, Alexandria, Virginia (last date accessed: 4 June 2008).

USGS (U.S. Geological Survey), 2007. The national map seamless server, National Elevation Data (NED) FAQ, URL: http://seamless.usgs.gov/faq/ned_faq.php, U.S. Geological Survey, Reston, Virginia (last date accessed: 23 May 2008).

Wang, J., G.J. Robinson, and K. White, 2000. Generating viewsheds without using sightlines, *Photogrammetric Engineering & Remote Sensing*, 66(1):87-90.

Yoeli, P., 1985. The making of intervisibility maps with computer and plotter, *Cartographica*, 22(3):88-103.

Yu, S.M., S.S. Han, and C.H. Chai, 2007. Modeling the value of view in high-rise apartments: a 3D GIS approach, *Environment and Planning B: Planning and Design*, 34(1):139-153.

Chapter 6

Chrisman, N., 2006. *Charting the Unknown: How Computer Mapping at Harvard Became GIS,* ESRI Press, Redlands, California, 218 p.

De Floriani, L., P. Marzano, and E. Puppo, 1994. Line-of-sight communication on terrain models, *International Journal of Geographical Information Science,* 8(4):329-342.

Doucette, P., and K. Beard, 2000. Exploring the capability of some GIS surface interpolators for DEM gap fill, *Photogrammetric Engineering & Remote Sensing*, 66(7):881-888.

El-Sheimy, N., C. Valeo, and A. Habib, 2005. *Digital Terrain Modeling: Acquisition, Manipulation, and Applications,* Artech House, Boston, Massachusetts, 270 p.

Ervin, S., and C. Steinitz, 2003. Landscape visibility computation: necessary, but not sufficient, *Environment and Planning B: Planning and Design,* 30:757-766.

ESRI (Environmental Systems Research Institute), 2007a. Geostatistical solutions, ArcGIS 9.2 Desktop Help, URL: http://webhelp.esri.com/arcgisdesktop/9.2/index.cfm?id=3266&pid=3259&topicname=Geostatistical_solutions, Environmental Systems Research Institute, Redlands, California (last date accessed: 5 May 2009).

ESRI (Environmental Systems Research Institute), 2007b. How inverse distance weighted (IDW) interpolation works, ArcGIS 9.2 Desktop Help, URL: http://webhelp.esri.com/arcgisdesktop/9.2/index.cfm?id=3304&pid=3302&topicname=How_Inverse_Distance_Weighted_(IDW)_interpolation_works, Environmental Systems Research Institute, Redlands, California (last date accessed: 1 May 2009).

Fisher, P.F., and N.J. Tate, 2006. Causes and consequences of error in digital elevation models, *Progress in Physical Geography*, 30(4):467-489.

Franke, R., 1982. Scattered data interpolation: tests of some methods, *Mathematics of Computation*, 38(157):181-200.

Gong, J., Z. Li, Q. Zhu, H. Sui, and Y. Zhou, 2000. Effects of various factors on the accuracy of DEMs: an intensive experimental investigation, *Photogrammetric Engineering & Remote Sensing*, 66(9):1113-1117.

Goodchild, M.F., and J. Lee, 1989. Coverage problems and visibility regions on topographic surfaces, *Annals of Operations Research*, 18:175-186.

Goovaerts, P., 1997. *Geostatistics for Natural Resources Evaluation,* Oxford University Press, New York, N.Y., 483 p.

Hirano, A., R. Welch, and H. Lang, 2003. Mapping from ASTER stereo image data: DEM validation and accuracy assessment, *ISPRS Journal of Photogrammetry and Remote Sensing*, 57(5):356-370.

Huss, R.E., and M.A. Pumar, 1997. Effect of database errors on intervisibility estimation, *Photogrammetric Engineering & Remote Sensing*, 63(4):415-424.

Kidner, D., M. Dorey, and D. Smith, 1999. What's the point? Interpolation and extrapolation with a regular grid DEM, *Geocomputation 99: Proceedings of the 4th International Conference on GeoComputation*, 25-28 July, Fredericksburg, Virginia, URL: http://www.geovista.psu.edu/sites/geocomp99/Gc99/082/gc_082.htm (last date accessed: 19 January 2009).

Kienzle, S., 2004. The effect of DEM raster resolution on first order, second order and compound terrain derivatives, *Transactions in GIS*, 8(1):83-111.

Krige, D.G., 1951. A statistical approach to some basic mine valuation problems on the Witwatersrand, *Journal of Chemical, Metallurgical, and Mining Society of South Africa*, 52(6):119-139.

Lam, N.S., 1983. Spatial interpolation methods: a review, *The American Cartographer*, 10(2):129-149.

Lloyd, C.D., and P.M. Atkinson, 2002. Deriving DSMs from LiDAR data with kriging, *International Journal of Remote Sensing*, 23(12):2519-2524.

Lloyd, C.D., and P.M. Atkinson, 2006. Deriving ground surface digital elevation models from LiDAR data with geostatistics, *International Journal of Geographical Information Science*, 20(5):535-563.

Longley, P.A., M.F. Goodchild, D.J. Maguire, and D.W. Rhind, 2005. *Geographic Information Systems and Science*, Second edition, John Wiley & Sons, West Sussex, U.K., 517 p.

MacEachren, A.M., and M.-J. Kraak, 2001. Research challenges in geovisualization, *Cartography and Geographic Information Science*, 28(1):3-12.

Maloy, M.A., and D.J. Dean, 2001. An accuracy assessment of various GIS-based viewshed delineation techniques, *Photogrammetric Engineering & Remote Sensing*, 67(11):1293-1298.

Maune, D.F., S.M. Kopp, C.A. Crawford, and C.E. Zervas, 2001a. Introduction, *Digital Elevation Model Technologies and Applications: The DEM Users Manual* (D.F. Maune, editor), American Society for Photogrammetry and Remote Sensing, Bethesda, Maryland, pp. 1-34.

Maune, D.F., J.B. Maitra, and E.J. McKay, 2001b. Accuracy standards, *Digital Elevation Model Technologies and Applications: The DEM Users Manual* (D.F. Maune, editor), American Society for Photogrammetry and Remote Sensing, Bethesda, Maryland, pp. 61-82.

NCFMP (North Carolina Floodplain Mapping Program), 2003. LIDAR and digital elevation data, North Carolina Floodplain Mapping Program Fact Sheet, URL: http://www.ncfloodmaps.com/pubdocs/lidar_final_jan03.pdf, State of North Carolina (last date accessed: 25 February 2008).

Oliver, M.A., and R. Webster, 1990. Kriging: a method of interpolation for geographical information systems, *International Journal of Geographical Information Systems*, 4(3):313-332.

Peucker, T.K., R.J. Fowler, J.J. Little, and D.M. Mark, 1978. The triangulated irregular network, *Proceedings of the ASP Digital Terrain Models (DTM) Symposium*, 9-11 May, St. Louis, Missouri (American Society of Photogrammetry, Bethesda, Maryland), pp. 516-540.

Su, J., and E. Bork, 2006. Influence of vegetation, slope, and lidar sampling angle on DEM accuracy, *Photogrammetric Engineering & Remote Sensing*, 72(11):1265-1274.

Watson, D.F., 1992. *Contouring: A Guide to the Analysis and Display of Spatial Data*, Pergamon Press, Oxford, 340 p.

Wise, S., 2000. GIS data modeling – lessons from the analysis of DTMs, *International Journal of Geographical Information Science*, 14(4):313-318.

Wood, J., and P.F. Fisher, 1993. Assessing interpolation accuracy in elevation models, *IEEE Computer Graphics and Applications*, 13(2):48-56.

Yang, X., and T. Hodler, 2000. Visual and statistical comparisons of surface modeling techniques for point-based environmental data, *Cartography and Geographic Information Science*, 27(2):165-175.

Yilmaz, H.M., 2007. The effect of interpolation methods in surface definition: an experimental study, *Earth Surface Processes and Landforms*, 32:1346-1361.

Chapter 7

Abidin, H., 2002. Fundamentals of GPS signals and data, *Manual of Geospatial Science and Technology* (J.D. Bossler, editor, J.R. Jensen, R.B. McMaster, and C. Rizos, associate editors), Taylor & Francis, London, U.K., pp. 95-113.

Arnaud, M., and A. Flori, 1998. Bias and precision of different sampling methods for GPS positions, *Photogrammetric Engineering & Remote Sensing*, 64(6):597-600.

Deckert, C., and P.V. Bolstad, 1996. Forest canopy, terrain, and distance effects on global positioning system point accuracy, *Photogrammetric Engineering & Remote Sensing*, 62(3):317-321.

Fisher, P., 2009. The representation of uncertain geographical information, *Manual of Geographic Information Systems* (M. Madden, editor), American Society for Photogrammetry and Remote Sensing, Bethesda, Maryland, pp. 235-264.

Huss, R.E., and M. A. Pumar, 1997. Effect of database errors on intervisibility estimation, *Photogrammetric Engineering & Remote Sensing*, 63(4):415-424.

Lachapelle, G., S. Ryan, and C. Rizos, 2002. Servicing the GPS user, *Manual of Geospatial Science and Technology* (J.D. Bossler, editor, J.R. Jensen, R.B. McMaster, and C. Rizos, associate editors). Taylor & Francis, London, U.K., pp. 201-215.

Lillesand, T.M., R.W. Kiefer, and J.W. Chipman, 2008. *Remote Sensing and Image Interpretation*, Sixth edition, John Wiley & Sons, New York, N.Y., 756 p.

Madden, M., R. Welch, T. Jordan, P. Jackson, R. Seavey, and J. Seavey, 2004. *Digital vegetation maps for the Great Smoky Mountains National Park*, URL: http://www.crms.uga.edu/nps/grsm/GRSM_Final_Report.pdf, Center for Remote Sensing and Mapping Science, Department of Geography, University of Georgia, Athens, Georgia (last date accessed: 20 November 2008).

Maune, D.F., J.B. Maitra, and E.J. McKay, 2001. Accuracy standards, *Digital Elevation Model Technologies and Applications: The DEM Users Manual* (D.F. Maune, editor), American Society for Photogrammetry and Remote Sensing, Bethesda, Maryland, pp. 61-82.

NGS (National Geodetic Survey), 2008. NGS Datasheet Page, downloaded metadata, URL: http://www.ngs.noaa.gov/cgi-bin/datasheet.prl, National Geodetic Survey, Silver Spring, Maryland (last date accessed: 29 May 2008).

Oderwald, R.G., and B.A. Boucher, 2003. GPS after selective availability: How accurate is accurate enough? *Journal of Forestry*, 101(4):24-27.

Plackner, A., 1998. GPS Q&A. *Earth Observation Magazine*, URL: http://www.eomonline.com/Common/Archives/1998jun/98jun_gps.html (last date accessed: 25 October 2008).

Rizos, C., 2002. Introducing the global positioning system, *Manual of Geospatial Science and Technology* (J.D. Bossler, editor, J.R. Jensen, R.B. McMaster, and C. Rizos, associate editors). Taylor & Francis, London, U.K., pp. 77-94.

Shi, W.(J.), 2009. Spatial data quality and uncertainty, *Manual of Geographic Information Systems* (M. Madden, editor), American Society for Photogrammetry and Remote Sensing, Bethesda, Maryland, pp. 201-224.

Stombaugh, T.S., and B.R. Clement, 1999. *The Ohio State University fact sheet: unraveling the GPS mystery, AEX-560-99,* URL: http://ohioline.osu.edu/aex-fact/0560.html, Ohio State University, Columbus, Ohio (last date accessed: 25 October 2008).

Wing, M.G., and A. Eklund, 2007. Performance comparison of a low-cost mapping grade global positioning system (GPS) receiver and consumer grade GPS receiver under dense forest canopy, *Journal of Forestry*, 105(1):9-14.

Wing, M.G., A. Eklund, and L.D. Kellogg, 2005. Consumer-grade global positioning system (GPS) accuracy and reliability, *Journal of Forestry*, 103(4):169-173.

Wong, D.W.S., and J. Lee, 2005. *Statistical Analysis of Geographic Information with ArcView GIS and ArcGIS*, John Wiley & Sons, Hoboken, N.J., 441 p.

Chapter 8

3D Nature, LLC, 2008. What is Visual Nature Studio?, URL: http://3dnature.com/vnsinfo.html, 3D Nature, LLC, Morrison, Colorado (last date accessed: 20 May 2009).

Amidon, E.L., and G.H. Elsner, 1968. Delineating landscape view areas...a computer approach, USDA Forest Service, Research Note PSW-180, Pacific Southwest Forest and Range Experiment Station, Berkeley, California.

Appleton, K., and A. Lovett, 2009. Visualizing rural landscapes from GIS databases in real-time – a comparison of software and some future prospects, *Manual of Geographic Information Systems* (M. Madden, editor), American Society for Photogrammetry and Remote Sensing, Bethesda, Maryland, pp. 815-836.

Appleton, K., A. Lovett, G. Sünnenberg, and T. Dockerty, 2002. Rural landscape visualisation from GIS databases: a comparison of approaches, options and problems, *Computers, Environment and Urban Systems*, 26:141-162.

Bishop, I.D., 2003. Assessment of visual qualities, impacts, and behaviours, in the landscape, by using measures of visibility, *Environment and Planning B: Planning and Design*, 30:677-688.

Ervin, S., and C. Steinitz, 2003. Landscape visibility computation: necessary, but not sufficient, *Environment and Planning B: Planning and Design*, 30:757-766.

ESRI (Environmental Systems Research Institute), 2002. ArcGIS 3D Analyst: three-dimensional visualization, topographic analysis, and surface creation, ESRI White Paper, URL: http://www.esri.com/library/whitepapers/pdfs/arcgis_3d_anal.pdf, Environmental Systems Research Institute, Redlands, California (last date accessed: 19 May 2009).

ESRI (Environmental Systems Research Institute), 2007. Raster to TIN (3D Analyst), ArcGIS 9.2 Desktop Help, URL: http://webhelp.esri.com/arcgisdesktop/9.2/index.cfm?id=961&pid=959&topicname=Raster_To_TIN_(3D_Analyst), Environmental Systems Research Institute, Redlands, California (last date accessed: 10 May 2009).

Gahegan, M., 1999. Four barriers to the development of effective exploratory visualisation tools for the geosciences, *International Journal of Geographical Information Science*, 13(4):289-309.

Germino, M.J., W.A. Reiners, B.J. Blasko, D. McLeod, and C.T. Bastian, 2001. Estimating visual properties of Rocky Mountain landscapes using GIS, *Landscape and Urban Planning*, 53(1):71-83.

Ghadirian, P., and I.D. Bishop, 2008. Integration of augmented reality and GIS: a new approach to realistic landscape visualisation, *Landscape and Urban Planning*, 86(3-4):226-232.

Haala, N., and M. Kada, 2009. Virtual GIS: efficient presentation of 3D city models, *Manual of Geographic Information Systems* (M. Madden, editor), American Society for Photogrammetry and Remote Sensing, Bethesda, Maryland, pp. 885-900.

Lee, J., 1991. Comparison of existing methods for building triangular irregular network models of terrain from grid digital elevation models, *International Journal of Geographical Information Systems*, 5(3):267-285.

Leica Geosystems (Leica Geosystems Geospatial Imaging, LLC), 2007. IMAGINE VirtualGIS® product description, URL: http://gi.leica-geosystems.com/documents/pdf/IMAGINEVirtualGISProductDEscription.pdf, Leica Geosystems Geospatial Imaging, LLC, Norcross, Georgia (last date accessed: 20 May 2009).

MacEachren, A.M., and M.-J. Kraak, 2001. Research challenges in geovisualization, *Cartography and Geographic Information Science*, 28(1):3-12.

MICRODEM, 2005. Drape map on DEM, MICRODEM Help files, URL: http://www.usna.edu/Users/oceano/pguth/website/microdem.htm, U.S. Naval Academy, Annapolis, Maryland (last date accessed: 3 February 2009).

Stoltman, A.M., V.C. Radeloff, and D.J. Mladenoff, 2004. Forest visualization for management and planning in Wisconsin, *Journal of Forestry*, 102(4):7-13.

Swanson, R., 2003. Line-of-sight algorithm/viewshed results against field data, Line of Sight Technical Working Group Meeting, 5 June 2003, URL: http://www.agc.army.mil/operations/programs/LOS/20030605/Viewshed%20Evaluation6-5-03.ppt, US Army Topographic Engineering Center, Alexandria, Virginia (last date accessed: 27 October 2008).

Wang, X., B. Song, J. Chen, T.R. Crow, and J.J. LaCroix, 2006. Challenges in visualizing forests and landscapes, *Journal of Forestry*, 104(6):316-319.

Winterbottom, S.J., and D. Long, 2006. From abstract digital models to rich virtual environments: landscape contexts in Kilmartin Glen, Scotland, *Journal of Archaeological Science*, 33:1356-1367.

Yu, S.M., S.S. Han, and C.H. Chai, 2007. Modeling the value of view in high-rise apartments: a 3D GIS approach, *Environment and Planning B: Planning and Design*, 34:139-153.

Chapter 9

Bossler, J.D., 2002. Coordinates and coordinate systems, *Manual of Geospatial Science and Technology* (J.D. Bossler, editor, J.R. Jensen, R.B. McMaster, and C. Rizos, associate editors), Taylor & Francis, London, U.K., pp. 8-15.

Colvocoresses, A.P., 1997. The gridded map, *Photogrammetric Engineering & Remote Sensing*, 63(4):377-380.

ESRI (Environmental Systems Research Institute), 2008a. How viewshed works, ArcGIS 9.2 Desktop Help, URL: http://webhelp.esri.com/arcgisdesktop/9.2/index.cfm?topicname=how_viewshed_works, Environmental Systems Research Institute, Redlands, California (last date accessed: 15 January 2009).

ESRI (Environmental Systems Research Institute), 2008b. Project raster (data management), ArcGIS 9.2 Desktop Help, URL: http://webhelp.esri.com/arcgisdesktop/9.2/index.cfm?id=1625&pid=1617&topicname=Project_Raster_(Data_Management), Environmental Systems Research Institute, Redlands, California (last date accessed: 2 April 2009).

Franklin, K.B., and P.L. Guth, 2005. The effects of DEM re-interpolation on viewshed computations, *Proceedings of the Sixth International Conference on Military Geology and Geography*, 19-22 June 2005, University of Nottingham, UK.

Germino, M.J., W.A. Reiners, B.J. Blasko, D. McLeod, and C.T. Bastian, 2001. Estimating visual properties of Rocky Mountain landscapes using GIS, *Landscape and Urban Planning*, 53(1):71-83.

Habib, A., 2002. Coordinate transformations, *Manual of Geospatial Science and Technology* (J.D. Bossler, editor, J.R. Jensen, R.B. McMaster, and C. Rizos, associate editors). Taylor & Francis, London, U.K., pp. 27-49.

Slocum, T.A., R.B. McMaster, F.C. Kessler, and H.H. Howard, 2008. *Thematic Cartography and Geovisualization*, Third edition, Pearson Prentice Hall, Upper Saddle River, New Jersey, 576 p.

Snyder, J.P., 1987. Map projections – a working manual, U.S. Geological Survey Professional Paper 1395, URL: http://onlinepubs.er.usgs.gov/djvu/PP/PP_1395.pdf, U.S. Geological Survey, Washington, D.C. (last date accessed: 11 June 2009).